Fouling of crude oil refinery preheat exchangers

Downey, Imelda Louise

Award date:
1993

Awarding institution:
University of Bath

FOULING OF CRUDE OIL REFINERY PREHEAT EXCHANGERS

Submitted by Imelda Louise Downey

for the degree of PhD

of the University of Bath

1993

ProQuest LLC
789 East Eisenhower Parkway
P.O. Box 1346
Ann Arbor, MI 48106-1346

C

FOULING OF CRUDE OIL REFINERY PREHEAT EXCHANGERS

ABSTRACT

This thesis investigates the relationship between fouling of industrial heat exchangers and their operational envelope. The work was based on a three year investigation period into the operation of a set of sixteen heat exchangers in an oil refinery crude oil preheat train. This extended period of observation allowed two operating cycles to be studied.

The objective of the study was to allow a detailed investigation into the effects of parameters such as tubewall temperature, velocity and fluid composition on fouling in an industrial setting. Thus complementing and expanding on previous laboratory based work.

The data gathered was used in the development of a simple correlation between the overall fouling rate and the tubewall temperature. The correlation was based on the data from the first operating cycle and took the form of an Arrhenius type relationship. The validity of the temperature model was tested using data from the second operating period. It was found that the model successfully predicted the steady reduction in the thermal performance of the exchangers in the preheat train whilst processing light crude oils. The activation energy for the fouling process was calculated as approximately 33 kJ/mol. A survey of the available literature showed that this value lies in a region which would indicate a mixture of both chemical and physical deposition methods.

Chemical analysis of the deposits removed from the exchangers at the end of the first operating cycle confirmed the presence of both inorganic and high molecular weight carbonaceous material, also indicating a combination of deposition methods.

The data set collected from the refinery is unique, and in order to gain maximum benefit from this valuable resource it was used to determine the validity of a previously published model (Minerva). The model was found to approximate the correct pattern of fouling rate change with changes in operational parameters. However when used on the second set of data there was a tendency for over prediction of the fouling resistance. This could be explained by a number of factors including the difficulty of allowing for shellside fouling and sensitivity of the models coefficients to exact crude types.

ACKNOWLEDGEMENTS

I am particularly grateful to the management and staff at the refinery operated by the Netherlands Refining Company (formerly BP Raffinaderij Nederland NV) for their time, enthusiasm and expertise during the three years of the project.

I am also especially grateful to Dr M F Self and Mr D King of BP International, and Mr D Cowie of BP research for their continued enthusiasm and support.

I also wish to express thanks for the help and encouragement of Drs Kolaczkowski and Crittenden, and other students and members of staff at the University of Bath.

Finally I would like to thank my family and friends who have put up with the long, protracted "writing-up" phase of this work.

Table of Contents

List of Figures

List of Tables

Nomenclature

A	Cross sectional area	m^2
A'	Arrhenius constant	
A_t	Cross sectional area at thermo-couple	m^2
c	Unit dirt content	
c_i	Temperature error corrective coefficient	
C	Constant eqn 3.29	-
C_{pc}	Specific heat capacity (Cold stream)	$J\ kg^{-1}\ K^{-1}$
$C_{A\text{-}D}$	Effectiveness factor related to crossflow	
D (d)	Tube inside diameter	m
De	Shell equivalent dia	m
d_o	Tube outside diameter	m
f	Friction factor	-
F	Underwood correction factor	
FF	Flow Fraction	-
G	Mass velocity	$kg\ s^{-1}\ m^{-2}$
h_i	Tube heat trans coeff	$W\ m^{-2}\ K^{-1}$
h_o	Shell heat trans coeff	$W\ m^{-2}\ K^{-1}$
k	Thermal conductivity	$W\ m^{-1}\ K^{-1}$
l	Tube length	m
N	Number of tube rows	-
P	Effectiveness number	
Pr	Prandtl number	-
P_T	Tube pitch	m

Q	Energy transfered	W
Qi	defined eqn 3.20 a&b	-
R	Universal Gas constant	kJ $kmol^{-1}$ K^{-1}
R'	defined by equation 3.7a	
R_f	Overall fouling resistance	K m^2 W^{-1}
R_{A-E}	defined eqn 3.21 a&b	-
Re	Reynolds number	-
r_w	thermal resistance of wall	
$R\phi$	thermal resistance tubeside foulant	km^2 W^{-1}
R_{fo}	thermal rsistance shellside foulant	km^2 W^{-1}
S	defined by equation 3.7b	
t	temperature (tubeside)	K (°C)
T	temperature (shellside)	K (°C)
t'	time	s (day or month)
U_c	Clean heat trans coeff	W m^{-2} K^{-1}
U_d	Dirty heat trans coeff	W m^{-2} K^{-1}
v	Velocity	m s^{-1}
W	Mass flowrate	kg s^{-1}
x	deposit thickness	m (mm)
Greek letters		
B	constant proportional to shear stress	
Δp	pressure drop	bar
Δt_c	temperature difference coldside	°C
μ	viscosity	N.s m^{-2}
ρ	density	kg m^{-3}

τ	shear stress
ϕ	μ/μ_w

Subscripts

A	A stream
B	B stream
C	C stream
D	D stream
E	E stream
b	Bulk
i	Inside
o	Outside
s	Shell side
t	Thermocouple
tw	In tube window
w	Wall

Superscripts

*	at asymptote

Chapter 1

1 Introduction

Heat exchanger fouling remains a major problem in refinery operations, especially in crude oil distillation unit preheat trains, causing throughput limitations and down time and thereby affecting profits. Its mechanisms and dependence on key operating parameters are still not fully understood. Increased knowledge in this area could lead to improved heat exchanger design allowing the exchangers to be more efficiently integrated into the refinery to reduce fouling.

This project was initiated with the objective of gaining a fundamental understanding of the complex dependencies of fouling rates in crude oil preheat trains on the key operating parameters of temperature, velocity and composition, by the use of actual data from an operating refinery.

The decision to use actual data from a refinery was taken due to the problems associated with laboratory studies. Carefully controlled laboratory-scale studies have been useful in showing the rate of fouling is strongly dependent upon surface and bulk temperatures, flowrates, feedstock composition and metallurgy. However since fouling on a refinery may take weeks or even months to reach significant levels, in laboratory studies it is necessary to modify one or more of the operating parameters so that an accelerated test lasting only hours or days can be achieved in the laboratory.

A common approach is to use actual feedstocks and realistic temperatures, pressures and metallurgy, but to greatly reduce the fluid flowrate thereby reducing the equipment size and power requirements. However special consideration must be given to maintaining representative fluid velocities and Reynolds numbers. It is not uncommon for laboratory-scale experiments to produce deposits that are dissimilar to those found in an industrial situation. The laboratory-scale deposits from crude oils often have unrealistically high organic contents as a result of the shift in balance between organic and inorganic fouling mechanisms in equipment of reduced scale.

The majority of laboratory-scale equipment[1,2,3] has been used to test the effectiveness of anti-fouling chemicals rather than to obtain fundamental relationships between fouling rates and operating parameters. Hence it is clear that there is a need to supplement laboratory scale studies with studies made on industrial plant if a more complete understanding of hydrocarbon fouling is to be obtained.

However using data from an operating refinery is not without its disadvantages which are principally;

(1) it is not possible to mount scientific experiments without interfering with the normal production of the refinery,

(2) the long time period over which fouling occurs in an industrial situation means that the process operating parameters will have changed many times during the observation period,

(3) instrumentation on a refinery is often limited by safety and operating considerations as all equipment around the exchangers has to be electrical zone classification one, and the instruments have to be robust enough to withstand the operating conditions on the preheat train.

The refinery at Rotterdam is ideally situated to take advantage of rapid changes in the oil spot market and so the refinery processes many different types of crude. This refinery was chosen for the project as it has the best instrumentation of the available refineries in the BP group, and had previously experienced fouling problems on the crude oil distillation units. There are three crude oil distillation units at the Rotterdam refinery which are described in Chapter 2. Crude oil distillation unit three (CDU3) was chosen for the study as it is refinery policy that this is the base operating unit with an approximately steady crude oil feed rate. Crude oil distillation units two and four are used intermittently as demand for petroleum products fluctuates.

Operating data namely flowrates and temperatures was collected from each exchanger in the preheat train of CDU3. This data along with the physical properties calculated

using an 'in-house' BP computer program was used to determine the fouling rate for each exchanger. The possible effects of inaccuracies in the collected data were determined and the data collection strategy was adjusted accordingly as described in Chapter 3.

The refinery is a profit-making unit and is subject to commercial pressures which dictate the flow of crude oil through the distillation unit and also the relative amounts of each of the product streams. Flow through the distillation unit can also be affected by other downstream units. These external factors make it impossible to mount controlled scientific experiments. The best that can be achieved is the acquisition of data at times of apparent significance, such as when heavy crude types are being processed, there are significant changes in the operating conditions and immediately before and immediately after a shutdown or start-up. Details of the chronological sequence of such events on the refinery with details of the crude oil types being processed when the data was collected are presented in Chapter 4 along with details of the shutdowns and start-ups witnessed during the project.

In Chapter 5 the fouling resistances calculated from the refinery data are presented, and allowing for the difficulties associated with a study on an industrial plant several valuable conclusions are drawn as to the effect of temperature, and to a lesser extent composition, on the fouling rate in the exchangers.

A simple mathematical model to predict the fouling rate based on the crude type and temperature is developed in Chapter 6. A more complex previously published model is also tested using the data from the refinery.

The conclusions from the study and suggestions for further work are presented in Chapter 7.

1.1 Fouling Of Crude Oil Distillation Unit Heat Exchangers

1.2 Effects Of Fouling

Fouling is the accumulation of dirt, scale, corrosion products or other material on a surface. It has the following two major effects:

(i) Reduction in the overall heat transfer coefficient; the deposit presenting a further resistance to heat transfer.

(ii) Reduction in the flow area, and possible increase in surface roughness exacerbating pressure drop for the same flowrate. Generally the deposits formed fall into one of three categories.

These effects combine to reduce the efficiency of the heat transfer equipment. Early observations of fouling were in boilers and steam generators. Somerscales [4] gives an historical review of the fouling of heat transfer surfaces. The costs attributable to fouling are difficult to determine due to the dearth of published information and the sensitivity of such data. Pritchard [5] estimated the cost of fouling in the United Kingdom to be £500 M (1979). This cost was based on four main categories:

(i) Additional capital expenditure;

(ii) Additional fuel costs;

(iii) Maintenance costs;

(iv) Lost production.

Van Nostrand [6] considered the cost of fouling for a hypothetical refinery utilising statistical data on refineries in the United States. The penalties incurred were classified into three categorise:

(i) Energy debits - due to increased consumption of process fuel;

(ii) Throughput debits - due to decreased flow area and increased down time;

(iii) Maintenance and cleaning costs.

It was calculated that for a 100,000 Bbl/sd (Barrels per stream day) refinery the annual penalties for the crude oil distillation unit were:

(i) Energy debits -	$1,020,000
(ii) Throughput debits -	$3,730,000
(iii) Maintenance costs -	$ 35,000
Total	$4,785,000

Extrapolating this data for the non-communist world gave a fouling related cost of $4.141 billion(US)/year. Approximately half of this is attributable to the crude oil distillation unit with much of the costs resulting from the increased fuel requirements due to the fouling of the preheat train.

Hence to improve the economic operation of refineries, the mechanisms of fouling in preheat exchangers need to be understood. This would enable mathematical models to be developed for predictive and design purposes.

1.3 Fouling Resistances

The majority of oil refineries currently in operation will probably have been designed using fouling resistances from the Tubular Exchangers Manufacturers' Association (TEMA) guide book[7]. These guidelines were developed with limited account being taken of the effects variables such as temperature, flowrate, and composition would have on the fouling process. Bott and Walker [8] compiled evidence which shows that in many oil refinery heat exchangers the TEMA resistances are exceeded in a short period of a few months. There have been few other guides to the selection of fouling resistances. Atkins [9] published a guide to the selection of time dependent fouling resistances for the petroleum industry, but these have not been regularly used for heat exchanger design. Lambourn and Derrieu[10] have published design fouling resistances for crude oil heat exchangers based on data from Total refineries that are an order of magnitude greater

then those from TEMA. They proposed that these fouling resistances may be used by Total to design heat exchangers. Table 1 gives details of published fouling resistances for refinery exchangers.

1.4 Fouling Deposits

Fouling deposits in heat exchangers generally fall into one of three categories as defined by Nelson[11].

(i) **Hard deposits**

The resistance of the hard dense deposit is directly proportional to the thermal conductivity of the foulant material. These are tenacious deposits that are removed by chemical treatment or sandblasting. Examples include hard thermally degraded coke.

(ii) **Porous deposits**

Porous deposits represent a high resistance to heat transfer due to the relatively low thermal conductivity of the fluid trapped in the pores. Porous deposits are removed by chemical treatment or high pressure steam or water jetting.

(iii) **Loose deposits**

Loose deposits can represent a high resistance to heat transfer primarily due to the liquid entrapped in the loose structure. Loose deposits are removed by air blowing or water washing.

Analysis of the deposits from exchangers can yield valuable information with regard to the mechanism of fouling. Eaton and Lux[3] gave detailed analysis of crude oil deposits formed in the laboratory and taken from industrial exchangers. There is an appreciable spread of data but generally those deposits formed in the laboratory have a higher pentane soluble (resin and free oil) fraction than those found in the industrial heat exchangers. However, it is difficult to draw comparisons as the type of crude oil used in the laboratory situation is different to that in the operating heat exchangers. In general Eaton and Lux

found that the samples from industrial exchangers were approximately 50% resin and free oil, 10% asphaltenes, 30% coke and 10% inorganic fractions such as calcium, sulphur, sodium and chlorine salts.

1.5 Fouling Mechanisms

Fouling of preheat exchanger trains results from one or more of the following mechanisms:

(1) Chemical reaction,

(2) Crystallisation or precipitation,

(3) Particulate deposition, and possibly

(4) Corrosion.

Fouling in complex industrial systems is often difficult to categorise as more than one mechanism may be involved. However Epstein[12] identified five stages that may be present in the development of fouling deposits throughout industry. These are:

(1) Induction period which is due to formation of free radicals, changes in surface roughness, or development of initiation sites.

(2) Transport/ deposition phenomena that are affected by turbulence, diffusion and thermophoresis.

(3) Attachment which can occur via Van der Waals forces, surface roughness and surface catalysis.

(4) Detachment which may be due to turbulence, pressure/temperature shocks and back diffusion.

(5) Ageing through recrystallisation and slow reactions.

1.5.1 Chemical Reaction Fouling

Chemical reaction fouling is the formation of deposits via chemical reactions either within the bulk, the product being transported to the surface, or at the wall with the heat transfer surface material possibly acting as a catalyst. Reviews of chemical reaction fouling have been given by Froment[13], (for high temperature fouling from hydrocar-

bons), and Crittenden *et al*[14].

The extent of the chemical reaction is dependent upon temperature, pressure, composition, including trace materials and velocity or residence time. The principal chemical reaction mechanisms for hydrocarbon streams are cracking, coking, autoxidation and polymerisation. Cracking and coking are usually associated with high temperatures (>650 K) and would not usually be applicable in a preheat exchanger train. It is generally accepted that deposition via chemical reactions in the range of temperatures observed in the preheat exchangers is from free-radical autoxidation and polymerisation reactions.

Autoxidation reactions are initiated by hydrogen removed from the hydrocarbon by a free-radical. The hydrocarbon radical thus formed may further react with molecular oxygen resulting in a chain reaction involving peroxy radicals and hydroperoxide molecules. Soluble salts such as those of iron, copper, chromium and nickel may catalyses the reaction by increasing the rate of hydroperoxide homolysis and possibly take part in the initiation reactions. The autoxidation mechanism summarised by Eaton and Lux[3] shows the key role played by asphaltenes in the formation of deposits.

Polymerisation reactions are the conversion of a monomer into a large chemical multiple of itself. If a polymer becomes insoluble in its monomer it precipitates as it forms. Oxygen, halides, sulphides and nitrogen compounds are able to initiate polymer formation. At certain temperatures mercaptans and sulphides can undergo reaction with the metal heat transfer surface. Such reactions can yield hydrocarbon radicals which in turn may initiate polymerisation and autoxidation reactions.

1.5.1.1 Temperature effects

It has generally been found [13],[14], that the fouling rate increases exponentially with temperature. Data is often fitted to an Arrhenius relationship of the following form,

$$\frac{dR_f}{dt} = A e^{\left\{-\frac{E}{(RT_w)}\right\}}$$

Crittenden and Khater [15], Vranos [16] and Taylor [17] have all found a more complex temperature dependence. There appears to be a transition temperature, often associated with a phase change, which is assumed to indicate a change in the reaction mechanism. Trace amounts of oxygen, sulphur, nitrogen compounds and other impurities can often affect the fouling rate/temperature dependence.

1.5.1.2 Composition effects

The Rotterdam refinery processes many different crude oils. Usually these are blended in tanks prior to processing. This makes it difficult to determine the exact composition of the crude oil being processed. There is little in the open literature on the fouling tendencies of particular crude oils. Atkins[9] categorises the fouling tendency of hydrocarbon streams on refineries according to the API gravity, with heavier hydrocarbons having a greater fouling tendency. Butler and McCurdy[18] showed that decreasing the salt content of a crude oil reduced the fouling rate. Fields,*etal*[19] published a guide to predicting crude oil fouling tendencies. They classified given crude oil slates as either high, moderate or low fouling but due to the confidential/commercial nature of the work did not give details of the specific crude studied. However they claim to have found a good correlation between the fouling tendency of a crude oils slate and such parameters as asphaltenes and sulphur content, with the extent of fouling increasing as the concentration of these components increased. They also found that heavier crude oils had a stronger fouling tendency.

The presence, in only trace amounts, of certain species can have a significant effect upon the fouling rate. Much of the work on composition effects has been done on laboratory-scale equipment, often using pure hydrocarbons so that the amount of each species can readily be determined. Nevertheless, many of the general conclusions should be applicable to crude oils.

(i) **Sulphur**

Sulphur compounds such as thiols, dissulphides and some condensed thiophenes at

concentrations of approximately 100ppm were found to breakdown forming the free radicals required to initiate chemical reaction fouling in oxygenated fuels [20].However it was found that diphenyl sulphides and dibenzothiophene were not deleterious. Johnson et al. [22] found that disulphides, polysulphides, free sulphur and particularly thiophenols promoted sludge formation in storage of jet fuels.

(ii) **Oxygen**

Crittenden and Khater [15] (studying fouling from kerosine), Taylor [17] (studying fouling from jet fuels), and Butler and McCurdy [18] (studying various refinery exchangers) found that exclusion of dissolved oxygen substantially reduced fouling.

(iii) **Nitrogen**

Thompson [23] investigated the effect of nitrogen compounds on fouling rates, and found that pyridenes and pyroles caused a drop in the stability of sour gasoline, which could lead to increased fouling.

(iv) **Chlorides**

Eaton and Lux [3] found that the presence of hydrogen chloride in crude oils, gave a dramatic increase in the fouling from hydrocarbons. The metal chlorides often found in crudes, such as iron, calcium, and magnesium hydrolyse to produce acids which may increase the fouling rate.

1.5.1.3 Velocity effects

It is generally thought that higher velocities usually help to reduce fouling. Nelson [11] worked with desalted crude over a range of velocities from 0.3-2.1 m s^{-1},in an industrial situation, and found that the deposition rate was less at higher velocities. Watkinson and Epstein [24] working with sour gas oils at Reynolds numbers in the range 9800 - 41900, also found a decrease in deposition rate with increased velocity.

Recent work by Crittenden et al. [14] working with polymerisation of styrene, found that above 150°C the initial deposition rate increased with increasing velocity, and that below this temperature the fouling rate decreased with increasing temperature. It was

postulated that at the higher temperature and high velocity, mass transfer of the monomer to the surface was the controlling step, whereas at the lower temperature the reaction kinetics were controlling.

1.5.2 Crystallisation Fouling

Crystallisation fouling is the deposition or formation of crystals from solution onto a surface. Bott[25] presents a general review of crystallisation fouling. Crystallisation fouling in crude preheat trains is usually attributed to the associated water. After the desalters crude contains upto 5% water as a result of water carryover and caustic injection. At high tubewall temperatures the water maybe vaporised and/or supersaturation conditions may be reached resulting in deposition of the inorganic salts.

Crystallisation fouling from hydrocarbons is often described as "freezing" or "solidification" fouling. This phenomena is found in crude carrying pipelines at or near the cloud point temperature, where the wax precipitates and deposits on the surface. However the relatively high temperatures in the preheat train preclude this type of fouling.

The dearth of published data on the complex supersaturation of species at the wall/fluid interface inhibits the development of mathematical models to describe crystallisation fouling. Further research into the basic concepts of mass transfer and solubility/temperature relationships is required, before predictive and design models based on operating parameters such as temperature and velocity can be developed.

1.5.3 Particulate Fouling

1.5.3.1 Isothermal fouling

Particulate fouling is the deposition on a surface of solid particles that were suspended in the fluid. Particulate fouling in refinery preheat trains is predominantly from corrosion products suspended in the process stream, and agglomerated particles of organics/inorganics. Initial work by Epstein[12] on particulate fouling was on isothermal systems with smooth surfaces and small particles. Under these conditions the extent of fouling is governed by the transport of particles to the surface. Epstein[26] proposed three

mechanisms for particulate fouling in the turbulent flow regime.

(i) **Diffusion** - suspended colloidal particles are carried to the surface by Brownian motion. The small particles are assumed to act as large molecules, allowing traditional mass transfer equations to be used in predictive models.

(ii) **Inertia** - larger particles suspended in the fluid have a free flight velocity sufficient to reach the surface. Predictive models are divided into two groups, those based on classical concepts of eddy diffusion and those based on stochastic approaches such as random walk or turbulent bursts.

(iii) **Impaction** - for particles of approximately 10 -20 microns diameter the response to turbulent variations is diminished, with transport coefficients similar to those for diffusion.

1.5.3.2 Temperature Effects

The introduction of thermal gradients to a system complicates the particulate fouling mechanism. The changing fluid properties with position, thermophoresis, and thermoelectric effects will influence the transport of particles to the surface. Whitmore and Miesen [27] developed a model to predict the thermophoretic velocity of a particle in both liquids and gases. The velocity is directly dependent upon the kinematic viscosity of the fluid. The models were compared to experimental results from other sources[28] and gave a satisfactory fit to the data. Typically the kinematic viscosity of a gas is an order of magnitude greater than that of a liquid, hence thermophoresis has a greater effect in gaseous systems. Hence it is unlikely to have a strong effect in the preheat exchangers.

1.5.4 Corrosion Fouling

Corrosive salts found in petroleum are primarily chlorides and sulphides. Chloride ions prevent the formation of a passive film on the heat transfer surface. Analysis of deposits[3] from refinery exchangers has shown that iron salts are frequently present in deposits. Often the corrosion in heat exchangers has occurred during storage before they go on-line. However it is possible for the corrosion to carry on during operation underneath other deposits. Oxygen also plays a significant role with the corrosion rate in neutral solutions being proportional to the oxygen concentration. Corrosion rates that are controlled by oxygen transfer often decrease with increasing temperature as the solubility of oxygen decreases. Corrosion fouling is usually dependent upon operating parameters in a similar manner to chemical reaction fouling, as it depends upon a reaction at the surface.

1.6 Summary

From consideration of the available literature it would be reasonable to expect the fouling of the preheat exchangers to be dependent upon temperature, velocity, and composition, and that the mechanisms involved would probably be a combination of chemical reaction fouling and particulate fouling with possibly some corrosion fouling.

The fouling deposits would be expected to be porous type deposits that could entrap liquid crude oil and have a carbon content of 10-60% by weight. These hypotheses will be investigated in detail in subsequent chapters.

Table 1 PUBLISHED FOULING RESISTANCES.

Source	Process Fluid	Combined shell and tube side fouling resistance $Wm^{-2}K^{-1}$	Time in operation
TEMA[7]	Gas oil and Crude oil.	0.002	-
Butler *etal*[18]	Furnace oil and Crude oil.	0.004	3 months
Lambourne & Durrieu[10]	Crude oil and Residue	0.0065	100 days
Weiland *etal*[29]	Absorption oils	0.006	8 months

1.7 References

(1) Braun R (1977) " The nature of petroleum process fouling"
Materials Performance. **16**(11) 35-41.

(2) Hausler R.H (1973) "New test will show fouling tendency of process streams"
Oil and Gas J. **71**(23) 56-63.

(3) Eaton P and Lux R (1984) In: "Fouling in Heat Exchange Equipment" (Suitor J.W and Pritchard A.M eds.) pp33-42. HTD **35** ASME New York.

(4) Somerscales E.F.C (1988) "Fouling of heat transfer surfaces an historical review" 50th Anniversary Commemoration of the Heat Transfer Division of ASME.

(5) Pritchard A.M (1979) "Heat exchanger fouling in British industry"
Fouling Prevention Res Dig **1** (1-4) iv-vi

(6) Van Nostrand W.L, Leach S.H and Haluska J.L (1981) " Economic penalties associated with the fouling of refinery heat transfer equipment"
In: "Fouling of Heat Transfer Equipment" (Somerscales E.F.C and Knudsen J.G eds) pp 619-643. Hemisphere Washington.

(7) Tubular Exchangers Manufacturer's Association (1978) "Standards of the Tubular Exchangers Manufacturer's Association" pp 138-142. New York.

(8) Bott T.R and Walker R.A (1971) "Fouling in heat transfer Equipment"
Chem Eng (11) 391-394.

(9) Atkins G.T (1962) "What to do about high coking rates"
Petro Chem Eng **34**(4) 20-25.

(10) Lambourn G.A and Durrieu M (1986) " Fouling in crude oil preheat trains " In: "Heat Exchanger Source Book" (Palen J.W ed) Hemisphere Washington.

(11) Nelson W.L (1934) "Fouling of Heat Exchangers"
Ref and Nat Gas Man **13**(7) 271-276.

(12) Epstein N (1978) "Fouling in Heat Exchangers"
Proceedings of 6th International Heat Transfer Conference.
p 235-254.

(13) Froment G.F (1981) "Fouling of heat transfer surfaces by coke formation in petrochemical reactors " In: "Fouling of Heat Transfer Equipment" (Somerscales E.F.C and Knudsen J.G eds) pp 411-435. Hemisphere Washington.

(14) Crittenden B.D, Kolaczkowski S.T and Hout S.A (1987) *"Modelling Hydrocarbon Fouling". Chem Eng Res Dev* **65** (2)

(15) Crittenden B.D and Khater (1987) *" Fouling from Vapourising Kerosine". ASME J Heat Trans* **109** 583-589.

(16) Vranos A, Marteney P.J and Knight B.A (1981) " Determination of coking rates in jet fuels" *Ind Engng Chem Pro Res Dev* **20** 167-169.

(17) Taylor W.F (1969) "Deposit formation from deoxygenated hydrocarbons". *Ind*

*Engng Chem Pro Res Dev***13** 133-138.

(18) Butler R.C, McCurdy N.M and Linden N.J (1949) "Fouling rates and cleaning methods in refinery exchangers." *Trans ASME* **11** 843-847.

(19) Fields D.E, Freeman R.F and Wright B.E (1988) "Predicting crude oil fouling tendency" *Energy Prog* **8** (4) 21-26.

(20) Taylor W.F (1969) "Kinetics of deposit formation from hydrocarbons (Fuel composition studies)" *Energy Prog* **8** 375-380.

(21) Taylor W.F (1968) "Kinetics of deposit formation from hydrocarbons (Effect of trace sulphur compounds)" *Energy Prog* **7** 198-202.

(22) Johnson C.R and Fink D.F (1954) "Stability of aircraft turbine fuels" *Ind and Engng Chem* **46** (10) 2166-2173.

(23) Thompson R.B, Druge L.W and Chencek J.A (1949) " Stability of fuel oils. In storage: effect of sulphur compounds". *Ind and Engng Chem* **42** 2715-2721.

(24) Watkins and Epstein (1969) "Gas oil fouling in a sensible heat exchanger" *Chem Eng Prog Symp Ser* **65** 89-90.

(25) Bott T.R (1988) "Crystallistion fouling - Basic science and models" In: "Fouling Science and Technology" (Melo L.F, Bott T.R and Bernardo C.A eds.) Nato ASI Series E Applied Sciences Vol 45 KluwerAcademic Pub Dortrect.

(26) Epstein N (1988)"Particulate fouling of heat transfer surfaces: Mechanisms and models". In: "Fouling Science and Technology" (Melo L.F, Bott T.R and Bernardo C.A eds.) Nato ASI Series E Applied Sciences Vol 45 KluwerAcademic Pub Dortrect.

(27) Whitmore P.J and Meisen A (1977) "Estimation of thermo and diffusiophoretic particle deposition."
Can J Chem Eng **55** 279-285.

(28) Nishio G, Kitani S and Takahashi K (1974)
Ind Eng Chem Process Des Dev **13** 408-412.

(29) Weiland J.H, McCay R.C and Barnes J.E (1949) " Rates of fouling and cleaning of unfired heat exchanger equipment"
Trans ASME **71** 849-853.

CHAPTER 2

2 REFINERY DESCRIPTION

2.1 Overview Of The BP Raffinaderij Nederland NV Oil Refinery

In a refinery the incoming crude oil is converted into marketable products to prescribed quantities and qualities by the appropriate combination of several different processing techniques.

The principal processing units on the refinery are;

(i) Crude Distillation,

(ii) Hydrofiner, and

(iii) Fluid Catalytic Cracking.

Tables 2.1, 2.2a and 2.2b give details of the design and measured temperatures, flowrates and physical properties of various the streams from the refinery and the Crude Distillation Unit.

The streams from these units are then further purified and blended in the following units:

(i) H_2S recovery unit.

(ii) Sulphur recovery unit.

(iii) Motor spirit blender.

(iv) White oil blender.

(v) Gas oil blender.

(vi) Fuel oil blender.

The Rotterdam refinery is situated on an estuary near one of the largest ports in Europe. The crude arrives from all over the world in ocean going tankers and is held in storage in the offsites area prior to processing in the production area. The products from the refinery are distributed by ocean going tankers via the product loading jetties, or directly by pipeline to distribution terminals in the Rotterdam district.

2.2 Offsites

The incoming crude is stored in one of six tanks in the offsites area. The tanks are 80m in diameter and 20m high with a crude storage capacity of 100530m^3. Each of the tanks may contain a mixture of different crude types. The mixture can contain anything from one to fifteen or more crudes. To ensure even distribution of the crude types within a tank there are three 60HP mixers. Prior to processing the crude oil on the refinery, samples of crude are taken from the top, middle and bottom of the tank and tested for specific gravity and bottom sediment and water (BSW) content. The tank is considered to be stratified if the specific gravity at all three points does not agree to two decimal places. If the tank is stratified the mixers are left on for a longer period of time until the crude blend is suitable for processing. The offsites area also contains the product storage facilities with loading jetties for marine tankers, and a pumping station to supply other distribution terminals in the Rotterdam district.

2.3 Crude Distillation Units

A crude distillation unit consists of an atmospheric distillation column, with the associated ancillary equipment, for the initial fractionation of the crude oil. The overhead product from the atmospheric unit is then treated in a distillate hydrotreater (DHT) where the sulphur is removed. The desulphurised stream is then treated in the stabiliser unit to remove the dissolved gaseous hydrocarbons prior to separation in the distillate fractionation unit (DFU). The benzene and naphtha mixture is then treated in the catalytic reformer to produce a stream with a higher octane number. The gas oil streams from the atmospheric crude distillation column are treated in the gas oil hydrofiners to remove sulphur. The atmospheric residue stream and the streams from the distillate hydro-treater, distillate fractionation unit and hydrofiners are treated in the Fluid Catalytic Cracker Unit.

There are three crude distillation units at the refinery. CDU 2 is the smallest of the

units and has a design capacity of 330 m^3hr^{-1} (50,000 Barrels per stream day)). CDU 3 and 4 are identical with a design capacity of 1325 m^3hr^{-1} (200,000 Barrels per stream day) each.

2.4 Fluid Catalytic Cracker Unit (FCCU)

The fluid catalytic cracker unit consists of a vacuum distillation unit, a catalytic cracking unit, a visbreaker, a gas concentration unit, a gasoline unit, an H_2S recovery system and a sulphur unit. In the vacuum distillation unit heavy gas oil is produced from the atmospheric residue. This heavy gas oil then forms the feed for the catalytic cracking unit. The catalytic cracker upgrades the heavy gas oil to lighter hydrocarbon fractions, for blending with other streams to reach product specifications. The visbreaker unit can process a mixture of atmospheric and vacuum residue. Thermal cracking reduces the viscosity thereby allowing blending with gas oils to produce fuel oils.

The gas concentration unit separates and purifies the catalytic cracker overheads by absorption and distillation, producing propene, butene and heavy cracked gasoline. The gasoline units sweeten the catalytically cracked gasoline by removal of the sulphur. This is achieved by mercaptan oxidation over a charcoal catalyst. In the H_2S recovery unit the hydrogen sulphide in the liquid and gaseous LPG streams is removed by absorption in di-ethanolamine. The hydrogen sulphide from the H_2S recovery system and the hydrofiners is then treated in the sulphur unit. The sulphur unit uses the "Claus process" in which the H_2S feed is converted to liquid sulphur in three phases i.e. the thermal phase, the catalytic phase and an after burning phase.

2.5 Crude Distillation Unit 3 (CDU 3)

2.5.1 The Preheat Train

Crude oil is pumped from the tank farm to CDU 3 via three cold charge pumps. Each pump is designed to handle 35% of the total design flow rate on the unit. The discharge

pressure for each of the pumps is controlled between 15 and 20 barg by a pressure controller at the desalters. The desalters are maintained at a pressure of 8 barg and a temperature of approximately 130°C. The cold crude charge pumps are fitted with a fluid coupling that permits adjustment of the power input to the motors to regulate the discharge pressure in proportion to the pressure drop through the first six exchangers in the preheat train.

The incoming crude splits into two parallel trains (See Figure 2.1) and is heated from ambient (5-15°C) to approximately 130°C in the first six heat exchangers. For geometric details see Appendix A. In these exchangers the cold crude is heated by the product and pump around streams from the atmospheric distillation column. The crude then enters the desalters where caustic at approximately 0.5% w/w is injected to control the pH of the desalter effluent to between 6 and 7. A demulsifying agent is added to reduce the foaming in the desalters and to improve the oil/water separation. Water, 4% w/w, is added in the desalter to remove the salts that are present in the crude. A high potential field across the desalter assists in coalescing the brine droplets. The hot brine solution is removed from the desalters and the two crude streams are pumped via the "warm" crude charge pumps through the preheat train to the furnace and then to the atmospheric distillation column. Each of the pumps has a design capacity of 464 m^3hr^{-1} and a discharge pressure between 30 and 40 barg. The pumps are controlled by a pressure controller at the furnace which assures that the pressure to the furnace is sufficient to suppress vaporisation of the crude to enable flow regulation through the furnace.

The desalted crude is then heated in two parallel preheat trains from approximately 130°C to 250°C. This is achieved by heat exchange with the product and pump around streams from the atmospheric distillation column. Details of these streams are given in Tables 2.2a and 2.2b. A schematic diagram of the preheat trains on CDU 3 is given in Figure 2.1. The flow of crude through each of the trains can be adjusted by a hand control valve. By-passes are provided so that part of one train can be by-passed for on-stream

cleaning. Cleaning methods will be discussed in Chapter 4.

2.5.2 The Atmospheric Distillation Column

After being heated in the preheat train the crude enters the furnace. The furnace has 10 vertical high intensity burners which can be fired on fuel gas, fuel oil or a combination of the two. The furnace heats the crude from 250 °C to 350 °C. The crude liquid/vapour mixture leaves the furnace and flows via the transfer line directly into the flash zone of the column.

The column contains 31 trays in all. There are six residue stripping trays in a reduced diameter section in the bottom of the column, and twenty five fractionating and heat exchange trays in the section above the flash zone. There are three pump around streams that are used to control the temperature in the column, and four product streams, the specifications for which are given in Tables 2.2A and 2.2B. Pressure in the column is controlled at 1 barg by a split range pressure controller on the overhead drum, either admitting pressuring gas from the fuel gas system or venting gas to the low pressure fuel gas system.

2.5.3 Residue Stream

Atmospheric residue is stripped with super heated steam (5000 kg h^{-1}) introduced at the base of the tower, and is withdrawn under flow control reset based on the liquid level in the bottom of the column. The stripped residue is then cooled by heat exchange with the incoming crude and the stabilizer feed. After further cooling it is sent to the vacuum distillation unit.

2.5.4 Heavy Gas Oil (HGO) and Bottom Pump Around (BPA)

Heavy gas oil (HGO)is withdrawn from tray twelve of the atmospheric distillation column along with the bottom pump around (BPA) stream. The system is operated under

vacuum, using a two stage steam ejector. The HGO then flows to the HGO stripper and is transferred under level control via the crude heat exchangers to the drier and thence to storage.

The BPA stream flow is controlled on the return temperature to the atmospheric distillation column. The required temperature is achieved by partial by-passing of the crude/BPA exchangers in the preheat train.

2.5.5 Light Gas Oil (LGO) and Middle Pump Around (MPA)

Light gas oil (LGO) and middle pump around (MPA) are withdrawn from tray nineteen. The flow control and processing for LGO is similar to that for HGO. The middle pump around is returned on tray twenty one of the atmospheric crude distillation column, after heat exchange with the crude feed. The flow is controlled on temperature as for the BPA stream, however there is no by-passing of the crude/MPA exchangers; a variable fan air cooler is used to adjust the return temperature.

2.5.6 Top Pump Around and Top Product

Top pump around (TPA) is withdrawn from tray twenty nine. The flow is controlled on the temperature at the top of the column at approximately 180°C by exchanging heat with the crude feed and use of a variable fan air cooler. The top product withdrawn from tray thirty one is cooled by exchanging heat with the crude feed. It is then pumped to the distillate hydrotreater.

2.6 Instrumentation

2.6.1 Instrumentation Available On CDU3 Preheat Train

In order to determine the extent of fouling in a given heat exchanger the flowrate, temperature, and in some cases the pressure, of each of the streams is required. Prior to this project, the extent of fouling was only assessed when there was a requirement to increase refinery throughput or when the outlet temperature from the preheat train

dropped below 240°C. This sporadic monitoring did not require extensive instrumentation, hence the monitoring equipment had to be improved to allow the extent of fouling for each exchanger in the preheat train to be assessed.

From discussions with the refinery personnel it was found that previous fouling problems on CDU 3 had been predominantly on the exchangers after the desalter. Hence it was decided to concentrate the project on the sixteen post desalter exchangers with crude oil on the tubeside (E2104a-E2110d).

2.6.2 Temperature Measurement

Table 2.3 gives the details of the instrumentation available at the start of the project (October 1986). There was no fixed method of measuring the shellside outlet temperatures for any of the exchangers. However there are thermowells in the shellside outlet pipework. Experiments were carried out at the University of Bath (see Appendix D) to ensure that the temperature read by a probe in a thermowell, under the range of conditions observed on the refinery, was representative of the temperature of the fluid inside the pipe.

The initial set of readings (13.11.86) were taken by BP personnel using a rototherm inserted into the thermowells. However the location of the thermowells makes insertion and reading of the rototherm difficult. Also the fragility of the instrument meant that it was unsuitable for such use.

Two hand held Comark digital thermocouples were purchased and calibrated at British Petroleum Research Centre Sunbury. These were used in place of the rototherm. It was decided to utilize the thermowells in the crude stream pipework and to use the thermocouples to measure all the temperatures around each exchanger to reduce any errors that may have been introduced by using different instruments for each of the readings. The thermocouples were kept at the University of Bath and regularly checked against calibrated thermocouples.

To ensure safe working conditions it was decided (26.4.88) to install permanent thermocouples (details in Table 2.4) in the inaccessible thermowells that were wired to a safe terminal, and could be used with the same indicators as the hand held instruments. These permanent thermocouples were periodically checked against the hand held probes.

2.6.3 Flowrate Measurement

Shellside flowrates measured and calculated from energy balances with the first sets of data showed that there were significant errors in the data collected at the refinery see Table 2.5. It was assumed that temperature readings were the more accurate (as the thermocouples had been calibrated and were checked regularly) than shellside measured flowrates. Discussions with the refinery staff revealed that the shellside flow meters had a history of inaccuracy and blockage and were used only as an approximate guide by the operators. The flow meters were of an orifice type, designed flows of 30-80% greater than that measured, and for viscosities upto 300% less than those observed during the project. Hence it was decided to use the shift crude tank dip data to measure the flow of crude oil through CDU3, and to calculate the shellside flowrate assuming the measured temperatures were correct. The crude tank dip was chosen as the standard as it is the measurement used by customs and excise officers to establish the flow of crude oil through the refinery for tax purposes, and hence is checked regularly. Each of the tanks has been previously calibrated so that if the level of fluid in the tank is known then the exact volume of fluid can be calculated. The level in the tank is then checked regularly so that the volume change of crude over a given time period can be determined.

Analysis of the equations used to determine the extent of fouling, (discussed in Chapter 3 Section 3.4), showed that errors in flowrate were less critical than errors in temperature, confirming that it would be potentially less inaccurate to adjust the shellside flowrate to ensure an energy balance than to adjust any of the temperatures.

Table 2.1
Refinery Product Streams
Data supplied by BP Raffinaderij Nederland NV

Design crude	Typical Product streams	Approx API
Throughput 2980 m^3hr^{-1} Kuwait crude API 31.14	Petroleum Auto diesel Marine diesel Benzene Fuel oil Gas oil	75 40-50 40-50 45 25-30 28

Table 2.2A
Crude Distillation Product Streams Temperatures and Flowrates

Stream	Flowrate kg h^{-1}	Flowrate kg h^{-1}	Temp °C	Temp °C	Temp °C	Temp °C
	Design	Range measured	Design	Design	Range measured	Range measured
			in	out	in	out
Crude	581,728	436,296 to 319,950	121	250	129 to 123	252 to 241
TPA[1]	736,365	708,000 to 184,577	208	183	201 to 178	169 to 164
MPA[2]	727,270	720,527 to 188,865	280	188	276 to 253	208 to 194
BPA[3]	545,455	142,567 to 94,011	317	262	350 to 335	292 to 251
LGO[4]	167,430	390,743 to 123,179	263	178	280 to 243	212 to 177
HGO[5]	112,215	560,80 to 11,934	314	204	329 to 310	315 to 165
RES[6]	626,955	645,230 to 31,024	280	219	269 to 217	228 to 205

1 TPA Top Pump Around
2 MPA Middle Pump Around
3 BPA Bottom Pump Around
4 LGO Light Gas Oil
5 HGO Heavy Gas Oil
6 RES Residue

Table 2.2B

Crude Distillation Product Streams Physical Properties

Stream	Specific Gravity		Specific Heat Capacity kJ $kg^{-1}K^{-1}$		Thermal Conductivity W m^{-2} K^{-1}		Viscosity cp	
	Des	(Meas)	Des	(Meas)	Des	(Meas)	Des	(Meas)
Crude	0.870	0.889	2.3	2.48	0.127	0.129	3.19	10.24
		0.837		2.42		0.124		2.85
TPA	0.687	0.803	2.5	2.66	0.131	0.148	0.12	1.57
		0.731		2.53		0.134		0.37
MPA/LGO	0.872	0.870	2.6	2.51	0.133	0.132	1.15	4.18
		0.817		2.41		0.125		1.14
BPA/HGO	0.897	0.893	2.3	2.44	0.117	0.125	4.68	10.98
		0.861		2.38		0.121		3.55
RES	0.937	0.968	2.0	2.33	0.111	0.117	266	290.83
		0.923		2.24		0.111		116.87

Table 2.3

Instrumentation Available

Exchanger	Flowrate measuring instrument		Temperature measuring instrument		
	Tubeside	Shellside	Tubeside		Shellside
			inlet	outlet	outlet
E2104a	F-1012	F-1017	TI-1066	TI-1067	TI-1052
E2104b	F-1013	F-1017	TI-1075	TI-1076	TI-1052
E2105	F-1012	F-1023	TI-1067	TI-1068	TI-1057
E2106	F-1013	F-1024	TI-1076	TI-1077	TI-1059
E2107a	F-1012	F-1018	TI-1068	TI-1069	N/A
E2107b	F-1013	F-1018	TI-1077	TI-1078	N/A
E2108ab	F-1012	F-1002	TI-1069	TI-1071	N/A
E2108cd	F-1013	F-1002	TI-1078	TI-1080	N/A
E2109a	F-1012	F-1018	TI-1071	TI-1072	TI-1053
E2109b	F-1013	F-1018	TI-1080	TI-1081	TI-1053
E2110ab	F-1012	F-1019	TI-1072	TI-1074	TI-1054
E2110cd	F-1013	F-1019	TI-1081	TI-1083	TI-1054

Table 2.4

Thermowells With Permanent Temperature Probes.

Exchanger	Tubeside	Shellside
E2104a	outlet	inlet
E2104b	outlet	inlet
E2105		inlet and outlet
E2106		inlet and outlet
E2107a		inlet
E2107b	inlet	inlet and outlet
E2108ab		inlet
E2108cd		inlet
E2109a		inlet
E2109b		inlet
E2110ab		inlet
E2110cd		inlet

Table 2.5

Energy Balance Data

Shellside flowrates m^3hr^{-1}

Exchanger	13.11.86			30.01.87			04.03.87		
	calc	meas	err	calc	meas	err	calc	meas	err
E2104a	481	293	39	1106	272	75	659	246	63
E2104b	396	293	26	2052	272	87	634	246	61
E2105	234	252	-8	191	229	-20	201	171	15
E2106	36	38	-5	17	15	12	106	29	73
E2107a	486	283	42	385	274	29	213	219	-3
E2107b	235	283	-20	349	274	21	392	219	44
E2108ab	94	142	-51	302	220	27	142	159	-12
E2108cd	52	142	-173	330	220	33	146	159	-9
E2109a	552	283	46	464	274	41	355	219	38
E2109b	480	283	41	431	274	36	325	219	33
E2110ab	148	161	-9	535	157	71	125	105	12
E2110cd	198	161	19	572	157	73	144	105	27

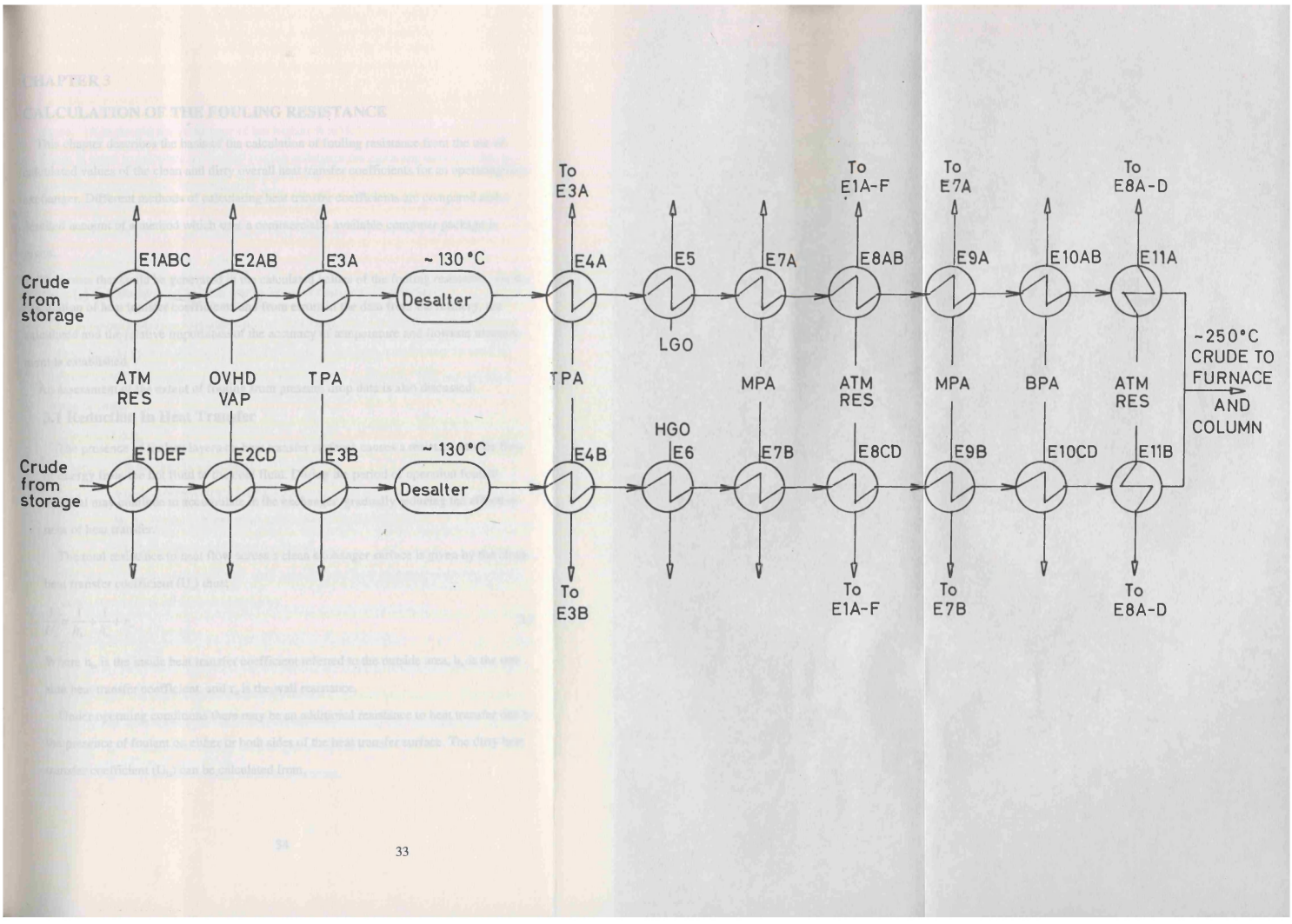
Crude from storage
E1ABC
E2AB
E3A
~ 130 °C
Desalter
E4A
E5
E7A
E8AB
E9A
E10AB
E11A
To E3A
To E1A-F
To E7A
To E8A-D
LGO
ATM RES
OVHD VAP
TPA
TPA
MPA
ATM RES
MPA
BPA
ATM RES
~250°C CRUDE TO FURNACE AND COLUMN
Crude from storage
E1DEF
E2CD
E3B
~ 130 °C
Desalter
E4B
HGO
E6
E7B
E8CD
E9B
E10CD
E11B
To E3B
To E1A-F
To E7B
To E8A-D

CHAPTER 3

CALCULATION OF THE FOULING RESISTANCE

This chapter describes the basis of the calculation of fouling resistance from the use of calculated values of the clean and dirty overall heat transfer coefficients for an operating heat exchanger. Different methods of calculating heat transfer coefficients are compared and a detailed account of a method which uses a commercially available computer package is given.

The errors that could be generated in the calculated values of the fouling resistance, via the calculation of heat transfer coefficients and from errors in the data from the refinery, are calculated and the relative importance of the accuracy of temperature and flowrate measurement is established.

An assessment of the extent of fouling from pressure drop data is also discussed.

3.1 Reduction In Heat Transfer

The presence of foulant layers on heat transfer surfaces causes a resistance to the flow of energy from the hot fluid to the cold fluid. During the period of operation foulant material may continue to accumulate in the exchanger, gradually reducing the effectiveness of heat transfer.

The total resistance to heat flow across a clean exchanger surface is given by the clean heat transfer coefficient (U_c) thus;

$$\frac{1}{U_c}=\frac{1}{h_{io}}+\frac{1}{h_o}+r_w \qquad 3.1$$

Where h_{io} is the inside heat transfer coefficient referred to the outside area, h_o is the outside heat transfer coefficient, and r_w is the wall resistance.

Under operating conditions there may be an additional resistance to heat transfer due to the presence of foulant on either or both sides of the heat transfer surface. The dirty heat transfer coefficient (U_D) can be calculated from,

$$\frac{1}{U_D} = \frac{1}{U_C} + R_f \qquad 3.2$$

where R_f is the thermal resistance of the foulant $Wm^{-2}K^{-1}$

Hence in order to calculate the overall fouling resistance the clean and dirty heat transfer coefficients are required. From equation 3.2,

$$R_f = R_f = \frac{1}{U_D} - \frac{1}{U_c} \qquad 3.3$$

3.1.1 Calculation Of The Dirty Heat Transfer Coefficient

Although fouling is a dynamic process, the fouling rate is usually sufficiently low such that at any time the steady-state rate equation for heat transfer may be used to calculate the instantaneous overall dirty heat transfer coefficient. This may be determined from,

$$Q = U_D A F \Delta T_{lm} \qquad 3.4$$

where Q is the energy transferred,

A is the area available for heat transfer,

Δt_{lm} is the logarithmic mean temperature difference, and

F is the Underwood correction factor.

For even multiple tube pass/single shell pass counter flow exchangers the logarithmic mean temperature difference is given by,

$$\Delta t_{lm} = \frac{(T_1 - t_2) - (T_2 - t_1)}{\ln \frac{(T_1 - t_2)}{(T_2 - t_1)}} \qquad 3.5$$

where T_1 is the hot stream inlet temperature

T_2 is the hot stream outlet temperature

t_1 is the cold stream inlet temperature, and

t_2 is the cold stream outlet temperature.

and the Underwood correction factor,F, is given by,

$$F = \frac{\sqrt{(R^2+1)}\ln\frac{1-S}{(1-RS)}}{(R-1)\ln\frac{2-S\left(R+1-\sqrt{R^2+1}\right)}{2-S\left(R+1+\sqrt{R^2+1}\right)}} \qquad 3.6$$

where

$$R = \frac{T_1 - T_2}{t_2 - t_1} \qquad 3.7a$$

$$S = \frac{t_2 - t_1}{T_1 - t_1} \qquad 3.7b$$

To reduce the propagation of errors from the plant data the energy balance for the cold stream (crude oil) is used, (discussed in Chapter 2)

Hence the energy balance for the cold stream is given by,

$$Q = MC_{pc}\Delta t_c \qquad 3.8$$

Where M is the mass flowrate,

C_{pc} is the cold stream specific heat capacity and

Δt_c is the cold stream temperature difference.

3.1.2 Calculation Of The Clean Heat Transfer Coefficient

The clean heat transfer coefficient is determined from the tube and shellside heat transfer coefficients using equation 3.1 The calculation of heat transfer coefficients has been the subject of much research[1,2,3,4,5,6]. The following sections give details of the available methods for the calculation of heat transfer coefficients.

3.1.2.1 Tubeside Film Heat Transfer Coefficient

Early work[1] on a correlation for the inside heat transfer coefficient of a fluid flowing through a tube was based on heating hydrocarbon oils and water in pipes. This correlation was later developed by Sieder and Tate[2] and is expressed thus for a heating situation:

$$\frac{h_i D}{k} = 0.027(Re)^{0.8}(Pr)^{1/3}\left(\frac{\mu}{\mu_w}\right)^{0.14} \qquad 3.9$$

where Re is the Reynolds number,

Pr is the Prandtl number,

μ is the viscosity.

μ_w is the viscosity of the fluid at the wall,

D is the internal diameter of the tube, and

k is the thermal conductivity of the fluid.

Equation 3.9 was used by Kern[3] for Reynolds numbers above 4000. This correlation, with modifications for such details as tube entrance effects, and free convection enhancement[7], forms the basis of modern computer design and simulation packages. However, as shown in Section 3.1.3, the effects of these modifications are not considered to be significant for the range of Reynolds numbers calculated from the data for the refinery studied in this thesis.

3.1.2.2 Shellside Film Heat Transfer Coefficient

Kern[3] used a correlation of a similar form to that for the tubeside heat transfer coefficient.

$$\frac{h_o D_e}{k} = 0.36(Re)^{0.55}(Pr)^{1/3}\left(\frac{\mu}{\mu_w}\right)^{0.14} \qquad 3.10$$

where D_e is the shellside equivalent diameter.

However this correlation takes no account of the complex flow patterns of the shellside fluid as it traverses the tube bundle. From a concept developed by Tinker[4], Bell[5] formulated a method of calculating the shellside heat transfer coefficient, based on an empirical relationship between the Reynolds number and the tube layout. The method however does not calculate the magnitude of the flow in each of the by-pass streams (illustrated in Figure 3.1) proposed by Tinker. The streams are labelled as,

A - tube to baffle leakage,

B - cross flow stream,

C - bundle to shell by-pass,

D - baffle to shell leakage,

E - tube field partition by-pass,

The method uses a correction factor to modify the heat transfer coefficient. It was not originally tested on commercial size exchangers, the data coming from the following:

(i) experimental results obtained at the University of Delaware,

(ii) Tinker's data on small diameter exchangers,

(iii) a few widely scattered points from industry.

Determination of the shellside heat transfer coefficient using Bell's method requires the solution of many iterative calculations and is limited to situations in which the by-pass flow areas are less than 30% of the minimum cross flow area at the centre of the bundle. The increase in the availability and power of computers in the 1960's led to a reassessment of the streams proposed by Tinker. This work was carried out by organisations such as Heat Transfer Research Incorporated (HTRI) and Heat Transfer and Fluid Flow Service (HTFS). The commercial nature of this work meant that the results were maintained confidential and rarely published in the open literature. A synopsis of the development of the HTRI method is provided by Palen and Taborek[6].

The HTFS method uses the streams proposed by Tinker. In order to calculate the shellside heat transfer coefficient the flow for each of these streams must be determined. The flow rate is given implicitly by the pressure drop.

$$\Delta P = C^1 R\left(\frac{W}{A}\right)^2 \qquad 3.11$$

where R is the resistance to flow defined below,

C is a constant,

W is the flowrate, and

A is the flow area.

On going from the centre of one baffle it is assumed that the stream splits into the previously defined flows and then recombines (see Figure 3.1).

Hence the pressure drop from a given centre of separation to a corresponding point of recombination must be the same for each stream.

$$\Delta P_A = \Delta P_B = \Delta P_C = \Delta P_D = \Delta P_E \qquad 3.12$$

The mass balance is thus

$$W = W_A + W_B + W_C + W_D + W_E \qquad 3.13$$

Hence definition of the relative crossflow areas and the resistance to flow for each streams enables the flow fractions to be calculated.

Determination of the flow resistance coefficients.

Calculation of the flow resistance coefficients R_A to R_E is the crucial part of the "Stream Analysis Method". For the crossflow resistance, R_B, that of an ideal tube bank is used.

$$R_B = 4F_B N\phi \qquad 3.14$$

where f_B is the crossflow friction factor

N is the number of tubes in the cross flow area per baffle space.

ϕ is the viscosity gradient correction factor.

and

The tube-to-baffle and baffle-to-shell leakage resistance coefficients R_A and R_E were correlated from the University of Delaware data on ideal bundles with varying leakage areas.

$$R_{A,E} = k_m + 4f_i\left(\frac{t}{d}\right)\phi \qquad 3.15$$

where t is the baffel thickness,

and d is the bundle to shell clearence.

The parameter k_m accounts for momentum changes on entering and leaving the exchanger and is a function of the flow channel geometry and the Reynolds number. This correlation is stored internally to the commercial computer package as a function of Reynolds number.

The bundle by-pass resistance R_c was correlated mainly from HTFS's data on commercial size bundles with bypass clearances simulating a representative spread typical to industrial applications.

The pass partition resistance R_E was determined from HTFS data on commercial size units.

Determination of the flow fractions

The flow fractions for each of the streams is then calculated using

$$FF_i = \frac{Q_i}{\Sigma Q_i} \qquad 3.15$$

where Q is the ratio of stream flow to hypothetical correct path stream

FF is the flow fraction in stream i

i refers to the stream under consideration ie. A to E.

and

Determination of the Reynolds number.

In order to use the ideal tube bank equation the effective heat transfer Reynolds number must be calculated.

For crossflow

$$Re = \frac{DW}{A_A \mu}\left(C_B(FF_B) + C_A\left(1 - \frac{2N_{tw}}{N}\right)FF_A + C_E(FF_E) + C_D(FF_D) + C_C(FF_C)\right) \qquad 3.16$$

where W is the flowrate

D is the tube diameter

A is the cross-sectional area

C is the effectivness factor refered to crossflow.

and for the window flow

$$Re = \frac{DW}{A_W \mu}\left(C_B(FF_B) + C_A\left(\frac{2N_{TW}}{N}\right)FF_A + C_E(FF_E) + C_D(FF_D) + C_C(FF_C)\right) \qquad 3.17$$

Where C_A to C_E are the effectiveness factors. These were determined empirically from the data available to the HTFS group. It was found that the B stream (crossflow) was the most effective and the D stream which flows along the surface of the shell the least effective.

Due to the complexity of the technique and its reliance on parameters that have been calculated by HTFS but not published in the open literature, the commercial computer package is the only way to calculate the shellside heat transfer coefficient using the Stream Analysis method.

3.1.3 Comparison Of Heat Transfer Calculation Methods

An example heat exchanger on the refinery, see Table 3.1, was used to compare three methods of calculating the heat transfer coefficients. A Fortran program was written to use Kern's method. The commercial package STEP 5 (supplied by HTFS) was used for the Bell and HTFS methods. The results are compared in Table 3.2. The tube and shellside heat transfer coefficients were calculated for a range of Reynolds numbers between 25,000 and 40,000 which were typical of the range encountered in this study on the refinery.

From Table 3.2 and Figure 3.2 it can be seen that there is little difference between the methods for the prediction of the tubeside film heat transfer coefficient, with Kern's

method giving slightly lower values than the Bell's and HTFS's methods. However these differences are well within the 15% accuracy claimed for the calculations.[6,9] This is shown with the error bounds in Figure 3.3.

A summary of the three readily available methods for the calculation of shellside heat transfer coefficient is given in Table 3.3. The results of a comparison between the methods using the data from Table 3.2 are given in Figure 3.4. The high values of the shellside Reynolds number in Kern's method are due to the fact that the other methods allow for the different flow paths and by-passing of the shellside fluid. It can be seen that Kern's method gives shellside heat transfer coefficients that are lower than those from the Bell and HTFS methods, with the error bounds within the claimed accuracy of the predictions (±20% for Kern and ±30% for Bell and HTFS) overlapping. This is shown in Figure 3.5.

3.2 Determination Of Error Propagation In The Calculations

3.2.1 Calculation Of The Fouling Resistance

The error in the calculated value of R_f is dependent upon the errors in the calculated values of the clean and dirty heat transfer coefficients. Random errors in the dirty heat transfer coefficient are indeterminate and result from an inability to,

(i) control the experimental conditions accurately; and

(ii) read instruments accurately and consistently.

The errors in the clean heat transfer coefficient are dependent upon the accuracies of correlations used to calculate the film heat transfer coefficients and the resistance of the tube wall. These are systematic errors which it may be possible to reduce or eliminate by "calibration" of the predictive correlations with well controlled plant and laboratory data. For the function

$$R_f = R_f(U_c, U_d) \qquad 3.18$$

$$dR_f = \frac{dR_f}{dU_c} dU_c + \frac{dR_f}{dU_d} dU_d \qquad 3.19$$

If the errors in U_c and U_d are δU_c and

δU_d respectively, then the error induced in R_f is

given by,

$$\delta R_f = \frac{\delta R_f}{\delta U_c}\delta U_c + \frac{\delta R_f}{\delta U_d}\delta U_d \qquad 3.20$$

The maximum value of δR_f would occur when all the terms on the right hand side are

either positive or negative, i.e. the errors compound rather than eliminate each other.

$$\delta R_f = \left|\frac{\delta R_f}{\delta U_c}\right|\delta U_c + \left|\frac{\delta R_f}{\delta U_d}\right|\delta U_d \qquad 3.21$$

Thus

$$\delta R_f = \frac{\delta U_c}{U_c^2} + \frac{\delta U_d}{U_d^2} \qquad 3.22$$

Equations 3.1 and 3.5 can be treated similarly to determine the error in U_c and U_d respectively. (Details are given in Appendix B).

Using data from the refinery, detailed in Appendix B, and assuming an error in the temperature measurements of $\pm 1^{o}C$ and an error of ±5% in the flow rate, but no error from the correlation for the calculation of the clean heat transfer coefficient, then the maximum error in R_f would be approximately 28%.

The error in the calculated fouling resistance can be shown to be strongly dependent upon the relative temperature difference of each of the streams. (Appendix B) Decreasing the temperature difference on either side of the exchanger would increase the error, with the effect being greatest for crude oil side temperature difference. This could have an effect on the results for those exchangers that can be by-passed, ($E2108_{a-d}$ and E2105), because when the by-passes are open there is only a small change in crude temperature through the exchanger.

The inlet and outlet temperatures of each of the streams as expressed by the parameter W,

$$W = (T_1 - t_2) - (T_2 - t_1)$$

and also has a strong effect on the accuracy of the calculated fouling resistance, see Appendix B. The greater W the less the error. Hence exchangers in which the inlet temperatures approach each other may have greater errors than those exchangers with greater temperature driving forces. This is the case with E2108 $_{A\text{-}D}$. These exchangers have the widest fluctuations in temperature driving force, which is due to varying amounts of energy being removed from the residue stream in the stabilizer reboilers prior to these exchangers.

The parameter W would be lower at start-up when the exchangers are clean and performing well, as the tube side temperatures t_1, and t_2 will be higher then design/ normal operation. This coupled with the inherent difficulties of obtaining reliable data during start-up may cause increased errors in the initial fouling resistances.

3.2.2 Effect Of Errors In Heat Transfer Coefficient Correlations

The clean heat transfer coefficient is calculated via equation 3.1. With the relative error in the clean coefficient, assuming accurate tubewall resistance given by,

$$\frac{\delta U_c}{U_c} = \frac{h_o}{h_{io} + h_o}\frac{\delta h_{io}}{h_{io}} + \frac{h_{io}}{h_{io} + h_o}\frac{\delta h_o}{h_o} \qquad 3.23$$

Using the typical refinery data detailed in Appendix B and assuming flowrate and temperature measurements to be accurate then

$$\frac{\delta U_c}{U_c} = 0.23 \qquad 3.24$$

However for the example refinery data the contribution to the error in the fouling resistance of the error in the clean heat transfer coefficient is approximately a third of that of the dirty heat transfer coefficient. Hence the error in the temperature measurement

would have to be less than 0.5 °C and the flowrate error would have to be less than 1% for the error from the worst scenario in the film heat transfer coefficient correlations to exceed the error from the measured parameters.

3.3 Selection Of Heat Transfer Calculation Method

From the comparison of the three readily available methods of clean heat transfer coefficient calculation it is clear that there would be little difference in the determination of the fouling resistance.

The HTFS method was selected to calculate the overall clean heat transfer coefficient, as it was areadily available, and a recognised method and was accessibleas a commercial computer package" Step 5". This package is similar to those used internally at British Petroluem, and hence would be useful as a check against results calculated at BP. Step 5 gives an easy to interpret print out in a format familiar to the BP staff.

However to expedite the development of simple predictive models it was decided that Kern's method would be suitable. It is easily converted into a short computer programme which requires significantly less computing time and memory and as such the experimental data gathered over long operating periods of upto 18 months can easily be stored and run readily on a personal computer, rather than over night on the main frame, as was the case for the commercial package.

3.4 Using Pressure Drop Data

Generally interest in heat exchanger fouling is focused on the limitations imposed on the heat transfer rate. However the foulant may cause higher pressure drops or reduced flowrates through a heat exchanger. The reduced flowrate situation would result in lower heat transfer coefficients and exacerbate the decrease in heat transfer efficiency. As the fouling deposit develops the area available for flow decreases, so at a constant mass flowrate the velocity of the fluid increases. Relatively modest reductions in flowrate area will give substantial increases in pressure drop, as pressure drop varies as the square of velocity.

$$\Delta p = \frac{fv^2 \rho l}{2d} \qquad 3.25$$

where Δp is the pressure drop,

f is the Fanning friction factor,

ρ is the fluid density

l is the tube length

d is the tube diameter, and

v is the fluid velocity.

The pressure drop will be further increased if the deposit has a rougher surface than the clean tube.

Flow maldistribution between the tubes may increase the pressure drop through the equipment. If the maldistribution exists in the clean condition different rates of fouling will occur in different tubes. This is likely to aggravate the maldistribution, giving rise to excessive velocities in some tubes and low velocities in other tubes. The overall effect would be an increase in pressure drop through the exchanger. This effect was observed in the exchangers under study and is reported in Chapter 4.

The pressure drop through the tubeside of an exchanger can also be used to give an estimate of the thickness of the deposit in the tube. From equation 3.25 it can be seen that the pressure drop is inversely proportional to the tube diameter. After fouling the diameter decreases which would increase the velocity for the same volumetric flowrate. The velocity is proportional to the reciprocal of diameter to the power four. Thus the relationship between pressure drop and diameter can be described by;

$$\frac{\Delta p}{M^2} = \frac{c^1}{d^5} \qquad 3.26$$

Where c' is a proportionality constant and can be determined using the design data for the exchanger. The reduced diameter can then be calculated assuming even flow distribution

tribution and no change in surface roughness.

From pressure drop and flowrate measurements on the preheat exchangers it is possible to estimate the approximate thickness of the foulant from;

$$x = \frac{d - d_1}{2} \qquad 3.27$$

Then from the deposit thickness the fouling resistance can be calculated thus,

$$R_f = \frac{k}{x} \qquad 3.28$$

where k is the thermal conductivity.

However this requires knowledge of the thermal conductivity which is both difficult to measure and estimate for this type of deposit.

Assuming that measurement of thermal conductivity are accurate, a similar error analysis method to that used for the calculation of the fouling resistance from the reduction in heat transfer, yields the result that for a 5% error in the flowrate and a 5% error in each of the pressure measurments the maximum error in the fouling resistance could be 256%. This high potential error is due to the fact that the pressure drop across an exchanger is relatively small (1 bar) hence any error in the measured pressures leads to a large error in the fouling resistance. To reduce such errors the same pressure gauge was used for each of the measurements. However the pressure tapping points were in inaccessible locations and so pressure drop surveys were difficult to make. This combined with the difficulties of thermal conductivity estimation negated the use of the pressure drop method to determine the fouling resistance. Nevertheless historically pressure drop limitation is the main factor that has caused CDU3 to be shut down for cleaning. Approximately ten years ago (1980) there were permanent pressure transducers on each of the exchangers in the preheat train. However it was found that they were not robust enough for conditions on the refinery and excessive maintenance costs resulted in them

being removed. During the project two sets of individual pressure drop measurements have been taken for each of the post-desalter exchangers, the results are given in Chapter 5.

Table 3.1 Typical heat exchanger details (E2107a)

Heat Exchanger Details		
Number of tubes	1640	
Number of tube passes	4	
Number of baffles	20	
Baffle spacing	0.3	m
Tube inside diameter	0.01283	m
Tube outside diameter	0.01588	m
Shellside diameter	1.27	m
Tubes square pitch	0.0254	m
Process fluid details		
Tubeside		
Viscosity	$4.5x10^{-4}$	N s m^{-2}
Thermal conductivity	0.138	W m^{-1} K^{-1}
Specific heat capacity	2.085	kJ kg^{-1} K^{-1}
Density	832	kg m^{-3}
Shellside		
Viscosity	$3.3x10^{-4}$	N s m^{-2}
Thermal conductivity	0.131	W m^{-1} K^{-1}
Specific heat capacity	1.742	kJ kg^{-1} K^{-1}
Density	867	kg m^{-3}

Table 3.2 Comparison of heat transfer coefficient calculation methods.

Tube flow kg h^{-1}	305550	355550	385550	405549	455549
Shell flow kg h^{-1}	223270	259805	281727	296341	332877
HTFS					
Re tube	26407	30729	33321	35050	39370
Re shell	12454	14493	15716	16532	18571
h_i Wm^{-2} K^{-1}	1488	1681	1794	1868	2044
h_o Wm^{-2} K^{-1}	1703	1886	1993	2061	2232
U_c Wm^{-2} K^{-1}	772	857	909	943	1028
BELL					
Re tube	26407	30729	33321	35050	39370
Re shell	20327	23653	25649	26979	23653
h_i Wm^{-2} K^{-1}	1488	1681	1794	1868	2044
h_o Wm^{-2} K^{-1}	1647	1823	1925	1993	2158
U_c Wm^{-2} K^{-1}	761	846	897	931	1011
KERN					
Re tube	26348	30659	33246	34971	39282
Re shell	55979	65139	70635	74299	83459
h_i Wm^{-2} K^{-1}	1471	1658	1772	1845	2027
h_o Wm^{-2} K^{-1}	1221	1329	1386	1425	1522
U_c wm^{-2} K^{-1}	664	738	789	806	886

Table 3.3 Shellside heat transfer calculation methods.

Method	Reynolds No range	Shellside flow pattern	Claimed accuracy
Kern	10,000+	No leakage	±20% [3]
Bell	1-40,000	By-pass streams	±30% [5]
HTFS	1-100,000	By-pas streams	±30% [6]

Figure 3.1 Overall Heat Transfer Coefficients

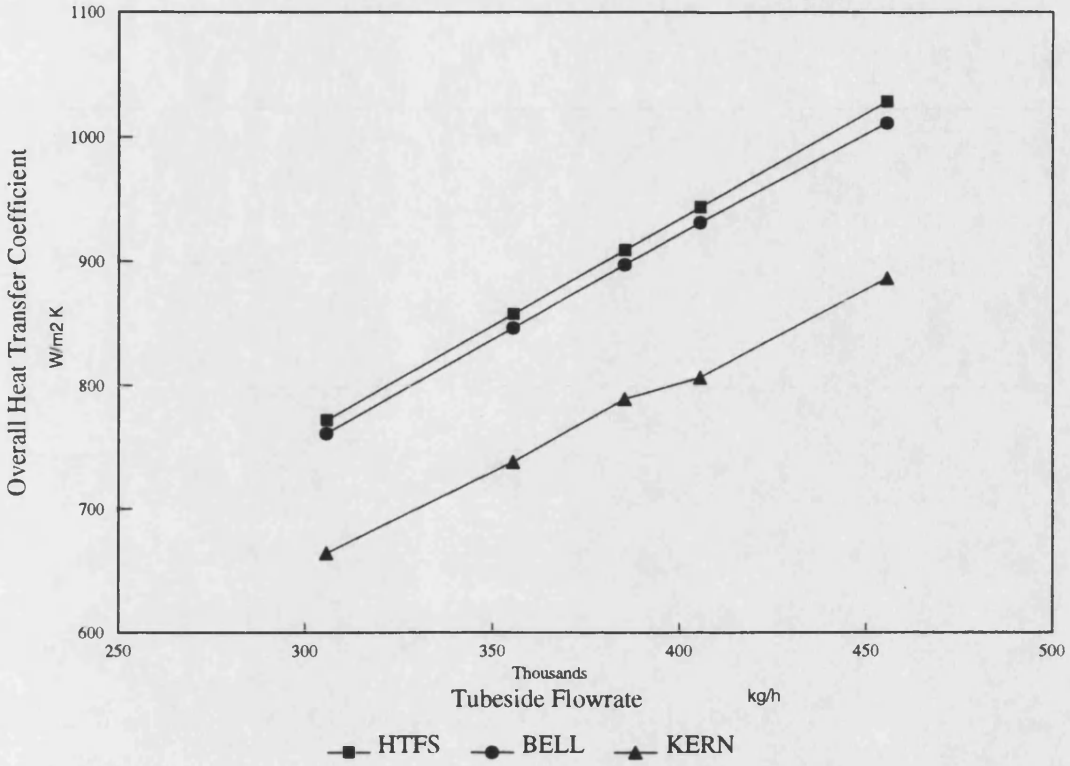

Figure 3.2 Tubeside Heat Transfer Coefficient

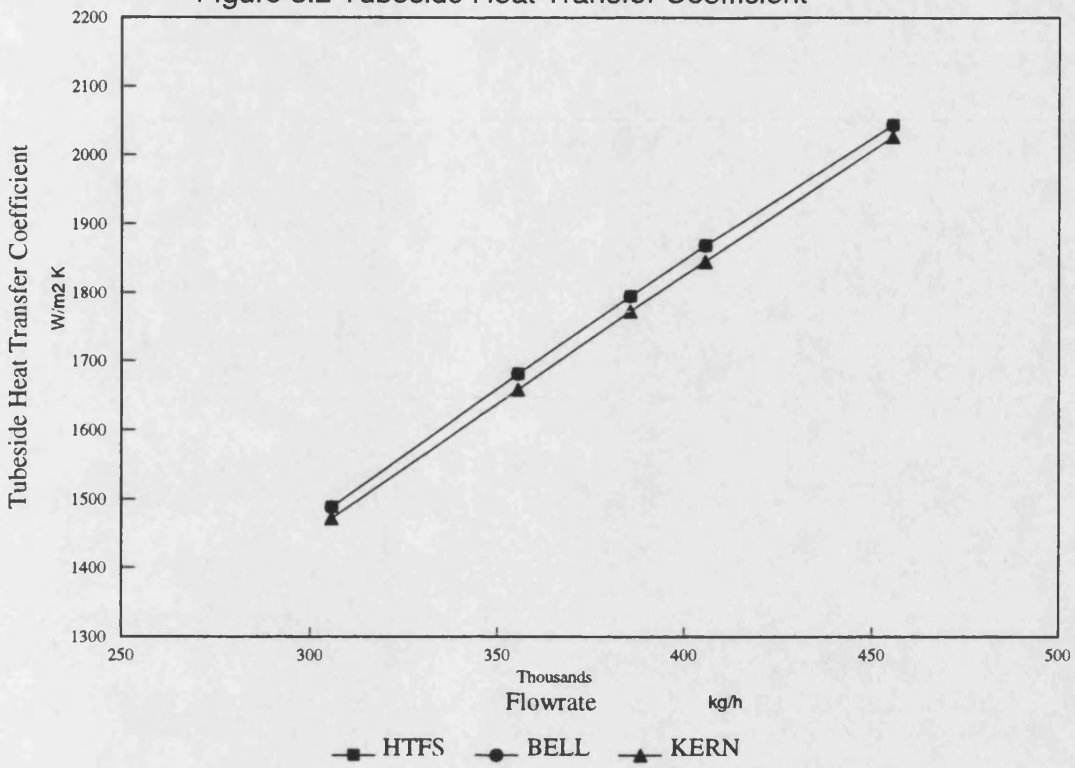

Figure 3.3 Tubeside Error Bound

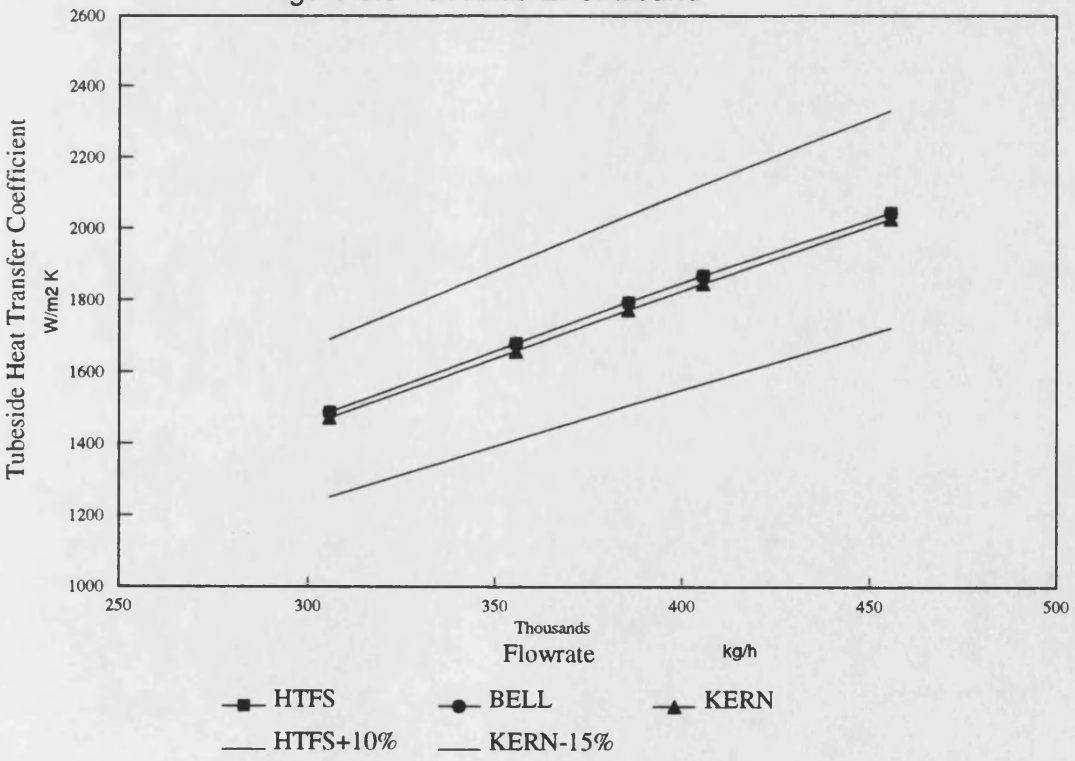

Figure 3.4 Shellside Heat Transfer Coefficient

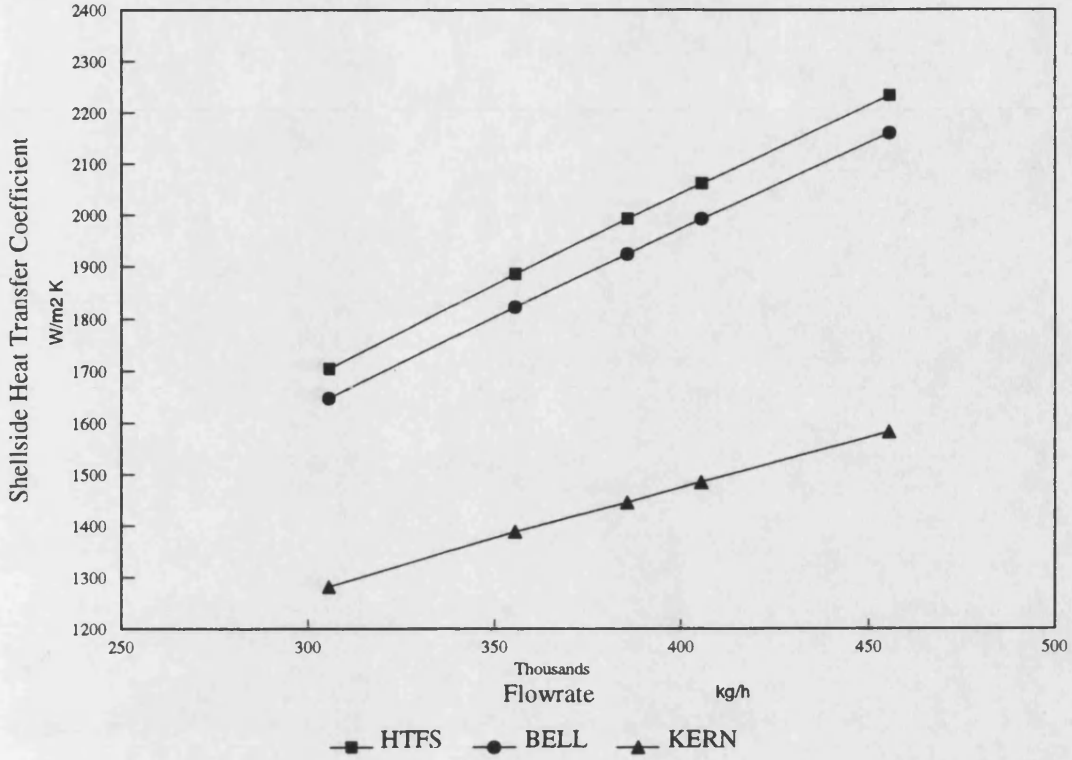

Figure 3.5 Shellside Error Bound

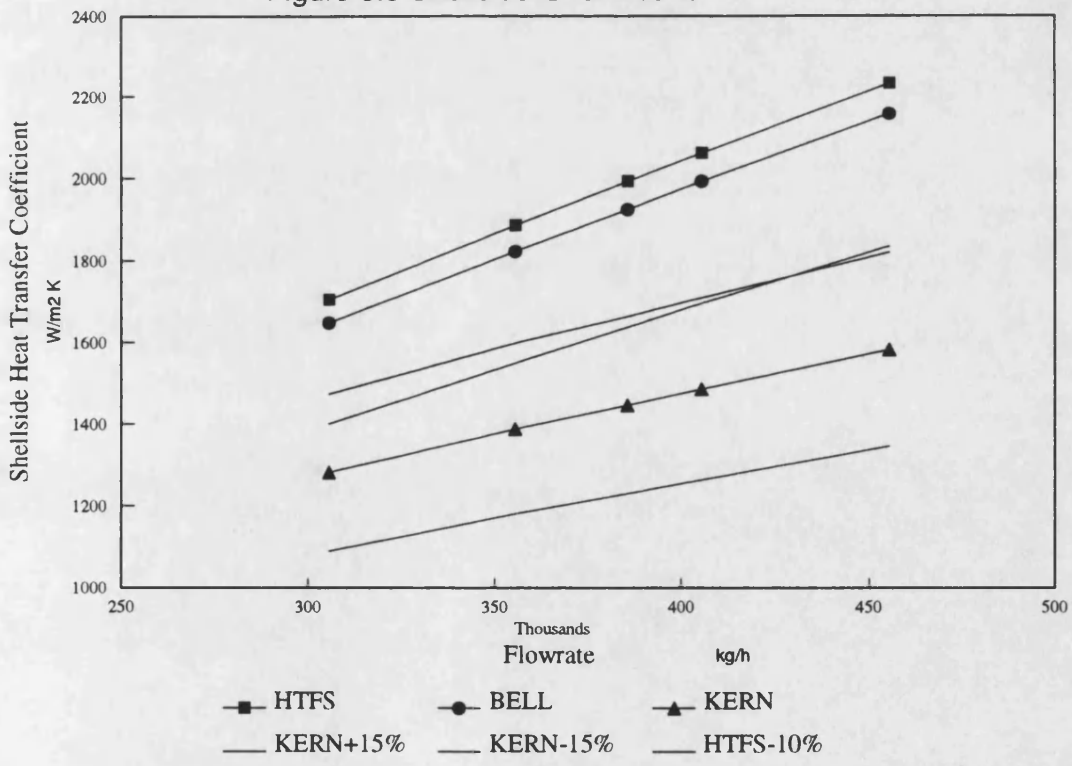

3.6 REFERENCES

(1) Morris and Whitman (1928) " Heat transfer for oils and water in pipes"
Ind Eng Chem Vol 20 P 234.

(2) Sieder and Tate (1936) "Heat transfer and pressure drop of liquids in tubes "
Ind Eng Chem Vol 28 pp 1429 - 1436.

(3) Kern D.Q (1950) "Process heat transfer"
Pub McGraw-Hill
New York.

(4)Tinker (1958) "General discussion on heat transfer"
Trans ASME Vol 80 pp 36 - 52.

(5) "Exchanger design based on the Delaware Bell research program"
1960 Petro and Chem Eng Vol 32 pp c26 - c40.

(6) Palen and Taborek (1969) "Solution of shellside flow pressure drop and heat transfer by the Stream Analysis method"
Chem Eng Prog Sym Ser No 92 Vol 65 pp 53 - 63.

Chapter 4

4 CHRONOLOGY OF EVENTS ON CDU3

This chapter presents the chronological order of events on the refinery during the research project. Details of the procedures followed at start-up, shut down and cleaning are discussed. The unit was operational before the start of the research project and the initial data (13.11.86) was provided by BP.

Two separate operating cycles of 499 and 295 days on stream were studied. The temperatures, flowrates and compositions of each of the streams in the preheat train were measured at approximately monthly intervals during each of the operating cycles. Each visit to the refinery lasted approximately a day, with the readings taken after a period of steady operation.

It was not possible to control the run length or conditions on the preheat train as the running of the refinery was dictated by commercial and/or operating decisions.

4.1 Operating Cycle 1

Date	Day No	Event	Comment
15.10.86	1	Start-up	Standard procedure followed
13.11.86	29	Data collection.	By BP personnel using rototherm.
30.01.87	107	Data collection.	Using rototherm.
4.03.87	139	Data collection.	Using rototherm.
14.03.87	149	Shutdown.	Standard procedure followed. High crude oil price low profit margin. Exchangers are flushed but not cleaned.
10.04.87	176	Start-up	Standard procedure followed
28.04.87	195	Data collection.	First use of hand held thermocouples. Refer to chapter 2 section
24.05.87	221	Shutdown	Standard procedure followed. High crude oil price low profit margin. Exchangers are flushed but not cleaned.
23.06.87	251	Start-up	Standard procedure followed
3.07.87	261	Data collection	Have been on low throughput 65% design, due to problems on the DHT. Flowrate will now be increased to 75% design.
14.08.87	303	Data collection	Hand held thermocouples used.
27.08.87	316	Data collection	Hand held thermocouples used. Checks on local short term temperature changes.
8.10.87	358	Data collection	Hand held thermocouples used.
09.11.87	390	Slops in feed	Slops sg=0.804
19.11.87	400	Data collection	Hand held thermocouples used.

Date	Day No	Event	Comment
3.12.87	414	Data collection Slops with feed. Pressure drop survey.	Hand held thermocouples used. Slops sg =0.8038.
10.12.87	421	Heavy crude	72% Merey in feed API=17.5
15.12.87	426	Tank Stratified	Tank 6 top sg=0.8968 mid sg=0.8992 bot sg=0.9063
17.12.87	428	Tank Stratified	Tank 2 top sg=0.8535 mid sg=0.8551 bot sg=0.8618
27.12.87	438	Minimum throughput	Throughput at 55% design low profit margin.
6.01.88	448	Throughput increased	Throughput at 65% design.
7.01.88	449	Data collection. Pressure drop survey.	Hand held thermocouples used.
10.2.88	483	Data collection.	Hand held thermocouple used.
25.02.88	499	Data collection.	Hand held thermocouples used.
27.02.88	501	Shutdown.	Standard procedure followed. Bundles were removed and both shell and tube sides cleaned. Samples were taken for analysis. Details given in Chapter 5
2.03.88 to 16.03.88		Shut-down. Cleaning of exchangers	
15.04.88		Permanent probes installed	These were checked against the hand held instruments.

4.2 Operating Cycle 2

Date	Day No	Event	Comment
18.04.88	1	Start-up.	Standard procedure followed
19.04.88	2	Data collection.	Hand held thermocouples used with permanent temperature probes. Cross checks carried out. Leaking problems on 7a & 9a steam lances used on the gaskets.
27.04.88	10	Data collection	Hand held thermocouples used with permanent temperature probes. Leakage on 6 caused it to be by-passed on the shellside and repaired.
17.05.88	30	Data collection.	Hand held thermocouples used with permanent temperature probes. Evidence of leakage around the majority of exchangers, due to low crude flowrate in preparation for DHT start-up.
14.06.88	58	Data collection.	Hand held thermocouples used with permanent temperature probes. Cross checks carried out.
9.08.88	114	Data collection.	Hand held thermocouples used with permanent temperature probes. Prior to these readings 13 days of minimum 55% design flow.
6.09.88	142	Data collection.	Hand held thermocouples used with permanent temperature probes. Further 20 days of minimum flow after last set of readings.
12.10.88	178	Data collection.	Hand held thermocouples used with permanent temperature probes. Cross checks carried out. Detail in appendix 1 section
17.10.88	183	A Train shutdown	Low profit margins allow A train to be shutdown and cleaned, whilst B train is operating.
20.10.88	186	Data collection.	Hand held thermocouples used with permanent temperature probes. B train only in operation. All flow shell and tube through B train.
3.11.88	210	Data collection.	Hand held thermocouples used with permanent temperature probes. Sudden change in crude price forced maximum throughput. Plan to clean B train abandoned.
14.12.88	251	Data collection.	Hand held thermocouples used with permanent temperature probes. Following last readings 8 days of maximum 80% design throughput. Crude price changed have run at minimum throughput 55% design for 6 days.
27.01.89	295	Shutdown	Standard procedure followed Exchangers cleaned insitu

4.3 Standard Start-up Procedure

This consisted of the following steps:

(i) Steam out the exchangers using low pressure steam.

(ii) Ensure the unit has been pressure tested, that it is free from leakages and that the O_2 content < 1%.

(iii) Start pumping crude at the minimum loading of one crude pump (75 m^3hr^{-1}). Use this pump to fill the system. As soon as there is crude at the bottom of the atmospheric distillation column start one of the residue pumps to produce circulation. Then steadily increase the feed rate to 650 m^3hr^{-1}.

(iv) Start the crude furnace raising the temperature by 20°C hr^{-1}. Then maintain a temperature of 120°C for two hours.

(v) Raise outlet temperature of crude furnace to 150°C and maintain this temperature for two hours. Then increase the temperature to 170°C and hold for two hours. Then raise the temperature by 20°C hr^{-1} to 220°C and hold for two hours. During this drying out period the pump around streams should be started on recycle, through the preheat train.

(vi) Adjust the flash zone temperature of the crude column to the required temperature (360°C).

(vii) Once the crude column is operating at normal temperatures and pressures, the product streams can be initiated and the DHT unit started.

4.4 Standard Shutdown Procedure

This consisted of the following steps:

(i) Reduce the unit throughput to 50% design flow, shutdown the desalters and reduce the furnace outlet temperature at a rate of 25°C hr^{-1} to 250°C.

(ii) Route the product streams to slops, keeping the pump-around pumps and the air coolers operating to reduce the column temperature.

(iii) Reduce the furnace outlet temperature by 30°C hr^{-1} to 150°C then shutdown the

furnace.

(iv) When no overheads are produced stop the cold crude charge pumps.

(v) When crude column base temperature is 200-250°C shut off the block valves after the preheat train. Use the 'warm' crude charge pumps to pump out the exchangers to slops.

(vi) Pump out the desalters to slops.

(vii) Flush with light cycle oil and the steam out prior to opening.

4.5 Standard Remote Cleaning

During the March 1988 turn around both the shell and tube side of the exchangers were cleaned. The bundles were removed from the shells using a bundle puller. They were the transferred on the bundle puller to the remote cleaning area. Water at 600 barg was used to clean the tubes inside and out. There were five cleaning prongs for the tube side and four for the shellside. The cleanliness of the tubes is checked using a scraping device, and if necessary the exchanger is cleaned again. The shellside cleanliness is visually inspected. The bundles are then left to dry in the open atmosphere during which time a thin layer of iron oxide formed on the surface of the tubes.

4.6 *In-situ* Cleaning

The end covers are removed but the floating heads are left in place. Manually operated flexible water lances are used with a design pressure of 500 barg. However an operating pressure of 300 barg is often used. *In-situ* cleaning does not allow the shellside to be cleaned. Also there can be problems with debris collecting in the floating head since this may not be flushed out through the lower passes. Usually the tubes are tested for cleanliness using a scraper device or an endoscope.

4.7 Conclusions

i) The sequence of operational changes on the preheat train will have an effect on the fouling resistances/deposits observed during the project. For example the inclusion of slops in the feed stream (18.11.87 and 3.12.87) may lead to increased fouling, especially

if the slops contain oxygen or sulphur as these could act as free radical autoxidation precursors. The type of crude processed could also have an effect on the extent of fouling. It is generally thought that the higher the asphaltene content the more deleterious the crude.

ii) Changes in throughput would also have an effect on fouling with the widely accepted view being that of increasing fouling rate with decreasing flowrate. These effects were further investigated in Chapter 5, in which the results of the fouling study were presented and in Chapter 6, in which predictive models are developed.

iii) The standard procedure for the shutdown of the exchangers involves flushing with hydrocarbon and water, before opening to the atmosphere. This process will have an effect on the fouling deposits. Some of the deposit may dissolve in the hydrocarbon, or be dislodged by the water stream. Hence the fouling deposits observed may not be fully representative of the foulant that was present at the end of the operating period.

iv) On start-up of the exchangers the desalter may not be operating at the optimum temperature and there may be some carry over of salt to the downstream exchangers. There is also initially a low flowrate through the exchangers which may cause fouling. However, the transient nature of the start-up makes the fouling at that stage difficult to determine. Fouling resistance at start-up are further discussed in Chapter 6.

Chapter 5

5 RESULTS

5.1 General discussion

This chapter contains the results of the fouling resistance calculations for each of those exchangers down stream of the desalters with crude oil on the tube side, in both the A and B preheat trains of CDU3 at BP's Rotterdam refinery. The fouling resistances were calculated using the commercial computer package STEP 5 as described in Chapter 3.

The data are presented in the form of fouling resistance against time graphs, starting with the exchangers which have the lowest crude oil temperature. A full listing of the clean and dirty heat transfer coefficients and the fouling resistances are given in Appendix C.

During the project two distinct operating cycles were monitored and a major shutdown for cleaning was observed. The general extent of the fouling is shown in Plates 5.1 and 5.2 which show the same set of tubes before and after cleaning. The individual results are presented for each exchanger. The observations during the cleaning of the exchangers are included in the discussion pertaining to each exchanger. During the shutdown the geometric details such as the number of baffles, the baffle spacing and the tube and shell diameters were checked against the design data, and were found to be correct.

A sampling device consisting of a long shaft with a scrapping device was used to remove samples of deposits from several of the tubes. These samples were then analysed to determine the composition of the deposits. However it should be noted that prior to the opening of the exchangers there was a washing out procedure as detailed in Chapter 4.

Two sets of pressure drop data were taken during the first operating cycle. From this pressure drop data the deposit thicknesses were estimated. During the major shutdown, but before the exchangers were cleaned the deposit thicknesses were measured.

Pate 5.1 BEFORE CLEANING

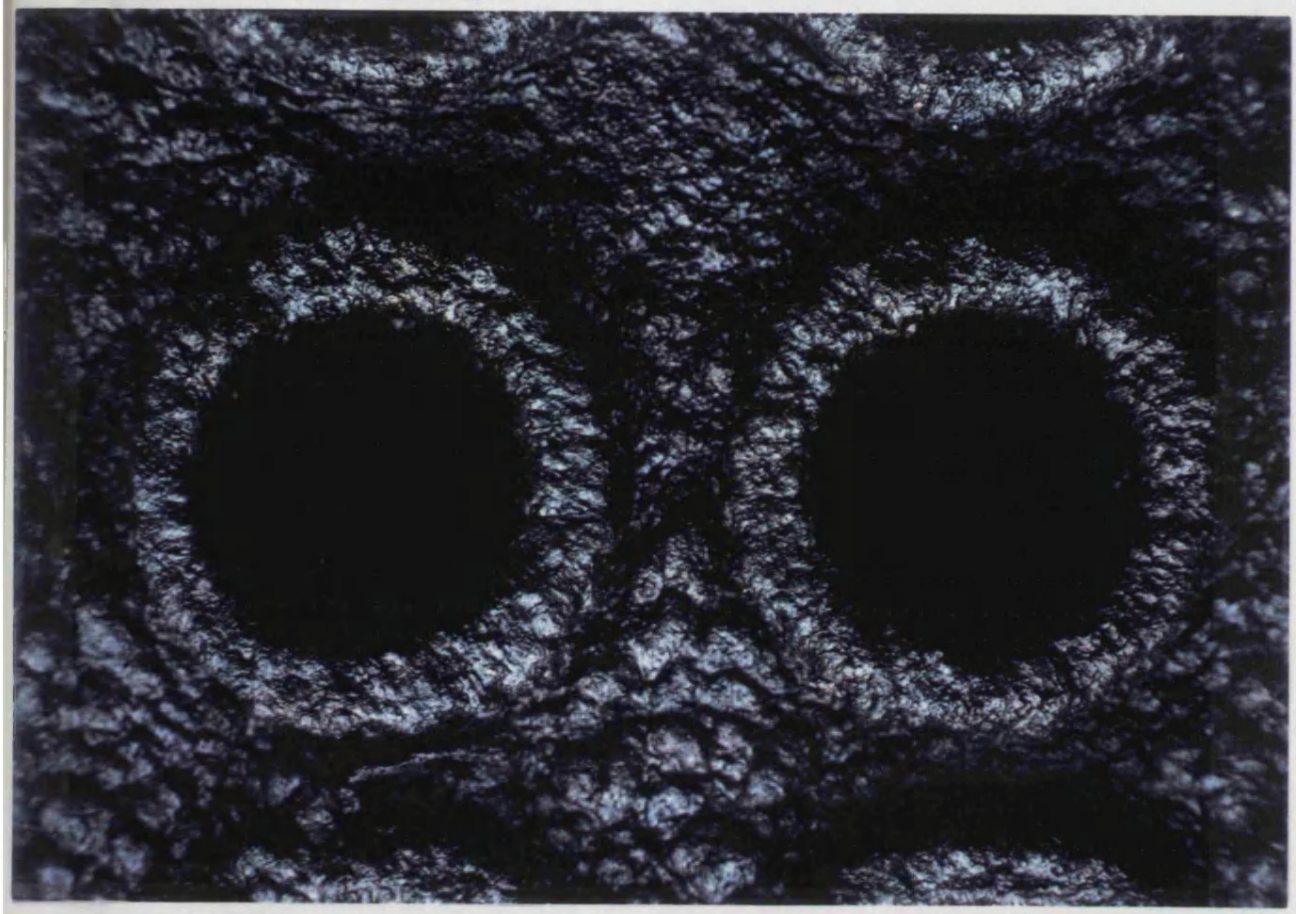

Plae 5.2 AFTER CLEANING

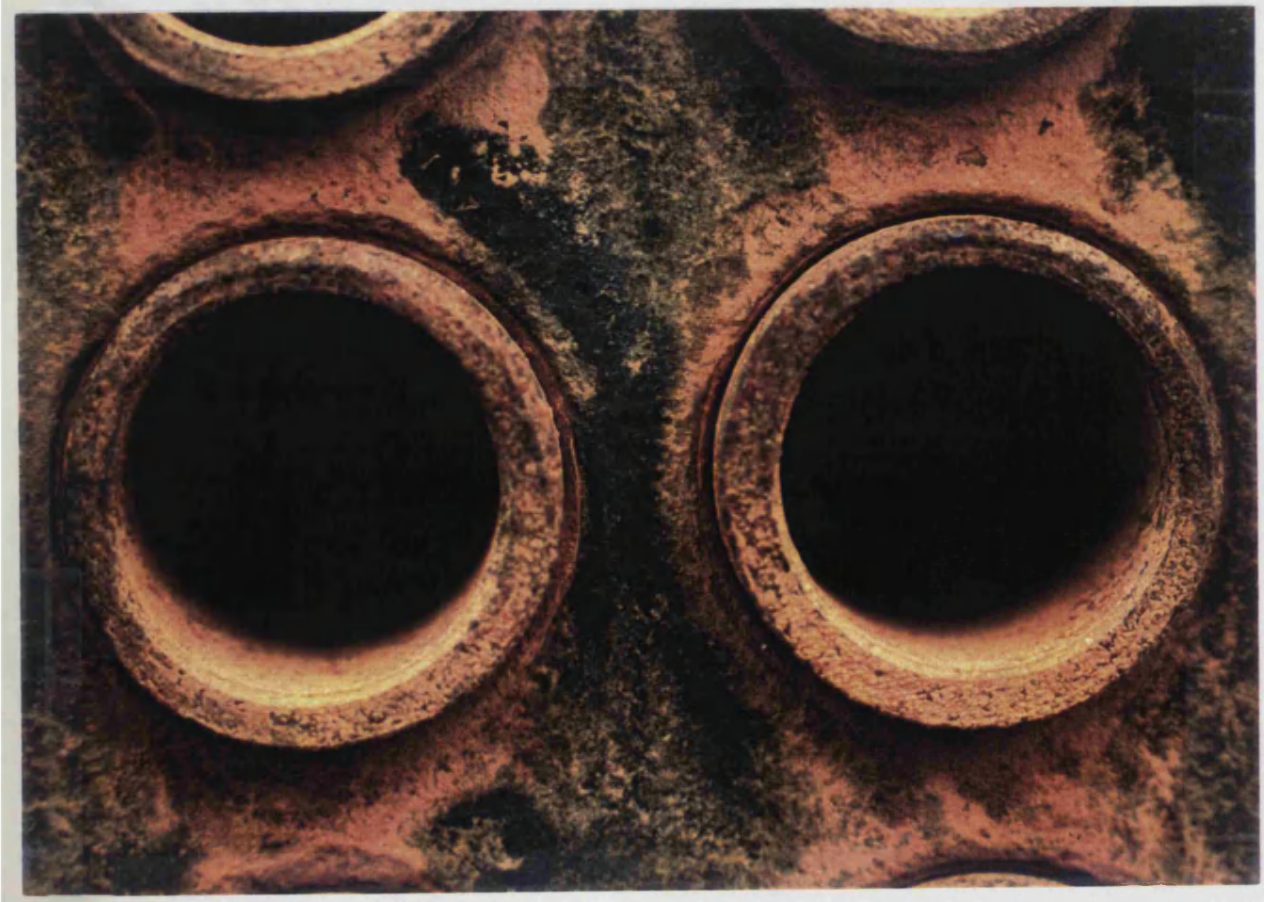

5.1.1 E2104a and E2104b

The E2104a and E2104b exchangers have two passes on the tubeside. The shellside is single pass with top pump around as the heating medium. During the study the velocity of the crude oil in the tubes ranged from 1.42 to 3.44 ms^{-1} and the tubewall temperature ranged from 153 to 182 °C.

The fouling resistances of E2104a and E2104b (Figures 5.1(a-c) and 5.2(a-C)) increase gradually with time but appear low when compared to the other exchangers in the train. This is probably due to the relatively low temperatures in these exchangers. Lawler[1], using data from a Gulf refinery preheat train, also found that there was relatively little fouling in the first exchangers following a desalter, or in exchangers where the bulk tubeside temperature was below 170-200°C.

The fouling resistance for E2104a remains almost constant during the study period. There is a modest increase in fouling resistance after the introduction of heavy crudes on day 324. The trend of increasing fouling resistance with heavy crudes is much more apparent in the E2104b exchanger, with a peak four fold increase in the fouling resistance after the heavy crude and slops were processed.

There is no obvious reason for the difference between the fouling resistances of the two exchangers as the velocities and temperatures were approximately the same over this period as can be seen from Figures 5.1b,c and 5.2b,c. One might speculate that the distribution of the fouling within the exchangers is different and that some of the tubes or a proportion of the return headers may be blocked in the E2104b exchanger. This would cause uneven flow distribution between the tubes in the exchanger and could exacerbate the fouling in those tubes which are partially blocked. (See Chapter 3). Unfortunately it was not possible to observe the opening of the E2104 exchangers, so the actuality of deposits in the header or uneven distribution of fouling between tubes could not be confirmed.

There was a period of minimum throughput between days 414 and 449 but this reduced velocity appears to have had little effect on the fouling resistance of E2104a, with the fouling resistance of E2104b dropping slightly. This may be due to the fact that the temperatures in these exchangers are relatively low compared with other exchangers in the train. Hence although reduced turbulence would have resulted in higher tubewall temperatures, the temperature probably would still not have been high enough for fouling to proceed rapidly.

When the tubeside velocity is increased there is little if any effect on the fouling resistance. This is probably due to the fact that there is only a small amount of fouling present and the effect of removal by shearing would not be as obvious as for exchangers that are heavily fouled.

On start-up of the exchangers after cleaning the E2104 exchangers showed an almost constant fouling resistance until the E2104a exchanger was shutdown for cleaning on day 753. Whilst the A train was being cleaned the B train was operating at maximum throughput. The increased velocity on both the shell and tubeside resulted in a reduction of fouling resistance, which then increased as the flowrates were reduced.

Figure 5.1(a)

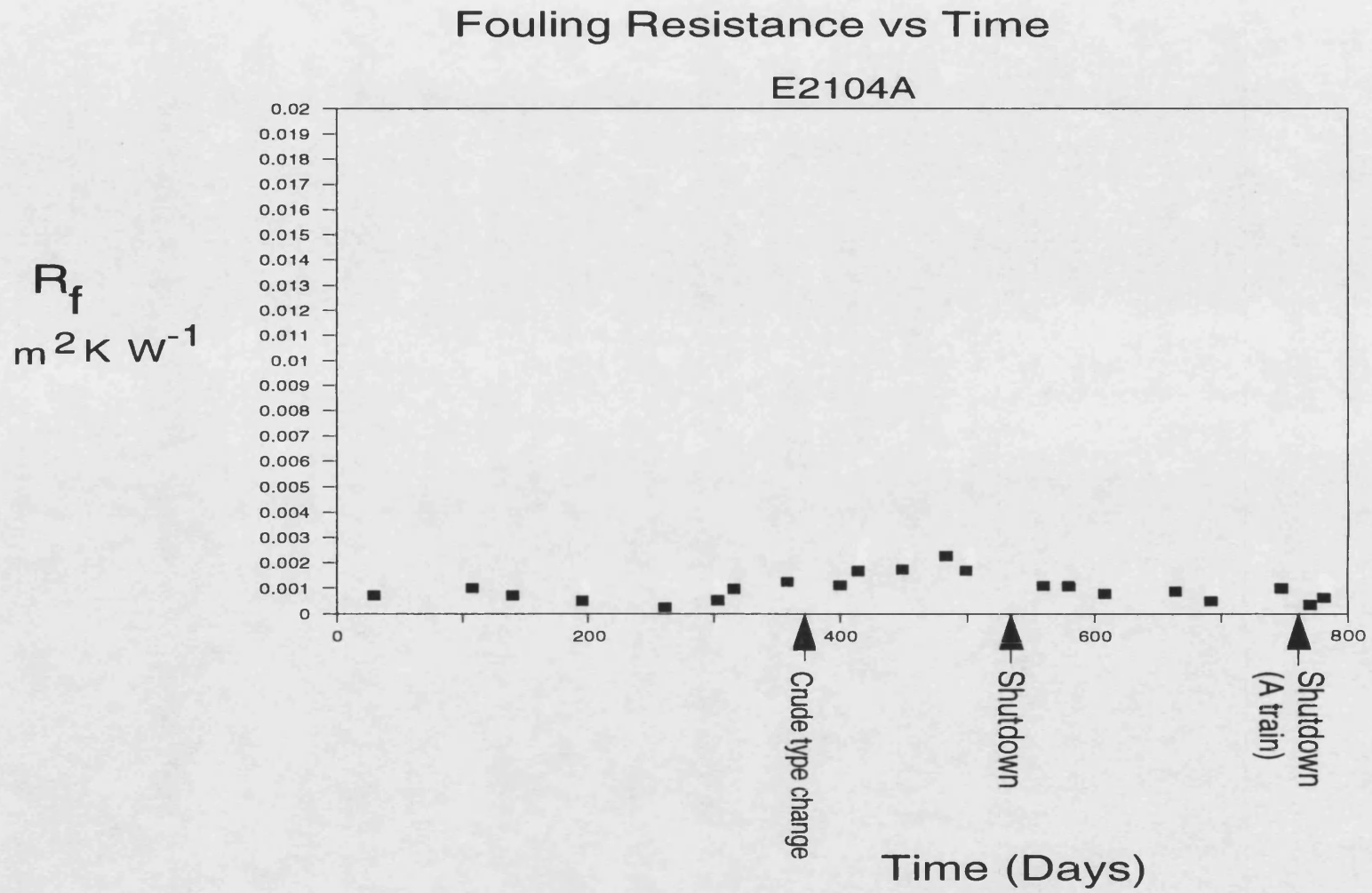
Fouling Resistance vs Time
E2104A
R_f
$m^2K\ W^{-1}$
0.02
0.019
0.018
0.017
0.016
0.015
0.014
0.013
0.012
0.011
0.01
0.009
0.008
0.007
0.006
0.005
0.004
0.003
0.002
0.001
0
0
200
400
600
800
Crude type change
Shutdown
Shutdown (A train)
Time (Days)

Figure 5.1(b)

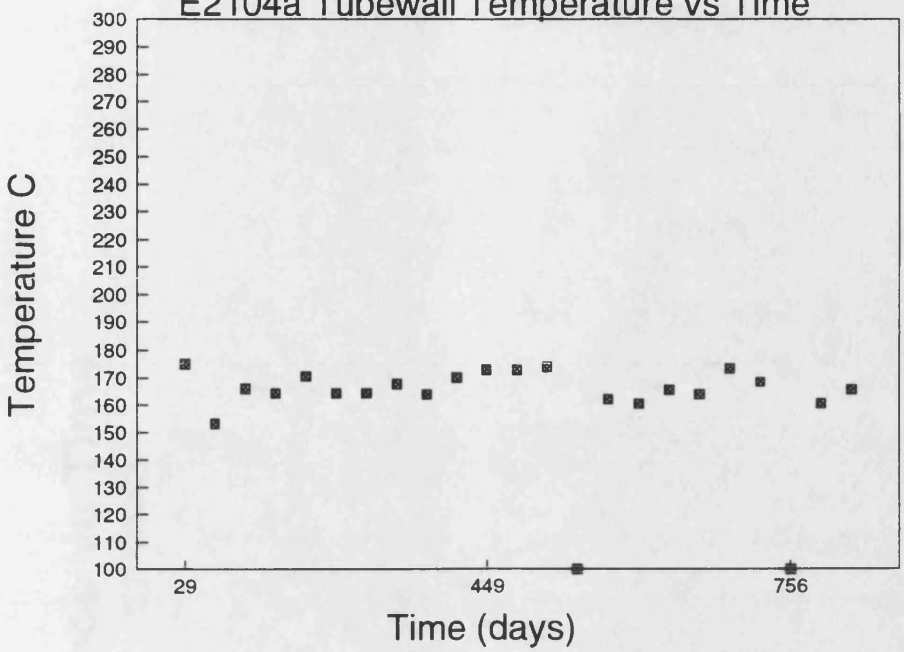

Figure 5.1(c)

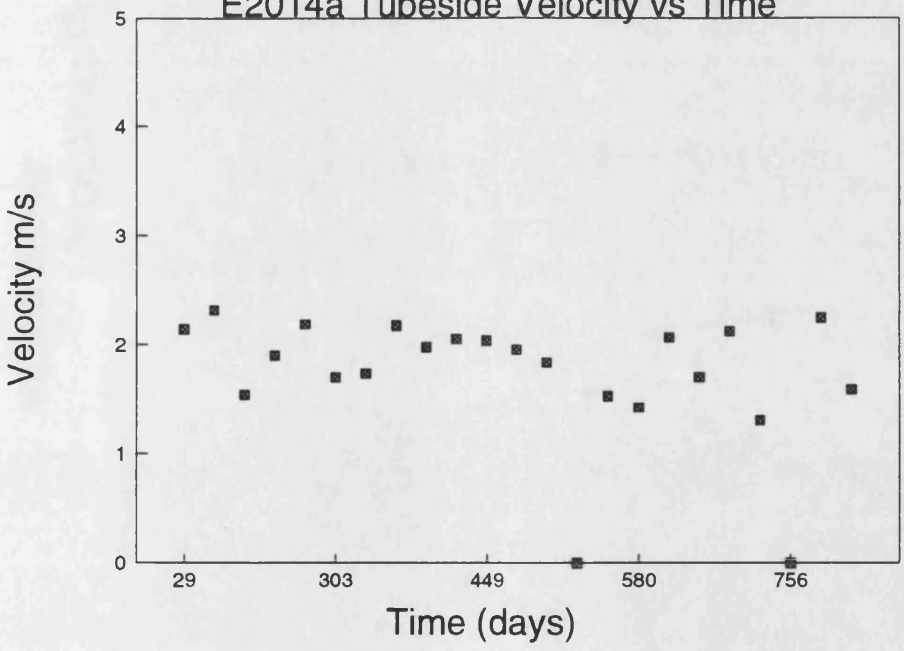

Figure 5.2(a)

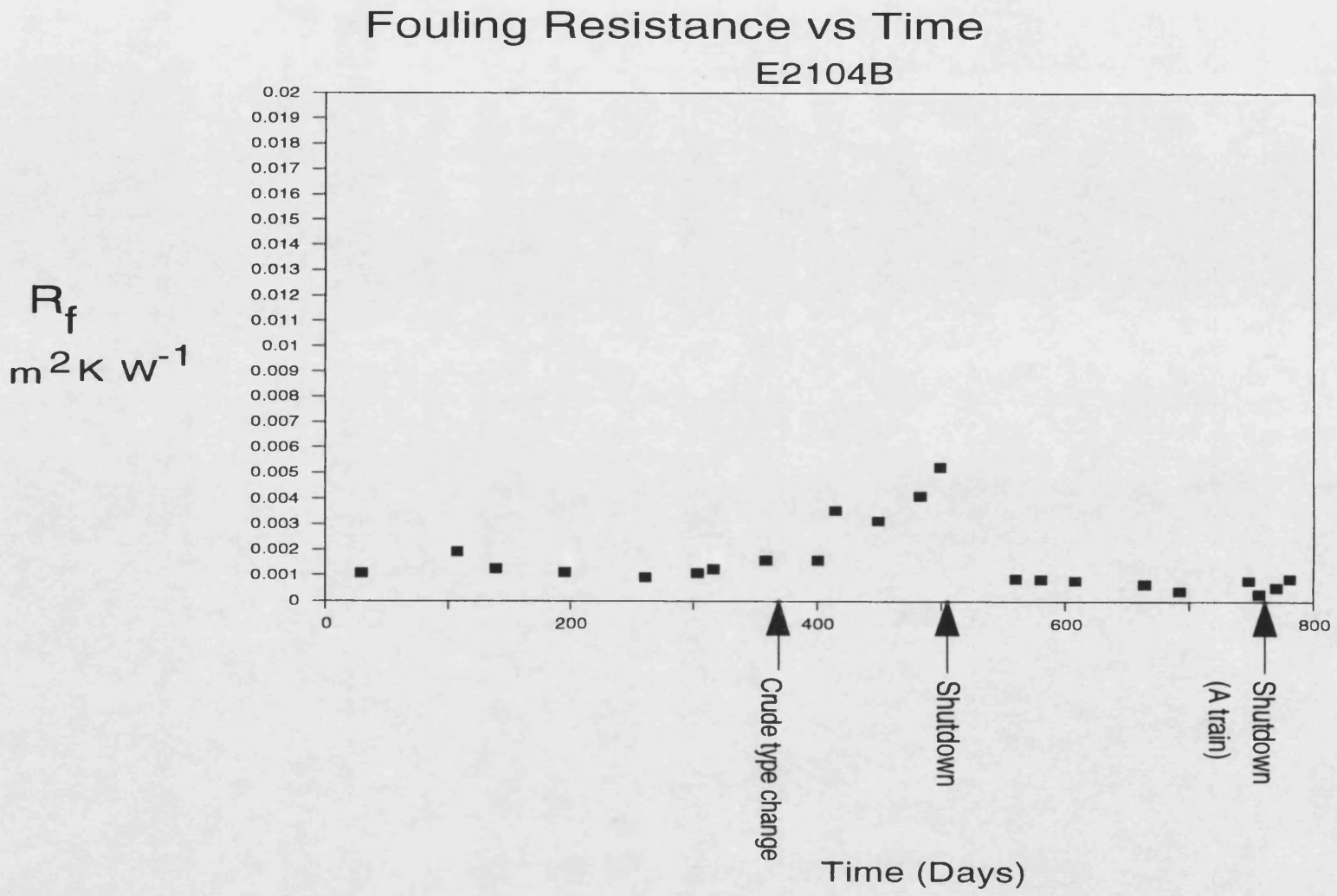
Fouling Resistance vs Time
E2104B
R_f
$m^2K\ W^{-1}$
0.02
0.019
0.018
0.017
0.016
0.015
0.014
0.013
0.012
0.011
0.01
0.009
0.008
0.007
0.006
0.005
0.004
0.003
0.002
0.001
0
0
200
400
600
800
Crude type change
Shutdown
Shutdown
(A train)
Time (Days)

Figure 5.2(b)

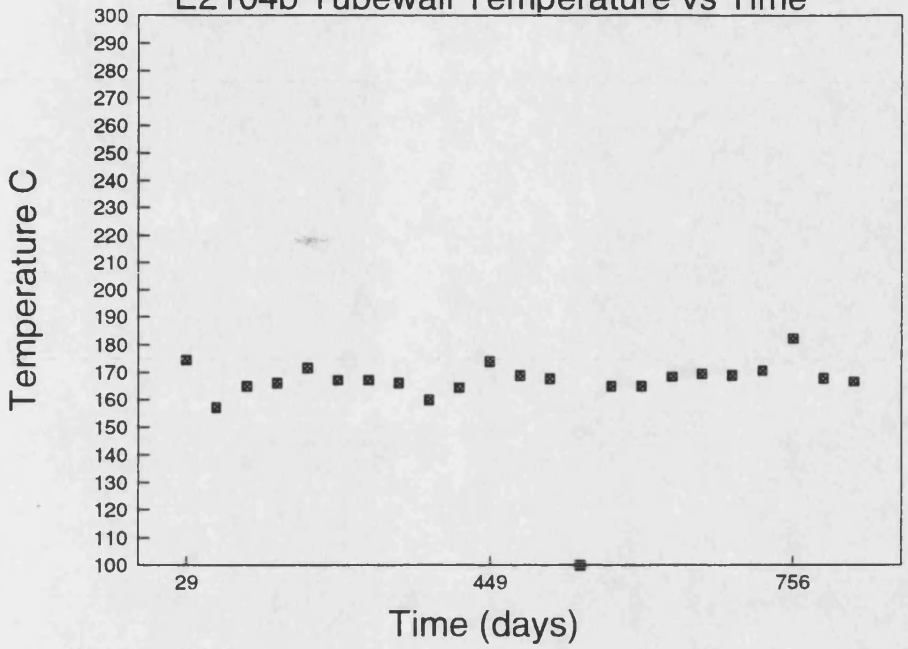

Figure 5.2(c)

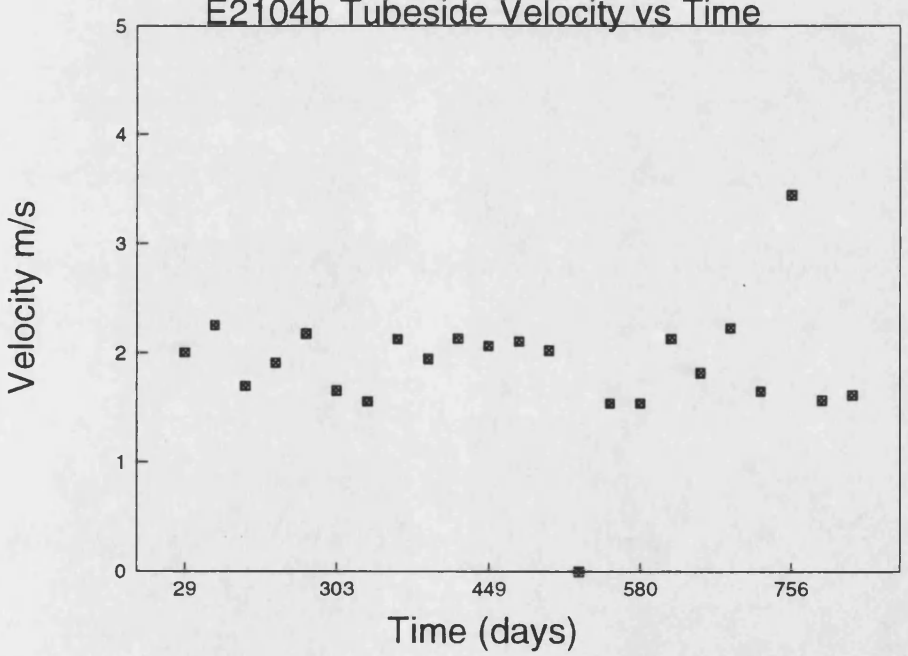

5.1.2 E2105

The E2105 exchanger has two passes on the tubeside. The shellside has a single pass with light gas oil as the heating medium. During the study the velocity of the crude oil on the tubeside ranged from 0.82 to 1.2 ms^{-1} (see Figure 5.3c) and the tubewall temperature ranged from 169 to 226 °C (see Figure 5.3b).

The fouling resistance against time graph for the E2105 exchanger (Figure 5.3) shows a general increase in fouling with time. The calculated fouling resistances for the exchanger are two to twelve times higher than those of the E2104a exchanger immediately upstream of it.

The average tubewall temperature is 207°C which is above the fouling temperature threshold observed by Lawler[1]. However it is unlikely that the increased temperature over that of the E2104 exchanger can be responsible for all of the difference in fouling resistance as the exchanger down stream of E2105, ie E2107a, has a generally lower fouling resistance but approximately the same tubewall temperature.

The E2105 exchanger has a design velocity approximately half that of the other exchangers. The reduced velocity will decrease the likelihood of deposit removal by fluid shear, and may facilitate the deposition of any particulate material suspended in the crude oil.

Hence the relatively high fouling resistance of E2105 compared to the exchangers immediately upstream and down stream is probably due to the tubewall temperature exceeding the temperature at which fouling will readily proceed, and to the low tubeside velocity in the exchanger.

The processing of heavy crudes and slops with the feed stream starting on day 390 resulted in an increase in the fouling rate for E2105. The period of minimum throughput between days 414 and 449 also had a detrimental effect upon the fouling resistance.

After the shutdown and cleaning during days 501 to 551 the fouling resistance of the E2105 exchanger shows an increase with time, with the *insitu* cleaning around day 756 having no apparent effect on the fouling resistance. This could be due to fouling on the shellside which would not have been removed during the *insitu* cleaning. Unfortunately the exchangers were not reopened during the project for this to be confirmed.

Figure 5.3(a)

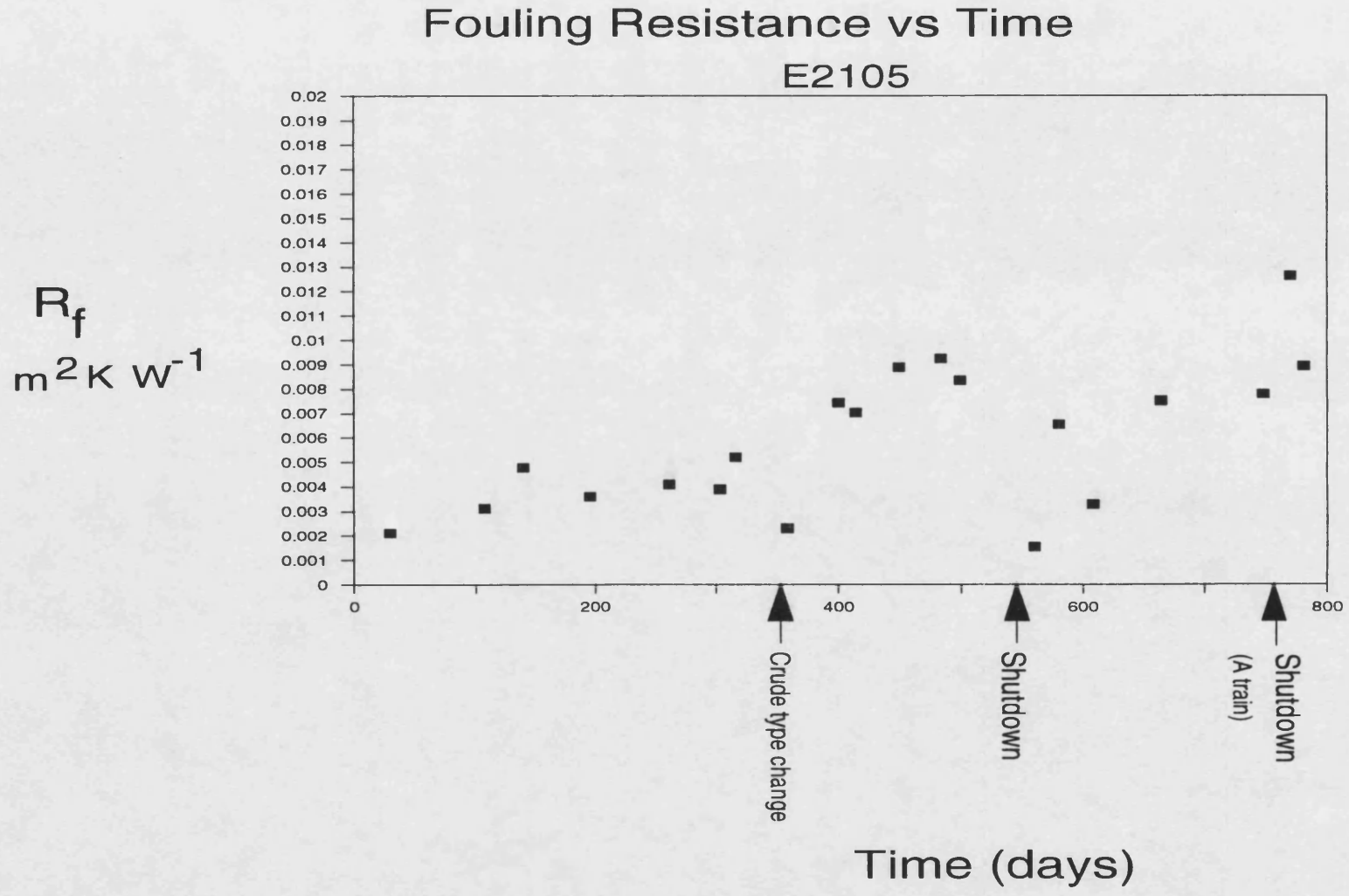
Fouling Resistance vs Time
E2105
R_f
$m^2 K W^{-1}$
0.02
0.019
0.018
0.017
0.016
0.015
0.014
0.013
0.012
0.011
0.01
0.009
0.008
0.007
0.006
0.005
0.004
0.003
0.002
0.001
0
0
200
400
600
800
Crude type change
Shutdown
Shutdown
(A train)
Time (days)

Figure 5.3(b)

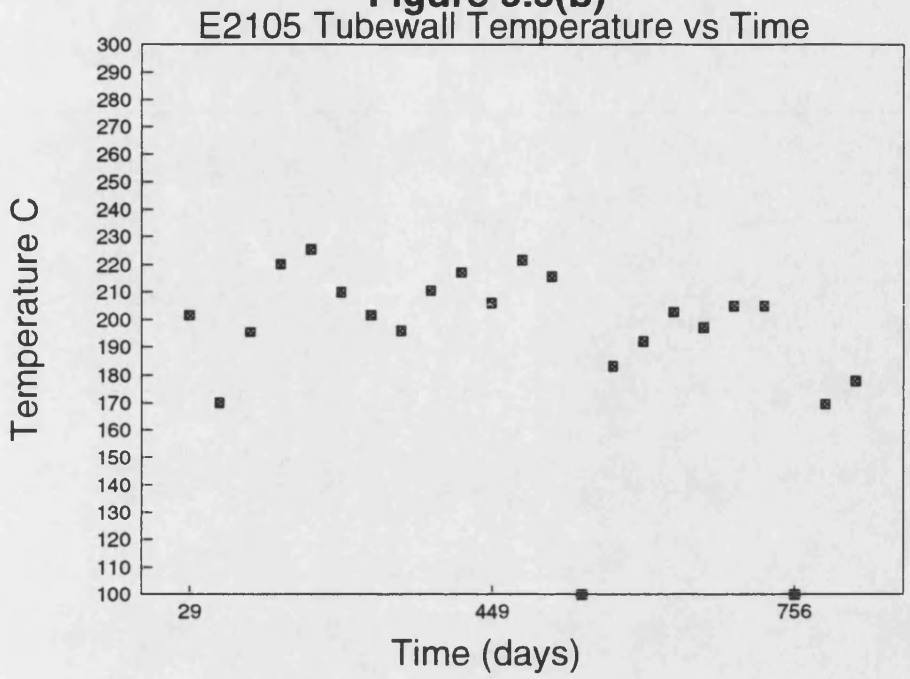

Figure 5.3(c)

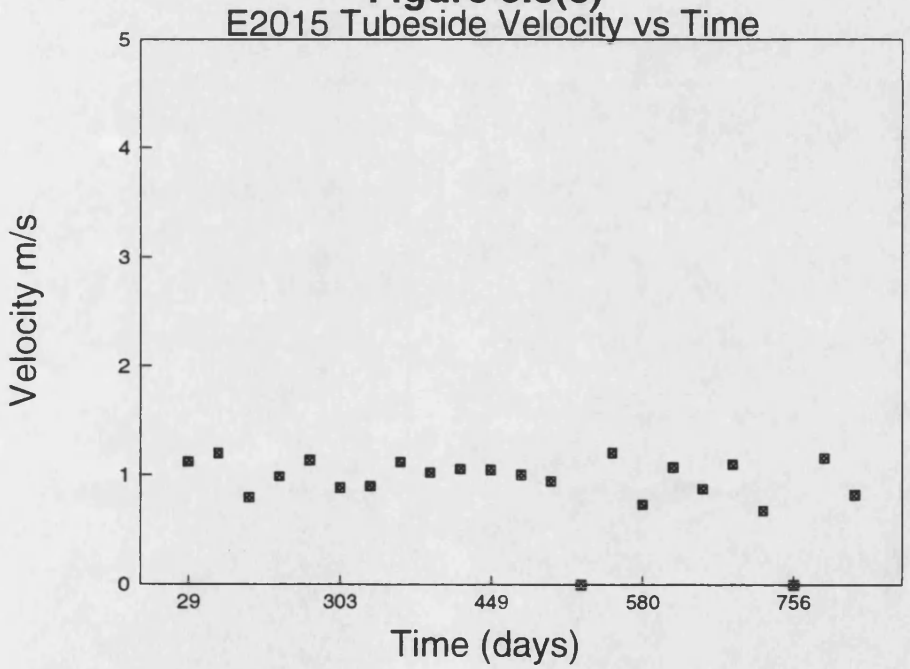

5.1.3 E2106

The E2106 exchanger has two passes on the tubeside. The shellside has a single pass with heavy gas oil as the heating medium. During the study the velocity of the crude oil on the tube side ranged from 1.51 to 2.27 ms^{-1} (see Figure 5.4c) and the tubewall temperature ranged from 155 to 291 °C (see Figure 5.4b).

The fouling against time graph for the E2106 exchanger (Figure 5.4) shows a general trend of increasing fouling resistance with time until the shutdown for cleaning on day 499. However there is scattering of the points. This could be due to the extremely low flowrate on the shellside of this exchanger which results from the volume of heavy gas oil produce having been reduced substantially since the preheat train was designed (see Chapter 2 Table 2a). This low shellside flowrate may mean that the apparently high fouling resistances calculated are due in part to the inefficient heat transfer on the shellside (probably with poor flow distribution) rather than due to presence of actual fouling deposits. This severe scattering of the data makes it virtually impossible to determine any relationship between the fouling resistance and the operating conditions.

On opening E2106 for cleaning a depth of 0.25 m of debris was clearly visible in the bottom of the shell. It is impossible to determine whether or not this debris would move around the exchanger under operating conditions. Assuming that due to the low flowrates the debris remained at the bottom of the exchanger it would effectively arrest any heat transfer to the bottom four rows of tubes, so reducing the thermal efficiency of the exchanger.

The severe fluctuations in the fouling resistance prior to the cleaning of the exchanger were not repeated when the exchanger was recommissioned, thus confirming that the oscillatory nature of the early results was probably due to the deposits observed on the shellside. It is worth noting that the exchanger had not been cleaned on the shellside for several years.

The A train exchangers were shutdown for cleaning around on day 753. This resulted in higher tubeside velocities in the E2106 exchanger. The fouling resistance stays at approximately the same level during this period of operation. This is at variance with the majority of the other exchangers in the B train in which the fouling resistance drops. It is suggested that it is the shellside fouling which gives the greater contribution to the overall fouling resistance for this exchanger.

Figure 5.4(a)

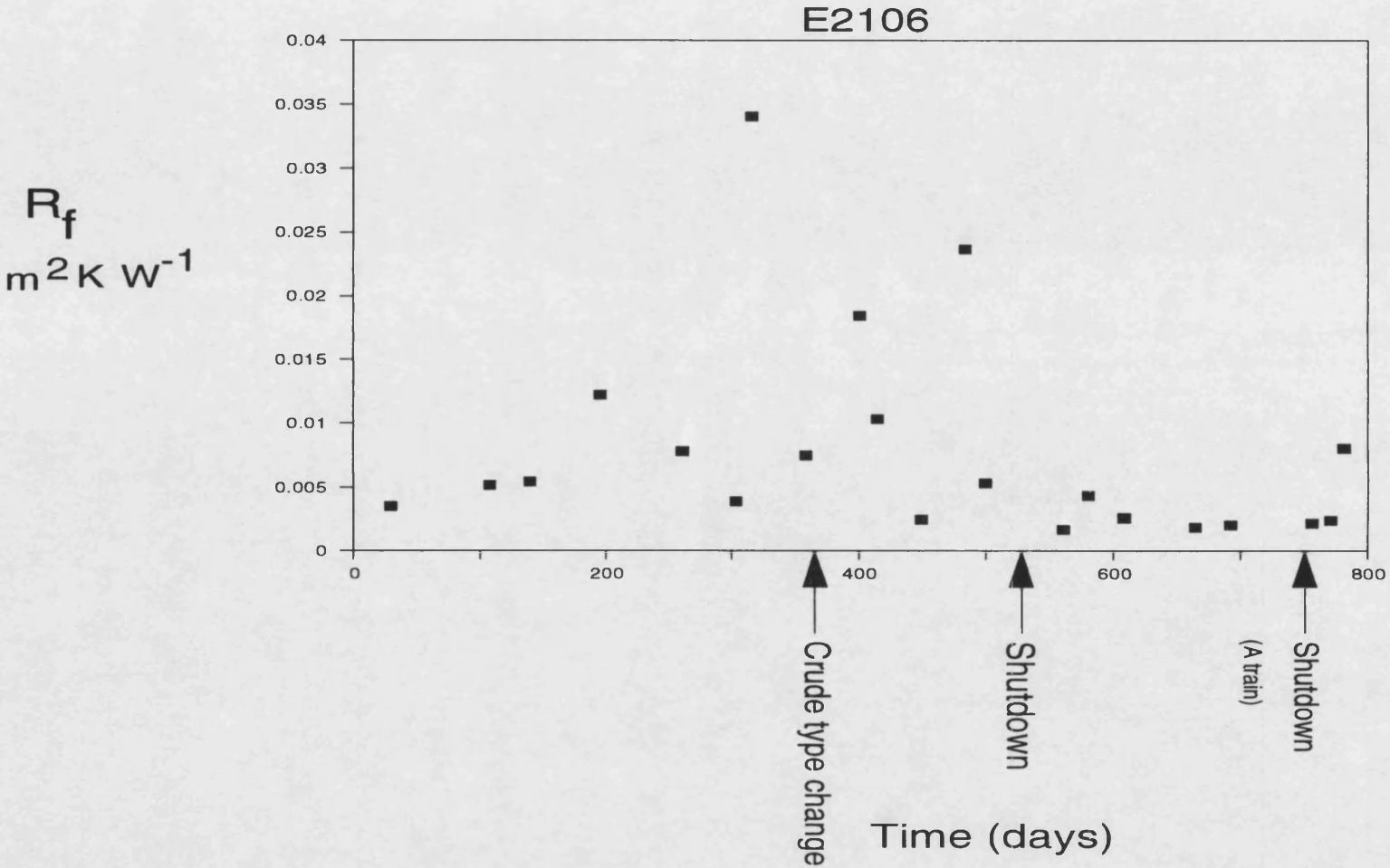
Fouling Resistance vs Time
E2106
R_f
$m^2 K W^{-1}$
0.04
0.035
0.03
0.025
0.02
0.015
0.01
0.005
0
0
200
400
600
800
Crude type change
Shutdown
(A train)
Shutdown
Time (days)

Figure 5.4(b)

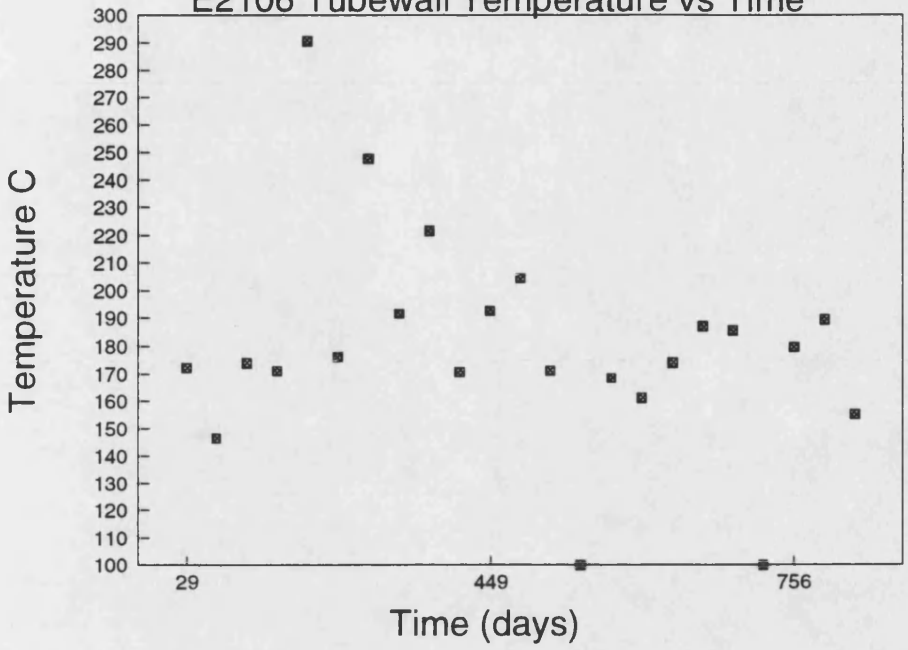

Figure 5.4(c)

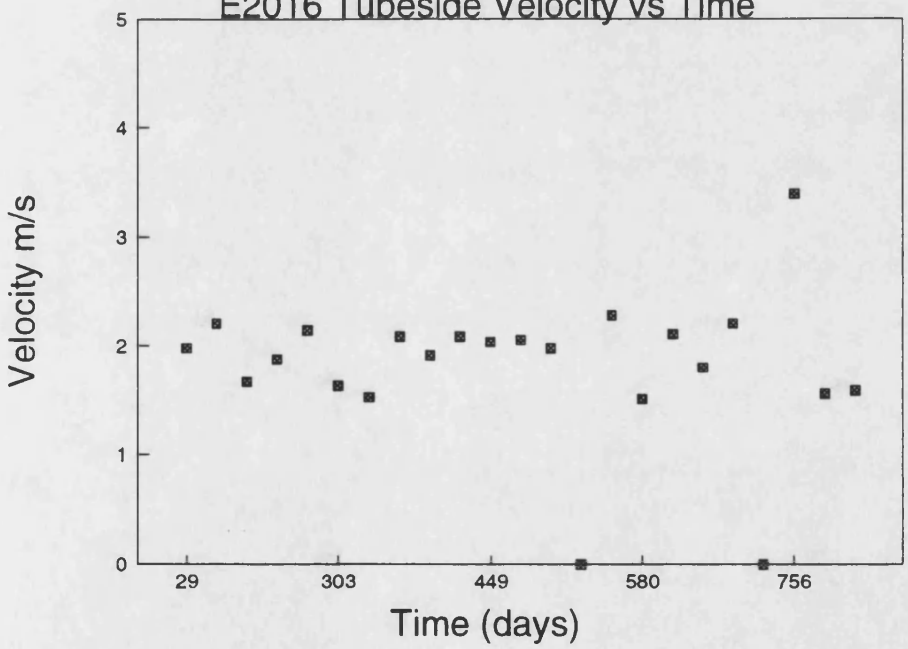

5.1.4 E2107a

The E2107a and E2107b exchangers are geometrically identical. Each exchanger has four passes on the tubeside. The shellside has a single pass with middle pump around as the heating medium. During the study the velocity of the crude oil on the tubeside ranged from 1.49 to 2.3 ms^{-1} (see Figure 5.5c) and the tubewall temperature ranged from 159 to 215 °C (see Figure 5.5b)

The fouling resistance against time graph for E2107a (Figure 5.5) shows a general trend of increasing fouling resistance with time. The fouling resistance increases steadily from the initial value of 0.0007 m^2KW^{-1} to 0.0037 m^2KW^{-1} and then decreases to almost the original value on day 261. This drop in fouling resistance corresponds with an increase in velocity of 0.7 ms^{-1} over the velocity at the peak fouling resistance during this period of operation. The increased velocity and hence shear stress may have removed some of the deposit from the tube wall.

On day 390 there was a change from light to heavy type crude oils and an introduction of slops into the feed stream. This resulted in an increased fouling rate for the E2107a exchanger.

When the exchanger was opened at the end of the first operating period there was an uneven distribution of the fouling deposit. E2107a is a four tube pass exchanger. The tubes in the first pass were relatively clean and the sampling tube could be run freely to its full length. However in the second and third passes the deposits appeared thicker and the sampler could only be pushed inside the tube to a depth of approximately ten centimetres. In the fourth pass the tubes were more heavily fouled and only a five centimetre length was passable with the sampler. This pattern of fouling corresponds with increasing crude oil temperature through the exchanger, with the deposit thickness at the tubeside outlet end generally greater than that at the tubeside inlet end.

The shellside of the exchanger had a fairly even cover of fouling approximately 1 mm thick. There was a small accumulation of deposit at the bottom of the exchanger. However this was relatively loose and could possibly have dropped from the outside of the tubes whilst the tube bundle was being removed. Plate 5.3 shows a sample of the fouling deposit from the outside of a tube in the E2107a exchanger.

On start-up of the exchangers after cleaning, the fouling resistance of E2107a increases until the exchanger is shutdown for cleaning around day 756. It is noteworthy that the three start-up values calculated for E2107a are approximately the same (0.0007,0.0007 and 0.0011 m^2KW^{-1}). This would seem to indicate that the shellside fouling deposit has little effect on the overall heat transfer coefficient and that the initial fouling resistances may result from errors in the start-up data.

Figure 5.5(a)

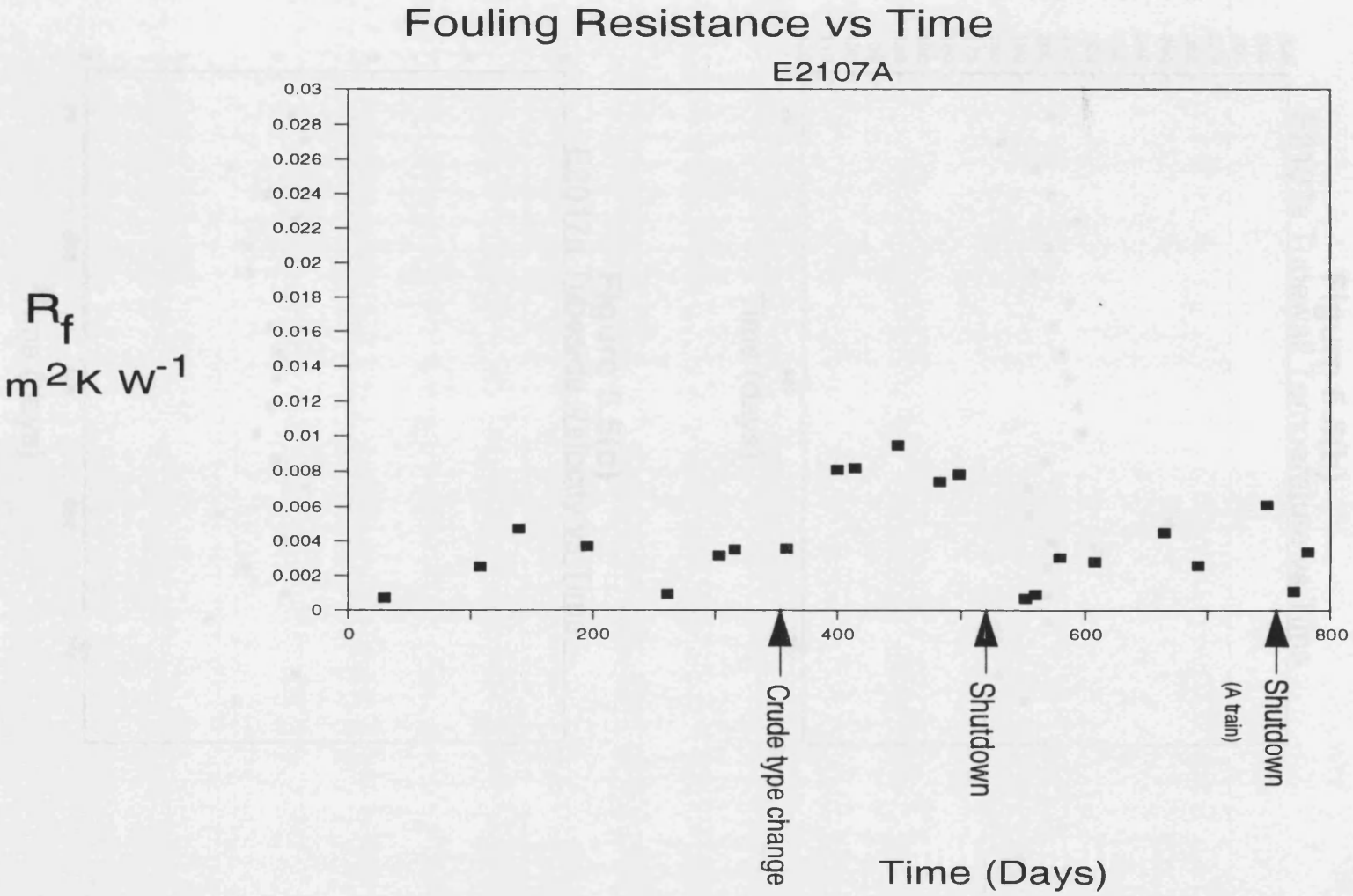
Fouling Resistance vs Time
E2107A
R_f
$m^2 K W^{-1}$
0.03
0.028
0.026
0.024
0.022
0.02
0.018
0.016
0.014
0.012
0.01
0.008
0.006
0.004
0.002
0
0
200
400
600
800
Crude type change
Shutdown
Shutdown
(A train)
Time (Days)

Figure 5.5(b)

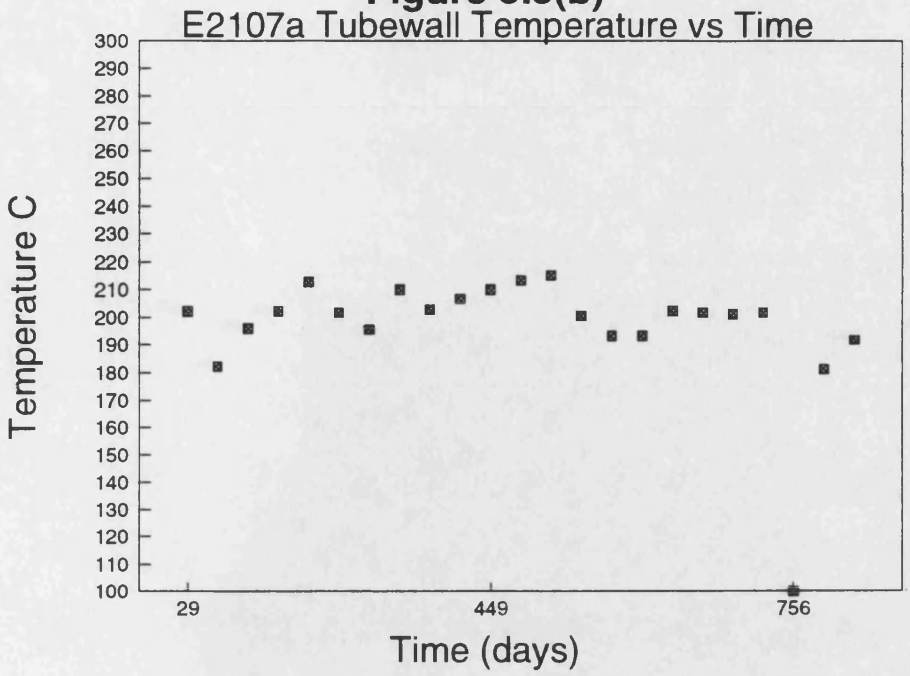

Figure 5.5(c)

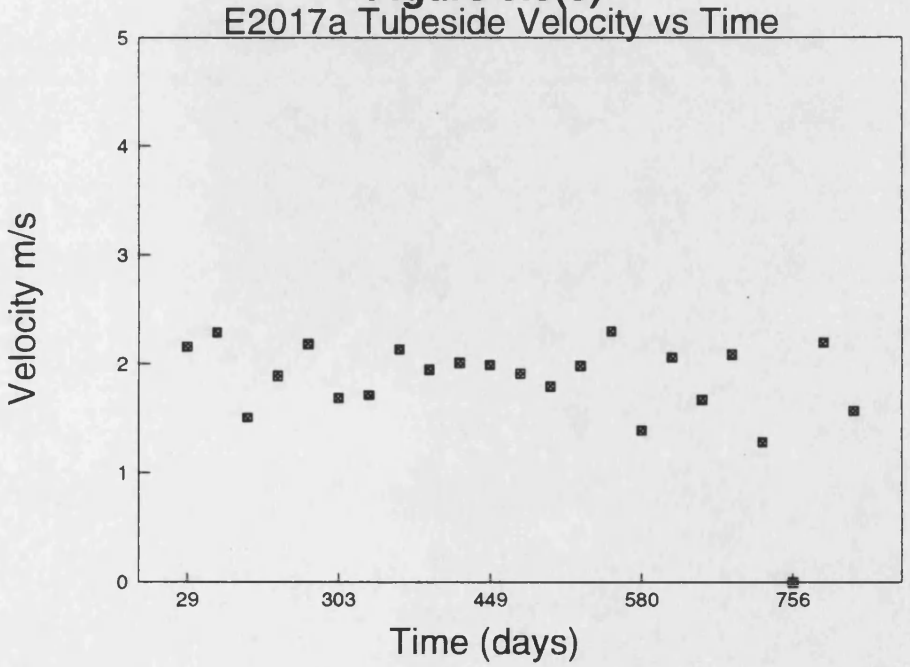

Plate 5.3 SHELLSIDE FOULING E2107a

5.1.5 E2107b

The fouling resistance against time graph for E2107b (Figure 5.6) shows that the exchanger was apparently clean after 29 days of operation, unlike the other exchangers in the train. It is possible, but unlikely, that this exchanger was more thoroughly cleaned than the others, but regrettably it was not possible to determine if this was the case. After the initial low value the fouling resistance increases steadily with time until day 261 when as for exchanger E2107a there is a decrease in fouling resistance corresponding to an increase in the tubeside velocity (see Figure 5.6c).

Throughout the study the fouling resistance of the E2107b exchanger is generally less than that of the geometrically identical E2107a exchanger. This could be due to the difference in operating temperature and thus tubewall temperature (see Figure 5.6b) between the two exchangers. The tubeside inlet temperature to E2107b is on average 15-20°C lower than the tubeside inlet temperature for E2107a. This lower temperature is due to poor heat transfer in the E2106 exchanger caused by low shellside flow.

On start-up of the exchangers after the cleaning during days 501 to 551 the E2107b exchanger showed an initial fouling resistance of approximately 0.001 m^2KW^{-1}. It is unlikely that the *insitu* cleaning prior to the start of the project would produce a cleaner surface than the remote cleaning during the major shutdown. This contrast in initial calculated fouling resistances highlights the likelihood of errors in the start-up fouling resistance which is further discussed in Chapter 3 and Chapter 6.

The fouling resistance of E2107b showed a general increase with time after the remote cleaning. Whilst the A train was shutdown for cleaning the flowrate on both the tube and shell side of the E2107b exchanger was increased. This resulted in a slight decrease in fouling resistance. However the fouling resistance returned to approximately the same level (0.0043 m^2KW^{-1}) when the velocities were reduced on the start-up of the A train.

Figure 5.6(a)

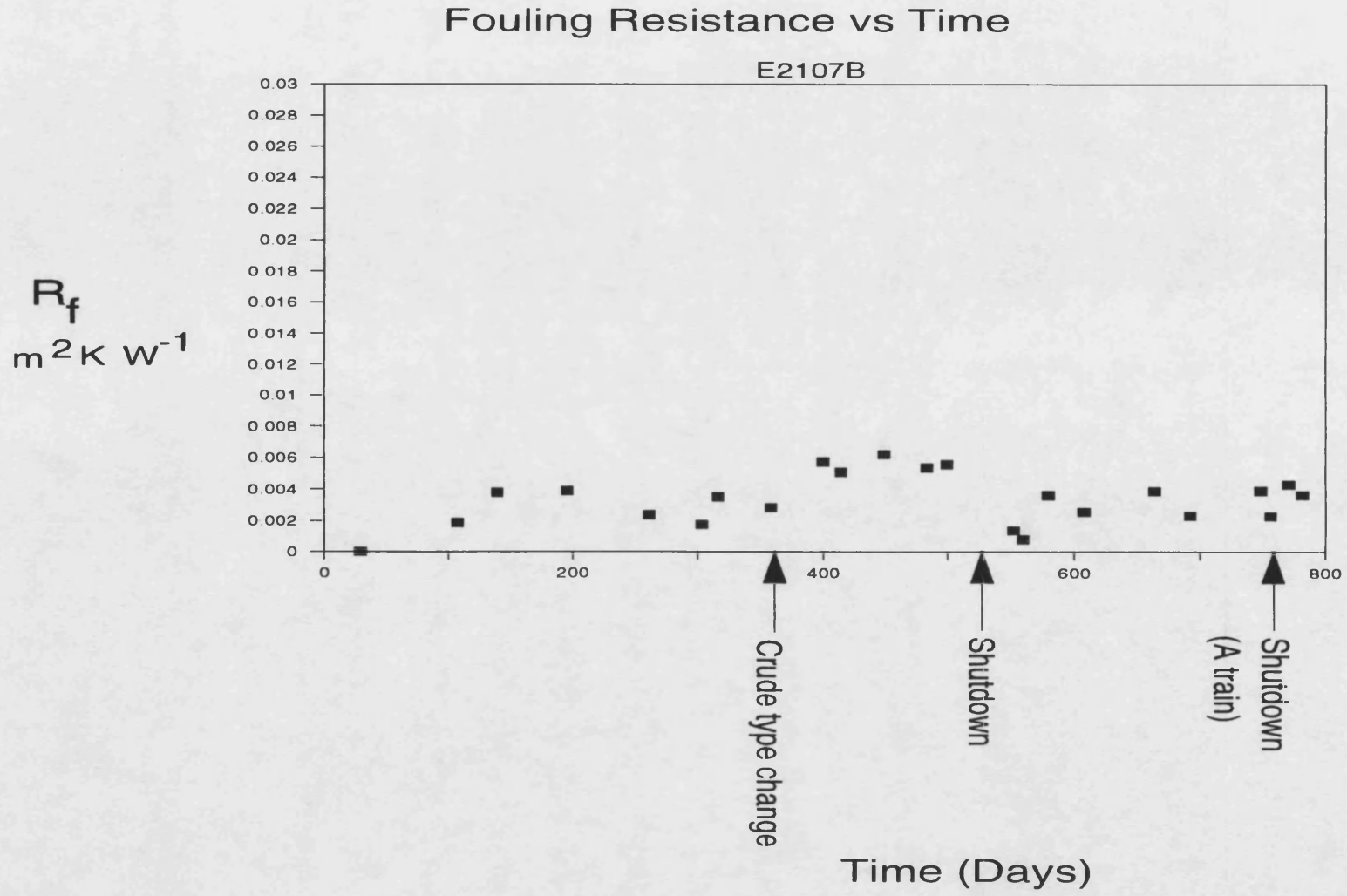
Fouling Resistance vs Time
E2107B
R_f
$m^2K\ W^{-1}$
0.03
0.028
0.026
0.024
0.022
0.02
0.018
0.016
0.014
0.012
0.01
0.008
0.006
0.004
0.002
0
0
200
400
600
800
Crude type change
Shutdown
Shutdown
(A train)
Time (Days)

Figure 5.6(b)

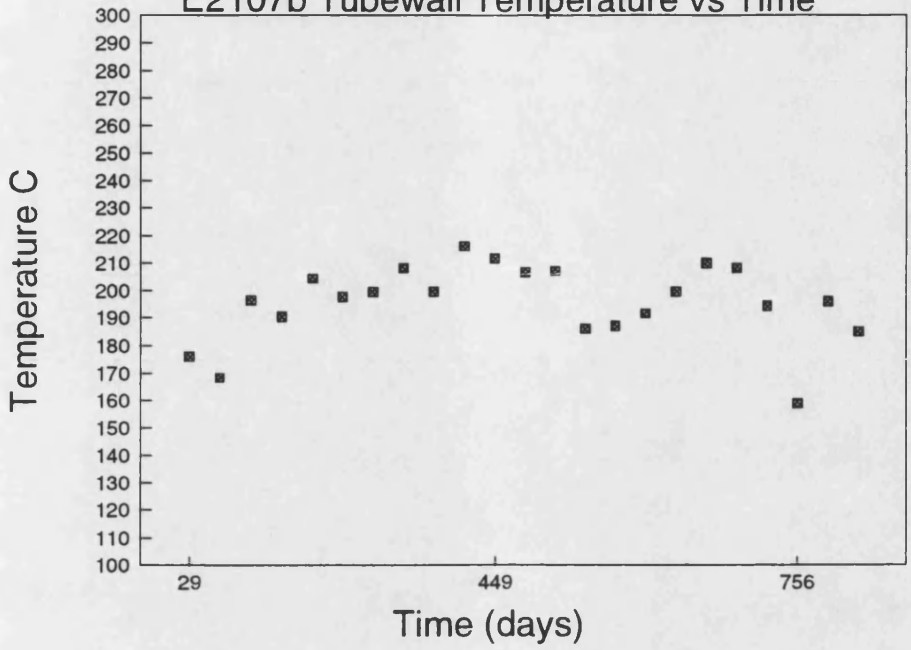

Figure 5.6(c)

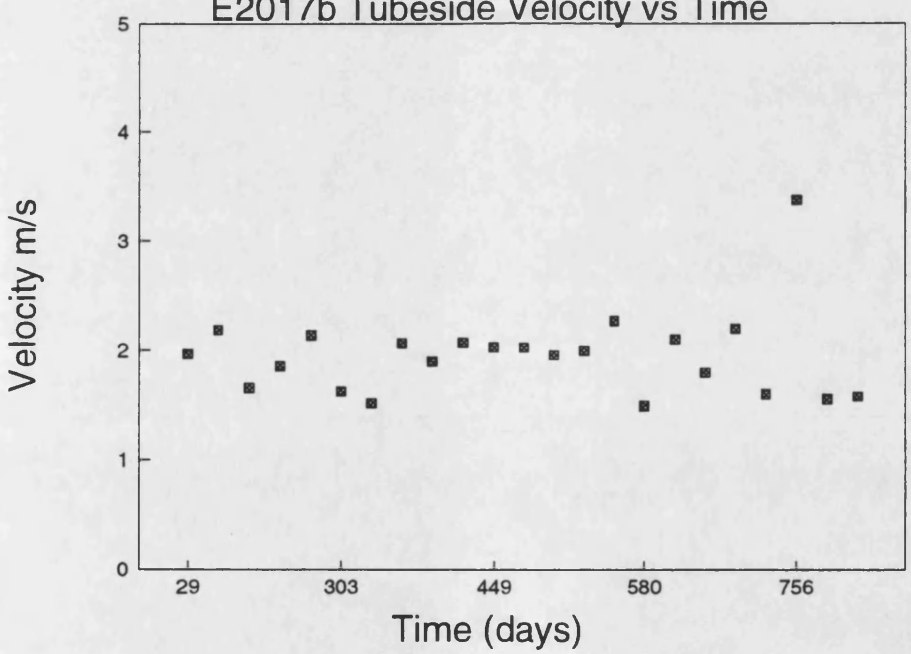

5.1.6 E2108ab

The E2108ab exchangers have two passes on the tubeside. The shellside has a single pass with middle pump around as the heating medium. During the study the velocity of the crude oil on the tubeside ranged from 1.1 to 2.9 ms^{-1} (see Figure 5.7c) and the tubewall temperature ranged from 184 to 227°C (see Figure 5.7b). It is not possible to measure the temperature of either the shellside or tubeside fluid between the E2108a and E2108b exchangers, hence the combined fouling resistance for the two exchangers in series has to be calculated.

The fouling resistance against time graph of E2108ab (Figure 5.7) shows the fouling resistance increases only slightly from the initial value of 0.006 m^2KW^{-1} until the introduction of slops and heavy crudes on day 390. There is then a marked increase in the fouling rate until the exchangers were shutdown for cleaning on day 501.

There is a significant amount of scatter of the points. This is probably caused by the periodic by-passing of the E2108 exchangers on the shellside to maintain the temperature in the stabilizer unit (see chapter 2 Section 2.1.2). This results in periods of low shellside flow when a fouling deposit may build up in this location, to be partially removed as the flow is increased again. Plate 5.4 shows a fouling deposit removed from the outside of a tube from the E2108a exchanger.

On opening the E2108ab exchangers for cleaning after day 510 there was a considerable difference in the appearance of these tube bundles compared to those of the upstream exchangers. The tubes were too severely blocked to allow the use of the sampling device, the samples for analysis being taken with a spatula. The outside of the bottom ten or so rows of tubes was caked in a thick deposit, which was distinctly layered. This confirmed that there was significant shellside fouling, which was probably responsible for at least some of the variations in the calculated fouling resistance.

On start-up of the exchangers on day 551 the initial calculated fouling resistance is significantly lower than that of the first operating period. This is probably due to the fact that both the shell and tubeside were cleaned during the shutdown whereas only the tubeside was cleaned prior to the start of the project.

There is an underlying increase in fouling resistance until the exchangers are shutdown and cleaned around day 756. After this *insitu* cleaning the initial fouling resistance was of the same order of magnitude as for the first operating period. The fact that this high shellside fouling resistance was reached from cleaned tubes in a period of 295 days could be considered indicative of the rapid asymptotic fouling by the heavy residue stream which is on the shellside of these exchangers.

Figure 5.7(a)

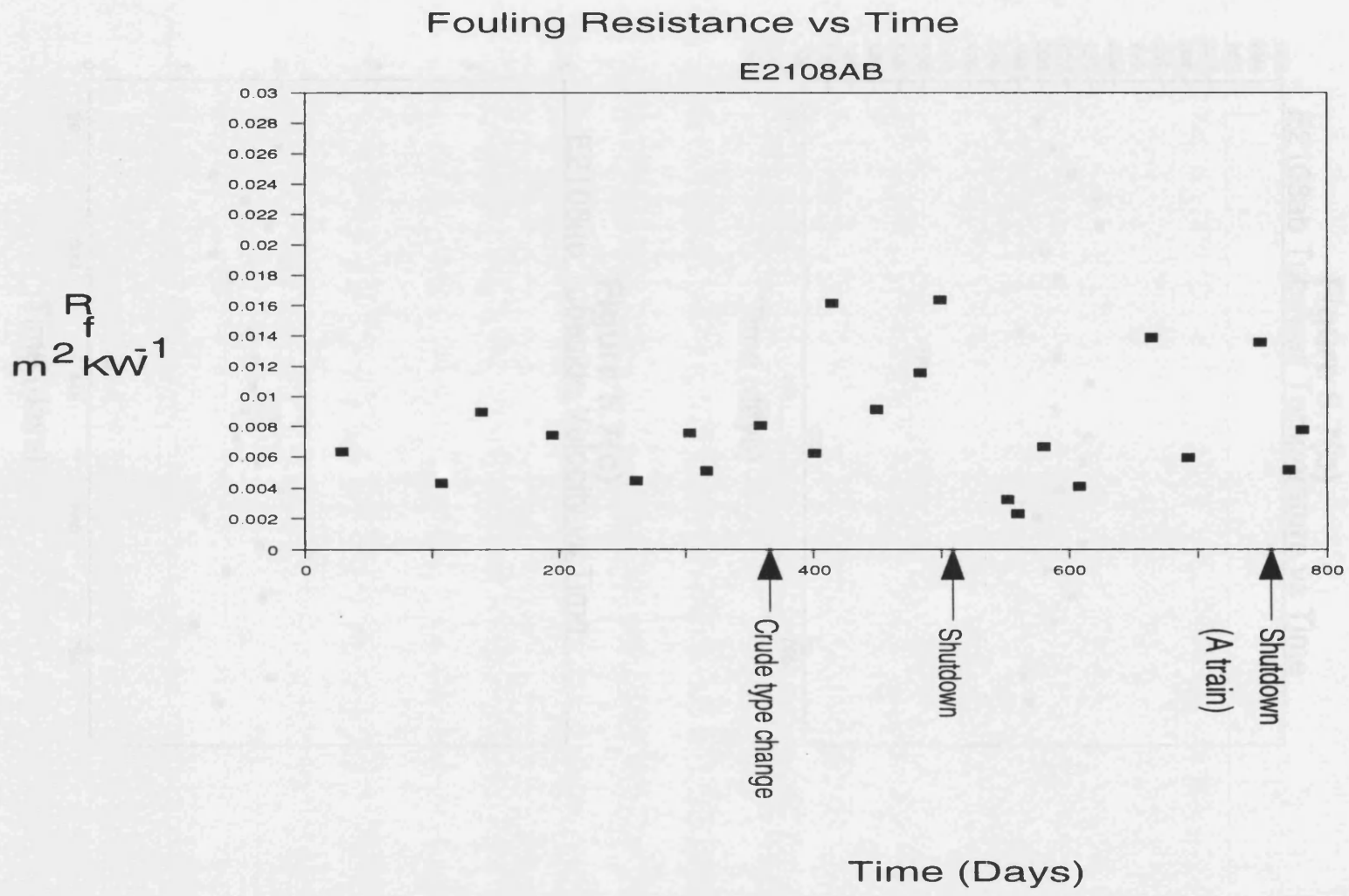
Fouling Resistance vs Time
E2108AB
R_f
$m^2 KW^{-1}$
0.03
0.028
0.026
0.024
0.022
0.02
0.018
0.016
0.014
0.012
0.01
0.008
0.006
0.004
0.002
0
0
200
400
600
800
Crude type change
Shutdown
Shutdown
(A train)
Time (Days)

Figure 5.7(b)

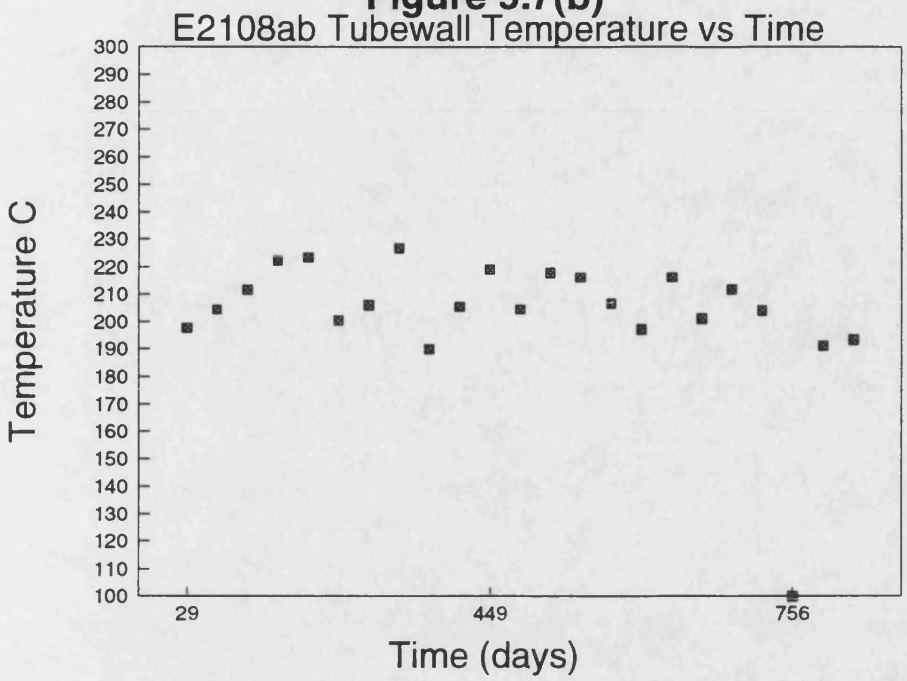

Figure 5.7(c)

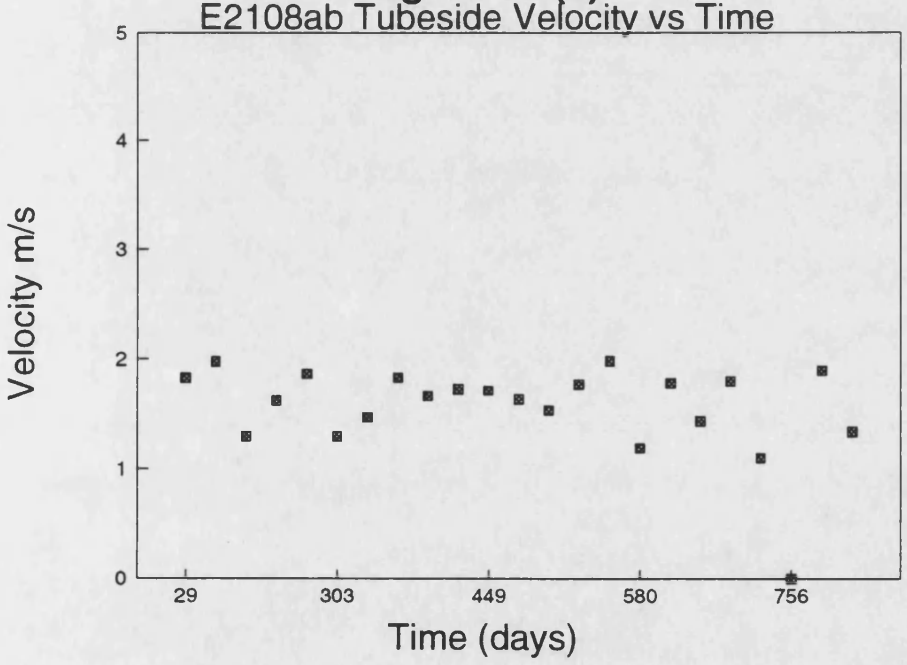

Plate 5.4 SHELLSIDE FOULING FROM E2108ab

5.1.7 E2108cd

The fouling resistance against time graph for E2108cd (Figure 5.8) shows approximately the same general pattern of fouling as E2108ab (figure 5.7) for the period of operation up to the introduction of heavy crudes and slops on day 390. The high calculated fouling resistance on day 414 is probably due to the slops present in the feed (see Chapter 4). However this small slops injection did not evoke such a dramatic change in the geometrically identical E2108ab exchangers. There is no obvious reason for the differing responses as the temperatures (see Figure 5.8b), flowrates and thus velocities (see Figure 5.8c) for the exchangers at this time were comparable. There were no recorded problems with the feed tank on this day but it may be possible that the slops were not evenly distributed, even though the specific gravity at each of the measuring points was the same. A concentrated parcel of slops may have passed through the E2108cd exchangers increasing the fouling deposit.

The calculated fouling resistance for both the E2108ab and E2108cd exchangers increases dramatically after day 414 and then decreases until the exchangers are shut down for cleaning. This return to the generally increasing fouling resistance pattern does not correspond to a change in tubewall temperature or tubeside velocity. The shellside inlet thermowell is common to both trains, therefore an error in this temperature measurement could produce the observed effect. Nevertheless the temperature measured is not obviously at variance with that measured on other days, although there is variation of up to $\pm 20^{o}C$ in this temperature, due to the periodic by-passing of the E2111 exchangers. From analysis of the system of equations used to calculate the fouling resistance (see Chapter 3) it was determined that a 20°C error would not be sufficient to produce such a large change in fouling resistance. Hence it would appear that the sudden increase in fouling resistance is not resultant from errors in the plant data or changes in the operating conditions. It must therefore be the result of composition changes, it is possible that the deposit formed from material in the slops was soluble in the next crude

oil type processed and was thus removed from the tubewall. It is most likely that these peak fouling resistances were the result of a combination of factors such as high shellside fouling due to by-passing of the exchangers and increased fouling due to the presents of a concentrated parcel of slops in the crude oil feed stream.

The initial fouling resistance for the E2108cd exchangers after the remote cleaning is significantly less than for the first operating period, confirming that the shellside fouling plays a considerable part in the fouling of these exchangers.

The fouling resistance on day 756 when the E2108ab exchangers were shutdown for cleaning is reduced compared to the previous values, probably due to the increased shell and tube side flowrates, however it returns to approximately the same value (0.0114 m^2KW^{-1}) when the A train comes back on line.

Figure 5.8(a)

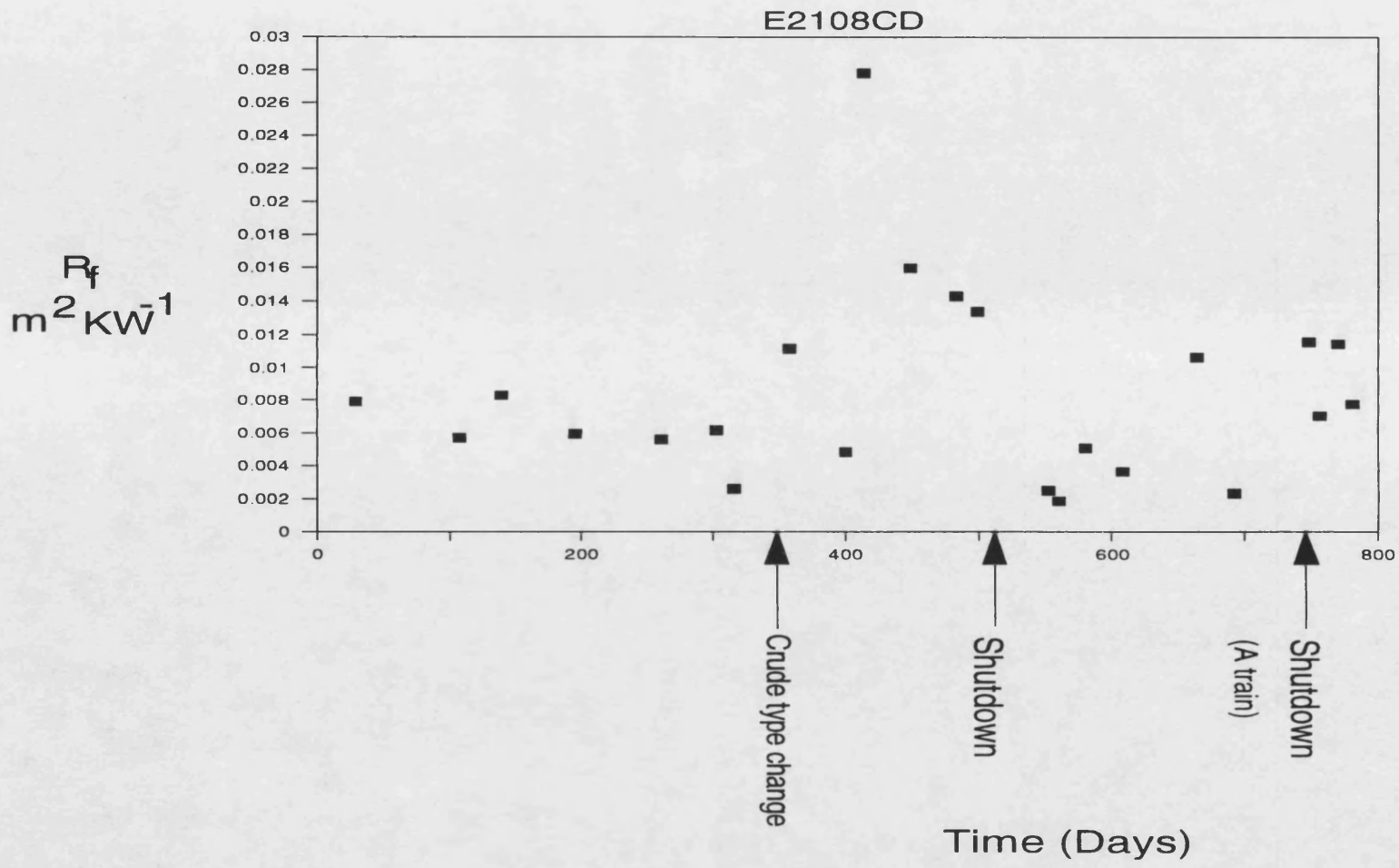
Fouling Resistance vs Time
E2108CD
R_f
m^2KW^{-1}
0.03
0.028
0.026
0.024
0.022
0.02
0.018
0.016
0.014
0.012
0.01
0.008
0.006
0.004
0.002
0
0
200
400
600
800
Crude type change
Shutdown
(A train)
Shutdown
Time (Days)

Figure 5.8(b)

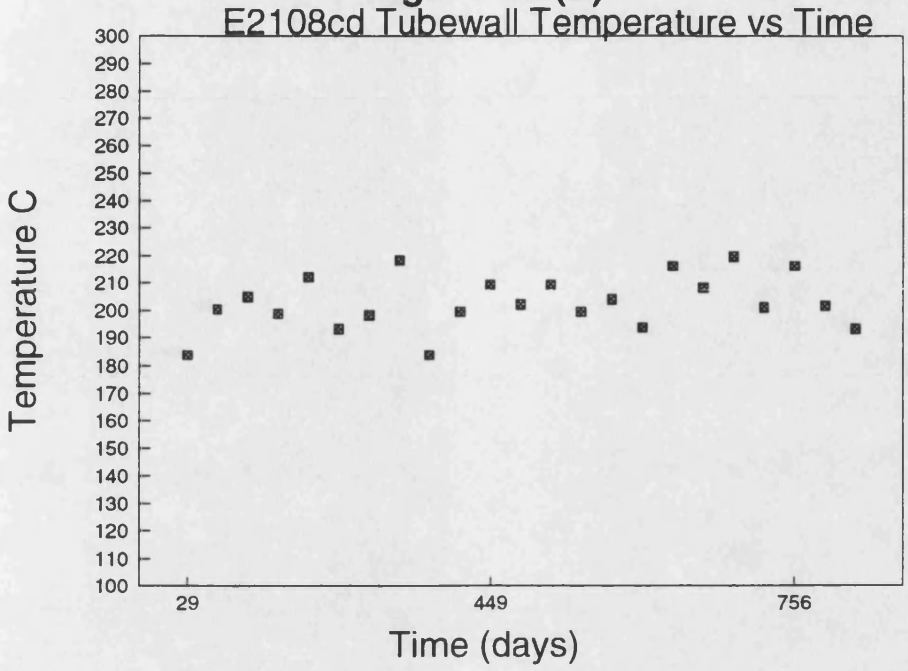

Figure 5.8(c)

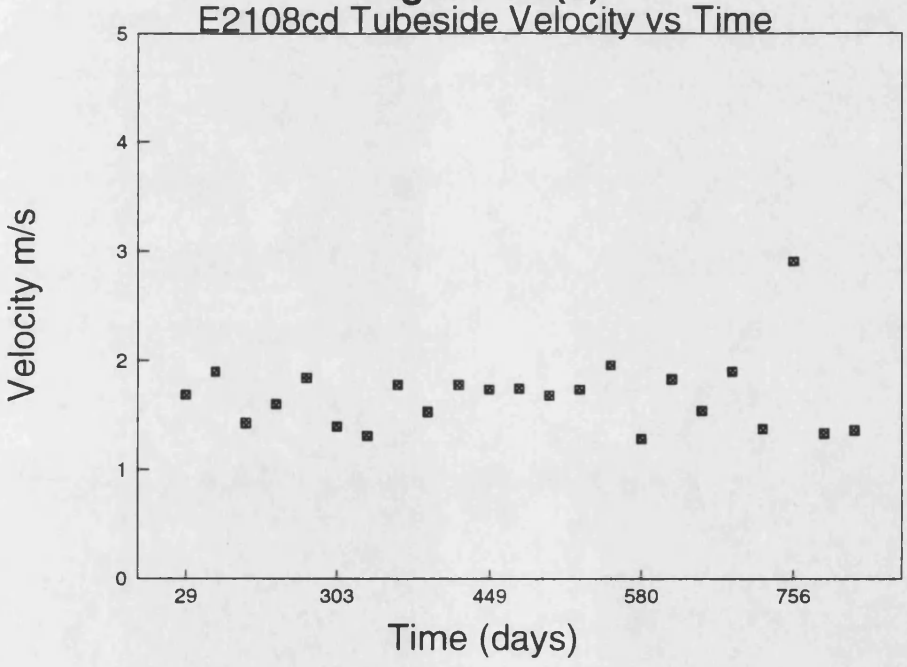

5.1.8 E2109a

The E2109a and E2109b exchangers are geometrically identical to the E2107 and E2107b exchangers and have four passes on the tubeside. The shellside has a single pass with middle pump around as the heating medium. During the study the velocity of the crude oil on the tubeside ranged from 1.31 to 3.47 ms^{-1} (see Figure 5.9c), and the tubewall temperature ranged from 163 to 241°C (see Figure 5.9b).

The fouling resistance against time graph for the E2109a exchanger (Figure 5.9) shows a general increase in fouling resistance with time. The E2109 exchangers are geometrically identical to the E2107 exchangers and have the same process fluids hence any differences in the fouling between them should be due to different operating conditions. The general trend during the first operating period is approximately the same for E2107a and E2109a although the fluctuation of the points is greatest in the cooler exchanger. It is plausible that this is because the deposit formed at the lower temperature is easier to remove.

The sudden increase in fouling resistance for E2109a on day 400 comes just after a slops injection in the feed on day 390. This injection of slops marks the start of the change in the fouling resistance pattern for the majority of the exchangers. The crude types from this point until the shutdown of the exchangers for cleaning were generally heavier than those already processed and there were occasional injections of slops. Nevertheless the E2109a exchanger has the most immediate and dramatic response to this feed composition change. The increased fouling resistance does not correspond to an increase in tubewall temperature or a noteworthy decrease in tubeside velocity. However it does correspond to the lowest calculated tubewall temperature for this exchanger (214°C). This tubewall temperature is more typical of an E2108 exchanger which as discussed previously may have been susceptible to fouling from slops in the crude oil. It could be possible that the reaction involving slops occurs to the greatest extent within a given temperature band which would appear from the data for the E2108

exchangers and E2109a to be in the region 200-215°C. This point requires further investigation. As with the E2108 exchangers the fouling resistance then returns to the general increasing pattern until the exchangers are shutdown for cleaning.

On removal of the tube bundle for cleaning a large amount of deposit fell from the outside of the bottom rows of tubes. At the hottest end of the exchanger the spaces between the tubes were completely blocked. Thus some of the calculated fouling resistance for the first period of operation would have been due to shellside fouling. The shellside fluid for the E2109 exchangers is middle pump around from the distillation column. This stream has a fairly constant flowrate and inlet temperature, and hence should give less fluctuations in the shellside fouling resistance than those exchangers in which the shellside operating conditions are more changeable.

After the exchangers had been cleaned on both the shell and tube sides the initial fouling resistance (0.0023 m^2KW^{-1}) was approximately the same as for the first operating period (0.002 m^2KW^{-1}), and again when the exchangers were cleaned *insitu* around day 756 the initial value on start-up (0.0029 m^2KW^{-1}) was also similar to that for the first operating period. This would appear to indicate that the contribution to the overall fouling resistance from the shellside deposit was small as the cleaning of the shellside appeared to have little effect. One explanation for this could be that the shellside deposit only formed during the first period of operation and was not present at the start of the project. This is unlikely as the exchangers had not been cleaned on the shellside for several years and there had been no significant change in operating conditions hence there is no reason to suppose that the exchangers suddenly started fouling on the shellside.

Another explanation could be that although there was a significant amount of deposit present it had a large thermal conductivity and thus presented little resistance to heat transfer. Unfortunately it was not possible to measure the thermal conductivity of the deposits.

In conclusion it would appear that for the E2109a exchanger the initial high fouling resistances probably stem from errors generated by the method used to calculate the fouling resistance at start-up rather than from shellside fouling.

Figure 5.9(a)

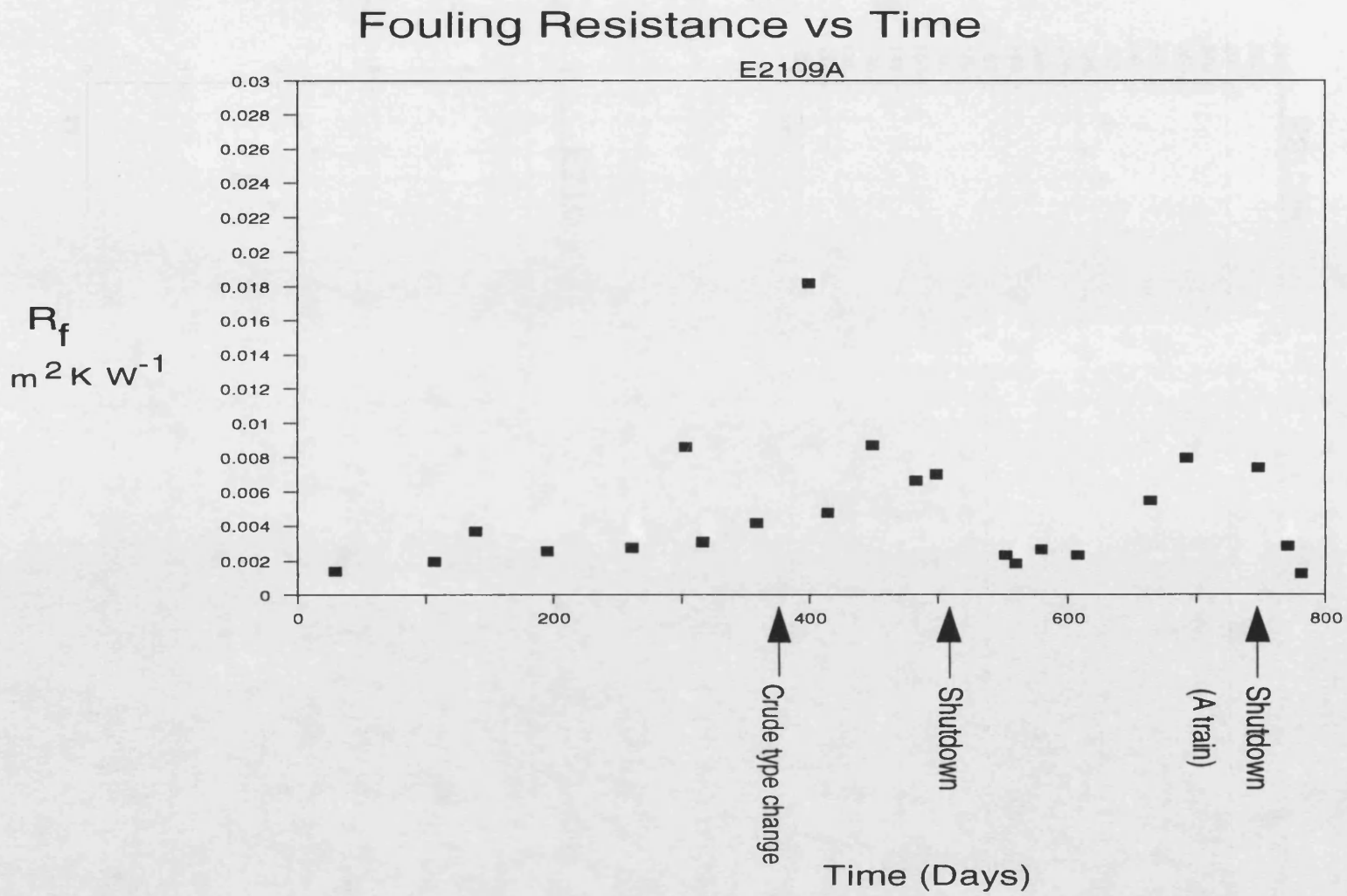
Fouling Resistance vs Time
E2109A
R_f
$m^2 K W^{-1}$
0.03
0.028
0.026
0.024
0.022
0.02
0.018
0.016
0.014
0.012
0.01
0.008
0.006
0.004
0.002
0
0
200
400
600
800
Crude type change
Shutdown
(A train)
Shutdown
Time (Days)

Figure 5.9(b)

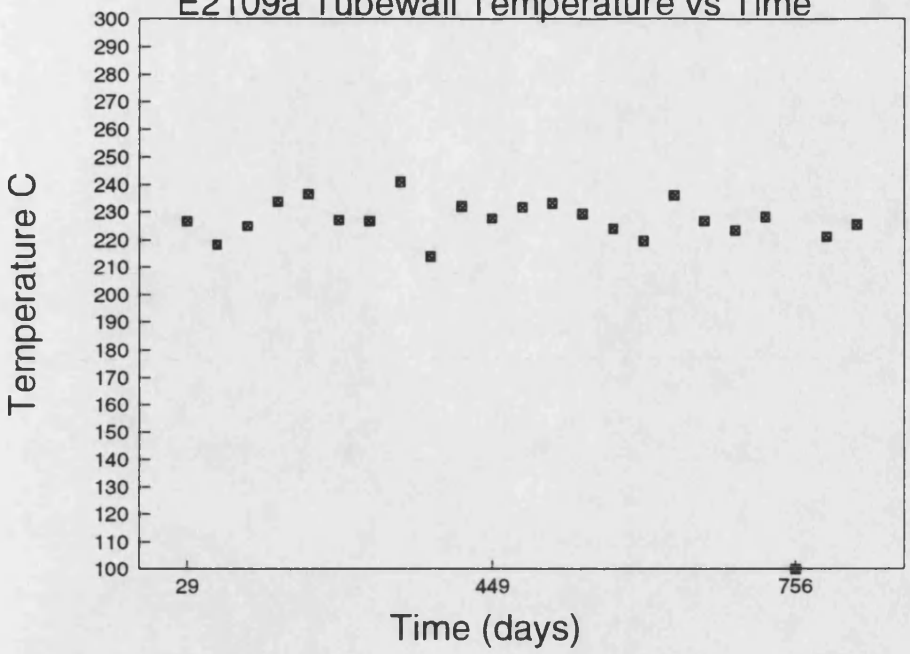

Figure 5.9(c)

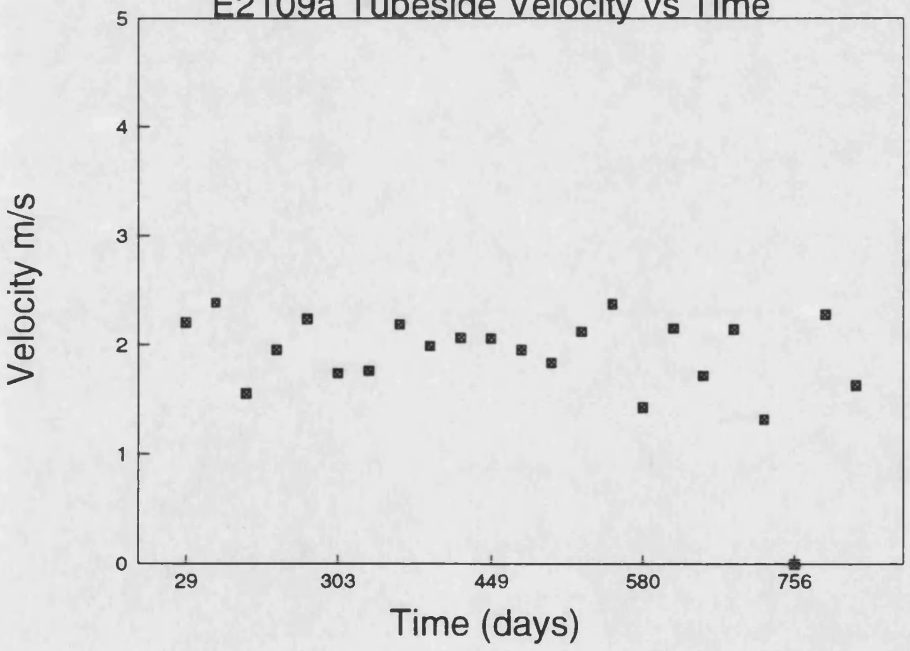

Plate 5.5 SHELLSIDE FOULING E2109a

5.1.9 E2109b

The fouling resistance against time graph for the E2109b exchanger (Figure 5.10) shows a general trend of increasing fouling resistance with time, with an increased fouling rate after the introduction of slops and heavy crudes on day 390.

The increase in the rate of fouling for E2109b on the introduction of slops and heavy crudes is much greater than that for E2107b, a geometrically identical exchanger operating with the same process fluids but at a lower temperature (see Figure 5.10b). This could suggest that the rate of fouling from this type of crude mixture increases with increasing temperature.

On removal of the tube bundle for cleaning the condition of the E2109b exchanger was much the same as the E2109a exchanger, although there appeared to be more shellside fouling, with a lot of debris falling from the outside of the bundle when it was pulled.

The start-up fouling resistance for the E2109b exchanger in the second period of operation was slightly less than for the first period of operation which may indicate that for this exchanger there was a slight effect from shellside fouling.

The increased shell and tube side flowrates and thus velocities (see Figure 5.10c) around day 756 whilst the A train exchangers were being cleaned resulted in a slight reduction in fouling resistance.

Figure 5.10(a)

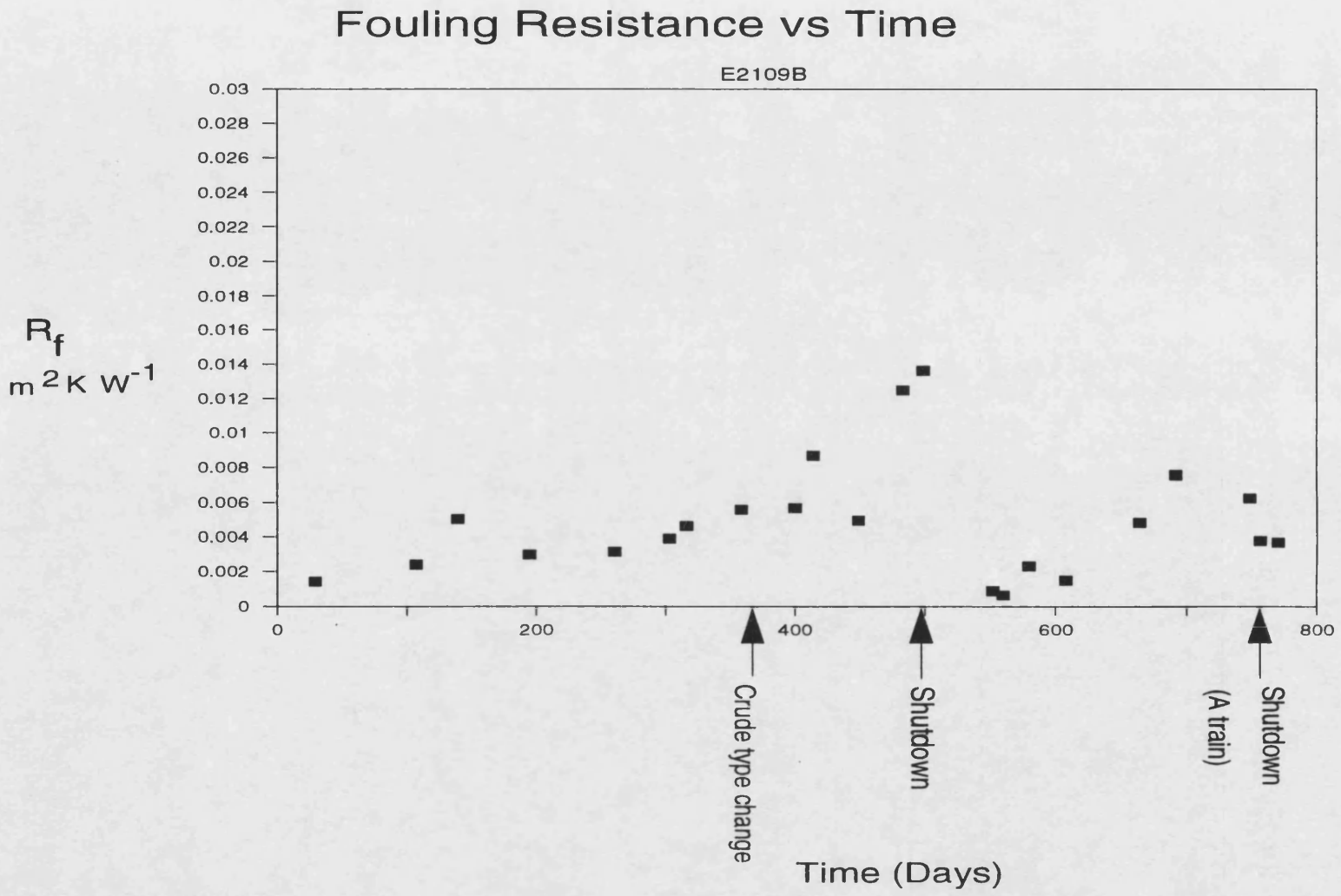
Fouling Resistance vs Time
E2109B
R_f
$m^2 K W^{-1}$
0.03
0.028
0.026
0.024
0.022
0.02
0.018
0.016
0.014
0.012
0.01
0.008
0.006
0.004
0.002
0
0
200
400
600
800
Crude type change
Shutdown
(A train)
Shutdown
Time (Days)

Figure 5.10(b)

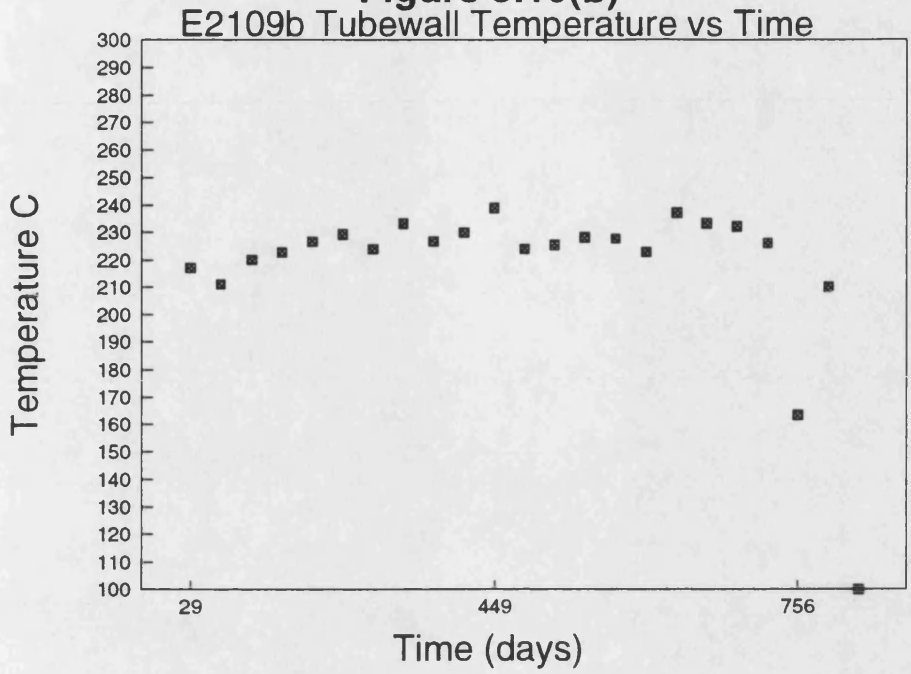

Figure 5.10(c)

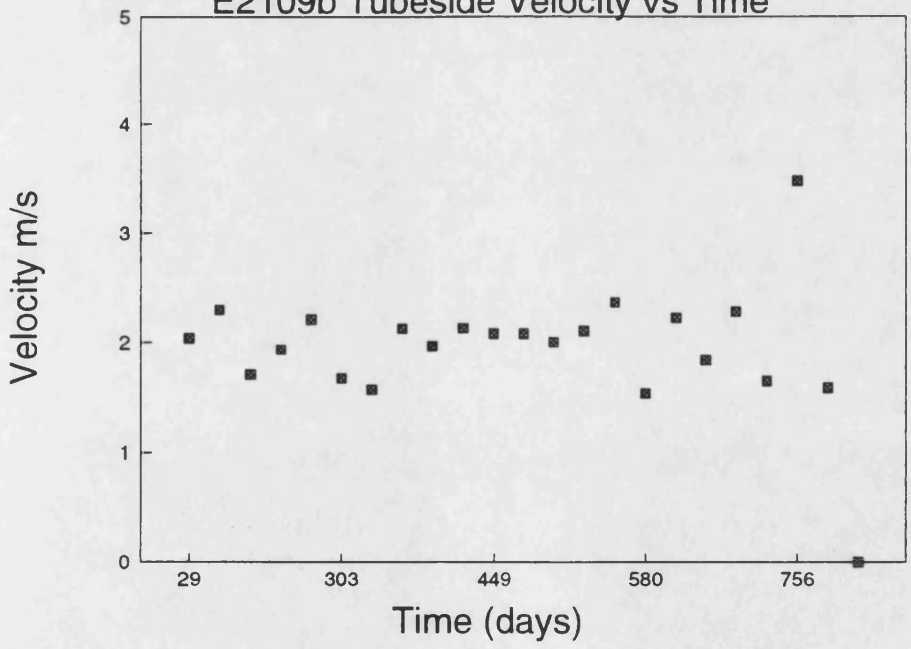

5.1.10 E2110ab

The E2110ab and E2110cd exchangers have two passes on the tubeside. The shellside is a single pass with bottom pump around as the heating medium. During the study the velocity of the crude oil on the tubeside ranged from 1.31 to 1.97 ms^{-1} (see Figure 5.11b), and the tubewall temperature ranged from 234 to 279°C (see Figure 5.11c). It is not possible to measure the temperature of either the shellside or tubeside fluid between the E2110a and E2110b exchangers, hence the combined fouling resistance for the two exchangers in series has to be calculated.

The fouling resistance against time graph for the E2110ab exchangers (Figure 5.11) shows a general increase in fouling resistance with time, with a marked increase in fouling rate after the introduction of heavy crudes and slops on day 390.

The E2110 exchangers are the last exchangers in the preheat train that have crude oil on the tubeside, and are consequently the hottest exchangers studied. With the exception of the E2108 exchangers previously discussed the E2110 exchangers have the highest fouling resistances showing that fouling from crude oil is probably temperature dependent.

There is a very dramatic increase in the fouling rate on the introduction of slops and heavy crudes into the feed. The peak fouling resistance on day 449 follows a period of minimum throughput and the processing of crude oils from stratified tanks (see Chapter 4). The throughput was then increased with the result that the fouling resistance returned to the generally increasing pattern before the exchanger was shutdown for cleaning.

On opening of the exchangers it was obvious that the tubes were more extensively fouled than those of the other exchangers. It was also apparent that the fouling was not evenly distributed with the hotter passes of the exchanger being more heavily fouled. There was a small amount of fouling on the shellside but not as much as for the other exchangers in the train. This is because these exchangers had new bundles in October 1986 and hence there was no residual shellside fouling.

The initial fouling resistance for the second operating period is slightly less than that for the first operating period. This could be considered as showing that there was a significant amount of fouling in the first 29 days of the first period of operation. If this were so allocating the whole of the difference between the first and second period initial points to shellside fouling may be erroneous. However the large amount of shellside fouling present when the exchangers were opened indicates that at least some of the initial fouling resistance must be due to shellside fouling.

After the shutdown for cleaning around day 756 the start-up value ($0.0012\ m^2KW^{-1}$) is approximately the same as for the second operating period ($0.0014\ m^2KW^{-1}$). However the fouling resistance then rapidly increases to exceed the peak value of the second operating period. This last point follows a six day period of minimum throughput, when low velocities may have caused rapid deposition.

Figure 5.11(a)

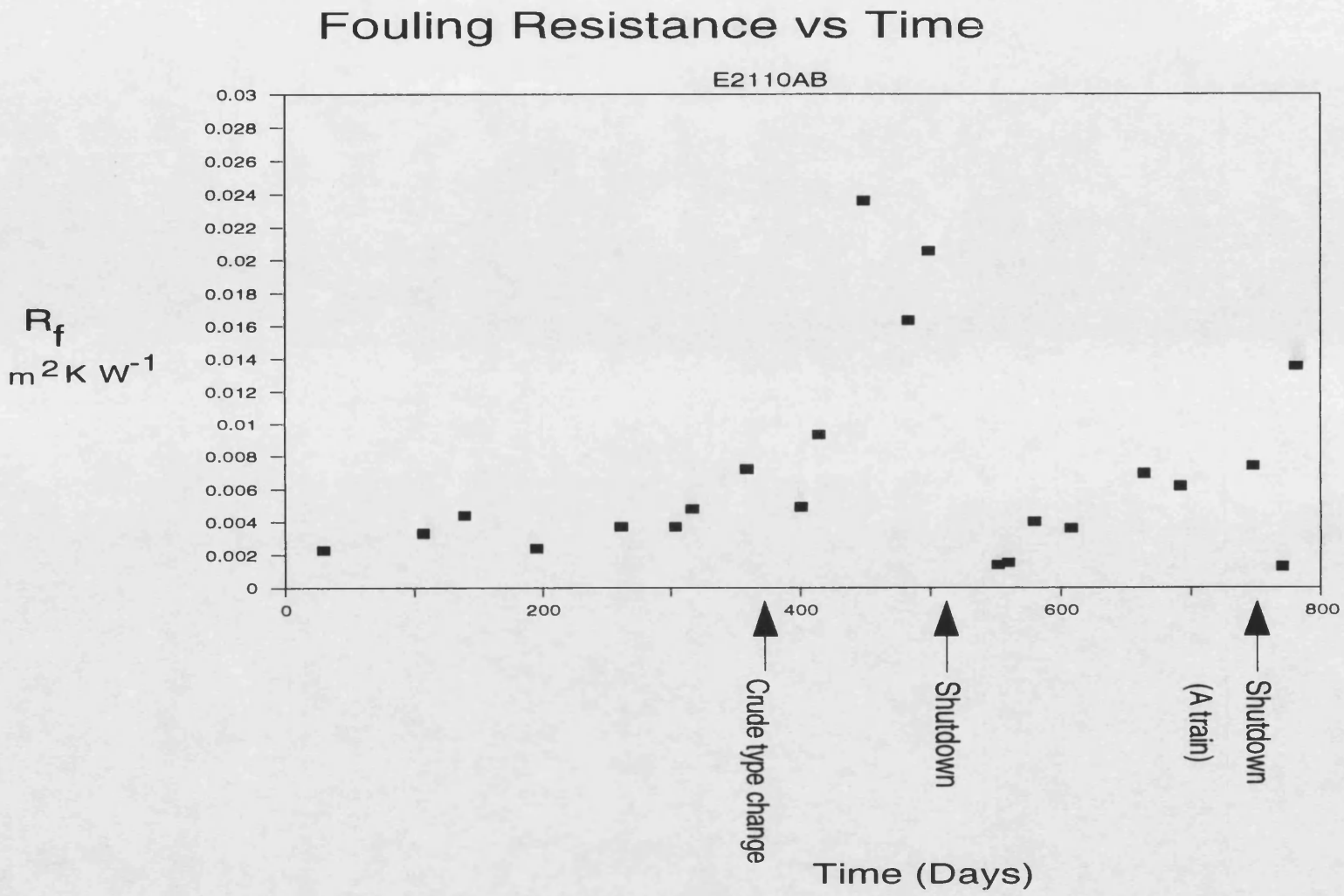
Fouling Resistance vs Time
E2110AB
R_f
$m^2 K W^{-1}$
0.03
0.028
0.026
0.024
0.022
0.02
0.018
0.016
0.014
0.012
0.01
0.008
0.006
0.004
0.002
0
0
200
400
600
800
Crude type change
Shutdown
(A train)
Shutdown
Time (Days)

Figure 5.12(b)

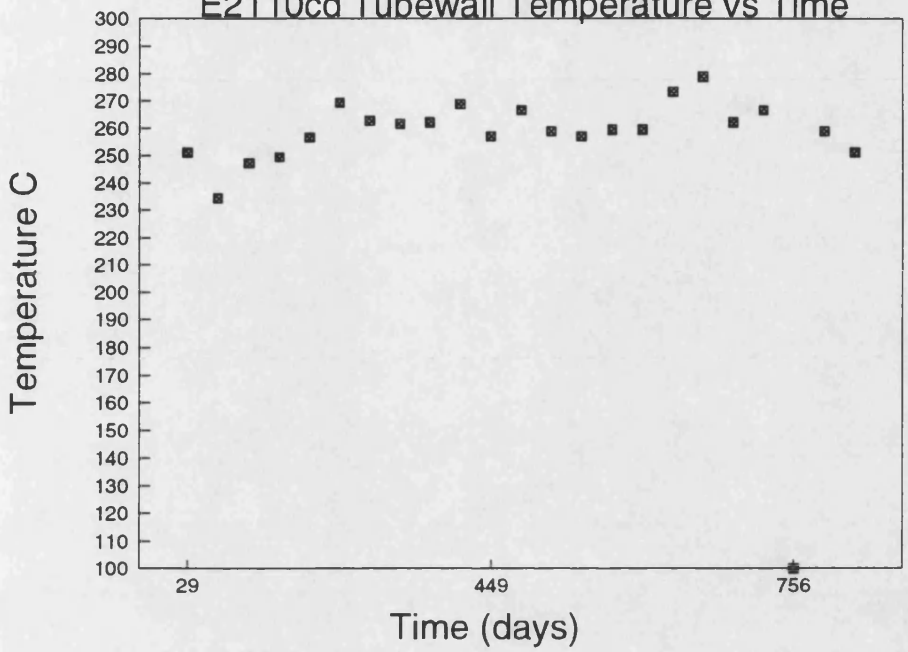

Figure 5.11(c)

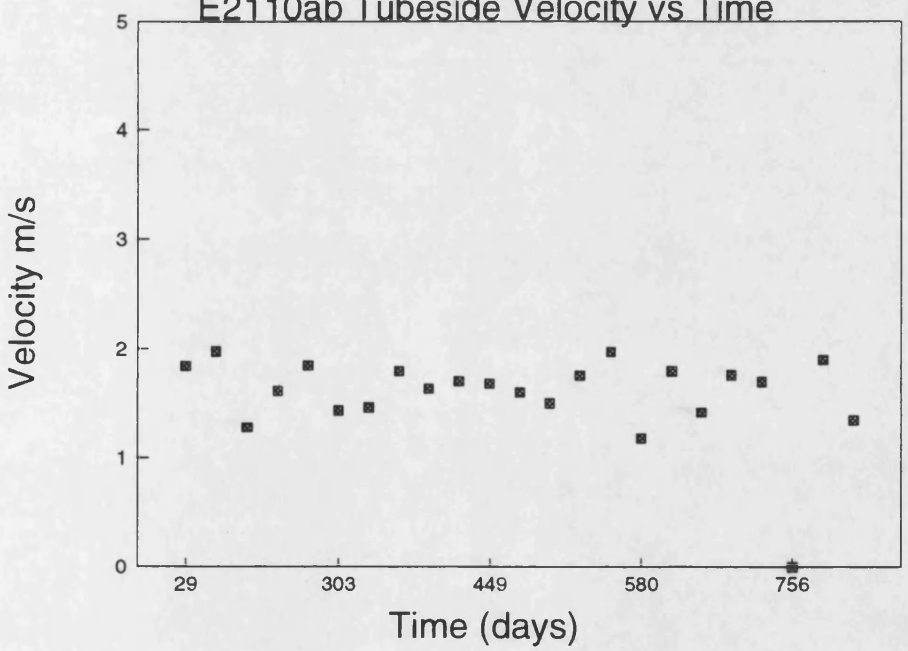

5.1.11 E2110cd

The fouling resistance against time graph for the E2110cd exchangers (Figure 5.12) shows a similar pattern to that of the E2110ab exchangers. The processing of slops and heavy crudes combined with a period of minimum throughput caused a peak in fouling resistance on day 449.

When the exchangers were opened for cleaning it was obvious that the tubes were extensively fouled with some of the tubes in the hottest pass being obviously completely blocked.

On start-up of the exchangers after cleaning the fouling resistance of E2110cd followed a similar pattern to the first period of operation until the flowrate on both the shell and tube side was increased to allow cleaning of the A train. This resulted in a reduction in fouling resistance.

Figure 5.12(a)

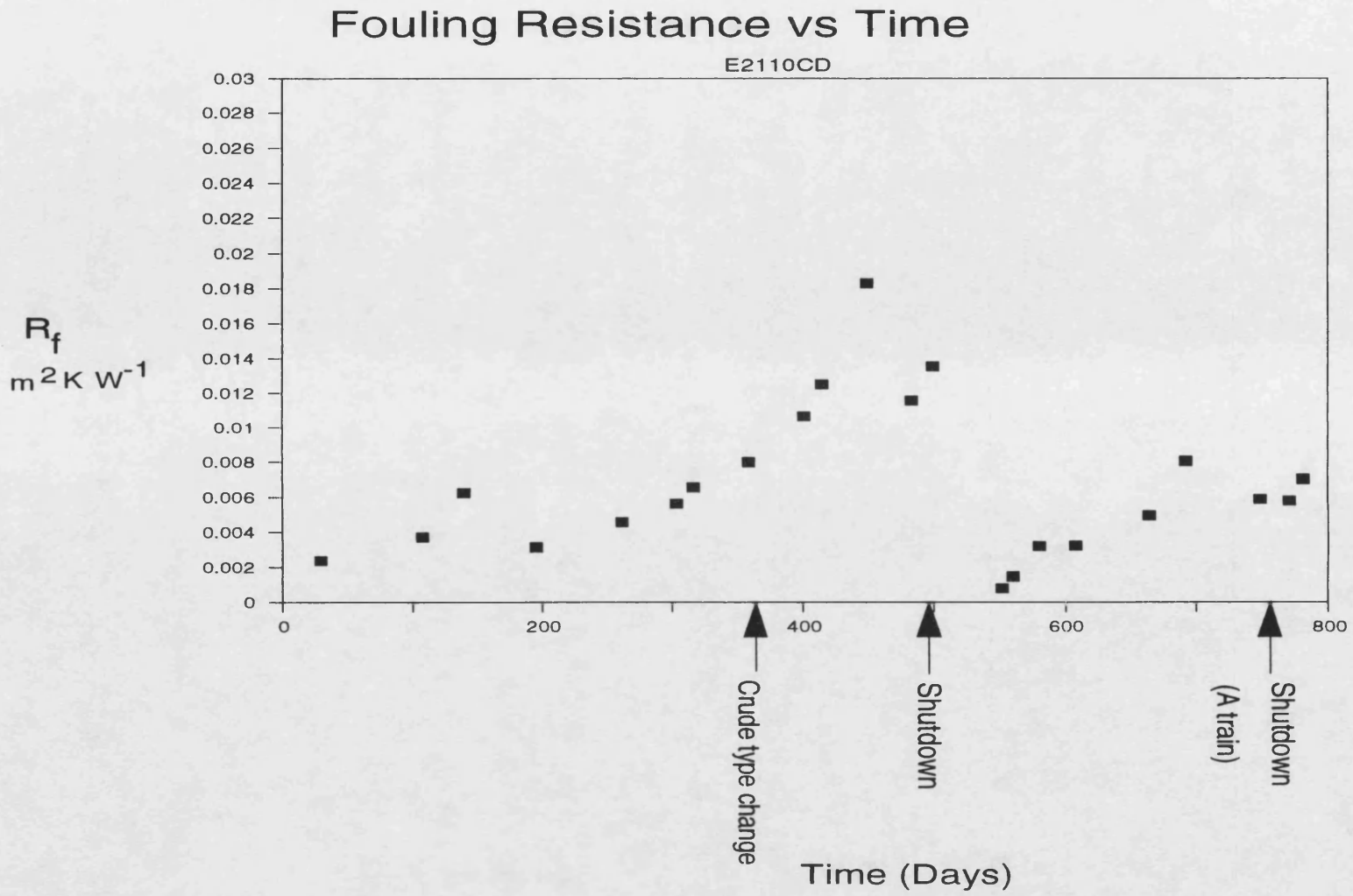
Fouling Resistance vs Time
E2110CD
R_f
$m^2 K W^{-1}$
0.03
0.028
0.026
0.024
0.022
0.02
0.018
0.016
0.014
0.012
0.01
0.008
0.006
0.004
0.002
0
0
200
400
600
800
Crude type change
Shutdown
(A train)
Shutdown
Time (Days)

Figure 5.12(b)

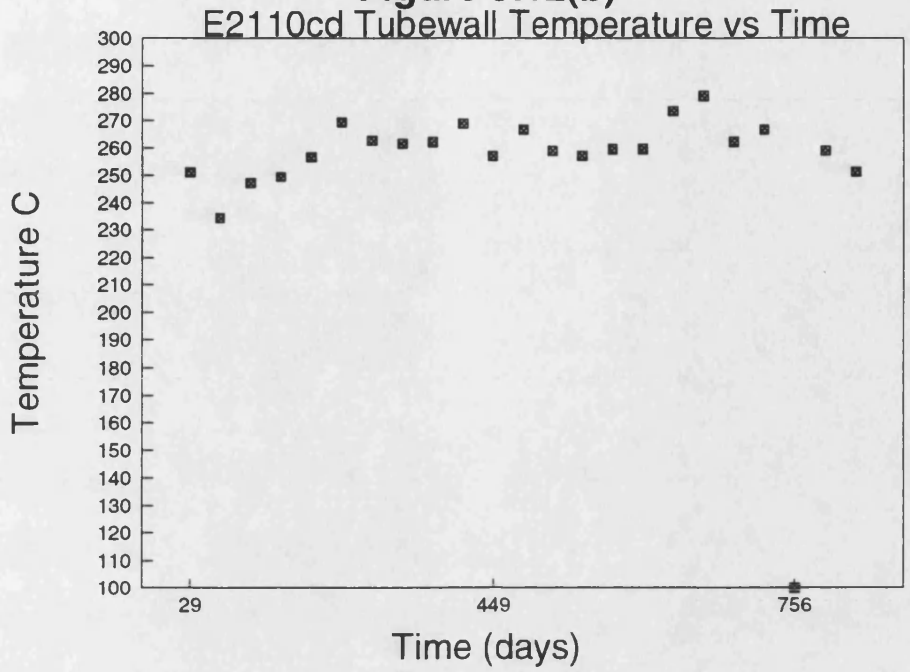

Figure 5.12(c)

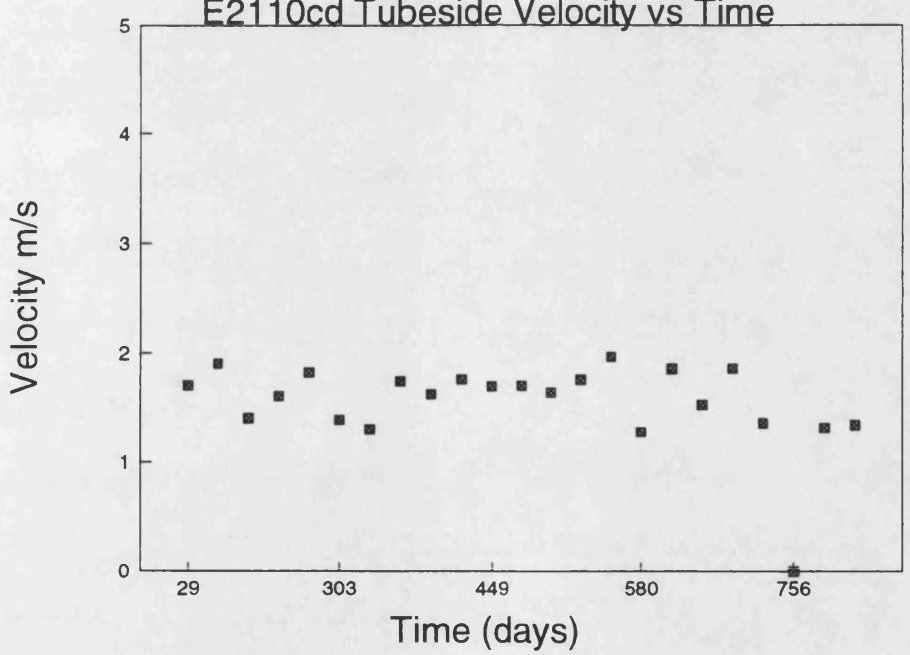

5.2 Estimation of fouling deposit thickness from pressure drop data.

Pressure drop measurements were made for the tubeside of each of the exchangers on 3.12.87 (day 414) and 7.1.88 (day 449). The data is presented in Table 5.1. All the readings were taken using the same pressure gauge. There were problems with the pressure tapping point on the outlet of E2104a, hence the reading for this exchanger is assumed to be erroneous.

An estimation of the deposit thickness was made using the procedure described in Chapter 3. The details are presented in Table 5.2. During the shutdown of days 501 to 551 the deposit thicknesses of some of the exchangers were measured using a set of callipers. The measurements were made at a distance of approximately 0.025 m from the end of the tube, and hence are only representative of the deposits at the ends of the tubes. The measured thicknesses are given in Table 5.3. Consideration should be given to;

- the fact that the callipers used may have indented slightly into the deposit,
- that some of the deposit may have been removed during the shutdown procedure,
- and also that the pressure drop measurements were made 85 and 50 days prior to the shutdown for cleaning and fouling deposits would presumably have continued to develop.

5.3 Comparison of estimated and measured fouling deposit thicknesses.

Table 5.3 shows that the mean measured deposit thicknesses broadly increase through the train with increasing operating temperature. The average deposit thickness measured for E2110a is slightly less than for the two downstream exchangers this may be due to the new tubes in the E2110a exchanger fouling to a lesser extent than the older tubes in the other exchangers. Although it should be noted that some of the tubes in the final

pass of the E2110b exchanger appeared to be completely blocked. Hence caution should be exercised in drawing detailed conclusions from this data as there was only sufficient time to measure a few tubes in each exchanger (the exchangers have on average 1305 tubes), and it is difficult to asses how representative those tubes in which the measurements were taken were. Nevertheless the data gives a qualitative indication of the amount of deposit present. The largest thickness measured was 2.8 mm which represents 15% of the tube inside diameter. The mean deposit thickness measured for the E2107a exchanger is less than that estimated from the pressure drop measurements. This could be due to some of the deposit being removed during the shutdown process and/or the callipers indenting slightly into the deposit during measurement.

The mean deposit thickness measured for the E2108a exchanger is greater than that estimated from pressure drop measurement. This may be due to the fact that the pressure drop for the E2108ab exchangers has to be measured across the two exchangers in series. Hence the estimated deposit thickness is the average between the two exchangers. Unfortunately it was not possible to measure the deposit thickness of the E2108b exchanger to determine if it were less than that of the E2108a exchanger. However from consideration of the slightly higher operating temperature of the E2108b exchanger it would be unlikely that it would foul to a lesser extent than E2108a. The discrepancy between the measured and estimated values is probably due to too few or non-typical deposit thicknesses being measured.

The mean deposit thicknesses measured for the E2110a exchanger is slightly less than that estimated from the pressure drop data. This could be due to the fact that some of the deposit was removed during the shutdown process and/or the callipers indented into the deposit during measurement.

This comparison of the estimated and measured deposit thicknesses shows that within the limited data afforded by this study it would appear that the pressure drop across an exchanger for which the design specifications are known provides a reasonable indication of the amount of deposit present.

5.4 Fouling Deposit Analysis

It was decided that the results of an analysis of the components present in the fouling deposits inside the tubes of the heat exchangers might prove advantageous in determining the type of fouling that was occurring in the preheat train. The analysis should also give an insight into those species within the crude oil that may contribute towards the fouling. The established techniques for analysis of such hydrocarbon deposits were used. This involved the following four fractions being obtained from a sample:

(i) the pentane soluble fraction, which is assumed to be resins and free oil contained within the sample,

(ii) the toluene soluble fraction which is assumed to be asphaltenes,

(iii) the coke fraction which is defined as the loss on ignition at 820K of the toluene insoluble fraction,

(iv) the remaining ash which is assumed to be inorganic and may be analysed using standard laboratory techniques such as mass spectroscopy or X-ray fraction scanning to determine those spices which are present.

Eaton and Lux[6] have published analysis of deposits both from the field and from laboratory simulations. They found that typically the pentane soluble, toluene soluble, coke and inorganic fractions are 50%,10%,30%, and 10% by weight respectively.

Samples of the tubeside fouling of four of the exchangers in the preheat train at Rotterdam were successfully shipped back to the laboratories at BP Sunbury for analysis. The exchangers were from the A train and were E2107A, E2108A, E2109a and E2110A.

The tests carried out on the samples at Sunbury were similar to those described by Eaton and Lux with the substitution of n-heptane for pentane and the use of X-ray fraction to conform with those methods used by BP. The results are presented in Table 5.4.

5.5 Conclusions

At all times the calculated fouling resistances for all of the exchangers were well in excess of the design (TEMA) figures. This is in agreement with the findings of other workers[1,2,3] and with data from other BP refineries. Inspection of Figures 5.1 to 5.12 shows that at start-up for the first operating period the exchangers were seemingly not perfectly clean, as on extrapolation of the graphs to time zero there is an apparent "clean" fouling resistance for the majority of the exchangers ranging from 0.0007 to 0.006 m^2KW^{-1}.

Lambourn and Durrieu[3], Butler and McCurdy[5] and Weiland *etal*[6] also present data from oil refinery exchangers which shows, on extrapolation, a fouling resistance in excess of the recommended TEMA value at start-up. However this apparent offset does not appear in the report by Lambourn and Durrieu[3] of laboratory experiments on the same crude oil types. This difference between refinery and laboratory studies may be due to the fact that experiments in the laboratory are more easily controlled thus reducing errors from measured parameters. This aspect is further discussed in Chapter 6.

Such a high initial fouling could result from a combination of the following factors;

(i) residual deposits on the tubeside after the *insitu* cleaning,

(ii) shellside deposits built up over a number of years,

(iii) errors in the first set of temperature data,

(iv) the exchangers fouled rapidly during the first twenty nine days of operation.

The recurrence of the apparent "clean" fouling resistances, albeit at a reduced level for many of the exchangers, after the remote cleaning during days 501 to 551 indicates that these calculated initial resistances are probably subject to error.

From analysis of the results from the exchangers in the preheat train the following general observations can be made.

a) The fouling resistance and the amount of deposit observed at shutdown increased along the exchanger train, with the coolest exchangers (E2104) having the lowest fouling resistances and the hottest exchangers (E2110) the greatest fouling resistances and the largest amount of tubeside fouling deposit. This would appear to indicate that the fouling from crude oils increases with increasing temperature.

b) The velocity of the crude oil through the tubes appears to have an effect upon the fouling resistance. The E2105 exchanger has a low design tubeside velocity but a higher fouling resistance than the next hotter exchanger. Also the majority of the B train exchangers exhibited a reduction in fouling resistance when placed on maximum throughput due to the simultaneous cleaning of the A train. Hence from this study it would appear that fouling from crude oils increases with decreasing velocity.

c) The composition of the feed stream had a dramatic effect upon the fouling rate. The majority of the exchangers in the preheat train showed a substantial increase in fouling resistance on the introduction of slops to the feed stream on day 390 and continued to foul at an increased rate as crudes such as Merey and further slops were processed. Merey is a Venezuelan crude it is a heavy crude with a specific gravity of 0.9495, it also has a relatively high sulphur content 2.28% by weight. (Kuwait oil the design crude oil for the refinery has a sulphur content of 0.36% by weight.) It is also a very viscous crude oil with a viscosity of 956 cSt at 20°C compared to 9.16 cSt at the same temperature for Kuwait crude oil.

d) The analysis of the deposits from the four A train exchangers shows that there are probably general similarities in the fouling mechanisms within the exchangers.

With the notable exception of the E2108a exchanger approximately 50% by weight of the deposit is n-heptane soluble i.e resins and free oil with only a small fraction 1-2% being toulene soluble i.e asphaltenes. Dickakian and Seay[7] claimed that asphaltene precipitation is the major mechanism in crude oil heat exchanger fouling. In a pilot unit it was found that the addition of asphaltenes to crude oil increased the fouling tendency. They proposed that the mechanism for fouling from ashaltenes is as follows:-

(i) incompatibility of the asphaltenes to the crude oil causes asphaltene precipitation,

(ii) the precipitated asphaltenes adhere to the hot surface,

(iii) the asphaltenes then carbonise to form coke.

Although the asphaltene weight percent of the deposits from the Rotterdam refinery was found to be low (1-2%). It may be that the third step in the proposed fouling sequence forms an open structure in which the other types of deposit become entrapped. The refinery at Rotterdam usually processed mixtures of several crude oils, this could be exacerbating the fouling problem due to incompatibility of the asphaltenes with the various crude oils. This is a phenomena which cannot be investigated using the data from the refinery as it would require detail knowledge of the asphaltene content of the mixed crude oils which is not readily available.

The deposit from the E2108A exchanger had approximately half the free oil and resins associated with the other deposit samples. The detailed X-ray analysis of the insoluble residue from this deposit showed that it had substantially higher sodium and chlorine levels. This could be considered to indicate that salt within the crude oil is being carried over from the desalting process and is being deposited in this exchanger. This may account for the somewhat erratic fouling pattern of this exchanger as it may be linked to the desalter performance. Unfortunately the data is not available to test this hypothesis.

Table 5.1 Pressure drop measurements.

Date		3.12.87 (Day 414)		7.1.88 (Day 449)	
Exchanger	ΔP expected at Design Throughput Bar g	ΔP measured Bar g	ΔP* corrected Bar g	ΔP measured Bar g	ΔP* corrected Bar g
	1.3	0	-	0.5	1.0
E2104a	1.3	0.8	1.5	1.0	1.8
E2104b	0.6	1.4	2.7	0.6	1.2
E2105	1.1	1.0	1.9	1.3	2.3
E2106	2.0	1.9	3.7	1.9	2.4
E2107a	2.0	2.1	4.0	1.2	3.4
E2107b	3.1	2.5	4.9	2.8	5.5
E2108ab	3.1	1.9	3.6	2.9	5.2
E2108cd	1.9	3.8	7.4	2.3	4.5
E2109a	1.9	3.7	7.0	2.5	4.9
E2109b	2.4	4.7	9.2	6.4	12.5
E2110ab	2.4	4.8	9.1	5.4	9.7
E2110cd					

* Pressure drop corrected to design flowrate.

Table 5.2 Deposit thickness estimated from pressure drop.

Exchanger	3.12.87 (Day 414)	7.1.88 (Day 449)
	Deposit thickness mm	Deposit thickness mm
E2104a	-	-
E2104b	0.25	0.49
E2105	1.96	0.96
E2106	0.79	1.06
E2107a	0.89	0.78
E2107b	0.98	0.26
E2108ab	0.63	0.75
E2108cd	0.20	0.71
E2109a	1.80	1.19
E2109b	1.70	1.20
E2110ab	1.77	2.11
E2110cd	1.76	1.83

Table 5.3 Measured deposit thickness.

Exchanger	Deposit Thickness mm	Exchanger	Deposit Thickness mm
E2107a	0.40	E2109a	1.28
	0.83		0.95
	0.38		1.35
	0.30		1.65
	0.28		1.05
	0.15		2.80
	mean 0.39		1.88
			1.80
			1.55
			1.55
			mean 1.59
E2018a	1.40	E2110a	1.08
	1.38		1.08
	1.50		1.23
	1.40		1.20
	1.10		1.60
	0.95		1.08
	1.63		0.40
	1.10		1.05
	mean 1.31		2.10
			1.00
			mean 1.18

Table 5.4 Deposit Analysis

Fraction Weight %	E2107A	E2108A	E2109A	E2110A
N-Heptane soluble	49.8	22.6	56.1	57.4
Toluene soluble	1.9	1.1	1.6	1.2
Insoluble residue	48.3	76.3	42.4	41.4
Total	100	100	100	100
Loss on ignition of insoluble residue.	32.8	37.2	24.5	25.3
Residue after ignition	15.5	39.2	17.5	16.1
Components in insoluble residue Weight % of total.	E2107A	E2108A	E2109A	E2110A
Iron	5.5	11.0	6.5	6.8
Sulphur	4.5	7.2	4.8	4.5
Sodium	3.1	11.6	3.8	2.9
Calcium	1.2	1.3	0.7	0.9
Zinc	0.4	0.4	0.5	0.5
Magnesium	0.2	0.2	0.1	-
Chlorine	-	5.5	0.2	0.1
Others	0.6	2.0	0.9	0.4
Unaccountable	32.8	37.0	24.5	25.3

References

(1) Lawler D. (1979) "Fouling by crude oil in refinery heat exchangers"

In: "Fouling Science or Art ?" (Pritchard A.M ed)

(2) Eaton P and Lux R (19) "Laboratory fouling test apparatus for hydrocarbon feedstocks"

(3) Lambourn G.A and Durrieu M (1986) "Fouling in crude oil preheat trains"

In: "Heat Exchanger Source Book" (Palen J.W ed) Hemisphere Washington.

(4) Bott T.R and Walker R.A (1971) "Fouling in heat transfer equipment"

Chem Eng (11) 391-394.

(5) Butler R.C, McCurdy W.N and Linden N.J (1949) "Fouling rates and cleaning methods in refinery heat exchangers"

Trans ASME **71** 843-847.

(6) Weiland J.H, McCay R.C and Barnes J.E (1949) "Rates of fouling and cleaning of unfired Heat exchanger Equipment"

Trans ASME **71** 849-853.

6 MODELLING

Operating data for the exchangers was collected from the refinery and the fouling resistance for each exchanger was calculated using the commercial computer package previously described in Chapter 3. From the calculated values of fouling resistance presented and discussed in Chapter 5, an indication of the dependency of fouling on temperature, velocity and composition was established. In this chapter these relationships are explored further and where possible mathematical models serviceable for predictive purposes are developed.

Due to the changing crude types and operating conditions throughout the project and the inherent errors that could be magnified in the calculation procedure there is some scatter of the results. This renders the development of meticulous mathematical models to predict fouling from the data collected on the preheat train difficult. The crude oil types and combinations processed change approximately every three days, and a given combination of crudes was never repeated during the project. This makes the establishment of correlations between crude oil type and fouling rate difficult. The data from the refinery was collected at approximately monthly intervals, with only a general impression of the operating strategy for the intervening period being acquired. Hence any models developed had to be based upon the incremental change in the operating conditions from month to month. This makes the modelling of velocity and composition effects difficult as the parameters can change significantly during the time intervals at which data is collected. However temperature effects are more easily correlated as all the exchangers operate at different temperatures but with the same tubeside fluid. Hence for a specific crude oil combination at a given flowrate a reasonable range of temperatures were observed.

6.1 Modelling of hydrocarbon fouling.

The wide range of feedstocks and operating conditions encountered in the oil refining industry raise difficulties in forming generalisations about the mechanisms involved in

the formation of fouling deposits. The majority of the published models assume that the fouling rate of a whole exchanger can be modelled in terms of a single averaged set of parameters such as temperature, velocity, composition and geometry. However it should be possible to apply the same models locally to determine the local fouling rates.

Crittenden *et al*[1] and Crittenden[2] provide detailed summaries of hydrocarbon fouling covering fouling from liquids. Froment[3] provides a review of high temperature gas phase fouling from hydrocarbons.

Nelson[4] developed one of the early refinery data based fouling models. Nelson presented a method to calculate the resistance of coke deposits from oil. This model suggests that the rate of deposition is dependent upon the thickness of the thermal boundary layer. The thicker this layer the more oil is exposed to high temperature and hence the more coke is formed. Data is presented to confirm that the fouling rate can be reduced by increasing velocity. This simple model does not allow for any removal of the deposit. Although the changing nature of the coke deposit with increasing temperature is mentioned by Nelson no attempt to determine what effect this would have on the fouling resistance was made.

Atkins[5] developed a two layer concept with a porous coke layer adjacent to the fluid and a hard coke layer adjacent to the wall. Atkins collated data from a range of fired heaters on oil refineries, and found a constant increase in coke resistance with time. From this data he published a guide to the selection of design fouling resistances for hydrocarbon streams. The fouling resistance is based on the sum of two resistances:

(i) the resistance of the porous coke layer in contact with the process fluid, based on the TEMA fouling factor, and

(ii) the coking rate resistance which is characterised by temperature and composition and varies with time. This resistance had to be read off a graph based on data collected at the refinery.

In this model there is no allowance for any removal of the deposit. Atkins' analysis gives rise to a linear dependence of fouling rate with time, but is not readily suited to situations where there would be frequent changes in operating conditions and/or feedstocks.

Much of the published work on refinery heat exchangers[6,7,8,9] has been concentrated on the comparison of cleaning methods or antifoulants. Few models based on refinery data have been published.

6.1.1 Temperature Effects

The mechanisms involved in fouling from hydrocarbon streams are complex as many of the fluids processed in industry are diverse mixtures of hydrocarbons with the possibility of many varied reactions involving the constituents. Hence a simple dependence of fouling rate on temperature is not always the case.

Several workers[10,11] have found that the rate of fouling from hydrocarbons increases exponentially with temperature. Watkinson and Epstein[10] investigated the fouling from sour gas oils in the laboratory. The data from these experiments can be fitted to an equation of the form;

$$\textit{instantaneous fouling rate} \propto e^{-\frac{E}{RT_w}} \qquad 6.1$$

Where E is the activation energy

R is the Universal gas constant

T_w is the tubewall temperature

The activation energy was calculated as 120 kJ mol^{-1}.

Taylor[12] obtained data that fitted the same type of relationship and found an activation energy of 40 kJ mol^{-1} from laboratory work with pure n-paraffins. Crittenden, Hout and Alderman[12] studied the polymerisation of styrene and determined an activation energy of 39 kJ mol^{-1}. Unfortunately there has been no published data from which a relationship

of this type can be determined for crude oils. However it would not be unreasonable to assume that the activation energy for chemical reaction fouling from crude oils would lie in the range of published values for other hydrocarbon systems.

6.1.2 Velocity effects

Kern and Seaton[14] developed a model to predict particulate fouling rates based on the physical and mathematical relationships between the pressure drop through a tube and the accumulation of fouling with time. The model so developed is the summation of a deposition term and a removal term.

The deposition rate is assumed to be constant with time and is expressed thus;

$$Rate \quad of \quad deposition \quad = kcW \qquad 6.2$$

where k is a proportionality constant

c is the unit dirt content of the fluid

W is the mass flowrate

This deposition rate appears to be independent of temperature. However the unit dirt content can be expressed as a function of temperature, for example as the solubility of the fouling species in the process fluid.

The removal mechanism is assumed to be shearing of the deposit from the wall and is expressed thus;

$$Rate \quad of \quad removal \quad = K_1 \tau x_\theta \qquad 6.3$$

Where K^1 is a proportionality constant

τ is the shear stress

x_θ is the deposit thickness at time θ

Hence the change in deposit thickness with time is given by,

$$\frac{dx_\theta}{dx\theta} = kcW - K_1 \tau x_\theta \qquad 6.4$$

From data on the fouling of refinery heat exchangers Kern and Seaton[14] observed that the fouling resistance increased asymptotically with time. This behaviour can be approximated with an equation of the form;

$$R_\theta = Rf^*(1 - e^{-B\theta}) \qquad 6.5$$

Where R^* is the fouling resistance at the asymptote

B is a constant proportional to the shear stress

Watkinson and Epstein[10] compared the results from laboratory tests on sour gas oils to this Kern and Seaton model. The data fitted the asymptotic fouling resistance model but the relationships between flowrate and the asymptotic fouling resistance were found to be at variance with those predicted by the Kern and Seaton model which is based on the difference between a deposition rate proportional to the mass flowrate and species concentration, and a removal rate which varies with shear stress and deposit thickness. Their analysis predicts that the asymptotic fouling resistance R_f^* is proportional to the mass flowrate divided by the shear stress.

$$R_f^* \alpha \frac{W}{\tau} \qquad 6.5a$$

Shear stress τ can be difined thus

$$\tau = \frac{f\rho w^2}{2} \qquad 6.5b$$

Subsitution into equation 6.5a gives

$$R_f^* \propto \frac{1}{W} \qquad 6.6$$

and as B is proportional to shear stress it follows form equation 6.5a that

$$B \propto W^2 \qquad 6.7$$

However the data collected by Watkinson and Epstein showed that;

$$R_f^* \propto \frac{1}{W^2} \qquad 6.8$$

and

$$B \propto W \qquad 6.9$$

The relationship between the initial fouling resistance and flowrate was also different. Differentiation of equation 6.5 as time tends to zero gives;

$$\frac{dR_f}{dt}|_{t\to 0} \propto BR_f^* \qquad 6.10$$

Substituting equations 6.6 and 6.7 into equation 6.10 gives;

$$\frac{dR_f}{dt}|_{t\to 0} \propto W \qquad 6.11$$

That is to say the initial fouling resistance is proportional to the mass flowrate. The data from the experiments of Watkinson and Epstein indicates that the initial fouling resistance decreases with increasing mass flowrate. However increasing the velocity of the fluid through the tubes would also reduce the tubewall temperature, via the increase in film heat transfer coefficient. In fact the data collected by Watkinson and Epstein showed that the change in fouling rate with velocity could be wholly attributed to this effect.

The effect of the velocity of the process fluid on the fouling rate is dependent upon the type of the prevalent fouling regime. If the fouling rate is mass transfer controlled then increasing the velocity could exacerbate the fouling rate. For reaction rate controlled systems consideration should be given to the effect that changes in velocity have on the tube wall temperature. Velocity has a direct effect upon the heat transfer coefficient ie $h_{io} \alpha Re^{0.8}$. The tube wall temperature can be calculated via

$$t_w = t_b + \frac{h_o}{h_{io} + h_o}(T_b - t_b) \qquad 6.12a$$

Thus increasing the tubeside velocity will increase h_{io} which will decrease the term $\frac{h_o}{h_{io}+h_o}$ and thus t_w would decrease. Hence it can be seen that the relationships between the fouling rate with temperature and velocity are inter linked. It is possible for the fouling rate from a given hydrocarbon to be controlled by either

temperature or velocity depending upon the prevailing conditions. Crittenden *etal*[11] postulated that at low temperature and high flowrates the reaction rate was the controlling factor (*ie* temperature) and that at high temperatures mass transfer of the reactant to the surface was the controlling step (*ie* velocity).

These simple dependencies have been expanded by several workers to include such parameters as first order reaction rate constants[13], particulate sticking probability[10], and back diffusion and convection[13]. However these models require detailed knowledge of the composition of the process streams and so cannot be readily utilised for the prediction of crude oil fouling, although Crittenden and Kolaczkowski[15] have modified their model so that lumped parameters can be approximated from plant data. This model is further discussed in Section 6.3

6.1.3 Composition effects

The composition of the crude oil processed and the presence of slops, which are spillages from various process units on the refinery and/or off specification products, had a profound effect on the fouling rate in the preheat exchangers (previously discussed in Chapter 5). There have been no published models relating the fouling rate and crude oil type. However several workers have found that the presence of certain species such as sulphur[12,16], oxygen[17], nitrogen[16], and chlorides[18] can have a significant effect upon the fouling rate of various hydrocarbons. The effect of these species is generally thought to be via the contribution of free radicals that promote autoxidation and polymerisation reactions (see Chapter 1). Few distinct models have been published based purely on the composition of a mixed hydrocarbon stream, primarily because the bulk of work on hydrocarbon fouling has been on pure hydrocarbons. The results from work investigating the effects of contaminants usually take the form of an adjustment to the relationship between fouling resistance and temperature, where the activation energy is modified by the presence of the contaminant (see Chapter 1).

6.2 Development of a fouling model from refinery data

6.2.1 The effect of temperature on fouling rate.

The data from the refinery was analysed to determine the relationship between the fouling rate and temperature. It was decided to exclude exchangers E2105 and E2106 from the initial modelling work as the shellside flow for these exchangers is erratic.

The fouling rate for each of the exchangers was determined from Figures 5.1 to 5.12. From inspection of the fouling resistances against time graphs for the first operating period of 501 days it can be seen that there are two distinct phases of fouling with the change in fouling rate coinciding with the introduction of heavy crudes and slops on day 390. (See Chapter 4).

The fouling for the light crudes up to day 390 was assumed to be linear with time and a straight line was fitted through the data to determine the fouling rate. During this period there was relatively little variation in the tubewall temperature for a given exchanger (detail in Appendix C). Hence the average tubewall temperature was plotted against the fouling rate to determine the relationship between fouling rate and temperature. (See Figure 6.1).

It has been generally found [10,11,12] that the fouling rate increases exponentially with temperature. Data is often fitted to an Arrhenius relationship

$$\frac{dR_f}{dt} = A e^{\frac{-E}{RT_w}} \qquad 6.12$$

Figure 6.2 shows how the data from the refinery fits this relationship. The fouling rate was developed by fitting a straight line through the first eight points on the fouling resistance versus time graph for each of the exchangers, (Figures 5.1 to 5.12). From the gradient of Figure 6.2 the activation energy E= 32.66 kJ mol^{-1}. The scatter in the data makes it difficult to estimate the precision of E but it is unlikely to be less than 20 or higher than 45 $kJmol^{-1}$. This compares favourably with values published in the literature.

liquid jet fuels[19]	E=42 kJ mol^{-1}	$149<T_w<260°C$
pure n-paraffins[12]	E=40 kJ mol^{-1}	$93<T_w<260°C$
styrene polymerisation[11]	E=39 kJ mol^{-1}	$22<T_w<98$ °C

Inspection of Figures 5.1 to 5.12 (Chapter 5) shows that at start-up the exchangers were apparently not perfectly clean as, on extrapolation of the graphs to time zero, there is an apparent "clean" fouling resistance for each of the exchangers, ranging from $7.04x10^{-4}$ to $2.64x10^{-3}$ m^2KW^{-1} (detail in Table 6.1a) This resistance may result from a combination of the following factors;

(i) residual deposits after the insitu cleaning (see Chapter 4),and/or,

(ii) errors in the calculation of the initial fouling resistance (see Chapter 3) and/or

(iii) very high initial fouling rates causing the fouling resistance to rise rapidly in the initial period of 29 days.

As it was not possible to monitor the start-up of the exchangers for the first operating period of 501 days it was not possible to determine the cause of the high initial fouling resistances. However in March 1988 the preheat train was shutdown and cleaned (see Chapter 4). The start-up of the exchangers was monitored closely. It was found that the high initial fouling resistances were repeated. As the exchangers were known to have been thoroughly cleaned it is unlikely that these fouling resistances was due to residual deposits. However the tube bundles were left to stand in the atmosphere for several days after cleaning, and developed a layer of iron oxide, which although it is unlikely to have caused the apparent high initial fouling resistances (deposit thickness would need to be > 1cm) it may provide a rough surface that could promote fouling from the crude oil. The first set of data was taken on the first day of "steady" operation, and the initial fouling rate would have to be very high ($7.04x10^{-4}$ to $2.64x10^{-3}$ $(m^2KW^{-1})day^{-1}$) to attain the high start-up fouling resistances.It is more probable that the initial high resistances are due to errors in the calculation of the fouling resistance at start-up.

Lambourn and Durrieu[9] in studies on refinery heat exchangers and several other wor-

kers[6,7,10] have found that the fouling resistance at time t=0 is not zero. However this apparent offset does not appear in the reports of experiments in laboratories[9]. This is maybe due to the fact that the experiments in the laboratory can be closely controlled reducing the errors from measured parameters.

Typically experiments in the laboratory are run with constant heat flux (using electrical heating) and use a thermocouple embedded in the tube wall to measure the surface temperature. The fouling resistance is then derived thus;

$$R_f = \left(\frac{1}{U_D} - \frac{1}{U_c} \right) \frac{d_i}{d_t}$$

where d_i is the tube internal diameter

d_t is the diameter at the thermocouple location

and the U values are determined from

$$U = \frac{Q}{A_t(T_t - T_b)}$$

where A_t is the cross-sectional area at the thermocouple

T_t is the temperature measured by the thermocouple

T_b

is the bulk temperature

Q the heat flux and A the surface area are accurately know from the electrical heater and the tube geometry respectively. Hence the errors in the fouling resistance will be smaller than for the field situation due to the virtual elimination of errors in Q which are relatively large in the industrial situation as U_c and U_d are calculated in completely different ways.

Also there are fewer temperatures to be measured hence less error will be introduced this way, and the measuring equipment used in the laboratory will probably be more accurate.

Table 6.1a shows the error in temperature measurement that would need to be present to give the start-up fouling resistances for the second period of operation from 19.4.1988. Given the transient nature of a start-up in an industrial situation this would not appear unreasonable, hence it may be that the apparent initial fouling resistances stem from a lack of precise control over the start-up of the CDU and are not truly representative of a fouling deposit.

The start-up for the first set of data (13.11.86 - 25.2.88) was not observed and hence it is impossible to determine the temperature errors that would have been required to give the offset. However inspection of Table 6.1b shows that the offset is approximately the same as for the start-up 19.4.88, with the exception of the $E2108_{a-d}$. However there would probably have been significant shellside fouling at the start-up of the first period of operation which will have contributed to the first apparent start-up fouling resistance.

The errors in the absolute value of the fouling resistance should decrease as fouling proceeds, when the temperature approaches would increase thereby diminishing the effect from temperature measurement errors. Hence it was decided to allow for this initial fouling resistance error in the temperature model with the addition of a constant thus the integrated form of equation 6.12 becomes:

$$R_F = c_i + \int A \exp(-\frac{E}{RT_w})dt \qquad 6.14$$

Where c_i is the initial fouling resistance for a given exchanger.

In order to use equation 6.14 for predictive purposes it is necessary to determine the relationship between the initial fouling resistance and the characteristics of the individual exchanger.

In Chapter 3 it was shown that the potential error in the calculated fouling resistance is strongly dependent on the temperature difference for each stream in the exchanger. Decreasing the temperature difference increases the potential error with the tubeside (crude oil) temperature difference having the greatest effect. It was also shown in the same section that the closer the inlet temperatures of the two streams the greater the potential error in fouling resistance.

The thermal effectiveness of an exchanger as defined in the Heat Exchanger Design Handbook (HEDH) is given by,

$$P = \frac{t_2 - t_1}{T_1 - t_1} \qquad 6.15$$

A low effectiveness could be the result of a low temperature driving force which would result in a low temperature gain on the tubeside i.e a small temperature difference on the tubeside and hence a relatively large potential error in the calculated fouling resistance. Hence it would not be unreasonable to expect the exchangers to have a low effectiveness and hence high potential fouling resistance error at start-up.

The relationship between the initial thermal effectiveness and the observed off-set on start-up is shown in Figure 6.3. This graph can be used to determine the initial fouling resistance c_i.

6.2.2 Testing the temperature model.

Equation 6.14 developed from the data for the first operating cycle during the processing of light crudes was then used to predict the fouling resistance of the exchangers in the preheat train after they had been shut down and cleaned i.e in the second operating cycle. The results are shown in Figures 6.4 to 6.13.

From inspection of Figures 6.4 to 6.13 it can be seen that the temperature model over predicts the fouling resistances of E2104A and E2104B, but in general either correctly or slightly under predicts the fouling resistance of the other exchangers. This may be

indicative of a different deposition mechanism in the cooler E2104 exchangers to that prevailing in the hotter exchangers and this would seem to confirm the temperature threshold observed by Lawler[8] for crude oil.

However the temperature model only describes the deposition of a fouling deposit and it may be that the deposit formed at the lower temperature is more easily removed than that formed at the higher temperature. If this were the case it would seem to imply that the deposition term for those exchangers where the temperature model consistently under predicts the fouling resistance, E2108AB and E2018CD, is insufficient and there is the possibility that another form of fouling is taking place simultaneously with the chemical reaction fouling.

The tubeside surface temperature model was developed based on the assumption that all the fouling was on the tubeside. However as described in Chapter 5 there was a significant amount of fouling on the shellside of some of the hotter exchangers. The surface temperature on the shellside would be higher than on the tubeside and it would not be unreasonable to expect that if the two process fluids were the same that fouling would proceed more rapidly on the shellside. However the process fluids on the shellside are generally considered to be "cleaner" than crude oil and so would be expected to foul to a lesser degree. This is a composition effect as many of the "heavier" components, such as asphaltenes thought to cause fouling, are not present in the majority of the shellside streams with the exception of the bottom pump around and residue streams.

Reinforcement of this hypothesis is given by the fact that the temperature model for those exchangers with cleaner fluids, such as the pump around streams E2107a and b, E2109a and b, and E2110ab and cd, Figures 6.6, 6.7, 6.8, 6.9, 6.12, 6.13, fit the data reasonable well with in many cases the predicted fouling resistance line cutting across the saw-tooth pattern of the measured values. In contrast the temperature model for the E2018 exchangers (Figures 6.8 and 6.9) consistently under predicts the fouling resis-

tance. These exchangers have the residue stream on the shellside a fluid which has a large proportion of the "heavier" components and were found to have been badly fouled when the exchangers were opened, (see Chapter 5).

Detailed consideration of the effects for shellside fouling from various process streams is beyond the scope of this project and would require knowledge of the distribution of the fouling resistance between the shell and tube sides which could not be easily gained from a study based on industrial heat exchangers.

Since it was assumed that the only deposition process in the exchangers in the preheat train is that of chemical reaction fouling, and that the deposition is fully described by the temperature model developed then any difference between the measured and the predicted deposition rate must be due to the effects of velocity and/or composition and the omission of shellside fouling.

6.2.3 The effect of velocity on fouling rate

The design velocities for the exchangers in the preheat train, with the notable exception of the E2105 exchanger, are approximately either of two values. The E2108 and E2110 exchangers have a design velocity of approximately 2.6 m s^{-1} and the E2104 E2107 and E2109 exchangers have a design velocity of approximately 3 m s^{-1}. Thus the tubeside velocity through the exchangers for any given crude flowrate is approximately the same. This lack of variation of tubeside fluid velocity between the exchangers reduces the ability to develop a velocity based fouling model from the refinery data.

A further difficulty with the refinery data arises from the fact that the data was collected as discrete sets of readings at monthly intervals. Hence comparison between the results for one month with those of other months is difficult as sufficient detail of changes in the operating conditions in the intervening periods were not available.

With due consideration to these limitations the data from the refinery was analysed to determine the relationship between velocity and fouling rate. Figure 6.14 shows the tubeside velocity plotted against the difference between the measured fouling resistance

and the deposition rate predicted from the temperature model. The data is scattered about zero difference, which would appear to indicate that the velocity effect is accounted for in the change in surface temperature as found by Watkinson and Epstein[10] and discussed in Section 6.1.2. However if the effect of velocity is reflected solely in the change in surface temperature then it cannot be removal of the deposit by shearing that causes the saw tooth pattern of the measured fouling resistance graphs. The removal of the deposit from the tubes possibly by back diffusion, with the deposit from one type of crude being soluble in another may cause this type of fouling.

6.2.4 The effect of composition on fouling rate.

The refinery at Rotterdam processes blends of several different crude oils. It takes approximately three days to process the contents of one storage tank dependent on throughput. Hence the crude oil blend changes approximately twice a week, with the number of crude oils in a blend ranging from 1 to approximately 15. This makes correlation of fouling rate against composition very difficult, as the composition of the feedstock is almost constantly changing.

During the first 390 days of the first period of operation, the crude oils processed were generally light crudes (S.G < 0.87). The classification of crude oils into heavy and light is somewhat arbitrary and was developed in the crude oil processing industry based on the experience of blending and processing various crude types. Heavy crudes tend to have a higher asphaltene and sulphur content, constituents which are generally thought to promote fouling. The presence of a heavy crude oil or slops in the crude oil blend appears to have a significant effect on the fouling rate. There was an appreciable increase in the measured fouling rate after the introduction of 2% v/v of slops on day 390. The slops can come from almost any part of the refinery as all spillages and overflows are routed to the slops tank. Hence it is virtually impossible to determine the exact com-

position of this stream. The slops are usually mixed with the crude oil in the storage tanks and then processed through the distillation unit, at no greater than 5% v/v of the feed stream.

Heavy crudes such as Merey (sg = 0.9495) and Hoorn (sg = 0.9) were also processed during the period from day 390 to the shutdown. Unfortunately no readings were taken on the days when these crudes were being processed so it is not possible to determine the precise effect of the heavy crude oils. The primary effect of the heavy crude oils is a modification to the fouling rate/velocity relationship. A temperature model developed from the data for the operating period covering the processing of the heavy crude oils was developed in a similar manner to that described in section 6.2.1. The heavy crude oils have a lower activation energy of 21.25 $kJmol^{-1}$ see Figure 6.15, which would give a greater fouling rate than the light crude oils at the same surface temperature. Regrettably it was not possible to test the model for the heavy crude oils as these crude oil types were not processed again during the project.

Investigation of the back diffusion of deposits into various different types of crude oil is beyond the scope of this project due to the frequent changes in feedstock and the lack of repetition of a given combination of crude oils.

6.3 Testing the validity of a published temperature and velocity fouling model.

Crittenden *et al*[15] and Kolaczkowski *et al*[20] have shown that a simplified version of a mass transfer and kinetic deposition model (Kolaczkowski[21]) could be used to predict fouling in a heat exchanger network. This is the first attempt at incorporating predictive fouling models into a crude oil network simulation program. In the absence of plant data they were unable to validate this novel approach. The full derivation of the coefficients is available in Kolaczkowski[21]. The simplified version has also been described in the subsequent publications[15,20]. The manner in which the characteristics of the exchanger

are modelled has also been described in the explanations of the simlified technique. In this section the technique proposed[15] of calculating the model's coefficients is applied and the model is tested on plant data. The coefficients are determined from historical plant data. The program known as Minerva was developed in microsoft quickbasic (v 4.0) and runs on an IBM AT or compatible machine. When the model was run in simulation mode, known variations in: crude flow, shellside flow, and shellside ilet temperatures were modelled. In the model it is assumed that the fouling rate is the sum of a deposition rate and a removal rate. In the simplified version[15] the deposition rate is assumed to be kinetically controlled and the deposit removal is assumed to be via fluid shear. In addition, fouling is assumed to occur on the tubeside only. A further simplification is introduced by ignoring the effect of deposit build-up on fluid velocity and hence on removal by shearing. Thus the fouling rate is defined as

$$\frac{dR_{fi}}{dt} = A\exp\left(-\frac{E}{RT_{fi}}\right) - \frac{CM^2R_{fi}}{\rho\pi^2\left(\frac{d}{2}\right)^4} \qquad 6.3.1$$

integrating equation 6.3.1 at constant M gives,

$$R_{fi}(t) = \frac{A}{cu^2\rho}\exp\left(-\frac{E}{RT_{fi}}\right)(1-\exp(cu^2\rho t)) \qquad 6.3.2$$

where

$$R_{fi}(\infty) = \frac{A}{cu^2\rho}\exp\left(-\frac{E}{RT_{fi}}\right) \qquad 6.3.3$$

When t=0,

$$\left.\frac{dR_{fi}}{dt}\right|_{t=0} = A\exp\left(-\frac{E}{RT_{fi}}\right) \qquad 6.3.5$$

The coefficient A, C and E can be be described in a simplified from as follows:

A is a pre-exponential factor which is dependent upon feedstock composition.

C is a function of the Fanning friction factor and the physical characteristics of the deposit.

E is the activation energy and if also a function of feedstock composition.

For a more detailed description then consult Kolaczkowski[20]

In order to use this model the coefficients F, C, A and E need to be evaluated from plant data. For this to be done it must be assumed that the system under study exhibits asymptotic fouling.

The results of the calculated fouling resistances may be interpreted as having either an exponential or a linear variation with time. In Section 6.2.1 it was assumed that the fouling rate was linear with time over the first 390 days of operation. For some of the exchangers there is considerable scatter in the results and the pattern of fouling is open to interpretation. For example it could be considered that the exchanger E2104A exhibits asymptotic fouling as the fouling resistance increases by approximately 200% from day 261 to day 316 but then stays approximately constant until the shutdown for cleaning. Similarly if the result on day 358 were considered to be erroneous then the E2110A and B exchangers could also be considered to exhibit asymptotic fouling. The E2104A and E2110A and B exchangers represent the extremes of temperature measured in the preheat train, hence it was decided to use the data from these two exchangers to evaluate the coefficients in the model.

6.3.1 Determination of the coefficients A, C and E.

Since the Minerva computer program was written in British Engineering units, the coefficients A, C and E were determined in non SI units. The coefficients were determined using the plant data obtained in the first operating period. This requires the interface temperature, calculated using

$$Q = \frac{\Delta t}{\Sigma R} = \frac{T_i - T_b}{\frac{1}{h_{io}}}$$

and the simultaneous solution of equation 6.3.3 for both the exchangers. The data used from the two exchangers is presented in Table 6.3.

Simultaneous solution of the equations yields the following results for the light crudes.

E= 10327 Btu/(lb mol)

A/C= 7205 (h ft °F lb)/(Btu s^2)

C= 0.00045 (ft s^2)/ (month lb)

Although the units for the coefficients appear clumsy, they refeclt the convention adopted by the authors in calculating the initial rate of fouling on a monthly basis, showing the slow nature of the fouling process. These coefficients were then used in the Minerva program to predict the fouling of the exchangers on the Rotterdam refinery for those periods when light crude oil types were processed. The results are presented in Figures 6.16 to 6.21. Initially the coefficients were used to predict the fouling of those exchangers not used to determine them during the first operating period of 390 days. Then the coefficients were used to predict the fouling resistances of all the exchangers during the operating period after the shutdown for cleaning.

6.3.2 E2015

Figure 6.17 shows the fouling resistance predictions for this exchanger in the first operating period. It shows approximately the correct pattern of fouling with an overall increase in fouling resistance with time. The predicted values are generally less than those calculated from the plant data. This may be because the model takes no account of shellside fouling.

Figure 6.23 shows the predictions of the fouling resistance for this exchanger in the second operating period. The discrepancy between the predicted value and that calculated from the plant data is greater than for the first operating period. However the predicted pattern of fouling resistance is correct with an overall increase in fouling resistance with time but the actual predicted values are greater than those calculated.

This may indicate that the temperature relationship and particularly the activation energy could be different for those combinations of crude oil processed in the second operating period.

6.3.3 E2107A

Figure 6.18 shows the predictions of fouling resistance for this exchanger in the first operating period. It shows approximately the correct pattern of fouling. The predicted values are generally less than those calculated from the plant data. This may be because the model takes no account of shellside fouling.

Figure 6.24 shows the predictions of fouling resistance for this exchanger in the second operating period. The general pattern of fouling is correct with a general increase in fouling resistance with time. Although the predicted values are closer to the calculated ones for this exchanger than for E2105 the predicted values are still the highest.

6.3.4 E2108AB

Figure 6.19 shows the fouling resistance predictions for these exchangers in the first operating period. The Minerva program allows the A and B exchangers to be modelled separately. However it is not possible to separate the two exchangers using the data from the refinery hence both of the predicted values are presented on the graph for comparative purposes. The predicted general pattern of fouling for these exchangers is correct although the model does not predict the wide variations in fouling resistance that were calculated from the plant data. This maybe indicative that the fouling mechanism within these exchangers is different to that of the other exchangers in the preheat train a fact which is highlighted by the results of deposit analysis results previously discused in Chapter 5.

Figure 6.25 shows the predictions of the fouling resistance for these exchangers in the second operating period. With one exception the predicted values are greater than those calculated from the refinery data. The overall pattern of fouling is not as well modelled for these exchangers as it is for the other exchangers in the preheat train. If

the hypothesis of a different fouling mechanism in these exchangers is correct then it may be that this type of deposit is formed and/or removed by different methods than those used in the Minerva program.

6.3.5 E2109A

Figure 6.20 shows the predictions of fouling resistance for this exchanger in the first operating period. Generally the predictions for this exchanger are very close to those calculated from the refinery data. Figure 6.26 shows the predictions of fouling resistance for the exchanger in the second operating period. Whilst the pattern of fouling is correct Minerva again over predicts the fouling resistance.

6.4 Conclusions

6.5 Temperature based fouling model.

The data for the light crude oils processed during the first operating period was used to develop a temperature based fouling model of the form;

$$R_F = c_i + \int A \exp(-\frac{E}{RT_w})dt \qquad 6.14$$

Where c_i is a corrective coefficient arising from errors in the temperature measurements on start-up of the exchangers. This model was then tested on the data from the second operating period and was found to give a tolerable prediction of the fouling rate. The effect of increased velocity on fouling rate within the narrow limits of the measured velocities on the refinery, seemed to be accounted for by the decrease in surface temperature. The precise effects of the composition of the crude oil blend being processed on the fouling rate could not be quantified from the data collected on the preheat exchangers. However it was found that the activation energy of the heavy crude oils (E= 21 kJ mol^{-1}) was lower than that calculated for the light crude oils (E=32.66 kJ mol^{-1}). This would lead to a greater fouling rate from the heavy crudes for the same surface temperature, which corresponds with the observations on the refinery.

6.6 Temperature and velocity based fouling model

The results from the testing of the published model incorporated into the Minerva program would seem to indicate that the model can predict the general trends of fouling observed on the refinery. The results from the predictions for the first set of operating data are relatively close to those from the refinery data. The under prediction is probably resulted from the shellside fouling that was found to be present on the exchangers when they were opened up for cleaning.

When the model was used to predict the fouling resistances for the second operating period the tendency was for over prediction. This may be due to one or more of the

following factors.

(i) Over prediction may have resulted from the coefficients being determined from the data for the first operating period and hence would have included some contribution from the shellside foulant.

(ii) Although the crude oils processed in both operating periods were generally classed as light crude oils the coefficients would in reality have varied with the crude oil being processed. The coefficients A and E are both a function of the feedstock composition and C is a function of the physical characteristics of the deposit and so is also dependent upon the feedstock.

(iii) Minor process upsets for example salt carry over from the desalters and the introduction of small amounts of heavier feedstocks were not modelled.

(iv) Changes in operating conditions may have occurred between the dates on which detailed measurements of the operating parameters were taken. Since all the data required for the model would not be available for such changes they could not be incorporated into the model.

Figure 6.1 Fouling rate against temperature
Light crudes to day 390.

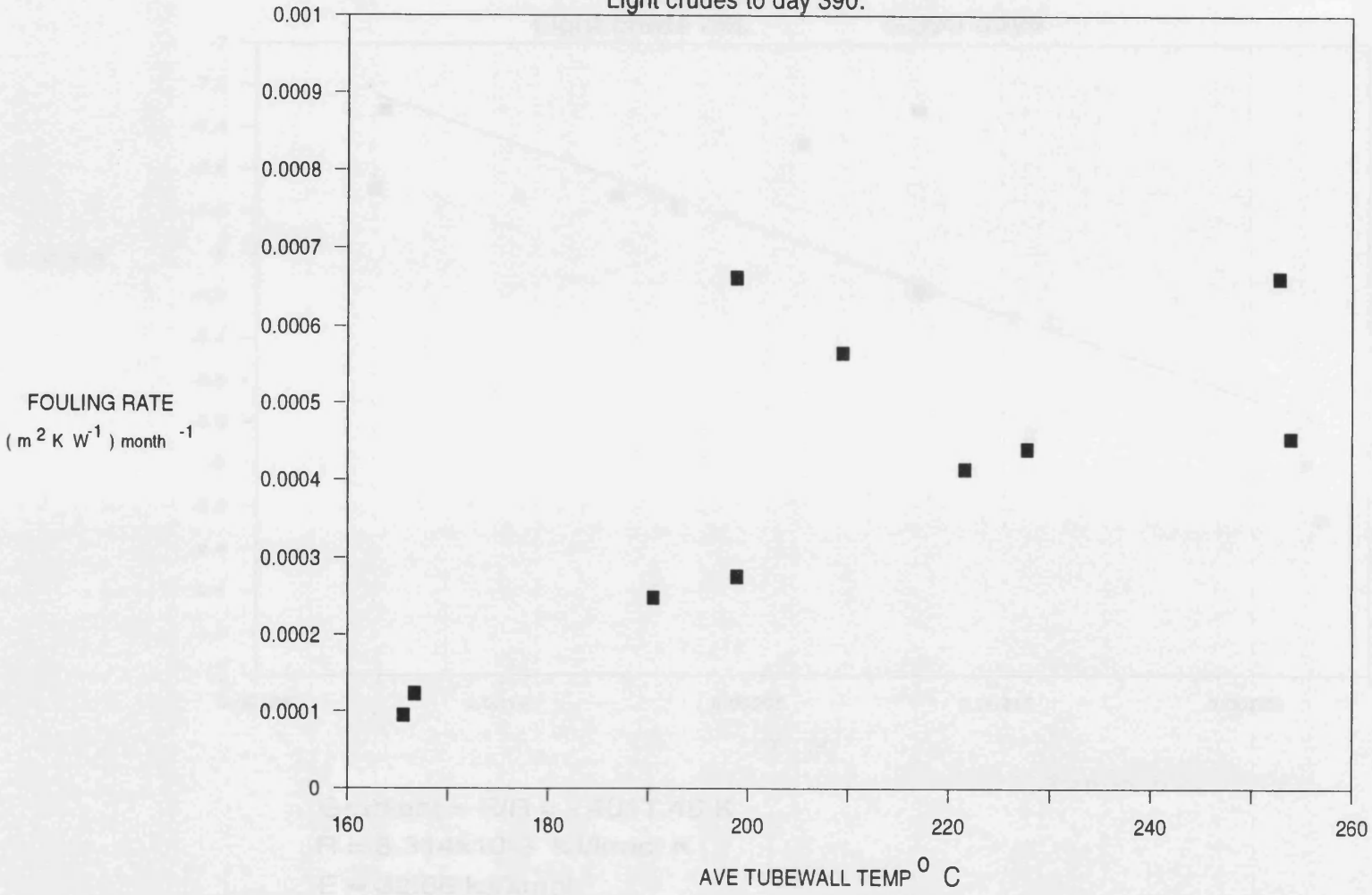

Figure 6.2

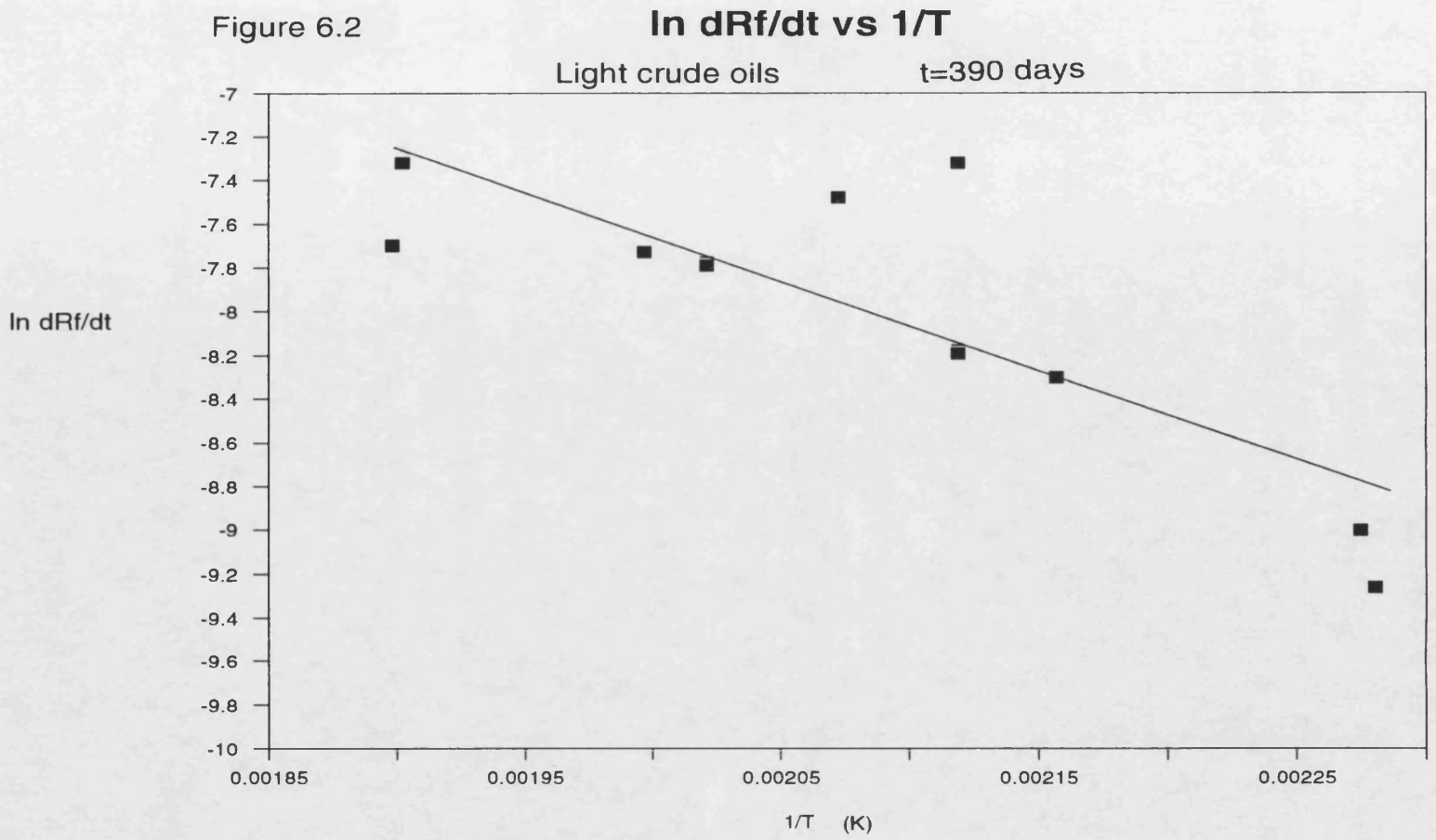

Gradient = E/R = - 4011.46 K

R = 8.314x10-3 kJ/kmol K

E = 32.66 kJ/kmol

Figure 6.3

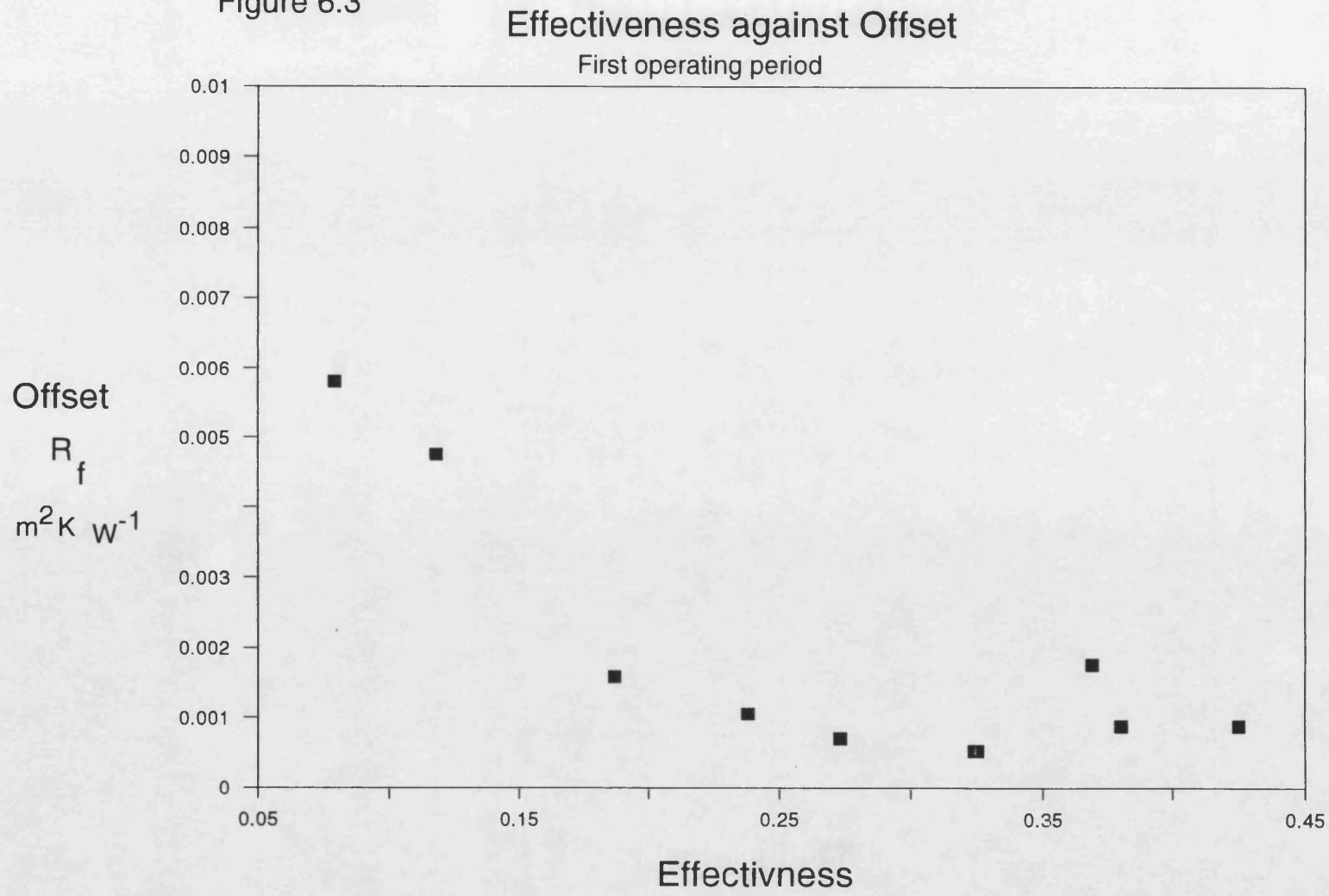
Effectiveness against Offset
First operating period
Offset
R_f
$m^2K\ W^{-1}$
0.01
0.009
0.008
0.007
0.006
0.005
0.003
0.002
0.001
0
0.05
0.15
0.25
0.35
0.45
Effectivness

Figure 6.4

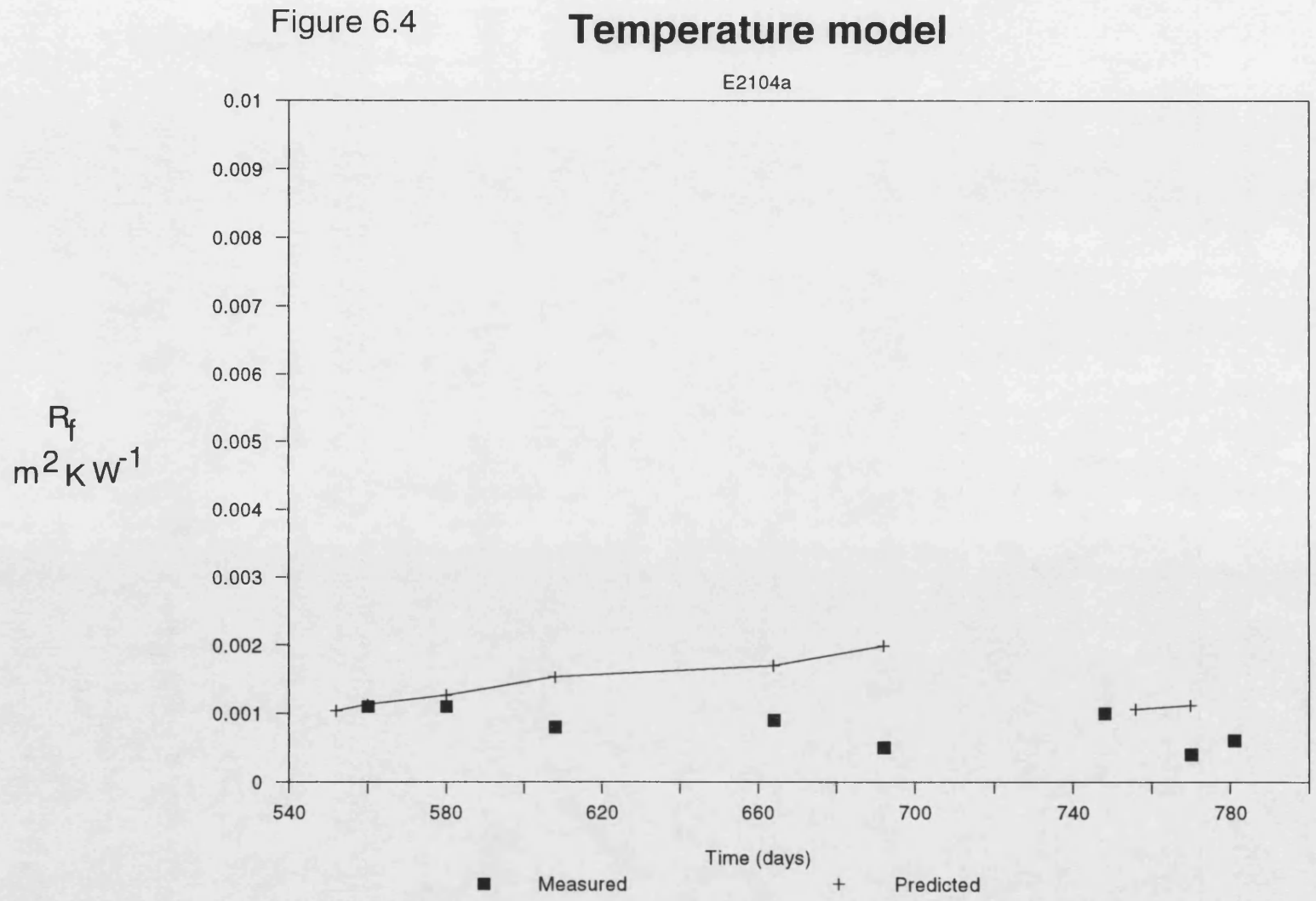
Temperature model
E2104a
R_f
$m^2 K W^{-1}$
0.01
0.009
0.008
0.007
0.006
0.005
0.004
0.003
0.002
0.001
0
540
580
620
660
700
740
780
Time (days)
Measured
Predicted

Figure 6.5

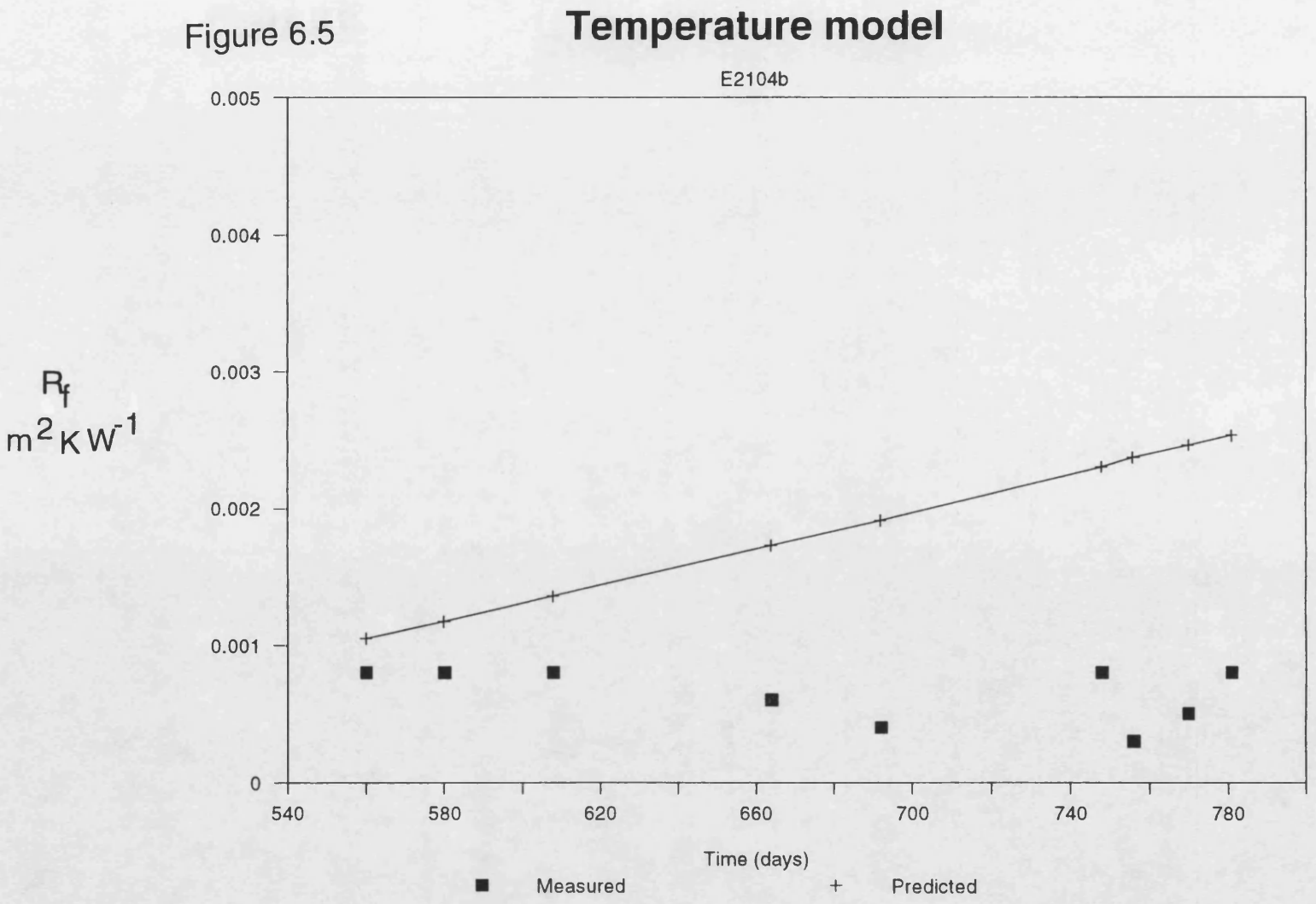
Temperature model
E2104b
R_f
m^2KW^{-1}
0.005
0.004
0.003
0.002
0.001
0
540
580
620
660
700
740
780
Time (days)
Measured
Predicted

Figure 6.6

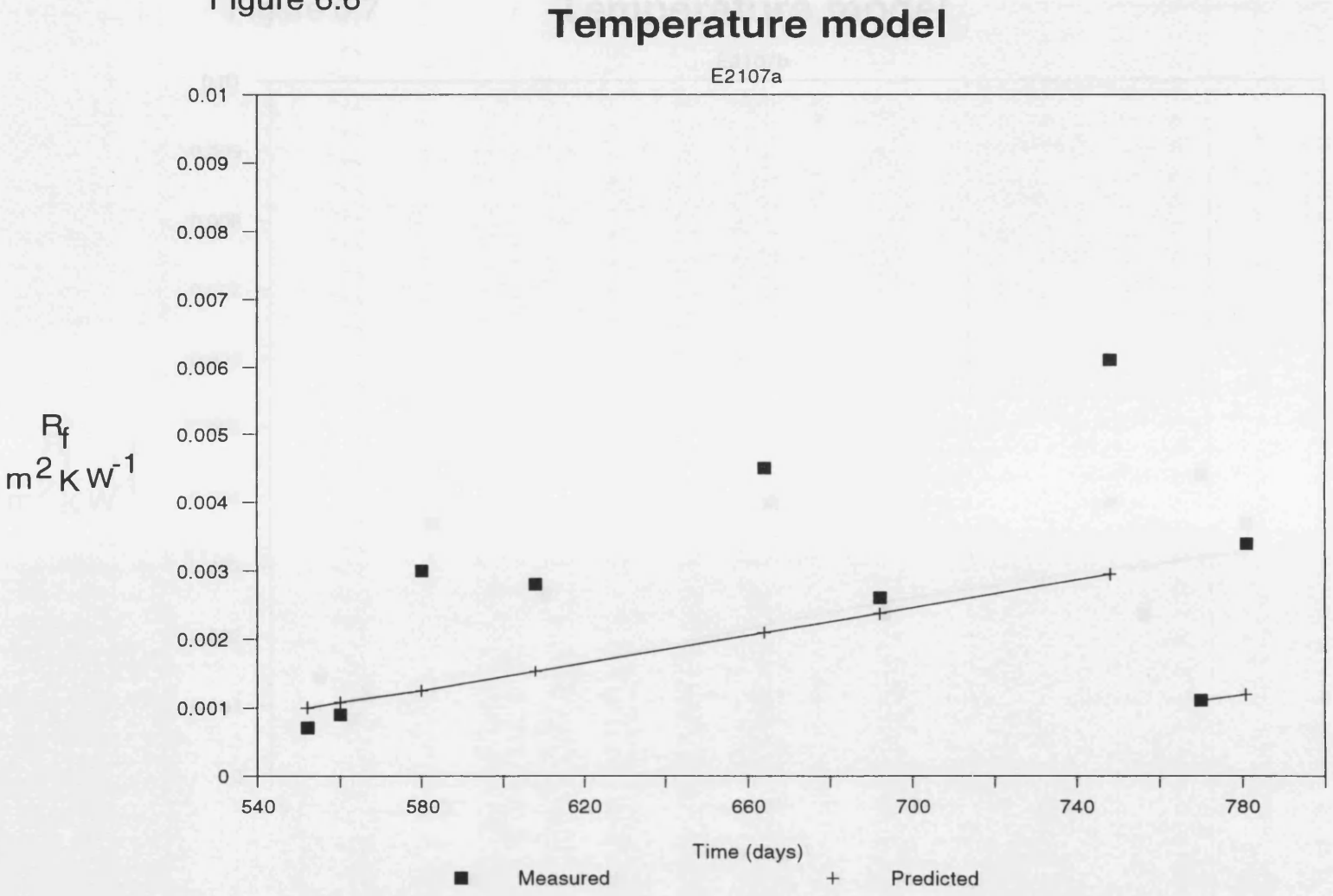
Temperature model
E2107a
R_f
$m^2 K W^{-1}$
0.01
0.009
0.008
0.007
0.006
0.005
0.004
0.003
0.002
0.001
0
540
580
620
660
700
740
780
Time (days)
Measured
Predicted

Figure 6.7 **Temperature model**

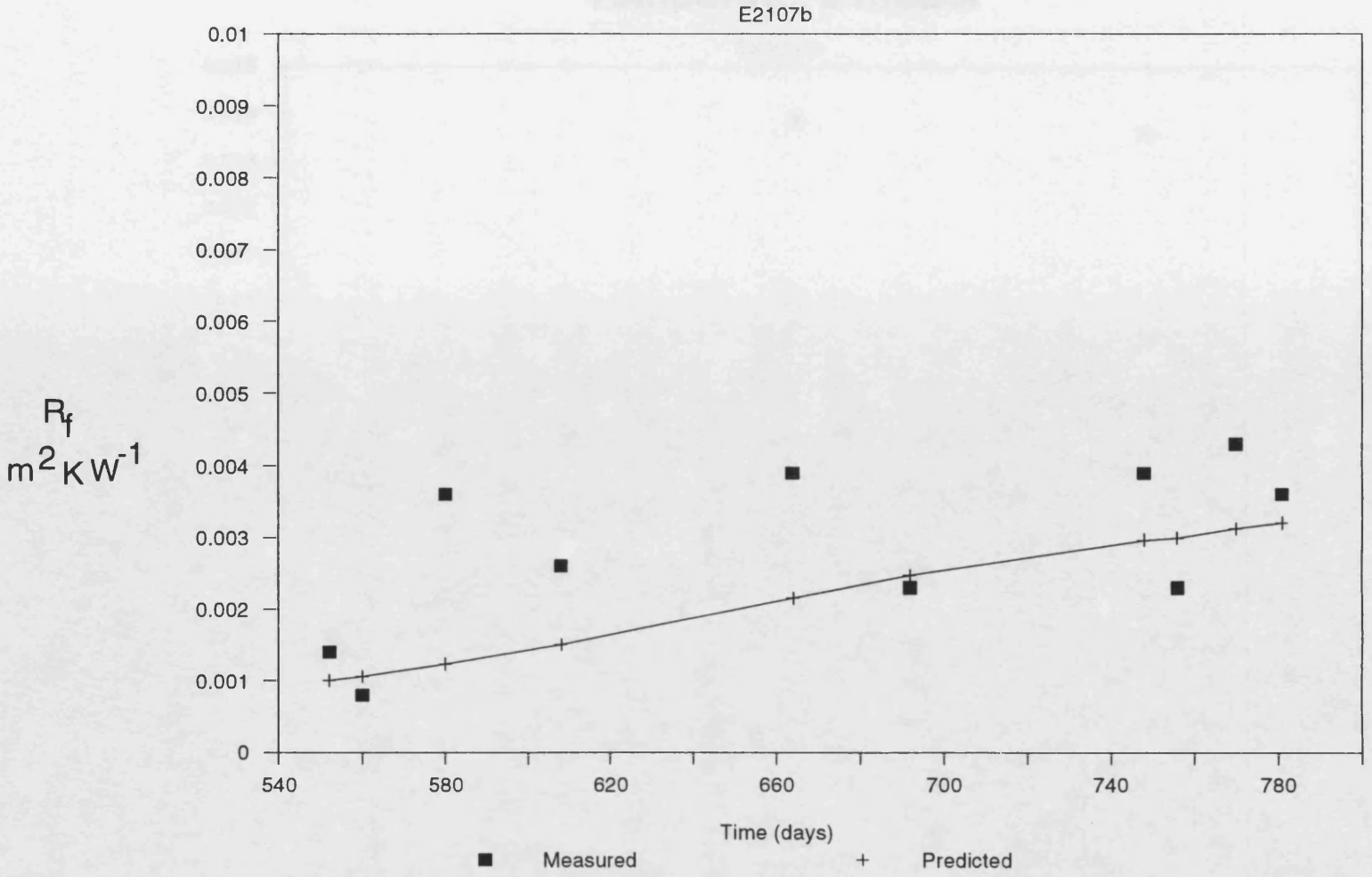

Figure 6.8

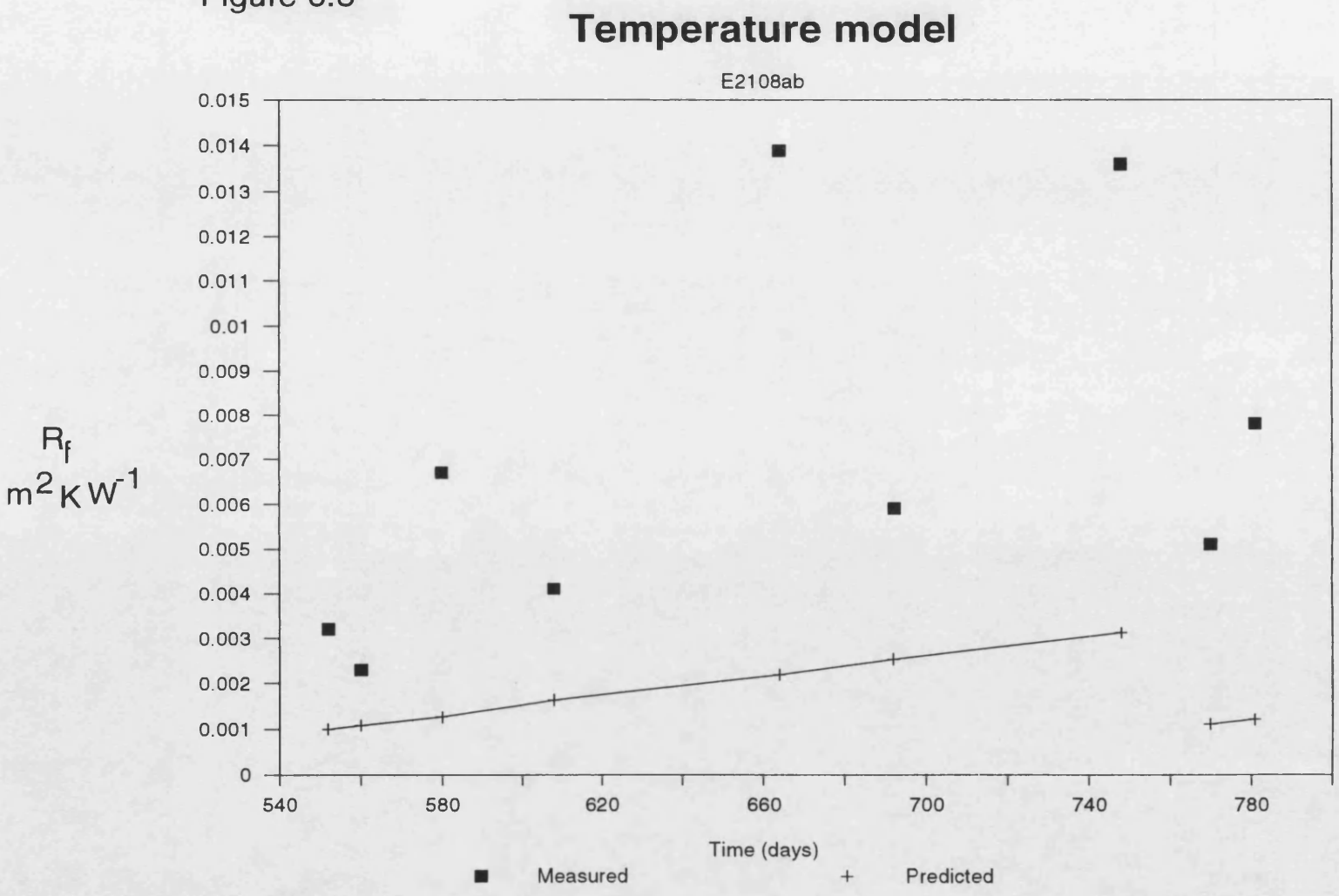
Temperature model
E2108ab
R_f
$m^2 K W^{-1}$
0.015
0.014
0.013
0.012
0.011
0.01
0.009
0.008
0.007
0.006
0.005
0.004
0.003
0.002
0.001
0
540
580
620
660
700
740
780
Time (days)
Measured
Predicted

Figure 6.9 **Temperature model**

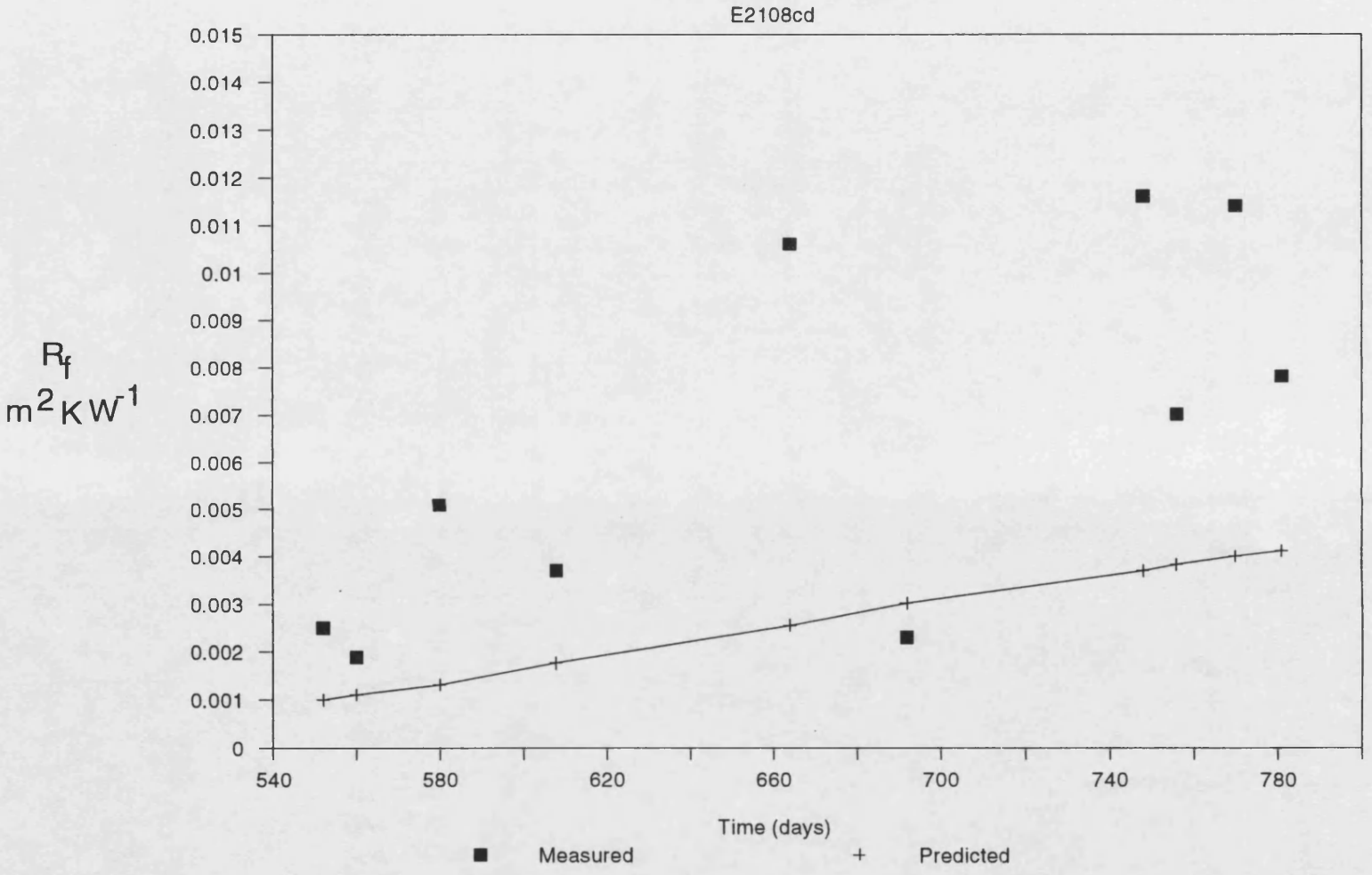

Figure 6.10

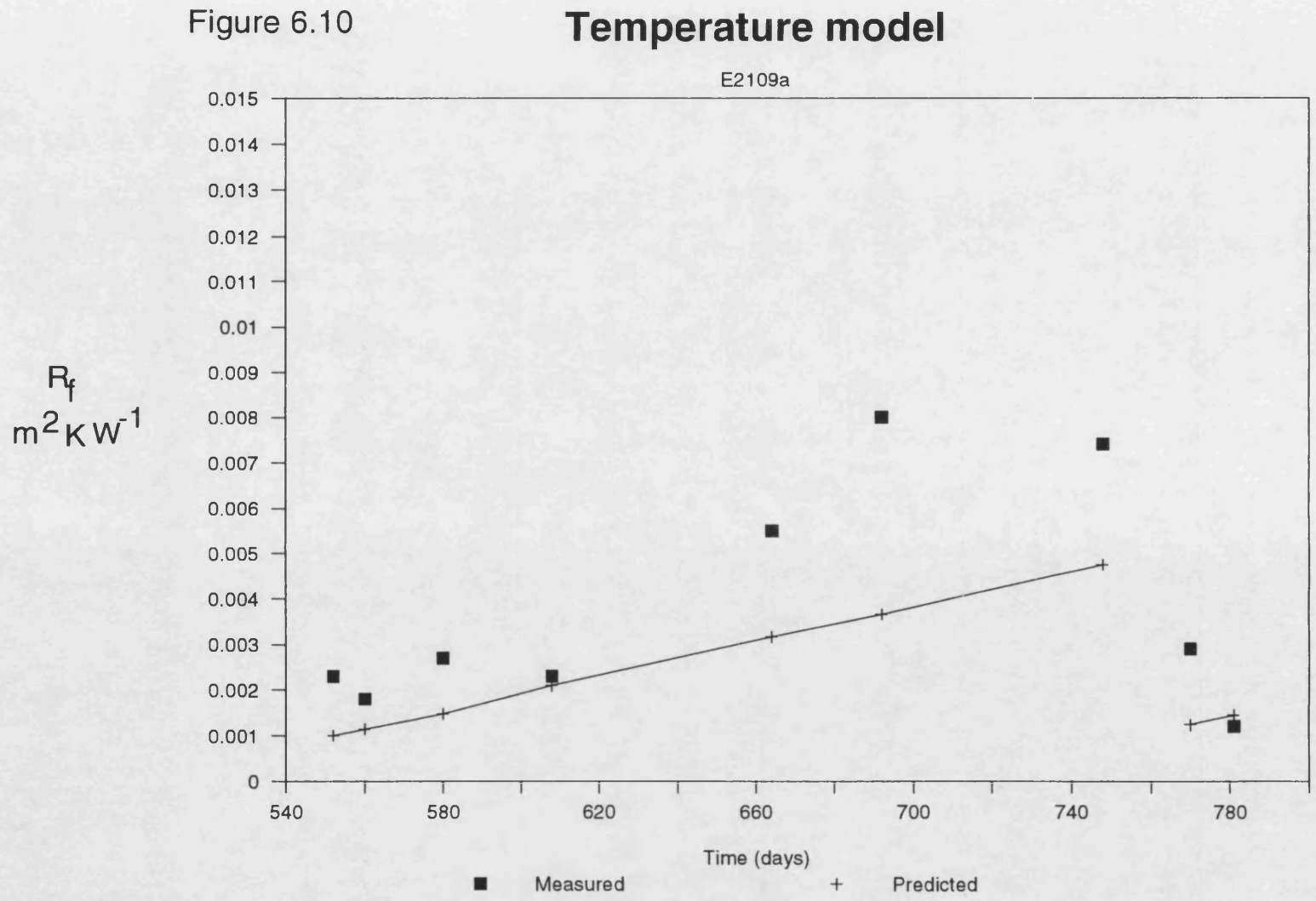
Temperature model
E2109a
R_f
$m^2 K W^{-1}$
0.015
0.014
0.013
0.012
0.011
0.01
0.009
0.008
0.007
0.006
0.005
0.004
0.003
0.002
0.001
0
540
580
620
660
700
740
780
Time (days)
Measured
Predicted

Figure 6.11 **Temperature model**

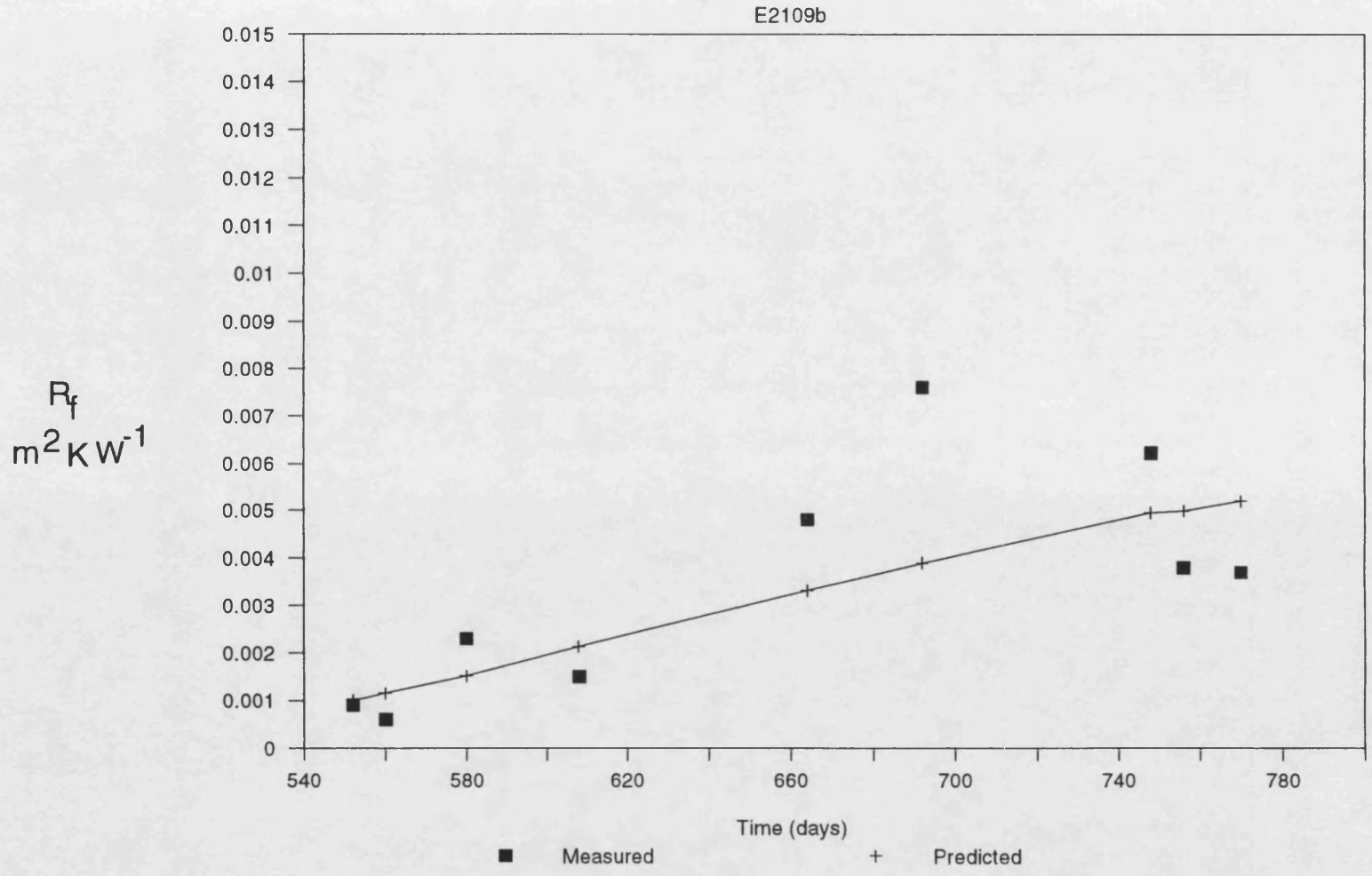

Figure 6.12

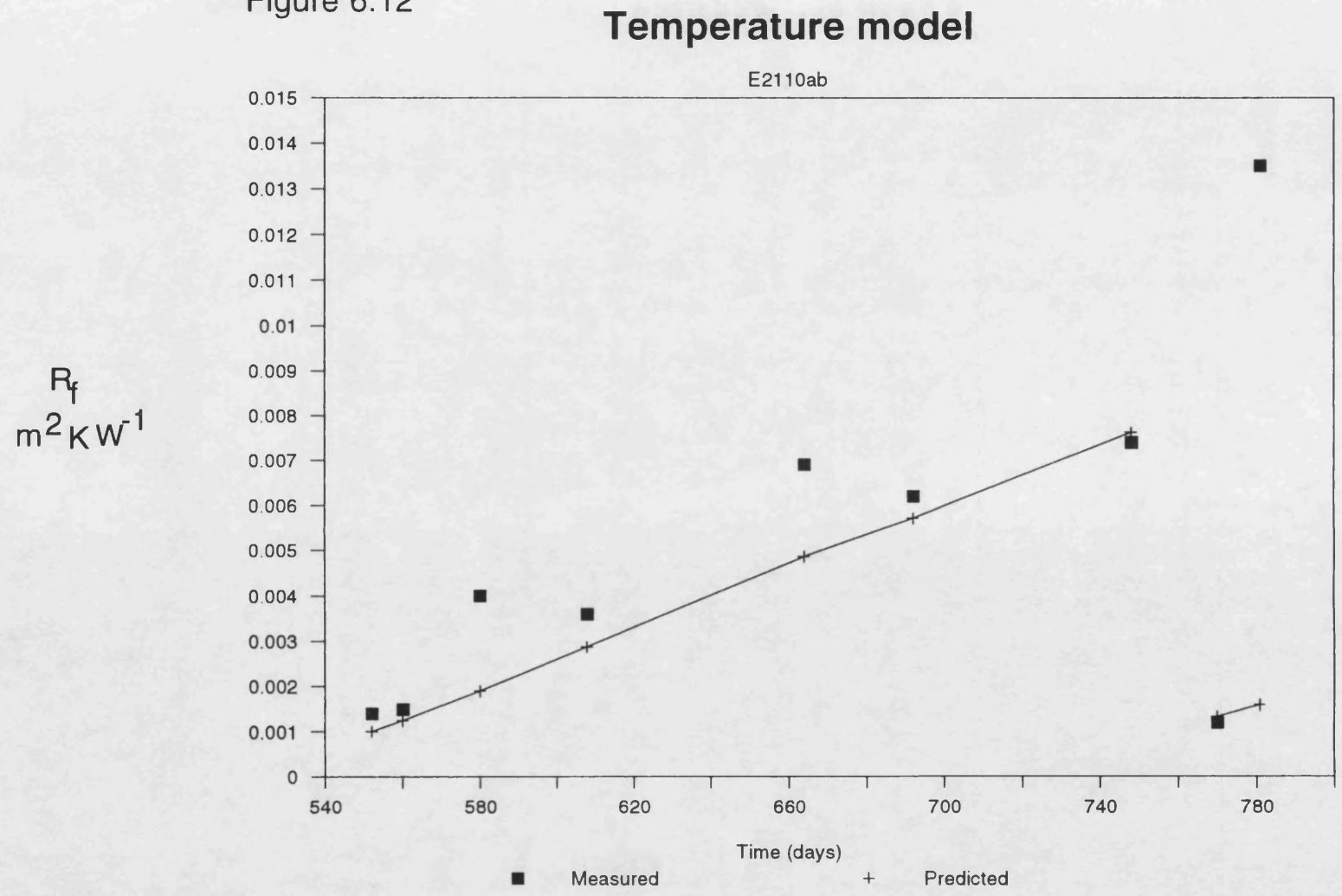
Temperature model
E2110ab
R_f
m^2KW^{-1}
0.015
0.014
0.013
0.012
0.011
0.01
0.009
0.008
0.007
0.006
0.005
0.004
0.003
0.002
0.001
0
540
580
620
660
700
740
780
Time (days)
Measured
Predicted

Figure 6.13

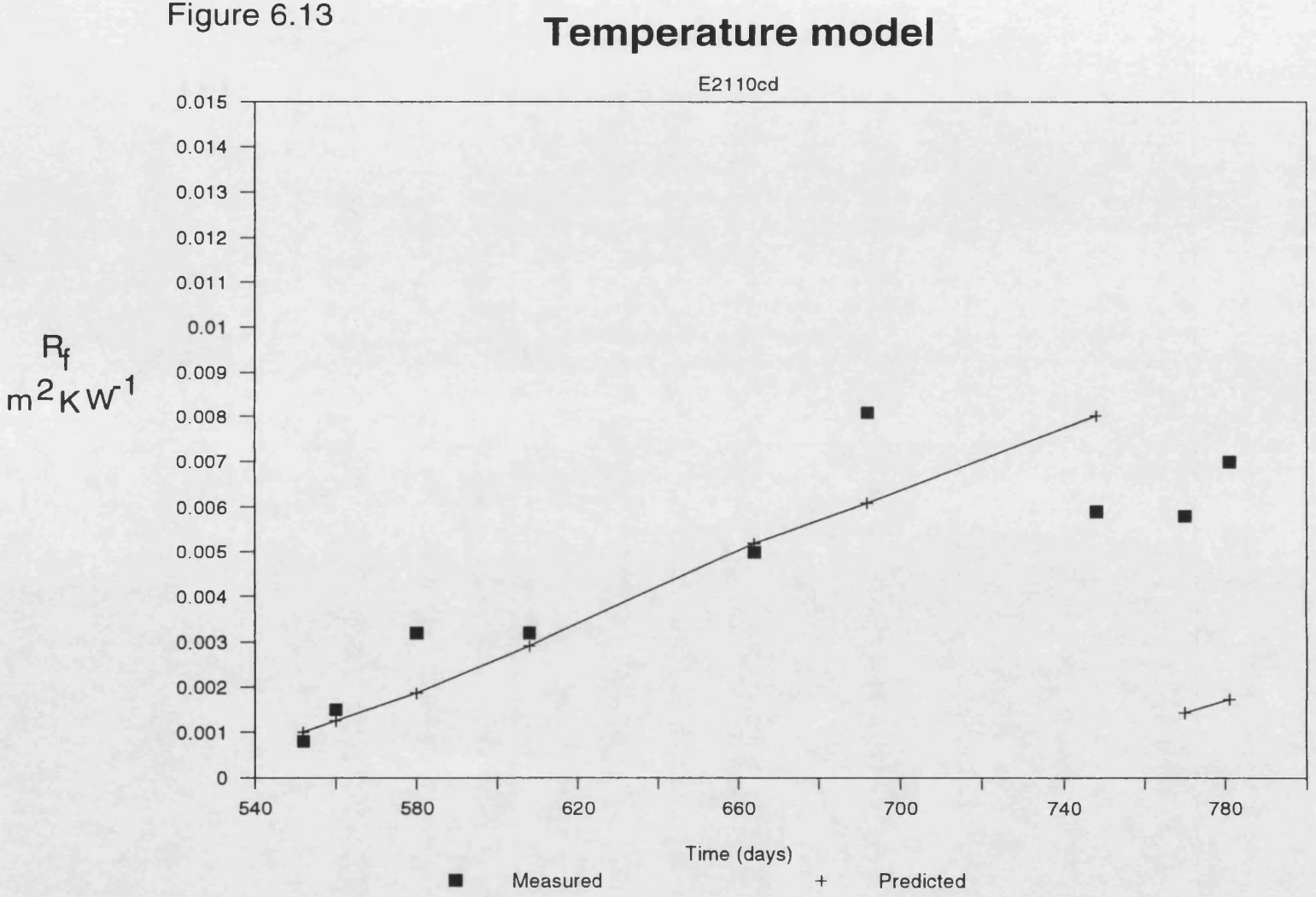
Temperature model
E2110cd
R_f
m^2KW^{-1}
0.015
0.014
0.013
0.012
0.011
0.01
0.009
0.008
0.007
0.006
0.005
0.004
0.003
0.002
0.001
0
540
580
620
660
700
740
780
Time (days)
Measured
Predicted

Figure 6.14

Velocity effects

E2104a&b

Figure 6.15

ln dRf/dt vs 1/T

Heavy Crudes and slops

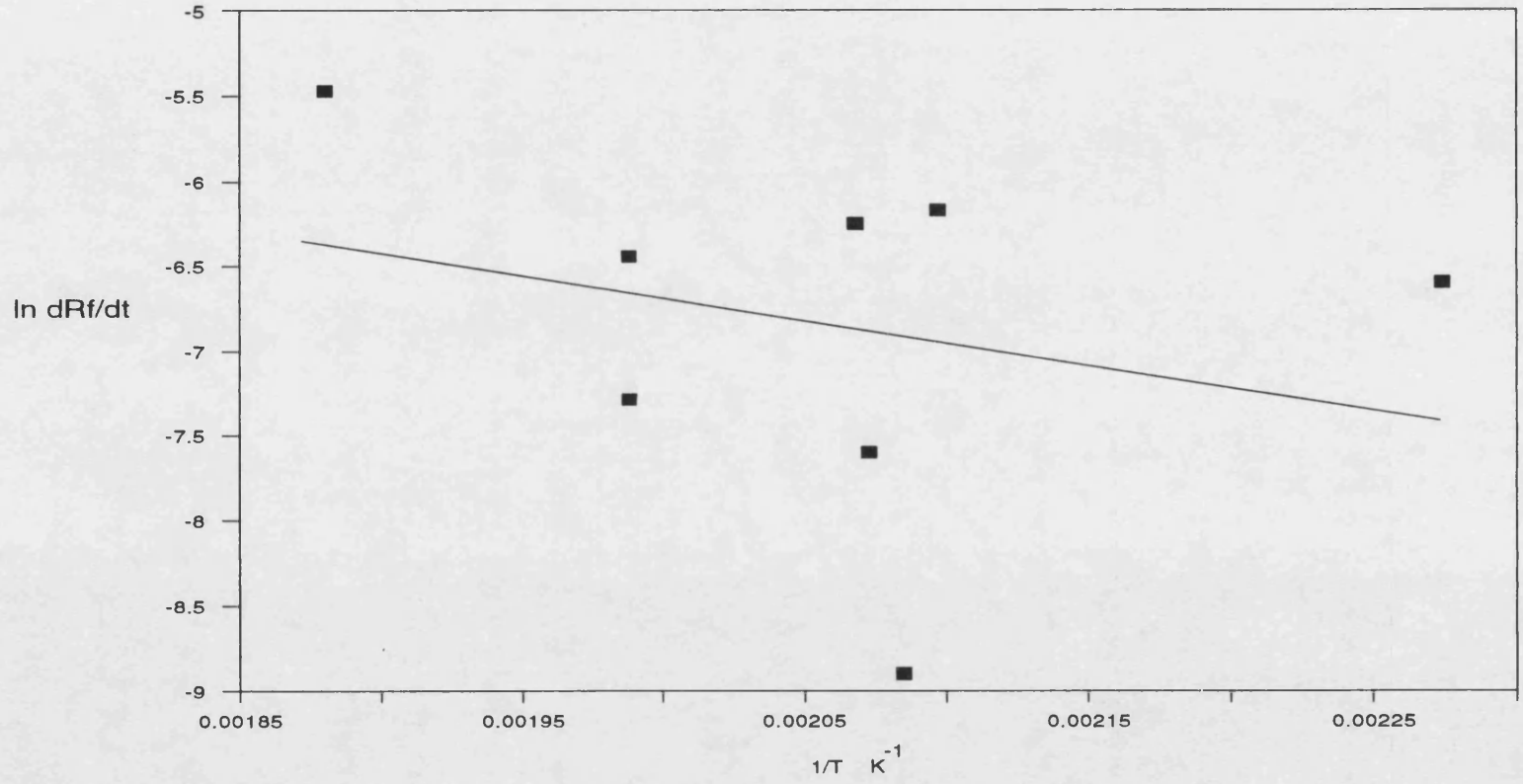

Gradient = E/R = -2555.67

R = 8.314x10-3 kJ/kmol K

E=21 kJ/kmol

Figure 6.16

Minerva predictions first operating cycle

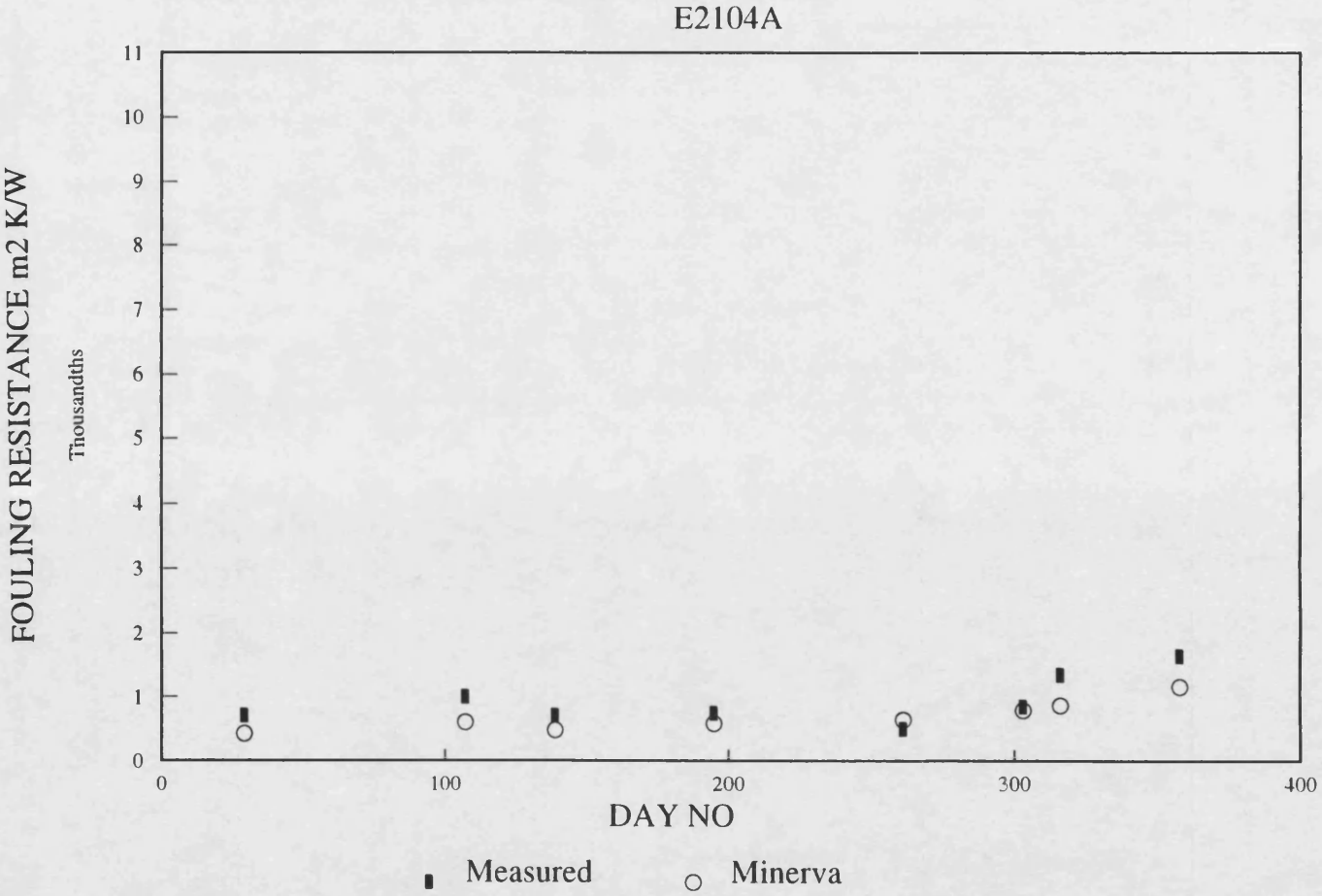

Figure 6.17

Minerva prediction first operating cycle

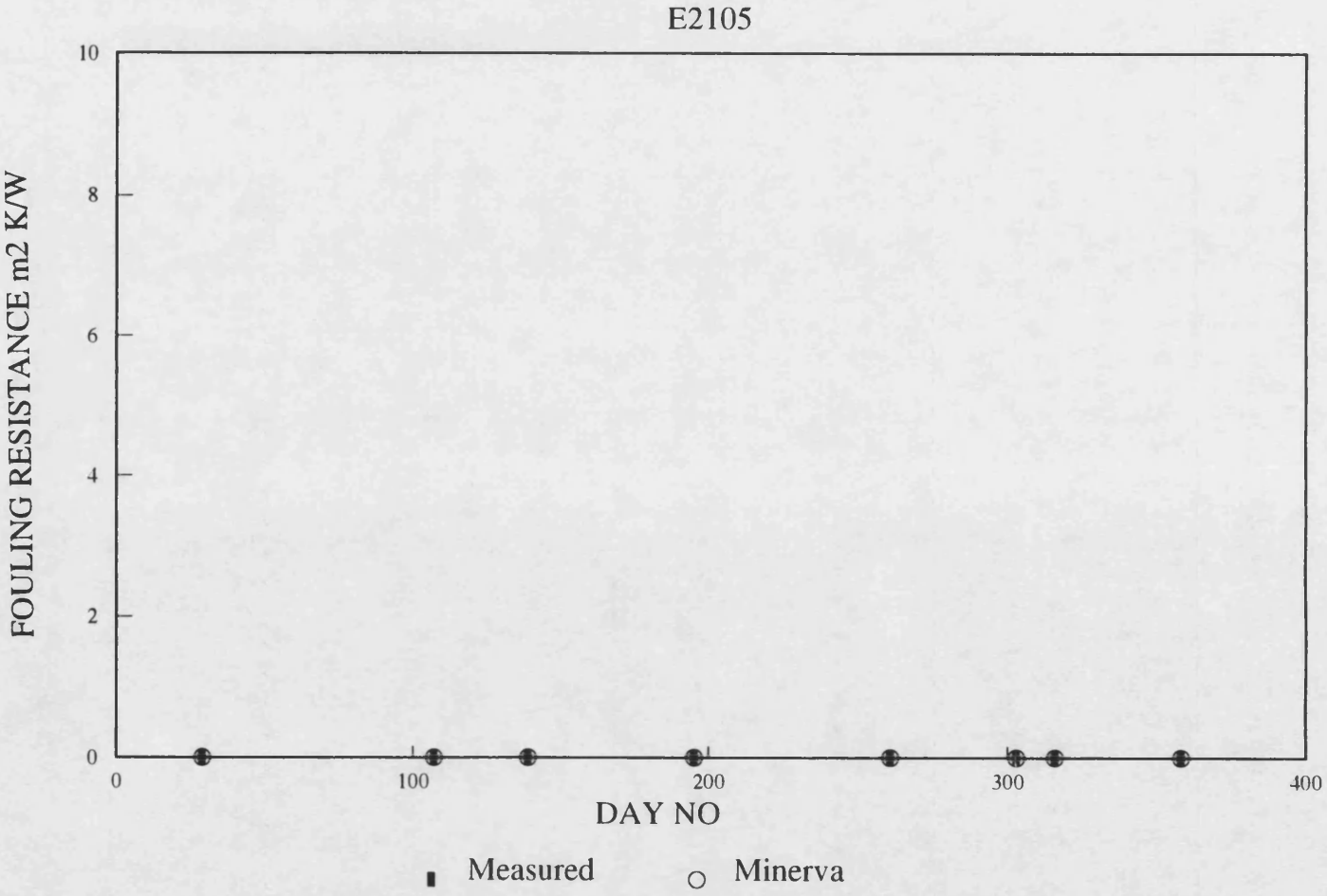

Figure 6.18

Minerva predictions first operating cycle

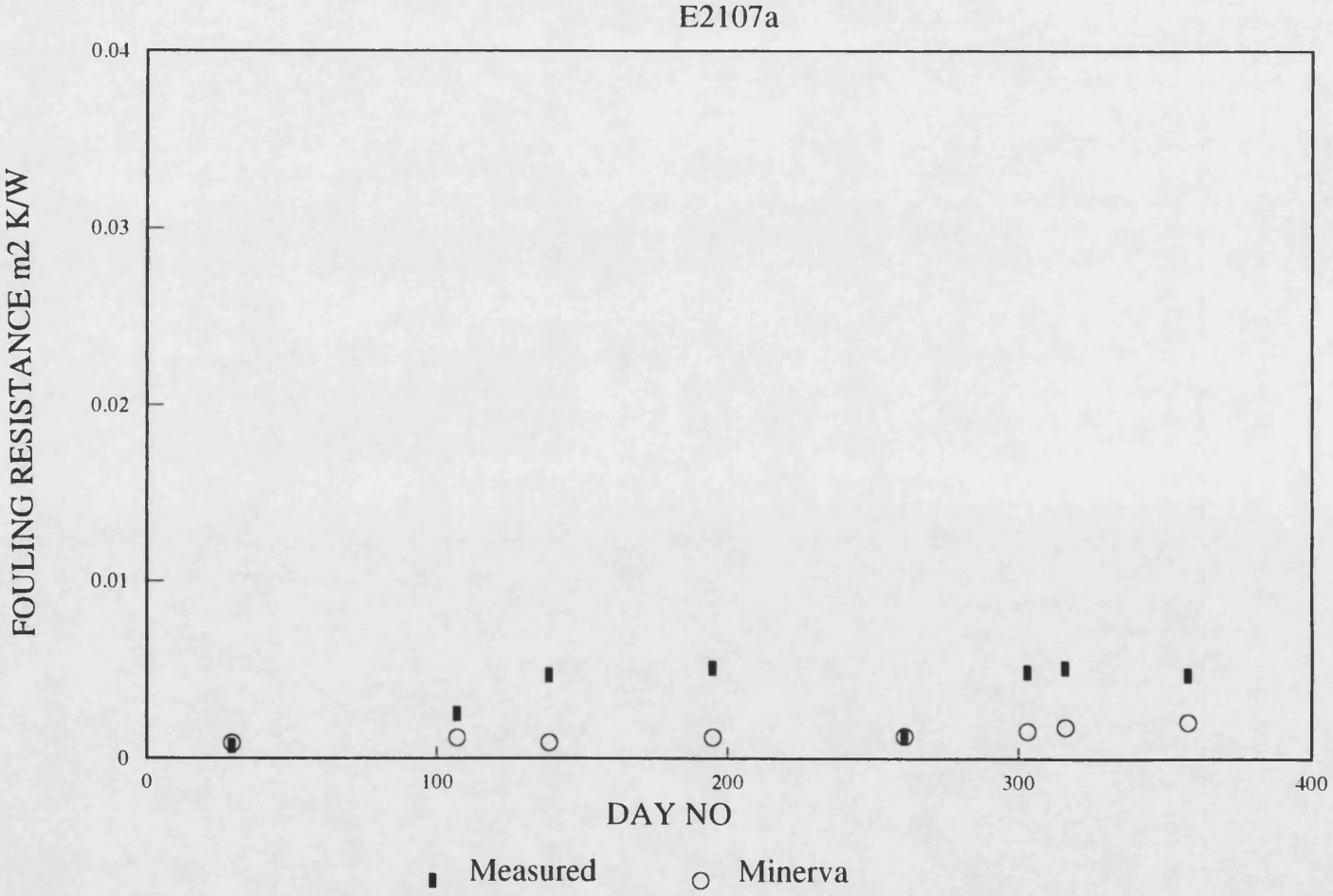

Figure 6.19

Minerva predictions first operating cycle

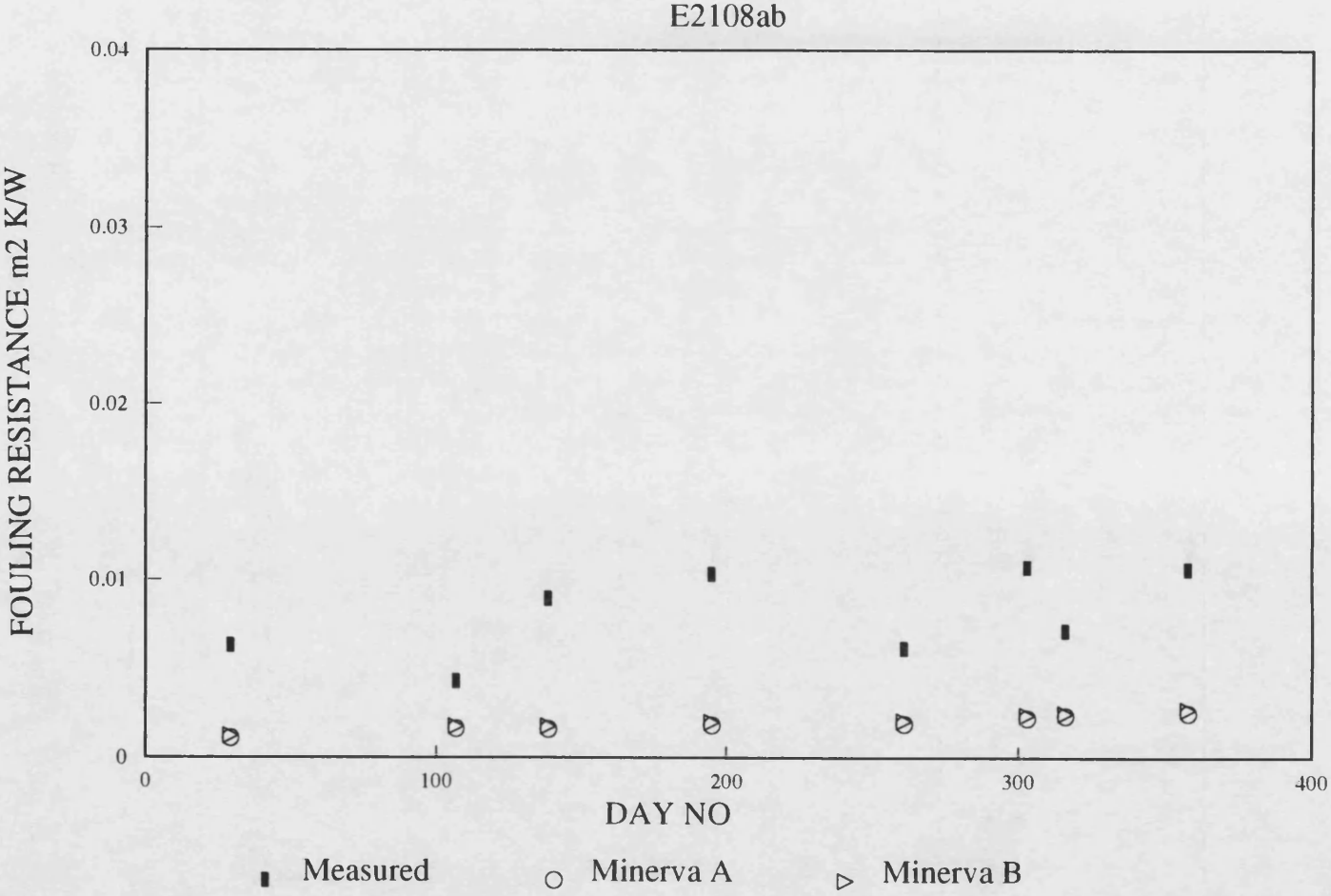

Figure 6.20

Minerva predictions first operating cycle

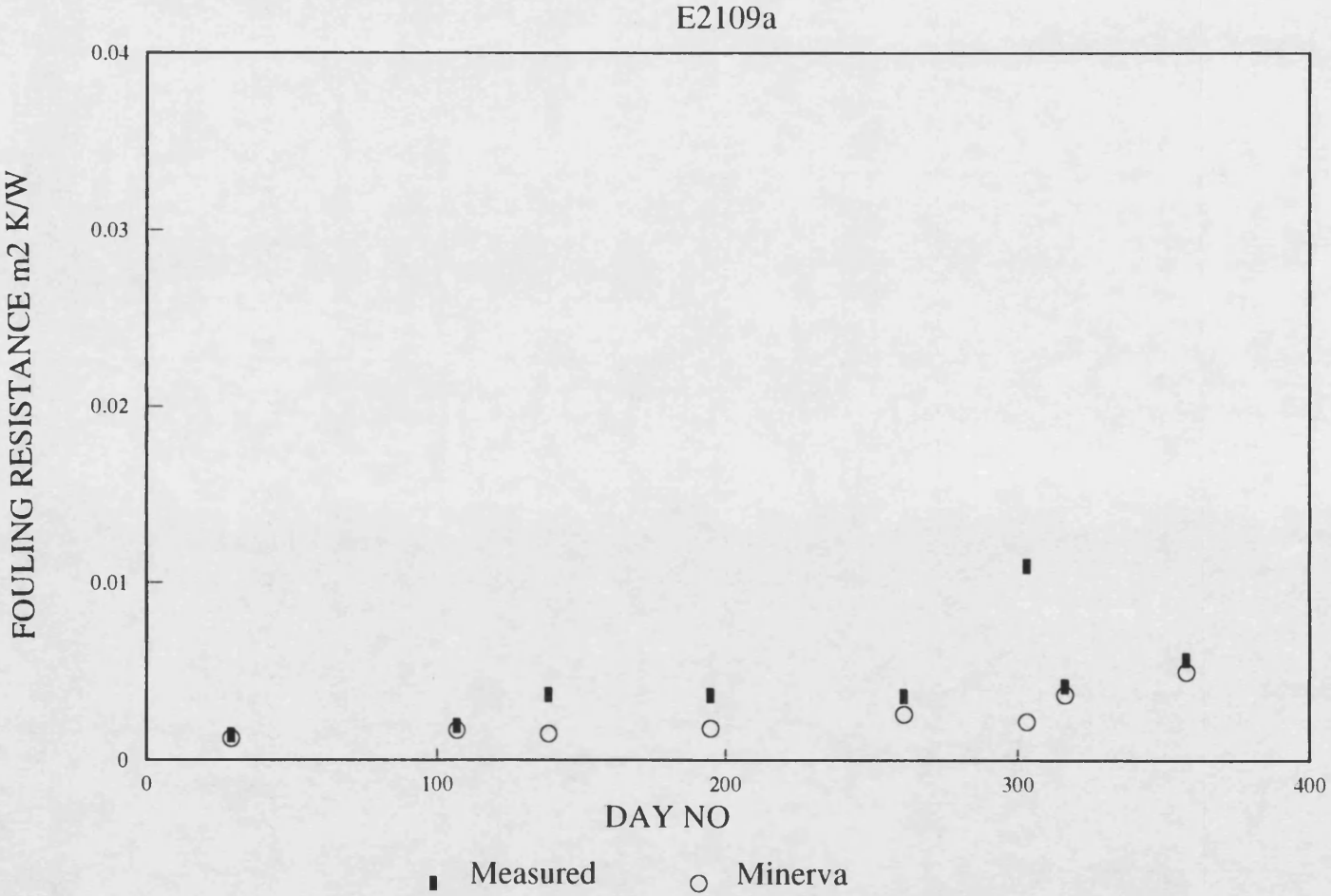

Figure 6.21

Minerva predicts first operating cycle

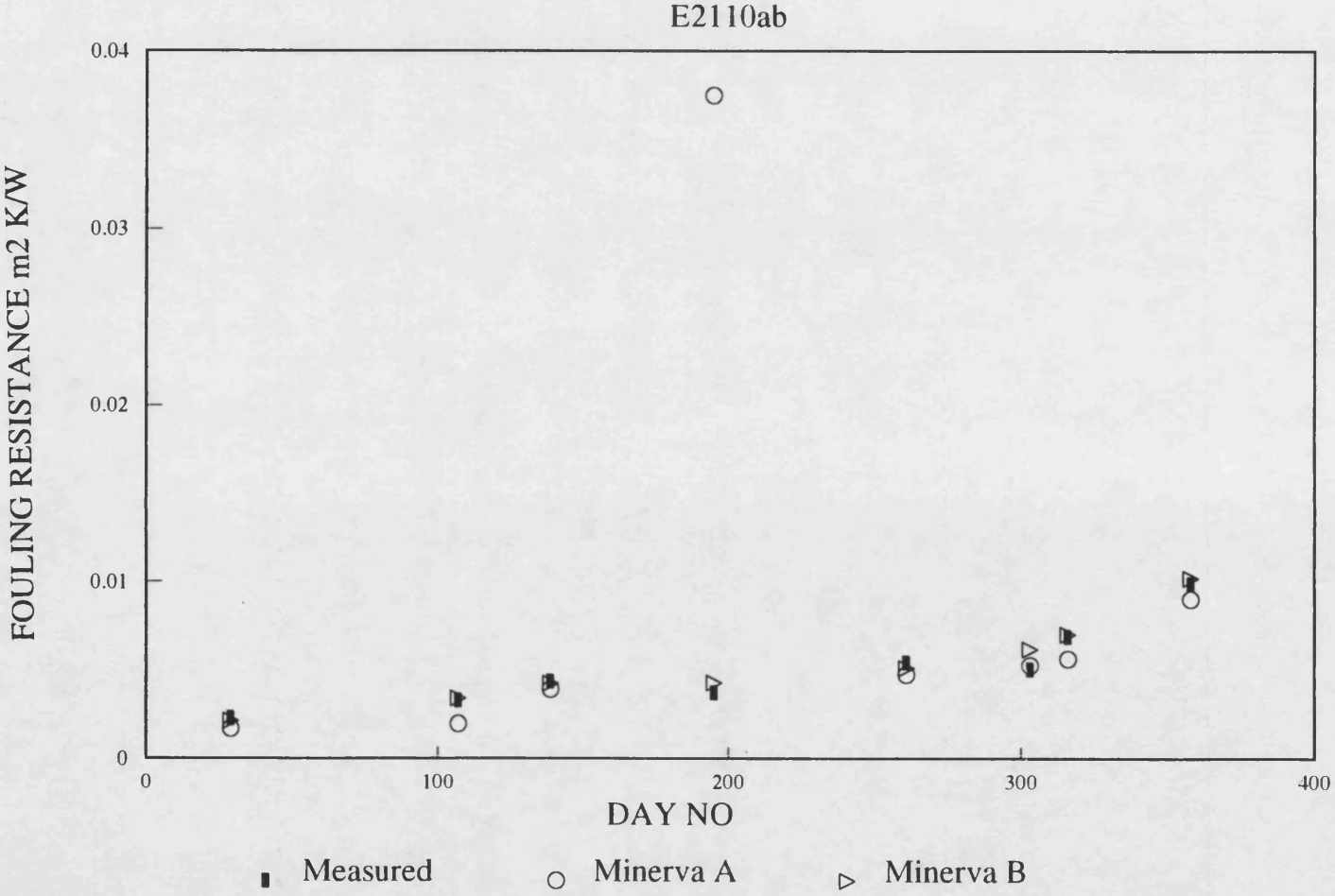

Figure 6.22

Minerva prediction post clean

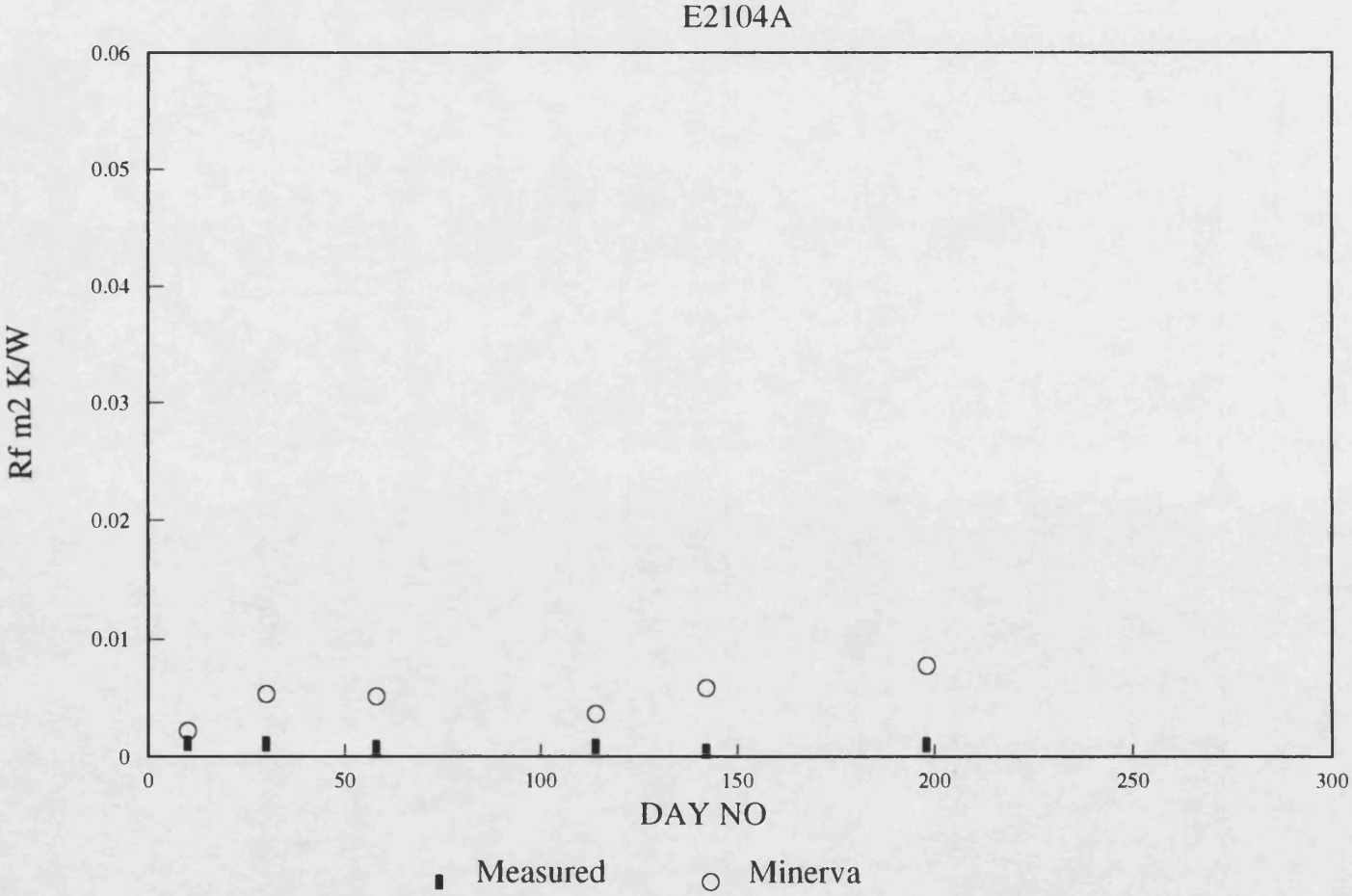

Figure 6.23

Minerva prediction post clean

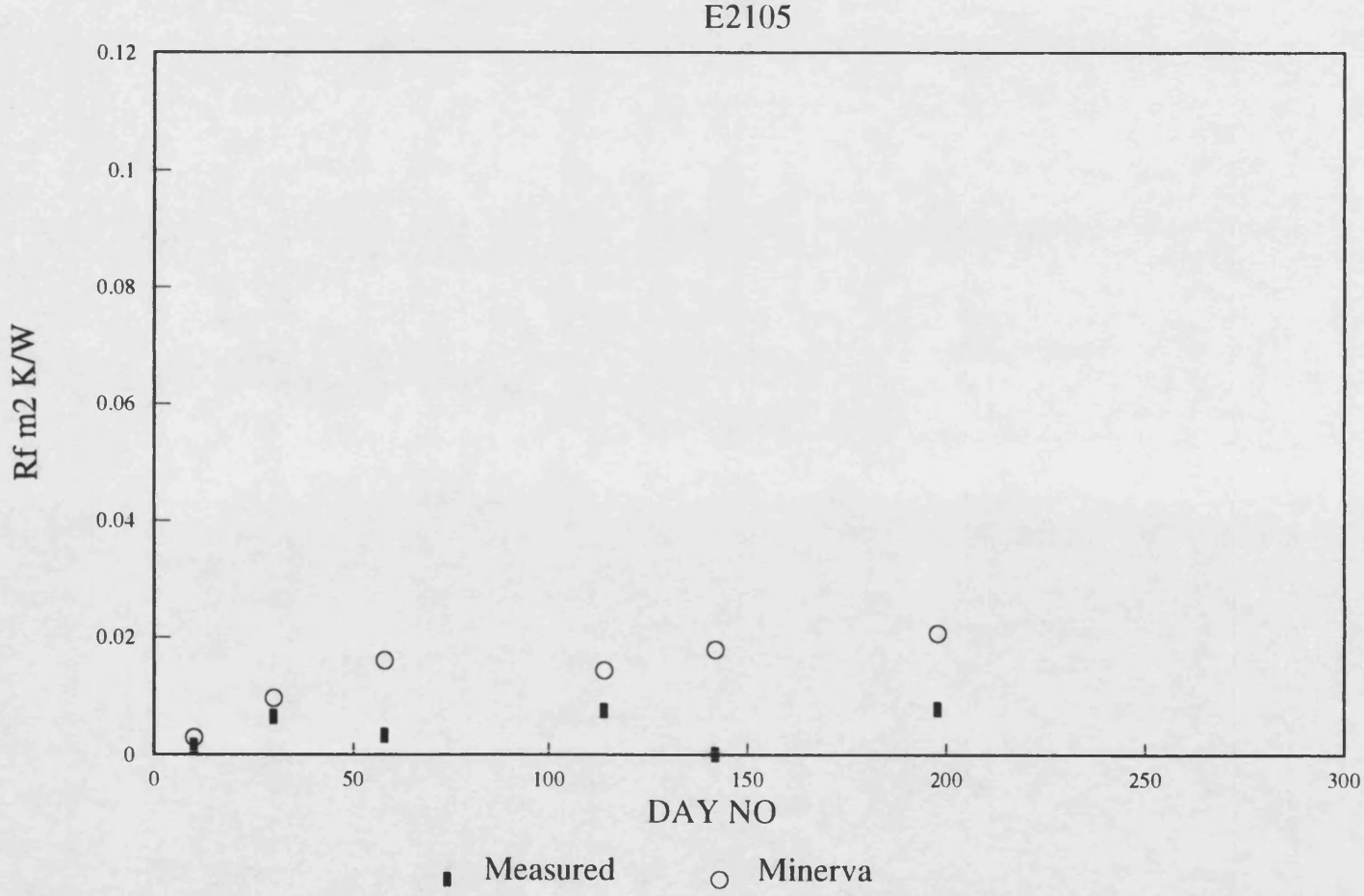

Figure 6.24

Minerva prediction post clean

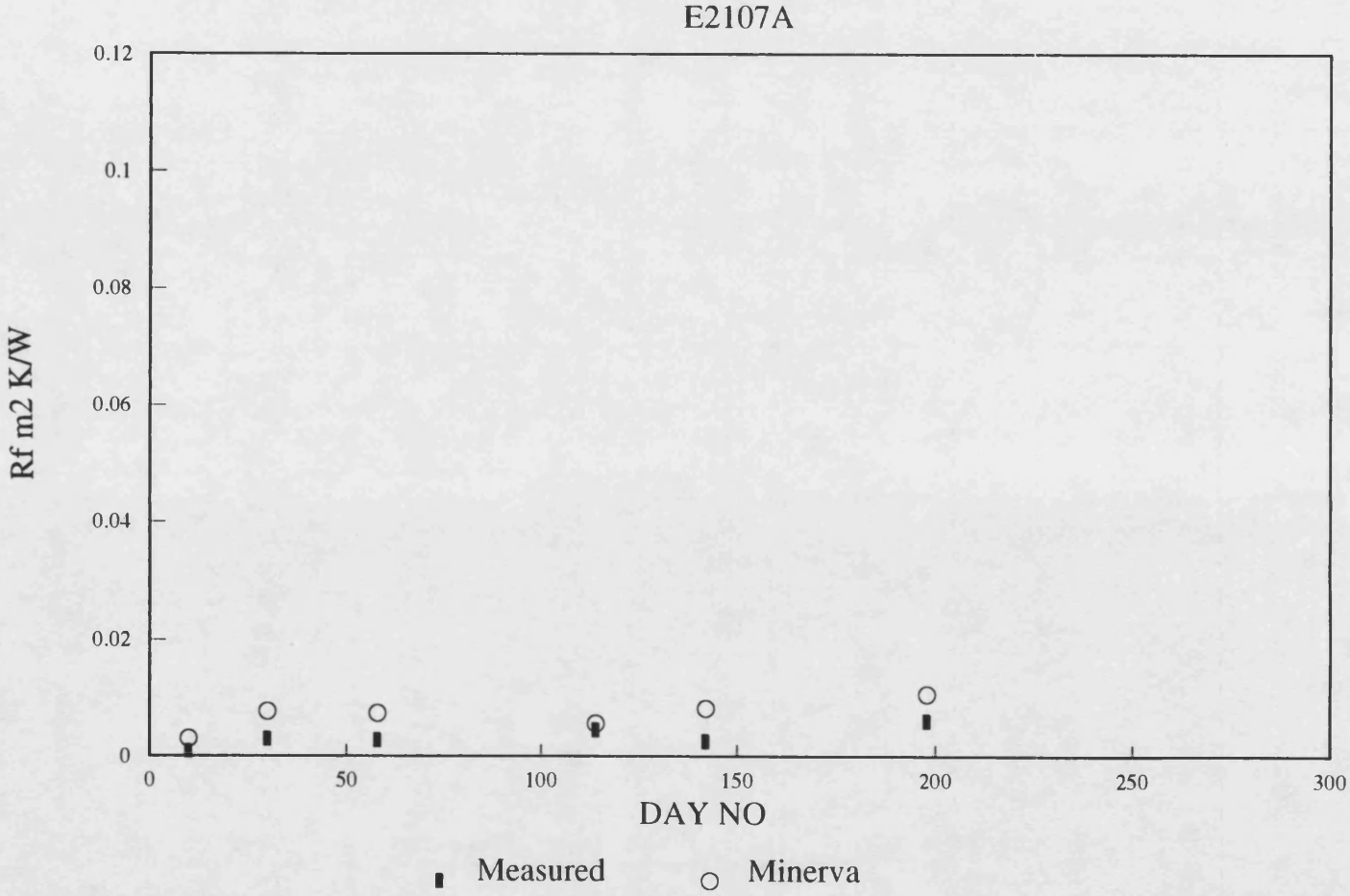

Figure 6.25

Minerva prediction post clean

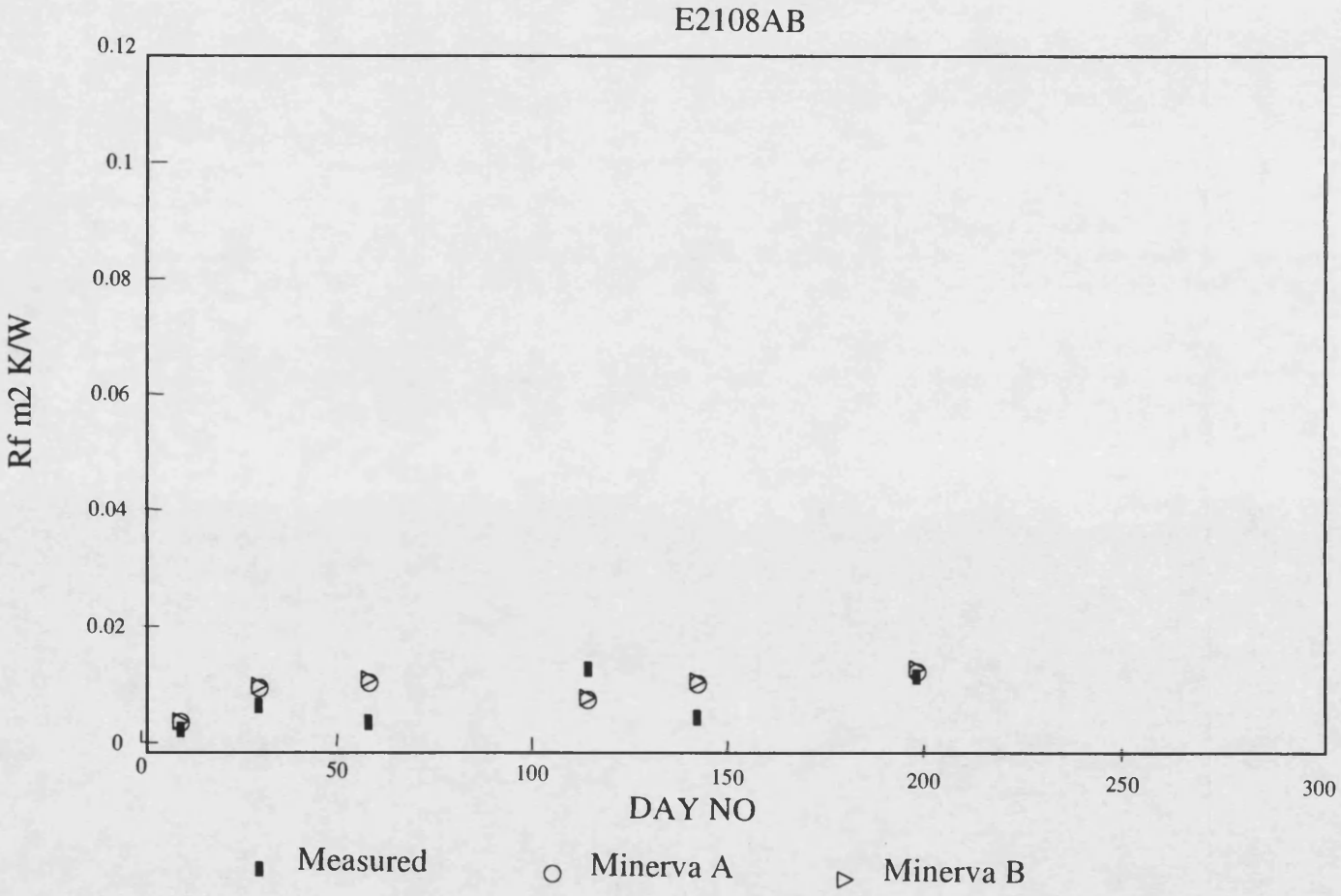

Figure 6.26

Minerva prediction post clean

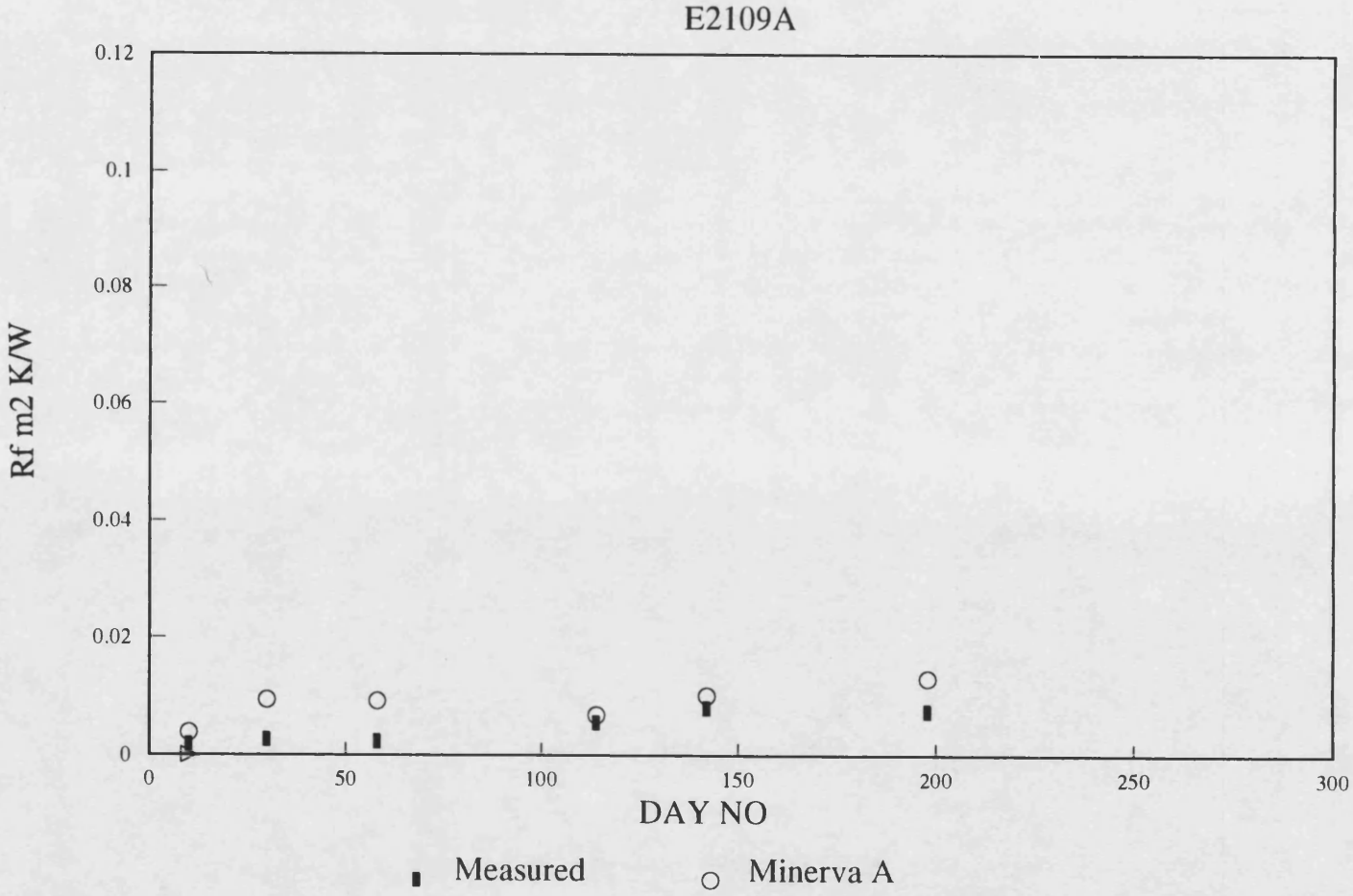

Figure 6.27

Minerva prediction post clean

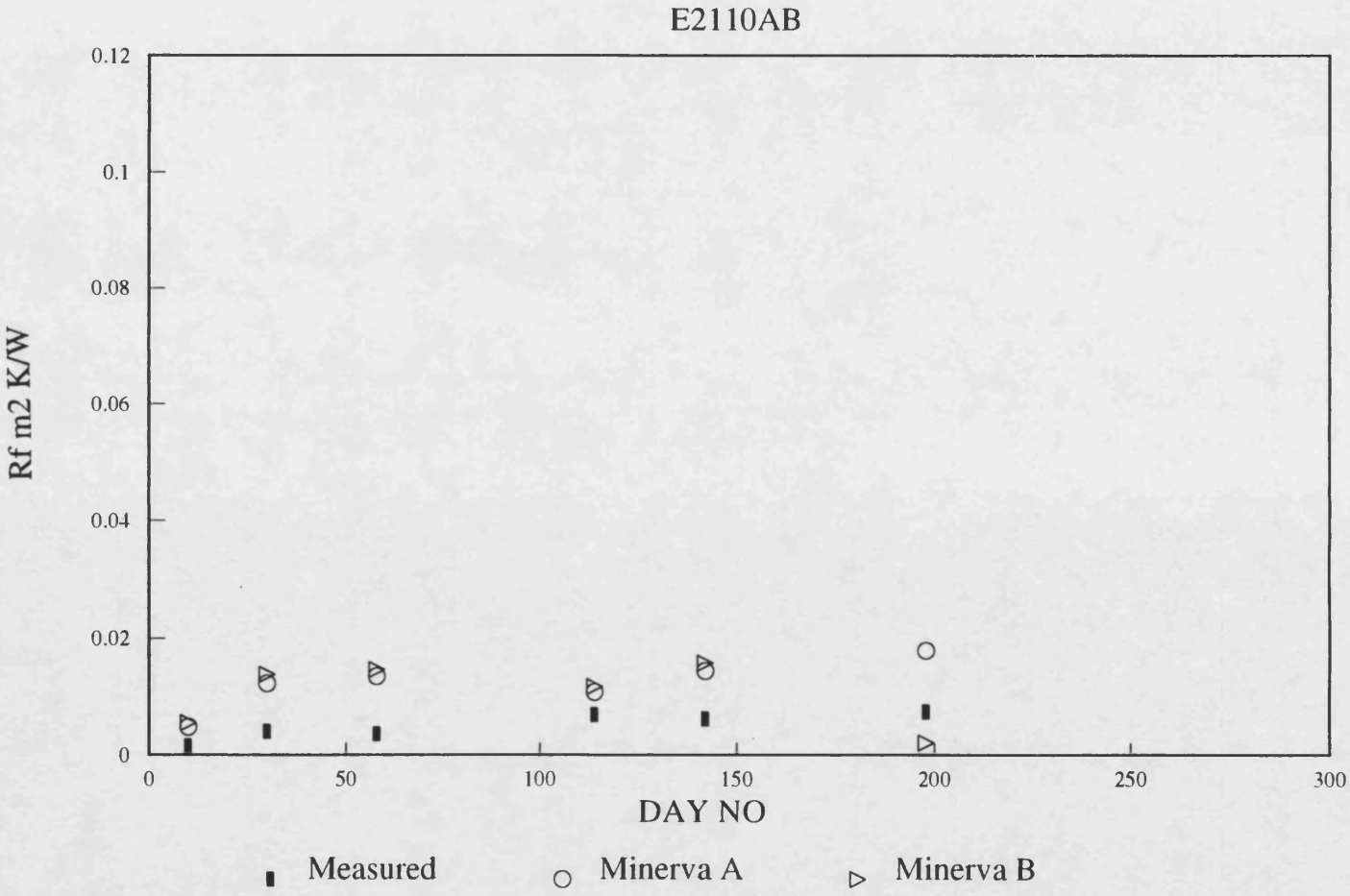

Table 6.1a Required Temperature Errors for Fouling Resistance Error

Required error in each temperature to give the initial fouling resistances observed in the second operating period.

Exchanger	Initial fouling resistance m^2KW^{-1}	Temperature Error °C
E2107a	0.00088	±2
E2107b	0.00141	±2
E2108ab	0.00264	±2
E2108cd	0.00211	±2
E2109a	0.00106	±2
E2109b	0.00070	±2
E2110ab	0.00106	±2
E2110cd	0.00141	±1.5

Table 6.1b Required Temperature Errors for Fouling Resistance Error

Required error in each temperature to give the initial fouling resistances observed in the first operating period (readings taken after 29 days operation)

Exchanger	Initial fouling resistance m^2KW^{-1}	Temperature Error °C
E2104a	0.000528	±3.5
E2104b	0.000704	±3.5
E2107a	0.00088	±3.0
E2107b	0.000528	±4.0
E2108ab	0.004752	±2.5
E2108cd	0.005808	±3.0
E2109a	0.00088	±4.0
E2109b	0.00176	±2.0
E2110ab	0.001584	±3.0
E2110cd	0.001056	±5.0

Table 6.2 Calculated Values of the Initial Thermal Efficiency

First operating period (readings taken after 29 days operation)

Exchanger	Initial thermal efficiency
E2104a	0.325
E2104b	0.273
E2107a	0.425
E2107b	0.324
E2108ab	0.118
E2108cd	0.079
E2109a	0.38
E2109b	0.369
E2110ab	0.187
E2110cd	0.238

Table 6.3 Data used to determine Minerva Coefficients

Data	E2014a	E2110ab
Density (lb ft^3)	47.4	43
Tubeside velocity (ft s^{-1})	5.68	4.79
Energy transfered (Btu h^{-1})	6847.28	7870.52
Bulk temperature (°F)	279	445
Inside heat transfer coefficient (Btu h^{-1} °F^{-1})	345	408
Outside heat transfer coefficient (Btu h^{-1} °F^{-1})	268.5	317.58
Asymptotic fouling resistance (°F h Btu^{-1})	0.0055	0.0272

References

(1) Crittenden B.D, Kolaczkowski S.T and Hout S.A (1987) "Modelling hydrocarbon fouling"

Chem Eng Res Des **65** 171-179.

(2) Crittenden B.D " Chemical reaction fouling of heat exchangers"

in "Fouling Science and Technology" Eds melo L.F, Bott T.R and Bernardo C.A NATO ASI Series E Vol 145

(3) Froment G.F (1981)

In: "Fouling of heat transfer Equipment" (Somerscales E.F.C and Knudsen J.G eds.) Hemisphere Washington

pp 411-435.

(4) Nelson W.L (1934) " Fouling of heat exchangers"

Ref and Nat Gas Man **13** (8) 292-298.

(5) Atkins G.T (1962) " What to do about high coking rates"

Petro Chem Eng **34** (4) 20-25.

(6) Weiland J.H McCay R.C and Barnes J.E (1949) " Rate of fouling and cleaning of unfired heat exchange equipment."

Trans ASME **71** 849-853.

(7) Butler R.C, McCurdy W.N and Linden N.J (1949) "Fouling rates and cleaning methods in refinery heat exchangers"

Ibid 843-847.

(8) Lawler D (1979)

Proc conf : Fouling Science or Art?"

ICorr Sci and Tech/IChemE London

pp 155-168.

(9) Lambourn G.A and Durrieu M (1986) "Fouling in Crude oil preheat trains"

In: "Heat exchanger source book" (Palen J. ed) Hemisphere London.

(10) Watkinson A.P and Epstein N (1969) "Gas oil fouling in a sensible heat exchanger"
Chem Engng Prog Symp Ser **65** (92) 84-90.
(11) Crittenden B.D, Hout S.A and Alderman N.J (1987)
Chem Eng Res Des **65** (2).
(12) Taylor W.F (1969) "Kinetics of deposit formation from hydrocarbons: Fuel composition studies"
Ind Engng Chem Prod Res Dev **8** 375-380.
(13) Crittenden B.D and Kolaczkowski S.T (1979) "Mass transfer and chemical kinetics in hydrocarbon fouling"
Proc conf: Fouling Science or Art?"
ICorr Sci and Tech/IChemE London
pp 169-187.
(14) Kern D.Q and Seaton R.E (1959) "A theoretical analysis of thermal surface fouling"
Brit Chem Eng **4** (5) 258-262.
(15) Crittenden B.D, Kolaczkowski S.T and Varley R (1979) "Efficient use of energy in oil refinery networks subject to fouling"
IChemE Symp Ser **105** 201-211.
(16) Thompson R.B, Druge L.W and Chenek J.A (1949) "Stability of fuel oils in storage: effect of sulphur."
Ind and Engng Chem **42** 2715-2721.
(17) Crittenden B.D and Khater E.M.H (1984) "Fouling from vaporising kerosine"
In: Fouling in heat exchange Equipment (Suitor J.W and Pritchard A.M eds)
ASME Publication HTD **35** New York.
pp57-64.
(18) Eaton P and Lux R (1984) "Laboratory fouling test apparatus for hydrocarbon feedstocks"
Ibid pp33-42.

(19) Vranos A, Marteney P.J and Knight B.A (1981)

In: "Fouling of heat transfer equipment" (Somerscales E.F.C and Knudsen J.G eds). Hemisphere Washington

pp 489-499.

(20) Kolaczkowski ST, Crittenden BD and Varley R (1988) " Operability of crude oil preheat exchangers: computer software to manage the problem."

Proc Int Conf on Fouling in Process Plant, ICorr Sci & Tech/ IChemE pp 52-67, 1988.

(21) Kolaczkowski (1977) "Two-phase heat transfer and fouling in hydrocarbon vaporizers" PhD Thesis, University of Bath.

7 CONCLUSIONS AND SUGGESTIONS FOR FURTHER WORK

7.1 Observations from the data collected on the refinery.

The unique, detailed set of industrial data, in-field deposit observation and measurement, and deposit composition analysis has enabled much insight to be gained into the fouling of refinery preheat exchangers. From an analysis of the large amount of data collected from the refinery the following general observations were made.

(i) At all times the calculated fouling resistances for all the exchangers were greater than the design (TEMA) values. This is in agreement with the findings of other workers and with the data from other BP refineries, possibly indicating that the TEMA values which are used through out industry may require revision.

(ii) There was an offset in the calculated "clean" heat transfer coefficients on start-up of the exchangers i.e $R_{f(t=0)} \neq 0$. From the data available form the refinery it was not possible to determine the exact cause of this. However it is a phenomena that has been observed by several other workers who have studied industrial exchangers. This offset is not as apparent in reports of studies on laboratory scale equipment and may be due to the lower degree of controlability in an industrial situation.

(iii) The fouling resistance and the amount of deposit observed at on shutdown of the exchangers for cleaning increased along the exchanger train. The coolest exchangers had the lowest calculated fouling resistances and the least amount of tubeside fouling deposit, with the highest calculated fouling resistance and the greatest amounts of fouling deposit being found in the hottest exchangers. This would appear to indicate the fouling from crude oils increases with increasing temperature.

(iv) The velocity of the crude oil through the tubes appears to have an effect upon the fouling rate. Several of the exchangers exhibited a reduction in fouling resistance when run at maximum throughput. However this effect was difficult to quantify as for commercial reasons the refinery was operated at a low and relatively steady flowrate for the period of the study.

(v) The composition of the feed stream had a dramatic effect on the fouling rate. The majority of the exchangers showed an increase in fouling resistance on introduction of the slops and heavy crude oil types. However due to the diversity of the feedstocks processed it was not possible to quantify this effect.

(vi) Analysis of the deposits from the heat exchangers showed that in the majority of them the composition by weight was approximately 50% by resins and free oil, 1-2% by asphaltenes, approximately 30% by coke and 18% inorganics. This compared favourably with the findings of other workers. The exception to this pattern was the E2108A exchanger where significant amounts of salt were found which were probably carried over from the desalters.

(vii) Pressure drop measurements were made on a few of the exchangers and from this data the average deposit thickness was estimated, these values compared favourably with measurements made when the exchangers were opened for cleaning. These results showed that pressure drop measurement can yield useful information as to the extent of fouling which would be of greater importance in systems that became throughput rather than heat transfer limited due to fouling.

7.2 Development and testing of mathematical models to predict fouling.

7.2.1 Simple kinetically controlled deposition model.

An insight into the relationship between the fouling rate and the tube wall temperature of the exchanger was gained by the development of a simple model. The fouling rate was correlated against temperature assuming a simple kinetically controlled deposition mechanism using a simple Arrhenius expression. This correlation yielded a value of 33 kJ mol^{-1} for the activation energy of the light crude oil type which compares favourably with published values for fouling from various hydrocarbon systems. This simple model was tested using data from the second operating period and was found to give a reasonable

prediction of the fouling resistance. The correlation yielded a value of 21 kJ mol^{-1} for the activation energy of the heavy crude oil types, indicating that there should be greater fouling for a given temperature, and in general this was found to be the case.

The offset observed in the fouling resistance on start-up of the exchangers was correlated against the initial thermal effectiveness of the exchangers. The results from this correlation were then used as a corrective constant in the simple model which improved the accuracy of the predictions.

7.2.2 Testing of published fouling models.

Crittenden and Kolaczkowski have published a kinetically controlled deposition and shear removal model, which has been developed into a form the can be used on a personal computer. The required coefficients were determined using the operating data from the first operating period. The model was then used to predict the fouling resistances in the second period of operation. The tendency was for over prediction of the fouling resistance. This may be considered as indicating that this more complex model is very sensitive to the feedstock composition and is hence not readily suitable, in the current form, for modelling a system with such diverse and frequent changes of feedstock.

7.3 Suggestions for further work.

7.3.1 Investigation of the effect of crude oil on fouling of industrial heat exchangers.

One of the major difficulties with analysisng the results from this study was the number of variables that could and often did change between data sets. It was diffficult to take account of the frequent changes in feed stocks, particularly as the feedstock was usually a mixture of several different crude oils and the feedstocks were not repeated. Repetition of the work in a situation where

(i) a refinery processed only a few crude oil types as single feedstocks for discreet operating periods, or

(ii) several refineries that process single feedstocks,

would allow a more thorough investigation into the composition effects. Also a preheat train that had a greater variation in tubeside velocity would allow the relationship between fouling rate and velocity to be evaluated on an industrial scale.

7.3.2 Laboratory Scale Experiments

The practicalities of an industrial scale project may render it too difficult or costly to mount. Hence it is further suggested that laboratory scale experiments be mounted using industrial tubes and actual crude oils at realistic temperatures and pressures. A small bundle of tubes with varing cross-sectional areas could be utilised to explore the fouling velocity relationship. Further investigation of the composition effects would be harder to reproduce in the laboratory due to the diverse types and large amounts of crude oil that would be required. Thus it is suggested that this investigative work would be best carried out over several refineries with the results from this study and subsequent velocity based studies being used to account for the effects of temperature and velocity thus hopefully exposing the composition effects.

The effect of temperature on fouling from certain species is a subject that warrents further investigation. During this study the it was discovered that the fouling from slops may only occur in a given temperature band (see Section 5.1.8). This is the type of investigation that could be carried out in the laboratory where it would be relatively easy to have several tubes seeing the same feed but having different tubewall temperatures.

APPENDIX A

HEAT EXCHANGER DETAILS

A1 HEAT EXCHANGER DETAILS

Chapter 2 describes the refinery and the preheat train on which the study was based.

Table A1 gives process and mechanical design details for the exchangers studied.

Table A1 Heat Exchanger Details

Exchanger	Tubeside Flowrate kg h^{-1}	Shellside Flowrate kg h^{-1}	Tube passes	Shell passes	Shell i.d. m	Tube length m
E2101a-f	581727.5	313477.5	2	1	1.24	6.096
E2102a-d	581727.5	161687.5	4	div flow	1.42	7.315
E2103a-b	581727.5	368182.5	2	1	0.838	4.877
E2104a-b	581727.5	368182.5	2	1	0.864	4.877
E2105	581727.5	167430.0	2	1	1.22	6.096
E2106	581727.5	112215.0	2	1	0.889	6.096
E2107a-b	581727.5	363635.0	4	1	1.27	6.096
E2108a-d	581727.5	313477.5	2	1	0.991	6.096
E2109a-b	581272.5	363635.0	4	1	1.27	6.096
E2110a-d	581727.5	272727.5	2	1	0.991	4.877
E2111a-b	313477.5	581727.5	4	div flow	0.965	6.096

Exchanger	Tube o.d. m	Tube i.d. m	Number of tubes	Baffle spacing m
E2101a-f	0.019	0.012	1610	0.4
E2102a-d	0.019	0.012	2065	0.5
E2103a-b	0.019	0.012	692	0.5
E2104a-b	0.019	0.012	740	0.48
E2105	0.019	0.012	1530	0.25
E2106	0.019	0.012	800	0.185
E2107a-b	0.019	0.012	1640	0.3
E2108a-d	0.019	0.012	970	0.5
E2109a-b	0.019	0.012	1640	0.3
E2110a-d	0.019	0.012	970	0.4
E2111a-b	0.019	0.012	894	0.49

APPENDIX B

PROPAGATION OF ERRORS

B1 INTRODUCTION

The error in the calculated value of the fouling resistance R_f is dependent upon the errors in the calculated values of the clean and dirty heat transfer coefficients.

The systematic errors that may be introduced in the calculation of the fouling resistance are discussed in Section 3.2.1 and were presented in the paper "Acquisition and interpretation of oil refinery plant data fro fouling studies." Crittenden BD, Downey IL and Kolaczkowski ST, Proc Int Conf on Fouling in Process Plant, ICorr Sci & Tech/ I Chem E, pp 32-51, 1988.

This paper is reproduced here with the kind permission of the co-authors, the detailed calculations that were used to establish the findings of the paper are presented in Section B2.

B1.1 ACQUISITION AND INTERPRETATION OF OIL REFINERY PLANT DATA FOR FOULING STUDIES

ACQUISITION AND INTERPRETATION OF OIL REFINERY PLANT DATA FOR FOULING STUDIES

B D Crittenden*, I L Downey and S T Kolaczkowski
School of Chemical Engineering
University of Bath
Bath BA2 7AY

ABSTRACT

Industrial plant data is invaluable for studying the effects of process variables on the loss of performance of heat exchangers processing oil refinery fluids. An analysis is presented of the potential errors which can arise when basic plant data is used to compute instantaneous fouling resistances. The analysis shows that even with reasonable allowances for inaccuracies in temperatures and flowrates, the maximum errors in thermal duty and fouling resistance can become significant. The use of an alternative method of representing the loss of thermal performance is explored.

1 INTRODUCTION

Fouling of oil refinery heat exchangers remains a major operational problem despite the amount of attention which has been paid to this subject by academia, by operating companies and by purveyors of anti-fouling chemicals and devices. The financial penalties are claimed to be very high. In 1979 the Exxon Chemical Company (Van Nostrand *et al*, 1981) estimated that the cost of fouling in a typical US 100,000 barrels per day oil refinery was approximately $10M per annum. About half of this cost was attributed to fouling in the crude distillation units (CDUs) in which all of the incoming crude oil is heated from ambient to elevated temperature in a network of shell and tube heat exchangers and furnaces. Other problematical exchangers are associated with the processes of hydrotreating, reforming and visbreaking.

In each unit the financial burden arises from a combination of the following:

- the reduction in throughput as exchanger flow channels become blocked;
- the additional energy which is required in furnaces in order to maintain feed temperatures to columns and reactors and to overcome increasing pressure drops;
- the maintenance and cleaning costs of fouled exchangers;
- the purchase of anti-fouling chemicals and devices in an attempt to alleviate the severity of fouling.

For most of the oil refineries which are currently operational, allowances for fouling in heat exchangers were made by including TEMA resistances (Tubular Exchangers Manufacturers' Association, 1978), or equivalent, at the design stage. Only scant regard would have been paid to the effects that process variables such as temperature, flowrate and composition would have on the fouling process.

2 INADEQUACY OF DESIGN FOULING RESISTANCES

Bott and Walker (1971) have compiled evidence which shows that in many oil refinery heat exchangers the TEMA resistance is exceeded in practice in very short time-scales. For continued operation after the design fouling resistance has been exceeded it is necessary to operate at reduced throughput, which, by virtue of the general effect that velocity has on fouling, will exacerbate the fouling problem. Alternatively, it may be possible to provide additional energy in furnaces. In many refineries some flexibility is obtained because the energy exchange occurs in complex but integrated networks.

3 INADEQUACY OF LABORATORY STUDIES

Fouling from hydrocarbons is a complex process which can involve a combination of mechanisms such as crystallisation, corrosion, chemical reaction and physical deposition. Carefully controlled laboratory-scale studies have been useful in showing that the rate of each of the above mechanisms of fouling is strongly dependent upon surface and bulk temperatures, flowrates, feedstock composition, equipment geometry and metallurgy (Epstein, 1981). As an example, the initial rate of fouling from sour gas oils in a small heated tube was found to depend exponentially on absolute surface temperature and to be inversely proportional to mass flowrate (Watkinson and Epstein, 1969). In another study (Crittenden and Khater, 1987), the initial fouling rate from odourless kerosene was found to be very high at low flowrates and to be strongly dependent upon surface temperature, pressure, oxygen content and degassing of the liquid phase during vaporisation.

Because fouling in refinery exchangers may take weeks or even months to reach significant levels, it is necessary in the laboratory to modify one or more of the operating parameters so that an accelerated test lasting only hours or days can be achieved. A common approach is to use actual feedstocks and realistic temperatures, pressures and

metallurgy, but to greatly reduce the fluid flowrate and thereby to reduce equipment size and power requirements. Special consideration needs to be given to preserving representative fluid velocities or Reynolds numbers. It is not uncommon to find that experiments which depend on reduced flowrates or unusual geometries yield deposits which are dissimilar in composition to those found in the industrial situation. For example, the laboratory-scale deposits from crude oils can often have unrealistically high organic contents as a result of the shift in balance between the organic and inorganic fouling mechanisms in equipment of reduced scale.

Several designs of laboratory-scale equipment are described in the literature (*eg* Braun, 1977; Hausler, 1973; Eaton and Lux, 1984), and have been used mainly to test the effectiveness of anti-fouling chemicals rather than to obtain fundamental relationships between fouling rates and operating and design parameters. Each method uses modified process parameters to give an accelerated fouling rate and therefore at best can only give a comparative effectiveness of a particular anti-foulant treatment.

It is clear therefore that in order to obtain a more complete understanding of hydrocarbon fouling, it is necessary to supplement laboratory-scale studies with studies made on industrial plant.

4 INDUSTRIAL PLANT DATA

The principal disadvantages of using industrial plant data in research are:

- it is not possible to mount scientific experiments without interfering with the normal business of production;
- since fouling in oil refineries may occur gradually over periods exceeding a year, it is quite likely that the process operating parameters will have changed many times before the "experiment" can be terminated, *ie* the plant is shut down for cleaning and maintenance and the exchanger surfaces can be inspected;
- the instrumentation is usually much more limited than would be possible in the research laboratory.

On a typical refinery exchanger the information which can normally be obtained at regular intervals is as follows:

- the inlet and outlet temperatures of both process streams, Figure 1;
- the flowrates of both process streams, Figure 1;
- the assays of fluids being processed;
- the pressures at some locations.

Although fouling is a dynamic process, the fouling rate is usually sufficiently low such that at any time the

steady-state rate equation for heat transfer may be used to calculate the instantaneous overall heat transfer coefficient:

$$Q = U_d A \text{ LMTD} \quad (1)$$

The fouling resistance is then calculated from:

$$R_f = \frac{1}{U_d} - \frac{1}{U_c} \quad (2)$$

in which U_c would be the instantaneous heat transfer coefficient for the exchanger if there were no fouling. It is important to note that at this stage it is not possible to determine how the value of R_f calculated from equation (2) is apportioned between shell and tube sides.

4.1 Errors in overall coefficients

Clearly the error in the calculated value of R_f is dependent upon the errors in the calculated values of both U_d and U_c. A computation of the error in R_f is a useful guide not only to the accuracy and reliability of the numerical value but also to the number of significant figures that should be quoted. Random errors in U_d are indeterminate and result from an inability to

- control the experimental conditions accurately; and
- read instruments accurately and consistently.

Both these aspects require careful attention. The coefficient U_c is computed from film heat transfer coefficients and the conductance of the tube wall. Thus errors in U_c are systematic and it should be possible to remove them by "calibration". In effect this can be achieved by testing predictive programs with extensive and well controlled plant and laboratory data. Vendors of exchanger software should be encouraged to supply the potential errors in U_c.

For the function

$$R_f = R_f (U_c, U_d) \tag{3}$$

$$dR_f = \frac{\partial R_f}{\partial U_c} dU_c + \frac{\partial R_f}{\partial U_d} dU_d \tag{4}$$

If the errors in U_c and U_d are δU_c and δU_d respectively, and are small relative to U_c and U_d, then the error induced in R_f is given by:

$$\delta R_f = \frac{\partial R_f}{\partial U_c} \delta U_c + \frac{\partial R_f}{\partial U_d} \delta U_d \tag{5}$$

The worst possible value of δR_f occurs when all of the terms on the right hand side of the equality are either positive or negative. Thus, taking δU_c and δU_d to be positive:

$$\delta R_f = \left|\frac{\partial R_f}{\partial U_c}\right| \delta U_c + \left|\frac{\partial R_f}{\partial U_d}\right| \delta U_d \qquad (6)$$

From equation (2):

$$\frac{\partial R_f}{\partial U_c} = \frac{1}{U_c^2} \qquad (7)$$

$$\frac{\partial R_f}{\partial U_d} = -\frac{1}{U_d^2} \qquad (8)$$

Thus $$\delta R_f = \frac{\delta U_c}{U_c^2} + \frac{\delta U_d}{U_d^2} \qquad (9)$$

Assuming that there is no error in the computation of U_c, then the error in the calculated fouling resistance is given by:

$$\delta R_f = \frac{\delta U_d}{U_d^2} \qquad (10)$$

or $$\delta R_f = \frac{1}{U_d}\left\{\frac{\delta U_d}{U_d}\right\} \qquad (11)$$

Equation (11) is plotted on Figure 2. For an exchanger which heats dry crude in the temperature range 149 to 259°C at an average velocity of 1 ms^{-1} with gas oil from a crude distillation unit, the combined fouling resistances taken from TEMA would be about 0.88 $m^2K\ kw^{-1}$. With U_d = 0.3 (± 27%) $kw\ m^{-2}K^{-1}$, it can be seen from Figure 2 that the

absolute error in R_f is equal to 0.88 $m^2K\ kw^{-1}$, *ie* the TEMA design value. Furthermore, if U_c = 1.0 (± 10%) kw $m^{-2}K^{-1}$,

$$\delta R_f = \frac{1}{U_c}\frac{\delta U_c}{U_c} + \frac{1}{U_d}\frac{\delta U_d}{U_d} \qquad (12)$$

$$= 0.1 + \frac{1}{0.3} \times 0.27$$

$$= 1\ m^2K\ kw^{-1}$$

The above analysis demonstrates the importance of determining U_c and U_d as accurately as possible if errors of the same order as TEMA resistances are to be avoided. As indicated above, it is possible, in principle, to eliminate errors in U_c by confirmation of predictive correlations. Clearly, an accurate physical property database is also required. On the other hand, errors in U_d depend upon the accuracy of plant data. Errors in U_d are related solely to errors in Q, A and LMTD [equation (1)].

4.2 Errors in operating parameters

In the following analysis the worst scenario is considered, that is, the errors in each of the four end temperatures and in each of the two flowrates compound, rather than eliminate each other. Using the notation given in Figure 1, the

instantaneous coefficient U_d is given by:

$$U_d = \frac{Q \ \ell n\left\{\frac{T_1-t_2}{T_2-t_1}\right\}}{A[(T_1-t_2)-(T_2-t_1)]} \qquad (13)$$

Thus, neglecting errors in the calculation of A,

$$\delta U_d = \left|\frac{\partial U_d}{\partial Q}\right|\delta Q + \left|\frac{\partial U_d}{\partial t_1}\right|\delta t_1 + \left|\frac{\partial U_d}{\partial t_2}\right|\delta t_2 + \left|\frac{\partial U_d}{\partial T_1}\right|\delta T_1 + \left|\frac{\partial U_d}{\partial T_2}\right|\delta T_2 \qquad (14)$$

Hence

$$\delta U_d = \left|\frac{\ell nX}{AW}\right|\delta Q + \left|\frac{Q(Z-\ell nX)}{AW^2}\right|\delta t_1 + \left|\frac{Q(\ell nX-Y)}{AW^2}\right|\delta t_2$$

$$+ \left|\frac{Q(Y-\ell nX)}{AW^2}\right|\delta T_1 + \left|\frac{Q(\ell nX-Z)}{AW^2}\right|\delta T_2 \qquad (15)$$

Or

$$\frac{\delta U_d}{U_d} = \frac{\delta Q}{Q} + \frac{1}{W}\left\{\left|\frac{Z}{\ell nX} - 1\right|\delta t_1 + \left|1 - \frac{Y}{\ell nX}\right|\delta t_2 + \left|\frac{Y}{\ell nX} - 1\right|\delta T_1\right.$$

$$\left. + \left|1 - \frac{Z}{\ell nX}\right|\delta T_2\right\} \qquad (16)$$

where $W = (T_1-t_2) - (T_2-t_1)$ (17)

$$X = \left\{\frac{T_1-t_2}{T_2-t_1}\right\} \qquad (18)$$

$$Y = \frac{W}{(T_1 - t_2)} \tag{19}$$

$$Z = \frac{W}{(T_2 - t_1)} \tag{20}$$

Equation (16) shows that the relative error in thermal duty needs to be assessed.

4.3 Error in the duty

The instantaneous thermal duty Q is given by

$$Q = M\, C_p (t_2 - t_1) \tag{21}$$

Assuming that there is no error in C_p, then

$$\delta Q = \left|\frac{\partial Q}{\partial M}\right| \delta M + \left|\frac{\partial Q}{\partial t_1}\right| \delta t_1 + \left|\frac{\partial Q}{\partial t_2}\right| \delta t_2 \tag{22}$$

or $$\delta Q = C_p (t_2 - t_1)\delta M + M C_p \delta t_1 + M C_p \delta t_2 \tag{23}$$

and $$\frac{\delta Q}{Q} = \frac{\delta M}{M} + \frac{\delta t_1 + \delta t_2}{(t_2 - t_1)} \tag{24}$$

4.4 Typical example

Consider an error of 2°C in each of the end temperatures and a 5% error in the flowrate measurement, *ie*

$$\delta t_1 = \delta t_2 = \delta T_1 = \delta T_2 = 2 \qquad (25)$$

$$\frac{\delta M}{M} = 0.05 \qquad (26)$$

For an exchanger in which

$$t_1 = 190°C, \quad t_2 = 210°C$$
$$T_1 = 310°C, \quad T_2 = 280°C$$

the error in Q is given by equation (24), *ie*

$$\frac{\delta Q}{Q} = 0.05 + \frac{(2 + 2)}{(210 - 190)}$$

$$= 0.25$$

Thus the maximum error in the duty could be as high as 25%.

Substituting values in equations (17) to (20) gives:

$$W = 10°C$$

$$X = 1.111$$

$$Y = 0.333$$

$$Z = 0.111$$

Substitution in equation (16) gives:

$$\frac{\delta U_d}{U_d} = 0.25 + \frac{2}{10}\left\{\left|\frac{0.111}{\ell n 1.111} - 1\right| + \left|1 - \frac{0.333}{\ell n 1.111}\right| + \left|\frac{0.333}{\ell n 1.111} - 1\right|\right.$$

$$\left. + \left|1 - \frac{0.111}{\ell n 1.111}\right|\right\} = 1.11$$

Hence the maximum error in the calculated value of the dirty coefficient for this example exchanger could be in excess of 100%. The consequences of such an error on the computation of R_f can be seen from Figure 2.

The major contribution to the error in U_d arises from the errors in the temperature measurements. If temperatures can be determined to within 1°C, whilst the error in flowrate remains at 5%, then the maximum error in U_d can be reduced to 59%.

4.5 Alternative methods of quantifying fouling

It is debatable whether the use of equation (2) is the best way of quantifying the loss of performance as a heat exchanger becomes fouled. The maximum absolute error in R_f calculated from equation (2) is given by equation (9). Since

$$R_f = \frac{1}{U_d} - \frac{1}{U_c} = \frac{U_c - U_d}{U_c U_d} \qquad (27)$$

the maximum relative error in R_f is given by

$$\frac{\delta R_f}{R_f} = \frac{1}{(U_c - U_d)} \left\{ \frac{U_d}{U_c} \delta U_c + \frac{U_c}{U_d} \delta U_d \right\} \qquad (28)$$

An alternative way of expressing the loss of thermal performance is as follows:

$$I_m = 1 - \frac{U_d}{U_c} = \frac{U_c - U_d}{U_c} \tag{29}$$

The maximum absolute error in I_m is given by

$$\delta I_m = \left|\frac{\partial I_m}{\partial U_c}\right| \delta U_c + \left|\frac{\partial I_m}{\partial U_d}\right| \delta U_d \tag{30}$$

$$= \frac{U_d}{U_c^2} \delta U_c + \frac{1}{U_c} \delta U_d \tag{31}$$

The maximum relative error in I_m is given by:

$$\frac{\delta I_m}{I_m} = \frac{1}{(U_c - U_d)} \left\{\frac{U_d}{U_c} \delta U_c + \delta U_d\right\} \tag{32}$$

A comparison of equations (28) and (32) shows that the maximum relative error in I_m will always be less than that in R_f since U_c/U_d is always greater than unity. The use of equation (29), rather than equation (2), has two further advantages; firstly, I_m is non-dimensional, and secondly, the range of I_m is more conveniently bounded by zero and unity.

5 DATA ACQUISITION

The above analyses reveal that it is extremely important to ensure that plant data for fouling studies is obtained as accurately as possible. In particular, it can be seen that errors in temperature measurements can have a profound effect on the accuracy of calculated fouling resistances. Whilst errors in temperature measurements cannot be eliminated entirely, it is possible to take precautions to ensure that inaccuracies are consistent and do not contribute in such a way as to maximise the error in R_f.

Figure 2 shows that for a given relative error in U_d, the absolute error in R_f increases as U_d decreases. Since U_d decreases with time, it might be inferred that the absolute error in R_f will increase with time as well. An additional complication is that as U_d decreases with time it is most likely that the relative error in U_d will increase. Thus the errors in R_f can vary substantially throughout the duration of a plant trial. At the beginning of a trial with a clean heat exchanger, R_f should be equal to zero. However, temperature approaches might be very small for a clean exchanger. The above analyses reveal that for a constant absolute error in temperature measurement, the absolute error in R_f can rise dramatically as the temperature approach is decreased. Hence high errors might also be expected in the period shortly after start-up from clean conditions.

6 CONCLUSION

Whilst it is desirable experimentally to use plant data to study the effects of process variables on fouling from oil refinery process streams, particular care needs to be taken in order to ensure that propagated errors do not become excessive. Errors in temperature measurements can have a profound effect.

7 ACKNOWLEDGEMENTS

The opinions given in this paper are entirely those of the authors and the data relates to a hypothetical refinery exchanger. Nevertheless, the authors wish to thank the Science and Engineering Research Council, BP International and British Petroleum Raffinaderij, Nederland, for their continued support of fouling research at the University of Bath.

8 NOMENCLATURE

A	exchanger surface area	m^2
C_p	process fluid specific heat	$kJ\ kg^{-1}K^{-1}$
I_m	parameter defined by equation (29)	-
LMTD	log mean temperature difference	°C, K
M	process fluid flowrate	$kg\ s^{-1}$
Q	exchanger thermal duty	kw
R_f	fouling resistance	$(kw\ m^{-2}K^{-1})^{-1}$
t_1	inlet temperature of process fluid	°C, K
t_2	outlet temperature of process fluid	°C, K
T_1	inlet temperature of shell-side fluid	°C, K
T_2	outlet temperature of shell-side fluid	°C, K
U_c	instantaneous overall heat transfer coefficient if there were no fouling	$kw\ m^{-2}K^{-1}$
U_d	instantaneous overall heat transfer coefficient	$kw\ m^{-2}K^{-1}$
W	parameter defined by equation (17)	°C, K
X	parameter defined by equation (18)	-
Y	parameter defined by equation (19)	-
Z	parameter defined by equation (20)	-

9 REFERENCES

Bott, T R and Walker, R A (1971), *The Chemical Engineer*, London, No 255, 391-395

Braun, R (1977), *Materials Performance*, 16 (11), 35-41

Crittenden, B D and Khater, E M H (1987), *ASME J Heat Transfer* 109, 583-589

Eaton, P and Lux, R (1984) in Suitor, J W and Pritchard, A M (eds) "Fouling in Heat Exchange Equipment", HTD Vol 35, ASME, New York, pp33-42

Epstein, N (1981) in Somerscales, E F C and Knudsen, J G (eds) "Fouling of Heat Transfer Equipment", Hemisphere, Washington, pp701-734

Hausler, R H (1973), *Oil Gas J*, 71 (23), 56-63

Tubular Exchangers Manufacturers' Association (1978), Standards of the Tubular Exchangers Manufacturers' Association, New York, pp138-142

Van Nostrand, W L *et al* (1981) in Somerscales, E F C and Knudsen, J G, "Fouling of Heat Transfer Equipment", Hemisphere, Washington, pp619-643

Watkinson, A P and Epstein, N (1969), *Chem Eng Prog Symp Ser* 65 (92), 84-90

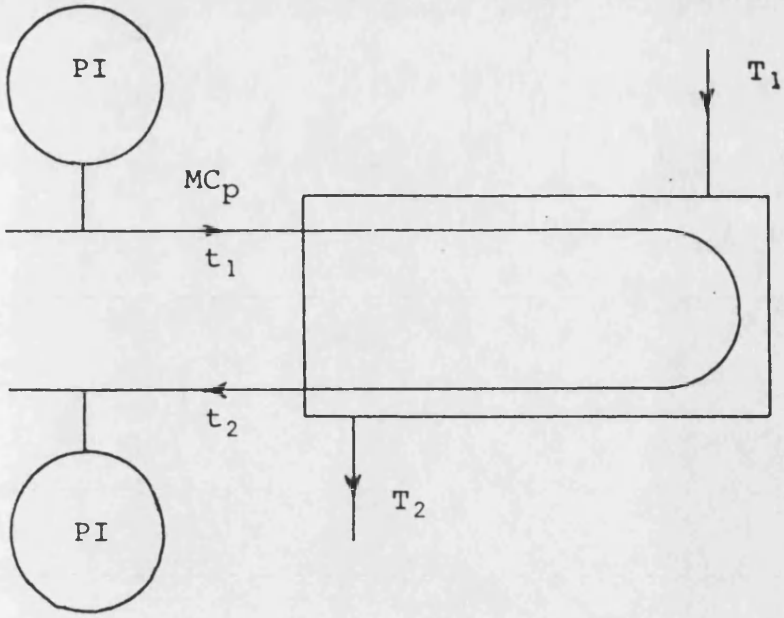

Figure 1 Hypothetical heat exchanger

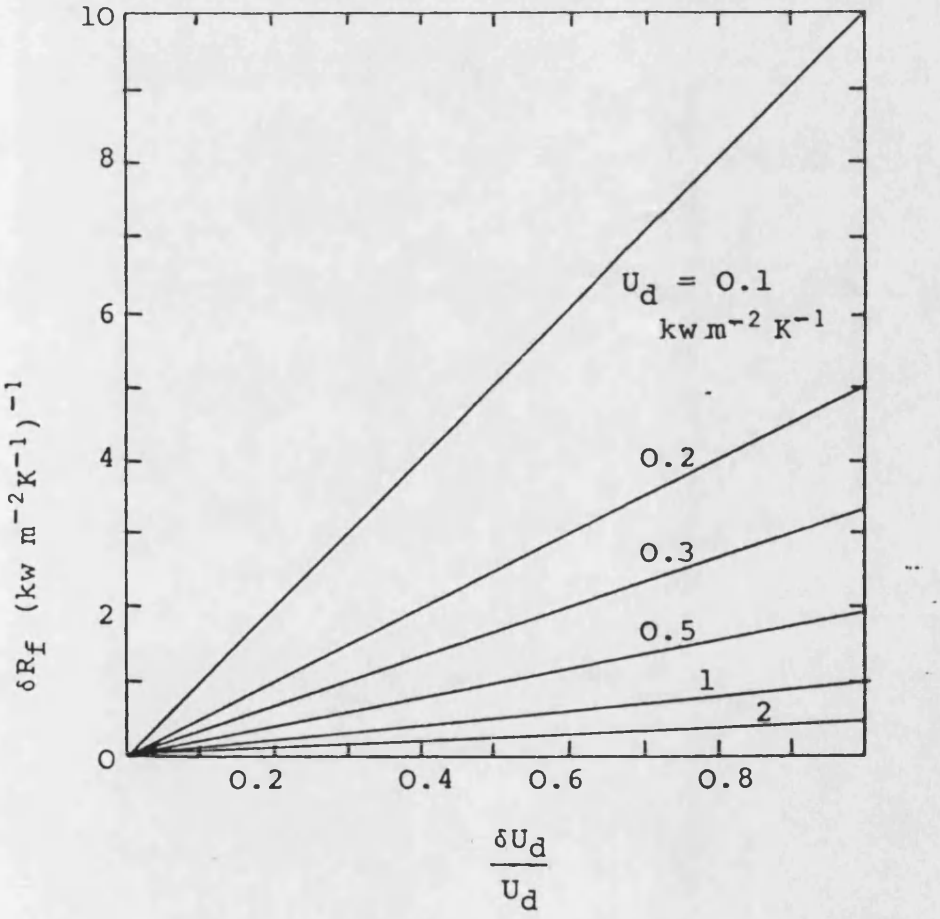

Figure 2 Maximum errors in fouling resistance (no error in clean coefficient)

B1.2 SUPPLEMENTARY INFORMATION

Equations 16 to 20 in Appendix B Section B1.1 were used to determine the maximum potential error in calculated values of fouling resistance. The following typical data was used in order to develop a system of equations that could be readily adapted for use in a sequential manner in a simple spreadsheet type format.

B1.2.1 Data Used

$t_1 = 193°C$ $h_o = 2000\ Wm^{-2}K^{-1}$

$t_2 = 213°C$ $h_i = 1700\ Wm^{-2}K^{-1}$

$T_1 = 310°C$ $U_c = 920\ Wm^{-2}K^{-1}$

$T_2 = 280°C$ $U_D = 325\ Wm^{-2}K^{-1}$

Substitution of this data into equation 17 gives

$$W = (310 - 213) - (280 - 193) = 10$$

Substitution into equation 18 gives

$$X = \frac{(310-213)}{(280-193)} = 1.1149$$

Substitution into equation 19 gives

$$Y = \frac{10}{310-213} = 0.10309$$

Substitution into equation 20 gives

$$Z = \frac{10}{280 - 193} = 0.1149$$

B1.2.2 System of equations

Substitution of the data from the above section into equation 24 gives

$$\frac{\delta Q}{Q} = \frac{\delta M}{M} + \frac{2\delta T}{20}$$

and into equation 16 gives

$$\frac{\delta U_d}{U_d} = \frac{\delta Q}{Q} + 0.1\ (0.217825 \quad \delta T)$$

The error in the clean heat transfer coefficient, assuming all physical properties are correct is dependent upon errors in the inside and outside heat transfer coefficients and thus the errors in the flowrate.

The heat transfer coefficients are related to the mass flowrate via the Reynolds number as detailed in Chapter 3, thus:

$$h_{io} \propto R_e^{0.8}$$

and

$$h_o \propto R_e^{0.55}$$

The clean heat transfer coefficient is related to the individual heat transfer coefficient thus,

$$U_c = \frac{h_{io} + h_o}{h_{io} h_o}$$

Thus the potential error in the clean heat transfer coefficient can be determined by substitution of the data in Section B1.2.1 to give

$$\frac{\delta U_c}{U_c} = 0.5405\left(0.8\frac{\delta M}{M}\right) + 0.4595\left(0.55\frac{deltM}{M}\right)$$

This allows the final equation in the system to be determined by substitution of the data into equation 12 in section B1.1

$$\frac{\delta R_f}{R_f} = 0.5462\left(\frac{\delta U_c}{U_c}\right) + 1.5462\left(\frac{\delta U_d}{U_d}\right)$$

This system of equations was then used sequentially to determine the maximum potential errors in the fouling resistance based on a given error in the measured data. The results are presented in Table B1, which is the basis for Figure 2 in Section B1.1.

Table B1 Calculation of Errors in Fouling Resistance

$\frac{\delta M}{M}$	δT (K)	$\frac{\delta Q}{Q}$	$\frac{\delta U_d}{U_d}$	$\frac{\delta U_c}{U_c}$	$\frac{\delta R_f}{R_f}$
0	0.05	0.05	0.0601	0	0.0929
0	1.00	0.10	0.1218	0	0.1883
0	1.50	0.15	0.1827	0	0.2825
0	2.00	0.20	0.2436	0	0.3767
0	2.50	0.25	0.3045	0	0.4708
0	3.00	0.30	0.3654	0	0.5650
0	3.50	0.35	0.4262	0	0.6590
0	4.00	0.40	0.4871	0	0.7532
0	5.00	0.50	0.6090	0	0.9417
1	0.05	0.06	0.0708	0.0069	0.1132
1	1.00	0.11	0.1318	0.0069	0.2076
1	1.50	0.16	0.1927	0.0069	0.3017
1	2.00	0.21	0.2536	0.0069	0.3959
1	2.50	0.26	0.3145	0.0069	0.4900
1	3.00	0.31	0.3753	0.0069	0.5841
1	3.50	0.36	0.4362	0.0069	0.6782
1	4.00	0.41	0.4971	0.0069	0.7724
1	5.00	0.51	0.6189	0.0069	0.9607

$\frac{\delta M}{M}$	δT (K)	$\frac{\delta Q}{Q}$	$\frac{\delta U_d}{U_d}$	$\frac{\delta U_c}{U_c}$	$\frac{\delta R_f}{R_f}$
10	0.05	0.15	0.1608	0.069	0.2863
10	1.00	0.20	0.2218	0.069	0.3806
10	1.50	0.25	0.2827	0.069	0.4748
10	2.00	0.30	0.3436	0.069	0.5690
10	2.50	0.35	0.4045	0.069	0.6631
10	3.00	0.40	0.4654	0.069	0.7573
10	3.50	0.45	0.5262	0.069	0.8513
10	4.00	0.50	0.5871	0.069	0.9455
10	5.00	0.60	0.7089	0.069	1.1338

B2 FOULING OF CRUDE OIL PRHEAT EXCHANGERS

The paper presented at the Internatioanl Conferenec on Fouling in Process plant held jointly by the Institue of Corrosion Science and Technology and the Institution of Chemical Engineers is presented overleaf.

FOULING OF CRUDE OIL PREHEAT EXCHANGERS

B. D. CRITTENDEN (FELLOW), S. T. KOLACZKOWSKI (FELLOW)
and I. L. DOWNEY (GRADUATE)
School of Chemical Engineering, University of Bath, Bath, UK

A simple refinery-specific correlation has been establishesd between the total fouling rate and tube wall temperature of individual heat exchangers in the preheat exchanger train of a crude oil distillation unit. The correlation has been obtained from plant data, and has subsequently been used successfully to predict the reduction in thermal performance of the preheat train with 'light' crude oils following a major shutdown for thorough cleaning. The activation energy for the fouling process for 'light' crude oils has been calculated to be about 33 kJ mol^{-1}, which lies in the region for a mixture of chemical and physical mechanisms. Chemical analyses confirm that the deposits contain a mixture of both inorganic materials and high molecular weight carbonaceous matter. The activation energy of the fouling process when 'heavy' crude oils are processed is much lower, at about 21 kJ mol^{-1}, which indicates the predominance of a physical mechanism.

INTRODUCTION

Fouling of heat exchangers remains a serious operating problem which leads to increased energy consumption, increased pressure drops, reduction or complete loss of throughput and increased maintenance costs. About half of the financial penalties due to fouling in an oil refinery is attributable[1] to the crude distillation unit (CDU) in which all of the incoming crude oil is heated from ambient to elevated temperature in a network of shell and tube heat exchangers and furnaces. The fouling mechanism is undoubtedly complex involving crystallisation of inorganics, corrosion, chemical reactions of organics and deposition of particulates[2]. To make matters worse, the controlling mechanism(s) may well vary from exchanger to exchanger in the preheat train.

An additional problem arises when the mechanism is not well understood, since it is clearly not easy to predict how much extra surface area should be provided in a new exchanger in order to cope with the problem. Chenoweth[3] has recently published information on the final report of the HTRI/TEMA Joint Committee to review the fouling section of the TEMA standards. Up till now, these standards[4] have normally been used to select design fouling resistances for refinery exchangers. Table 1 gives selected values from the new report[3] which are relevant to the research described in this paper. In most cases, the proposed design resistances are greater than or equal to those in the current standards[4].

RESEARCH METHODS

Research on CDU fouling in the laboratory is fraught with problems. Because fouling in refinery exchangers can take weeks or months to reach significant levels, it is common practice in the laboratory to modify one or more of the operating parameters so that an accelerated test lasting only hours or days can be achieved. One approach is to use actual feedstocks and realistic temperatures but to reduce greatly the fluid flowrate, and thereby reduce equipment size and power requirements. However, industrialists have indicated that experiments which depend on greatly reduced flowrates can yield deposits which have unrealistically high organic contents, indicating an over-emphasis of a particular fouling mechanism. On the other hand, operation at realistic flowrates in the laboratory would require continual

Table 1. Proposed design fouling resistances of relevance to CDUs, selected from Chenoweth[3].

fluid	temperature °C	velocity ms^{-1}	design R_f m^{2}K kW^{-1}	comment
crude oil	120	>1.22	0.35-0.70	desalted at ~120°C
crude oil	120-177	>1.22	0.53-0.70	desalted at ~120°C
crude oil	177-232	>1.22	0.70-0.88	desalted at ~120°C
crude oil	>232	>1.22	0.88-1.06	desalted at ~120°C
gasoline			0.35	
light distillate/ naphtha			0.35-0.53	
kerosene			0.35-0.53	
light gas oil			0.35-0.53	
heavy gas oil			0.53-0.88	
heavy fuel oil			0.88-1.23	
astmospheric tower bottoms			1.23	

0263-8762/92/$05.00 + 0.00

recycle of the crude oil even for a single tube experiment. Thus laboratory-scale equipment is normally only of value in comparative testing, and several designs for evaluating the effectiveness of anti-fouling chemicals are described in the literature[5].

The principal disadvantages of using actual plant data are associated with the difficulty in controlling the 'experiments'. Firstly it is necessary to assess the accuracy of the plant data, and secondly it is generally not possible to change the 'experimental conditions' on a CDU processing perhaps 100,000 barrels/day (*ca.* 660 $m^3 h^{-1}$), since the running of an oil refinery is dictated by commercial and operating decisions. Nonetheless, data acquired over relatively long periods of time can provide valuable information on the roles of key operating parameters on fouling rates.

CDU PREHEAT TRAIN

In this study, plant data were acquired over a three year period from one of the CDU preheat trains operated by the Rotterdam refinery of the Netherlands Refining Company (formerly BP Raffinaderij Nederland NV). A simplified flowsheet of the train is shown in Figure 1. On this figure, and in this paper, a notation such as E8AB signifies two exchangers in series (E8A and E8B) which, for practical reasons, could not be monitored individually.

The incoming crude oil is split into two parallel trains and heated from ambient to around 130°C in six exchangers in each train (E1A to E3B) using product and pump-around streams from the atmospheric distillation column. Each crude oil stream enters a desalter in which caustic soda at approximately 0.5% w/w is injected for pH control purposes. A demulsifying agent is added to reduce foaming and to improve oil-water separation. Water is added at 4% w/w to dissolve salts that are present in the crude oil.

The desalted crude oil is then pumped through a further network of heat exchangers (E4A to E11B) and its temperature is increased to around 250°C prior to passing into the atmospheric column via a furnace. In the post-desalter preheat exchangers, energy is obtained from streams which are taken from various positions within the atmospheric crude distillation column. Some of these streams are products taken from the column which require cooling whilst others, known as pump-around streams, are recycled back to the atmospheric column after cooling . Thus a middle pump-around is a recycle stream taken from somewhere near the middle of the distillation column. Details of relevance to this fouling study are shown in Figure 1 and Table 2. It should be noted that the two crude oil preheat trains are not identical downstream of the desalter.

All heat exchangers were of the multipass shell and tube type, in which, with the exception of E11A and E11B, the crude oil flows inside the tubes. Typical design data for the exchangers are shown in Table 2. A simplified schematic of a typical exchanger is shown in Figure 2 to demonstrate the nomenclature used in this paper.

ACQUISITION OF DATA

The chronology of major events is summarised in Table 3. Two separate operating cycles of 500 and 140 days continuously on-stream were studied. The temperatures, flowrates and compositions of each of the streams entering and leaving each exchanger (or pairs of exchangers, etc.) downstream of the desalter were recorded at frequent intervals during both operating cycles. Each visit to the refinery lasted approximately one day and the readings were taken after a period of steady operation. Between the two separate operating cycles the CDU was shut down and the exchanger bundles were removed for cleaning. This provided an opportunity to measure the thickness of deposits in some of the exchangers, although it must be borne in mind that the refinery's shutdown procedure may have had some effect on the foulant layers.

Stream temperatures were obtained using calibrated thermocouples located in thermowells. Crude oils were processed in batches and their flowrates were obtained

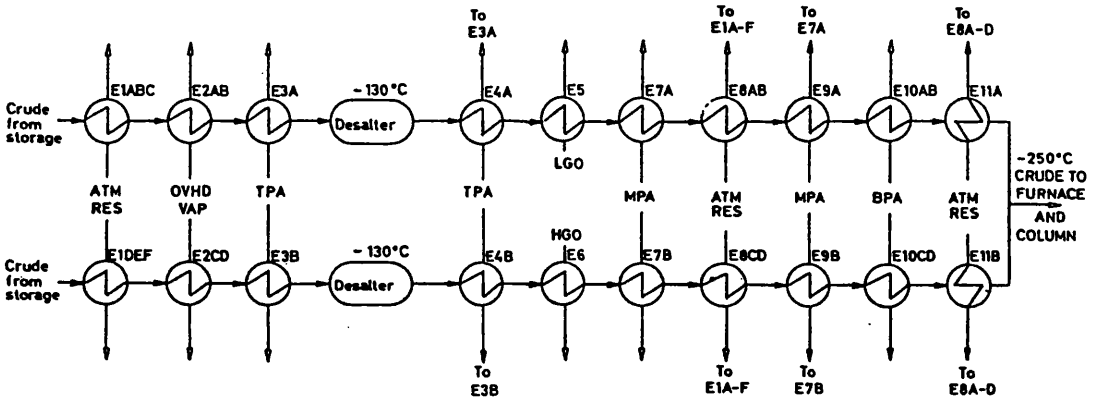

Figure 1. Simplified flow diagram of the crude oil pre-heat exchanger train: Key: E-shell/tube heat exchangers (see Table 2). The letters appearing after an exchanger number signify the number of shells in series, e.g. E1ABC signifies E1A, E1B and E1C in series. OHVD VAP overhead vapour, TPA top pump around; MPA middle pump around; BPA bottom pump around; LGO light gas oil; HGO heavy gas oil; ATM RES atmospheric residue.

Table 2. Basic description of CDU preheat exchangers.

exchanger train A	exchanger train B	description	tubeside fluid	tubeside passes	shellside fluid	shellside passes
E1ABC		3 in series	crude	2	atm residue	1
	E1DEF	3 in series	crude	2	atm residue	1
E2AB		2 in series	crude	4	o/head vapour	divided flow
	E2CD	2 in series	crude	4	o/head vapour	divided flow
E3A			crude	2	top pump around	1
	E3B		crude	2	top pump around	1
E4A			crude	2	top pump around	1
	E4B		crude	2	top pump around	1
E5			crude	2	light gas oil	1
	E6		crude	2	heavy gas oil	1
E7A			crude	4	middle pump around	1
	E7B		crude	4	middle pump around	1
E8AB		2 in series	crude	2	atm residue	1
	E8CD	2 in series	crude	2	atm residue	1
E9A			crude	4	middle pump around	1
	E9B		crude	4	middle pump around	1
E10AB		2 in series	crude	2	bottom pump around	1
	E10CD	2 in series	crude	2	bottom pump around	1
E11A			atm residue	4	crude	divided flow
	E11B		atm residue	4	crude	divided flow

Key. E: shell/tube exchangers. The letters appearing after an exchanger number signify the number of shells in series, e.g. E1ABC signifies E1A, E1B and E1C in series.

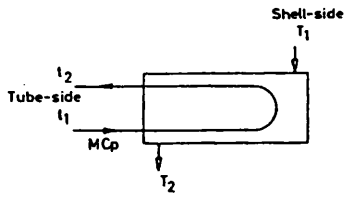

Figure 2. A single shell multi-tubular pass exchanger.

from tank dip data. Shell-side flowrates were obtained from orifice plate meters. Details of the crude oils being processed, together with other relevant operating information were obtained from data logged by the refinery.

The major shutdown for cleaning commenced at day 501 (the last data set being taken on day 499) and the CDU was restarted on day 552. Up to day 390, the crude oils being processed could be described as 'light', i.e. typically with a specific gravity of less than 0.87, but from this date up to the major shutdown, slop oils and 'heavy' crude oils were processed. Slop oils are hydrocarbons recovered from line and tank drainage/cleaning operations which are routed to a common tank, the slops tank. Heavy crudes typically have an SG > 0.87 and tend to have the highest asphaltene and sulphur contents. Following the major shutdown, 'light' crude oils were again processed for the remaining duration of the research project. The frequency of visits to the refinery for data acquisition can be obtained from the timing of the data points, see Figure 3, for example.

NATURE OF DEPOSITS

Several samples of tube-side deposits were taken from E7A, E8A, E9A and E10A at the major shutdown for cleaning (days 501 to 551), and analysed for:

Table 3. Chronology of major events.

operating cycle	start (day)	finish (day)	comment
shutdown		0	exchangers water-jetted on tube-side only E10A re-tubed
first	1	389	'light' crude oils processed
first	390	500	'heavy' crude oils and slops processed
major shutdown	501	551	— bundles pulled for remote cleaning of tube and shell-sides — deposit thicknesses measured — samples of deposits taken for analysis
second	552	692	'light' crude oils processed

- The heptane-soluble fraction which is assumed to be resins and free oil contained within the sample;
- the toluene-soluble fraction which is assumed to be asphaltenes;
- the coke fraction which is defined to be the loss on ignition at 820 K of the toluene-insoluble fraction;
- the remaining ash which can be subjected to elemental analysis.

Results of the analyses are given in Table 4. Not too much importance can be given to absolute numbers since the procedure to shut down the CDU involved flushing exchangers with both light hydrocarbons and water. Despite this, the analyses show general similarities, and

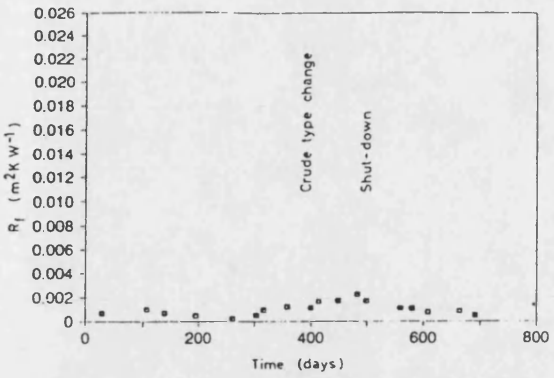

Figure 3. Exchanger E4A: fouling resistance as a function of time.

Table 4. Deposit analyses.*

fraction wt%	E7A	E8A	E9A	E10A
n-heptane-soluble	49.8	22.6	56.2	57.4
toluene-soluble	1.9	1.1	1.6	1.2
loss on ignition at 820K	32.8	37.2	24.6	25.3
remaining ash	15.5	39.1	17.6	16.1
Total	100.0	100.0	100.0	100.0
components in ash wt%				
iron	35.5	28.1	37.1	42.2
sulphur	29.0	18.3	27.4	28.0
sodium	20.0	29.6	21.7	18.0
calcium	7.7	3.3	4.1	5.6
zinc	2.6	1.0	2.8	3.1
magnesium	1.3	0.5	0.6	—
chlorine	—	14.1	1.1	0.6
others	3.9	5.1	5.2	2.5
Total	100.0	100.0	100.0	100.0

*courtesy of BP Research

indicate moderately high inorganic contents. Iron is almost certainly due to corrosion reactions, whilst sulphur probably originates from the crude oils themselves. The relatively high sodium content is probably due to the injection of caustic, which is carried out in order to control pH and hence corrosion. The high ash, sodium and chlorine content for E8A suggests that salt within the crude oil may have been carried over from the desalter to be deposited preferentially in this exchanger which is located well downstream.

The toluene-soluble fractions are small for all samples, indicating that the deposits contained little asphaltenic material. The coke fractions are relatively high, and thus it may be inferred that the fouling mechanisms include organic reactions as well as chemical and physical processes involving inorganic species.

With the exception of the low asphaltenic content, the analyses are broadly comparable with those found by Eaton and Lux[6], who studied deposit formation from crude oils using a laboratory-scale stirred apparatus. Dickakian and Seay[7] have suggested that asphaltene precipitation is the major mechanism in crude oil heat exchanger fouling. Steps proposed in their mechanism are:

- incompatibility of asphaltenes with crude oil, either through reactions or insolubility, causes precipitation;
- precipitated asphaltenes adhere to hot surfaces;
- asphaltenes then carbonise to form coke.

A similar mechanism involving both resins and asphaltenes has been proposed by Eaton and Lux[6]. The absence of asphaltenes in the deposits of this study does not infer that the asphaltene precipitation mechanism does not occur, since the third step could actually cause the disappearance of most of the asphaltenic content of a crude oil mixture to form a carbonaceous matrix which traps inorganic material.

DEPOSIT THICKNESSES

During the refinery shutdown from days 501 to 551, exchanger bundles were pulled from their shells and taken to a remote location for cleaning by high pressure water jetting. During the brief cleaning period, deposit thicknesses for some exchangers were measured using callipers. A more sophisticated measurement technique was not available. Several measurements were made at approximately 0.025 m from the open ends of exchanger tubes, and hence are only representative of this location. Also it is possible that the callipers may have indented the deposit slightly. The results, shown in Table 5, indicate that the average deposit thickness increased steadily from E7A to E9A, but then decreased to that found in E10A. The E10A exchanger was unique in being re-tubed prior to the first operating period, and thus would have been clean at day 1, unlike the remaining exchangers which had been water-jetted only on the tube-side, i.e. with no cleaning of the shell-side. Inspection of E10B in the parallel train at the major shutdown revealed partial blockage of tubes in the final pass. Thus, there is evidence of the deposit thickness increasing generally with crude oil temperature.

INTERPRETATION OF THERMAL DATA

STEP5, a commercial computer package available from the Heat Transfer and Fluid Flow Service, Harwell, was used to calculate fouling resistances. Although foul-

Table 5. Measured deposit thicknesses, mm (±0.1 mm).

E7A	E8A	E9A	E10A
0.4	1.4	1.3	1.1
0.8	1.4	1.0	1.1
0.4	1.5	1.4	1.2
0.3	1.4	1.7	1.2
0.3	1.1	1.1	1.6
0.2	1.0	2.8	1.1
	1.6	1.9	0.4
	1.1	1.8	1.1
		1.6	2.1
		1.6	1.0
Average 0.4	1.3	1.6	1.2

ing is a dynamic process, the fouling rate at any instant is usually sufficiently low such that the steady-state rate equation may be used to calculate the instantaneous overall heat transfer coefficient (based on outside tube surface area):

$$U_d = \frac{Q}{A_0 F(LMTD)} \quad (1)$$

F is the correction factor to the log mean temperature difference (LMTD) which takes account of the departure from pure countercurrent flow. All temperatures are measured values. In STEP5, the 'clean' heat transfer coefficient, U_c, is calculated from equation (2):

$$\frac{1}{U_c} = \frac{1}{h_i}\left\{\frac{D_0}{D_i}\right\} + \frac{1}{h_0} + \frac{(D_0 - D_i)}{2\lambda_t} \quad (2)$$

in which D_i and D_0 are the tube inside and outside diameters, and λ_t the tube thermal conductivity. The manual for STEP5 indicates the use of the thin wall assumption for the wall thermal resistance. In this study this approximation is acceptable in view of the high fouling resistances which are encountered.

The algorithms used in STEP5 are sophisticated, and allow for leakage around baffles, configuration correction factors and changes in physical properties. The tube-side film heat transfer coefficient, h_i, is calculated for the instantaneous operating conditions of flowrate, composition and temperature from correlations proposed by the Engineering Sciences Data Unit[8,9], and include laminar, transition and turbulent flow. STEP5 gives two options for the calculation of the shell-side film heat transfer coefficient, h_0, viz., the modified Bell-Delaware method and the HTFS stream analysis method. The shell-side coefficient is also calculated for the instantaneous operating conditions. Using both shell-side options, the values of h_0 were found to be similar for the conditions studied in this project[10].

STEP5 then computes the combined fouling resistance from equation (3):

$$R_f = \frac{1}{U_d} - \frac{1}{U_c} \quad (3)$$

Clearly, it is not possible to determine how the value of R_f is apportioned between shell- and tube-sides and, thus, values of R_f reported in this paper must be considered to be the total amount.

An energy balance around an on-line exchanger is required in order to calculate the instantaneous thermal duty Q for use in equation (1). For each exchanger Q was calculated from the flowrate and temperature change of the crude oil, i.e.

$$Q = MC_p(t_2 - t_1) \quad (4)$$

In using equation (4), due account was taken of the effects of temperature and crude oil composition on specific heat. The duty was not calculated from shell-side information since the shell-side flowrate data were considered to be the least accurate.

ACCURACY OF DATA

It has been demonstrated previously[11] that errors in plant data can readily propagate to give large errors in fouling resistances. Therefore careful consideration has been given not only to the accuracy of temperature and flowrate measurements but also to the method for evaluating the instantaneous combined fouling resistance, R_f.

Crude oil flowrates were obtained from tank dip data, rather than from flowmeter data, and were considered to have an accuracy close to $\pm 1\%$. Temperatures were obtained from thermocouples, either permanently installed or manually inserted into vacant thermowells. For the latter case, sufficient time was allowed for the thermocouple output to become steady. All thermocouples were calibrated and the random error in temperature measurements was found generally to be no more than $\pm 1°C$. Clearly the error in R_f is a function of the exchanger under consideration as well as the operating parameters including time. However, using the maximal error analysis[11], and assuming that the calculation method itself introduces no errors, then the likely accuracy of the computed fouling resistances was of the order of $\pm 20\%$. Details of the analysis are provided in the Appendix.

FOULING RESISTANCES

Fouling resistances were determined as a function of time for all the post-desalter exchangers except E11A and E11B, in which the crude oil flowed in the shell-side. Example plots are given in Figures 3, 4 and 5 for E4A, E8AB and E10AB, respectively.

Magnitude of fouling resistances

With few exceptions, the calculated fouling resistances for all the exchangers at all times were found to be in excess of the values recommended for design by TEMA[4] and the values shown in Table 1. This finding is in broad agreement with Bott and Walker's observations[12] and with the findings of other workers using refinery plant data[13–15]. The data also seem to indicate that at the start-up of the first operating period, the exchangers were seemingly not clean, as fouling resistances ranging from 0.0007 to 0.0026 $m^2K\ W^{-1}$ would be obtained on extrapolation of the graphs to day zero. There are several possible reasons for this. Firstly, at the shutdown prior to

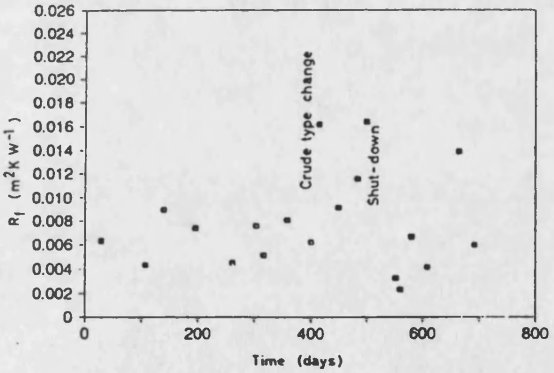

Figure 4. Exchanger E8AB: fouling resistance as a function of time.

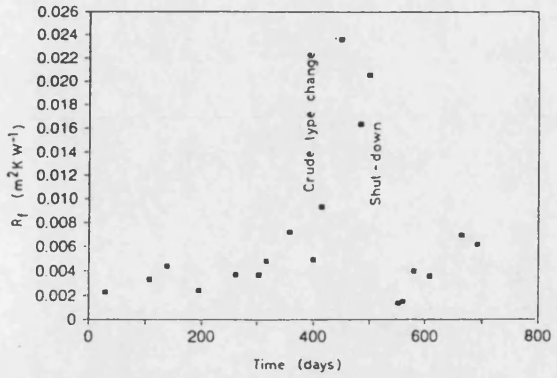

Figure 5. Exchanger E10AB: fouling resistance as a function of time.

day 1, the exchangers (with the exception of E10AB) had been cleaned only on the tube-side by high pressure water jetting with the exchangers *in situ*. Thus, not only would the shell-sides not have been cleaned, but also it may not have been possible to carry out as thorough a clean on the tube-sides as could be achieved by high pressure water jetting on the bundles pulled from the shells. Secondly, the exchangers may have fouled rapidly during the first 29 days of operation, the period up to the first data acquisition exercise. Thirdly, the calculation method itself, described above, could introduce errors. This is especially likely since U_d and U_c are determined by quite different procedures, both being subject to error.

During startup of the CDU, the transient variation in crude oil and shell-side flowrates is significant, and thus higher errors in the calculation procedure must be expected. Using the maximal error analysis[11], it has been estimated[10] that with, say, a 5% error in crude oil flowrate measurement, the error in each temperature would only need to be between ± 1 and 2.5°C to give the finite initial fouling resistances for the second operating period. Given the transient nature of startup of an oil refinery CDU, such variations in flowrate and temperature do not appear unreasonable, and could, therefore, possibly account for the initial values of calculated fouling resistances.

Non-zero fouling resistances were also found, although at reduced levels, for many of the exchangers during the second operating cycle (Table 3), i.e. after the cleaning during days 501 to 551, when the bundles had been removed from the shells. The authors witnessed thorough cleaning of both tube and shell-sides during the major shutdown, and thus the presence of such non-zero resistances so shortly after startup seems to indicate that the calculated initial resistances are subject to a degree of error.

It is particularly interesting to note that several other workers[13–15] have also presented data for oil refinery exchangers which show, on extrapolation, finite fouling resistances at startup. Significantly, this feature does not appear in the data obtained by Lambourn and Durrieu[15] from laboratory experiments on the same types of crude oil as used in their refinery study. Laboratory experiments are carried out under much better controlled conditions, and the number of parameters to be monitored is normally smaller than that for a refinery. It may be postulated, therefore, that the laboratory data provides a fouling resistance less prone to error. However, as noted earlier, the absolute value of the fouling resistance obtained in this way may not be representative of industrial operation.

Effect of temperature

In general, both the calculated fouling resistance at any time and the thickness of deposit measured at the major shutdown increased along each exchanger train. This indicates that fouling from crude oils increases with increasing oil temperature, as expected.

Effect of tube-side velocity

The tube-side velocity varied almost on a daily basis since it was related directly to the processing requirements of the refinery. In general a reduction in tube-side velocity caused an increase in the fouling rate and vice versa, although this relationship is complicated by the effect that the tube-side velocity has on the tube wall temperature, and possibly on removal mechanisms. Further evidence is available for the effect of velocity on fouling. Exchanger E5 was normally operated with a low tube-side velocity (in this range 0.7 to 1.0 m s^{-1}), and it yielded a higher fouling resistance at any time than the next hottest exchanger, E7A. All other exchangers were operated with velocities in the range 1.1 to 2.1 m s^{-1} up to day 500.

Effect of composition

The majority of the exchangers showed a substantial increase in fouling resistance when slop oils were introduced into the feed on day 390 and continued to foul at an increased rate as heavier crude oils, such as those from Merey and Maya, together with further slops, were processed up to the major shutdown on day 500. As an example, Figure 5 shows the dramatic effect of composition on the fouling rate for E10AB.

CORRELATION OF DATA

The fouling resistance-time data, together with much other supporting data, has been analysed to obtain simple mathematical relationships for the effects of tube wall temperature and crude oil types on fouling rates. No provision is made for deposit removal or release mechanisms, and thus the correlation developed is incapable of predicting asymptotic fouling resistances. Exchangers E5 and E6 were excluded from the analyses since, for refinery operational reasons, the shell-side flowrates for these exchangers were particularly variable and errors in R_f calculations were believed to be substantial.

Effect of temperature—'light' crudes

The fouling rates for the 'light' crudes up to day 390 were assumed to be constant (see Figures 3 to 5, for

example). That is a linear relationship between R_f and t was assumed. It was not assumed that $R_f = 0$ at $t = 0$. Since little variation in the average tube wall temperature of a given exchanger occurred in the period to day 390 (typically $\pm 8°C$ for E4A and $\pm 7°C$ for E7A), this temperature was used in the simplest manner to correlate fouling rates, by means of the modified Arrhenius equation:

$$\frac{dR_f}{dt} = A \exp(-E/RT_w) \quad (5)$$

The correlation is shown in Figure 6 from which the apparent activation energy for the fouling process is calculated to be 33 kJ mol^{-1}, a value which compares favourably with published data shown in Table 6 for other hydrocarbon fouling studies. The scatter in the data shown in Figure 6 makes it difficult to estimate the precision of E but it is unlikely to be less than 20 or higher than 45 kJ mol^{-1}. An activation energy below 40 kJ mol^{-1} probably indicates that both chemical and physical mechanisms are important.

The fouling rates for E8AB and also E8CD are high relative to adjacent exchangers, and create a high degree of scatter in the data shown in Figure 6. There are two possible reasons for this. Firstly, the deposits found in E8A at shutdown (and presumably those in E8B, C and D as well) were rich in chlorine. It is known[6] that the presence of chlorides in crude oil can have a pronounced effect on a fouling rate. Secondly, atmospheric residue is used on the shell-side of E8A-D, and thus it must be expected that some contribution to the overall fouling resistance would have come from the shell-side. This was confirmed by visual inspection at the major shutdown.

Since it was not possible to determine the predominant cause of the non-zero value of fouling resistance at day 0, this value has been considered to be an offset, or constant of integration in the correlation. Thus, equation (5) becomes:

$$R_f = C_i + \int [A \exp(-E/RT_w)]\, dt \quad (6)$$

in which the off-set C_i is unique to a particular exchanger. In order to be able to use equation (6) for predictive purposes, it is necessary to determine the relationship between the offset and the characteristics of individual exchangers.

The potential error in a calculated fouling resistance is strongly dependent on the temperature difference for each process stream[11]. Decreasing the temperature difference increases the potential error with the tube-side (crude oil) temperature difference having the greatest effect. Also, the closer the inlet temperatures of the two process streams, the greater the error in the fouling resistance is likely to be[11].

The thermal effectiveness P of the heat exchanger is given by:

$$P = \frac{t_2 - t_1}{T_1 - t_1} \quad (7)$$

As shown elsewhere[11], the error in the calculated fouling resistance in a given exchanger increases as the temperature approaches become smaller. Hence, at startup, the errors in the calculated values of initial R_f could be high. The offset values are plotted against effectiveness in Figure 7, from which a clear correlation is evident. Recent simulation studies on hypothetical exchangers, as yet unpublished[16], indicates that a correlation of this trend between the initial error in R_f and P is likely to be obtained when the fluid being cooled provides the controlling thermal resistance, and/or bypassing is used at startup. On the refinery CDU exchangers in this study, the shell-side coefficients are the lowest, and some bypassing is provided. Hence the trend in the correlation

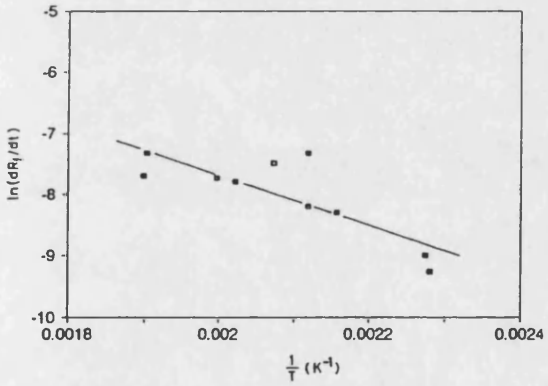

Figure 6. Light crude oil processing: the effect of temperature on fouling rates as an Arrhenius plot.

Table 6. Activation energies for hydrocarbon fouling.

fluid	activation energy kJ mol^{-1}	surface temperature range, °C	reference
sour gas oils	120	146-204	17
styrene polymerisation	39	22- 98	18
pure *n*-paraffins	40	93-260	19
liquid jet fuels	42	149-260	20
'light' crude oils	33	160-280	this study
'heavy' crude oils	21	160-280	this study

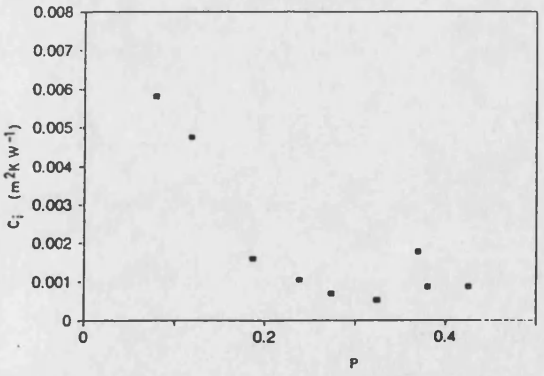

Figure 7. Offset, c_i as a function of thermal effectiveness, P.

shown in Figure 7 might be expected. Work is in progress to confirm the trend for refinery exchangers.

Testing the correlation

Equation (6), developed from the data for the first operating cycle, days 1 to 500, with 'light' crudes, was then used to predict the fouling resistances of the exchangers after the major shutdown for cleaning, from days 552 to 734. For each exchanger the mean tube wall temperature, required in equation (6), was obtained from STEP5. The comparisons between predicted and calculated resistances are shown in Figures 8 to 10 for E4A, E8AB and E10AB, respectively. In general, the correlation either correctly or slightly under-predicts the fouling resistances of most exchangers. The fit for E8AB is relatively poor, but, for reasons given earlier, and bearing in mind the high offset for these exchangers, this is perhaps not surprising.

The correlation has been developed based on the tube-side surface temperature, assuming that all the fouling

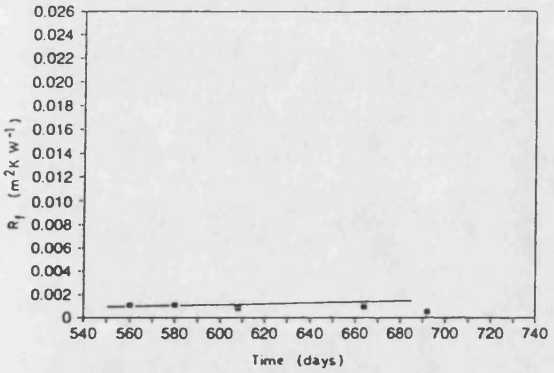

Figure 8. Exchanger E4A: predicted values (solid line) of fouling resistance for the second operating cycle ($C_i = 0.001$ m²K W^{-1}); squares are experimental data points.

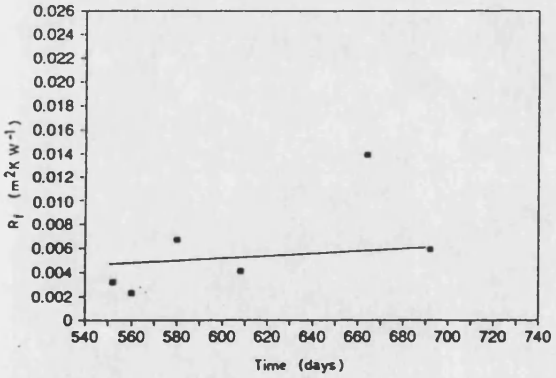

Figure 9. Exchanger E8AB: predicted values (solid line) of fouling resistance for the second operating cycle ($c_i = 0.0047$ m²K W^{-1}); squares are experimental data points.

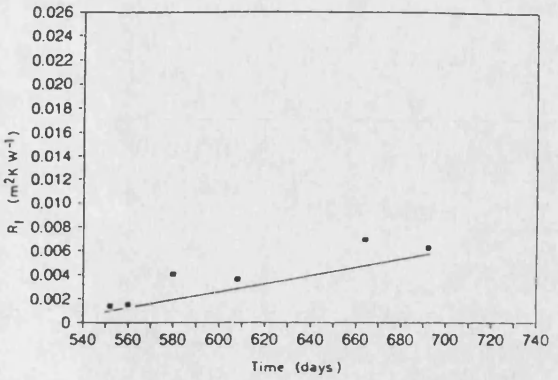

Figure 10. Exchanger E10AB: predicted values (solid line) of fouling resistance for the second operating cycle ($c_i = 0.001$ m²K W^{-1}); squares are experimental data points.

was on the tube-side. However, a significant amount of fouling on the shell-side of some of the hotter exchangers was witnessed at the major shutdown. The surface temperature on the shellside was always higher than on the tube-side, and it would not be unreasonable to expect that if the two process fluids were the same, that fouling would proceed more rapidly on the shell-side. However, the process fluids on the shell-side are generally considered to be 'cleaner' than crude oil, and so could be expected to foul to a lesser degree, This is a composition effect as many of the 'heavier' components, such as asphaltenes thought to cause fouling, are not present in the majority of the shell-side streams. This would seem to be confirmed by the fact that the simple correlation for those exchangers with cleaner fluids, such as the pump-around streams in E7A and B, E9A and B, E10AB and E10CD fits the data reasonably well with, in many cases, the predicted fouling resistance plot cutting across the saw-tooth pattern of the calculated values. The correlation for the E8AB and E8CD exchangers does not fit the data so well with a degree of under-prediction. In this case the two exchangers have the residue stream from the atmospheric column on the shell-side. The residue can be expected to have a large proportion of the 'heavier' components, and as expected, the E8 exchangers were found to be heavily fouled on the shell-sides when they were opened at the major shutdown.

The effect of velocity on fouling rate

The actual tubeside velocities for the exchangers in the preheat train, with the notable exception of E5, were in the range 1.1 to 2.1 m s^{-1}. The E8 and E10 exchangers were operated at slightly lower velocities than E4, E7 and E9. Thus the variation in tube-side velocity through the trains of exchangers was limited, making it difficult to derive a correlation which incorporated velocity. A further difficulty arises from the fact that the data were collected as discrete sets of readings at monthly intervals. Hence, comparison between the results for one month with those of other months is difficult, as sufficient details

of changes in the operating conditions in the intervening periods were not always available.

With due consideration of these limitations, the data from the refinery were analysed in an attempt to obtain the relationship between velocity and fouling rate. The results showed the difference between the measured fouling resistance and that predicted from the correlation was on average zero for the range of velocities studied. This would appear to indicate that the effect of velocity changes is accounted for by the change in surface temperature, as found by Watkinson and Epstein[17]. However, if the effect of velocity is reflected solely in the change in surface temperature, then it would not be removal of the deposit by shearing that causes the saw-tooth pattern of the measured fouling resistance graphs.

The effect of composition

The refinery at Rotterdam processed blends of several different crude oils. It took approximately three days to process the entire contents of one storage tank, and hence the blend could change approximately twice a week, with the number of crude oils in a blend ranging from 1 to approximately 15. This makes correlation of fouling rate with composition very difficult.

During the first 389 days of the first period of operation, the crude oils processed were generally 'light' (SG < 0.87). The classification of crude oils into 'heavy' and 'light' is somewhat arbitrary, and was developed in the crude oil processing industry based on the experience of blending and processing various feedstocks. 'Heavy' crudes tend to have higher asphaltene and sulphur contents, constituents which are generally thought to promote fouling. The presence of a 'heavy' crude oil or slops in the crude oil blend appears to have a significant effect on the fouling rate. There was an appreciable increase in the measured fouling rate after the introduction of 2% of slop oils on day 390. The slop oils can come from almost any part of the refinery and are routed to the slops tank. Hence it is virtually impossible to determine the exact composition of this stream. The slops are usually mixed with the crude oil in the storage tanks and then processed through the distillation unit, at no greater than 5% of the feed stream. 'Heavy' crudes such as Merey (SG = 0.9495) and Hoorn (SG = 0.9) were also processed during the period from day 390 to the major shutdown.

Despite this complexity, a correlation was developed from the data for the operating period covering the processing of the heavy crude oils in a similar manner to that described earlier for the 'light' crudes. Much scatter in the data was observed, and a much lower activation energy of 21 kJ mol^{-1} was obtained, which would give a greater fouling rate than 'light' crude oil at the same surface temperature. Regrettably, it was not possible to test the correlation in predictive mode for the heavy crude oils, as these crude oil types were not processed again during the three-year project. Nor was it possible to determine deposit characteristics which might have provided an insight as to whether the fouling process was more strongly dependent on physical rather than chemical processes, i.e. mechanisms with low activation energies.

CONCLUSIONS

A simple correlation has been established between the total fouling rate and tube wall temperature of individual heat exchangers in the preheat exchanger train of a particular crude oil distillation unit. For the refinery studied and the crude oils processed during this research project, the correlation obtained for 'light' crude oils is:

$$R_f = C_i + \int [4.9 \times 10^{-7} \exp(-33000/RT_w)\, dt \quad (8)$$

The dimensions and units of this correlation are provided in this paper in the section on symbols used. In order to predict absolute fouling resistances for this refinery, it is necessary to be able to predict the apparent initial fouling resistance (or offset c_i) for an individual heat exchanger. In this study, a good correlation between the apparent initial fouling resistance and the effectiveness of an exchanger has been obtained, as shown in Figure 7 for the refinery studied and the crude oils processed. The correlation has been successfully used to predict the reduction in thermal performance for the particular preheat train with 'light' crude oils following a major shutdown for thorough cleaning. The activation energy for the fouling process has been calculated to be about 33 kJ mol^{-1}, which lies in the region for a mixture of chemical and physical mechanisms. Chemical analyses confirm that the deposits contain a mixture of both inorganic materials and high molecular weight carbonaceous matter, the latter perhaps indicating some support for the view that asphaltene precipitation is an important mechanism. The activation energy of the fouling process when 'heavy' crude oils are processed is much lower, at about 21 kJ mol^{-1}, which indicates the predominance of a physical mechanism.

It is quite possible that the scatter in experimental data, seen in R_f versus t plots, such as Figures 8 to 10, is due to the removal and re-deposition elsewhere of foulant. Indeed, during the major shutdown for cleaning, deposits were seen to have accumulated not only inside the tubes but also at various other locations, e.g. the pass partition plates, in many of the exchangers. Since the correlation contains no provision for a deposit removal or release mechanism, it is therefore incapable of predicting an asymptotic fouling resistance. A more sophisticated scientific approach to modelling, such as that developed earlier[21], is required, and will be presented in due course.

Whilst the results and correlations given in this paper are clearly specific to the Rotterdam oil refinery and to the ranges and blends of crude oils processed during the project, nevertheless the principles of the analysis are readily applicable to other situations. Numerical values given in equation (8) are unique to the system studied. However, the form of this equation may well be suitable to other CDU preheat exchange trains.

APPENDIX

Error analysis

From equation (3), it is clear that the error in the calculated value of R_f is dependent upon the errors in the calculated values of both U_d and U_c.

For the function:

$$R_f = R_f(U_c, U_d) \quad \text{(A1)}$$

$$dR_f = \frac{\partial R_f}{\partial U_c} dU_c + \frac{\partial R_f}{\partial U_d} dU_d \quad \text{(A2)}$$

If the errors in U_c and U_d are δU_c and δU_d respectively, and are small relative to U_c and U_d, then the error induced in R_f is given by:

$$\delta R_f = \frac{\partial R_f}{\partial U_c} \delta U_c + \frac{\partial R_f}{\partial U_d} \delta U_d \quad \text{(A3)}$$

The worst possible value of δR_f occurs when all of the terms on the right hand side of the equality are either positive or negative. Thus, taking δU_c and δU_d to be positive:

$$\delta R_f = \left|\frac{\partial R_f}{\partial U_c}\right| \delta U_c + \left|\frac{\partial R_f}{\partial U_d}\right| \delta U_d \quad \text{(A4)}$$

From equation (3):

$$\frac{\partial R_f}{\partial U_c} = \frac{1}{U_c^2} \quad \text{(A5)}$$

$$\frac{\partial R_f}{\partial U_d} = -\frac{1}{U_d^2} \quad \text{(A6)}$$

Thus

$$\delta R_f = \frac{\delta U_c}{U_c^2} + \frac{\delta U_d}{U_d^2} \quad \text{(A7)}$$

It is possible, in principle, to eliminate errors in U_c by confirmation of predictive correlations. Clearly, an accurate physical property database is also required. On the other hand, errors in U_d depend upon the accuracy of plant data. Errors in U_d are related solely to errors in Q, A_0 and $LMTD$ [equation (1)].

Errors in operating parameters

In the following analysis the worst scenario is considered, that is, the errors in each of the four end temperatures and in each of the two flowrates compound, rather than eliminate each other. Using the notation given in Figure 2, the instantaneous coefficient U_d is given by:

$$U_d = \frac{Q \ln\left\{\frac{T_1 - t_2}{T_2 - t_1}\right\}}{A_0[(T_1 - t_2) - (T_2 - t_1)]} \quad \text{(A8)}$$

Thus, neglecting errors in the calculation of A_0,

$$\delta U_d = \left|\frac{\partial U_d}{\partial Q}\right| \delta Q + \left|\frac{\partial U_d}{\partial t_1}\right| \delta t_1 + \left|\frac{\partial U_d}{\partial t_2}\right| \delta t_2 + \left|\frac{\partial U_d}{\partial T_1}\right| \delta T_1 + \left|\frac{\partial U_d}{\partial T_2}\right| \delta T_2 \quad \text{(A9)}$$

Hence

$$\frac{\delta U_d}{U_d} = \frac{\delta Q}{Q} + \frac{1}{W}\left\{\left|\frac{Z}{\ln X} - 1\right| \delta t_1 + \left|1 - \frac{Y}{\ln X}\right| \delta t_2 + \left|\frac{Y}{\ln X} - 1\right| \delta T_1 + \left|1 - \frac{Z}{\ln X}\right| \delta T_2\right\} \quad \text{(A10)}$$

where

$$W = (T_1 - t_2) - (T_2 - t_1) \quad \text{(A11)}$$

$$X = \left\{\frac{T_1 - t_2}{T_2 - t_1}\right\} \quad \text{(A12)}$$

$$Y = \frac{W}{(T_1 - t_2)} \quad \text{(A13)}$$

$$Z = \frac{W}{(T_2 - t_1)} \quad \text{(A14)}$$

Error in the duty

The instantaneous thermal duty Q is given by equation (4). Assuming that there is no error in C_p, then

$$\delta Q = \left|\frac{\partial Q}{\partial M}\right| \delta M + \left|\frac{\partial Q}{\partial t_1}\right| \delta t_1 + \left|\frac{\partial Q}{\partial t_2}\right| \delta t_2 \quad \text{(A15)}$$

or

$$\delta Q = C_p(t_2 - t_1)\delta M + MC_p\delta t_1 + MC_p\delta t_2 \quad \text{(A16)}$$

and

$$\frac{\delta Q}{Q} = \frac{\delta M}{M} + \frac{\delta t_1 + \delta t_2}{(t_2 - t_1)} \quad \text{(A17)}$$

Typical example

Consider an error of 1°C in each of the end temperatures and a 1% error in the flowrate measurement, i.e.

$$\delta t_1 = \delta t_2 = \delta T_1 = \delta T_2 = 1 \quad \text{(A18)}$$

$$\frac{\delta M}{M} = 0.01 \quad \text{(A19)}$$

Consider for example E5A in a relatively clean condition

$t_1 = 152°C$, $t_2 = 189°C$

$T_1 = 280°C$, $T_2 = 183°C$

the error in Q is given by equation (A17), i.e.

$$\frac{\delta Q}{Q} = 0.01 + \frac{(1 + 1)}{(189 - 152)} = 0.064$$

Substituting values in equations (A11) to (A14) gives:

$$W = 60°C \quad \text{(A20)}$$

$$X = 2.935 \quad \text{(A21)}$$

$$Y = 0.659 \quad \text{(A22)}$$

$$Z = 1.935 \quad \text{(A23)}$$

Substitution in equation (A10) gives:

$$\frac{\delta U_d}{U_d} = 0.103 \quad \text{(A24)}$$

Hence the maximum error in the calculated value of the dirty coefficient for this example exchanger could be around 10%.

For an exchanger with $U_c = 0.6\ \text{kW m}^{-2}\text{K}^{-1}$ and $U_d = 0.1\ \text{kW m}^{-2}\text{K}^{-1}$, the fouling resistance would be $R_f = 8.33\ \text{m}^2\text{K kW}^{-1}$, i.e. typical of values shown in Figures 4 and 5. If the relative error in U_c is 5% and the relative error in U_d is 13%, then, from equation (A7):

$$\delta R_f = \frac{0.05}{0.6} + \frac{0.103}{0.1} = 1.11$$

and

$$\frac{\delta R_f}{R_f} = \frac{1.11}{8.33} = 0.13$$

Hence, assuming that errors are always additive, the maximum error in R_f for this example is 13%. For the majority of measurements the maximum error in R_f is no more than 20%. However, higher errors arise in the earlier stages of fouling, and shortly after startup, especially when the error in flowrate is substantially higher than 1%.

SYMBOLS USED

A	pre-exponential factor in Arrhenius equation	$\text{m}^2\text{K J}^{-1}$
A_o	outside surface area of tubes	m^2
C_i	initial fouling resistance of exchanger i	$\text{m}^2\text{K W}^{-1}$
C_p	specific heat of tube-side fluid	$\text{J kg}^{-1}\text{K}^{-1}$
D_i	inside diameter of tube	m
D_o	outside diameter of tube	m
E	activation energy	kJ mol^{-1}
F	correction factor for log mean temperature difference	—
h_i	inside film heat transfer coefficient	$\text{W m}^{-2}\text{K}^{-1}$
h_o	outside film heat transfer coefficient	$\text{W m}^{-2}\text{K}^{-1}$
$LMTD$	log mean temperature difference	°C, K
M	mass flowrate of tube-side fluid	kg s^{-1}
P	effectiveness of heat exchanger	—
Q	thermal duty of heat exchanger	W
R	Universal gas constant	$\text{J mol}^{-1}\text{K}^{-1}$
R_f	fouling resistance	$\text{m}^2\text{K W}^{-1}$
t	time	s
t_1	tube-side inlet temperature	°C, K
t_2	tube-side outlet temperature	°C, K
T_1	shell-side inlet temperature	°C, K
T_2	shell-side outlet temperature	°C, K
T_w	inside tube-wall temperature	°C, K
U_c	instantaneous clean overall heat transfer coefficient	$\text{W m}^{-2}\text{K}^{-1}$
U_d	instantaneous actual overall heat transfer coefficient	$\text{W m}^{-2}\text{K}^{-1}$
λ_w	thermal conductivity of tube wall	$\text{W m}^{-1}\text{K}^{-1}$

REFERENCES

1. Van Nostrand, W. L. Leach, S. H. and Haluska, J. L., 1981, In *Fouling of Heat Transfer Equipment*, eds Somerscales, E. F. C. and Knudsen, J. G., (Hemisphere, Washington) 619–643.
2. Crittenden, B. D., 1988, In *Fouling Science and Technology*, eds Melo, L. F., Bott, T. R. and Bernardo, C. A., Kluwer (Academic Publishers, Dordrecht) 293-313.
3. Chenoweth, J. M., 1990, *Heat Transfer Eng*, 11(1): 73-107.
4. Tubular Exchangers Manufacturers' Association, 1978 Standards, (TEMA, New York).
5. Chenoweth, J. M., 1988, In *Fouling Science and Technology*, eds Melo, L. F., Bott, T. R. and Bernardo, C. A., Kluwer (Academic Publishers, Dordrecht) 49-65.
6. Eaton, P. and Lux, R., 1983, In *Fouling in Heat Exchange Equipment*, eds Suitor, J. W. and Pritchard, A. M. ASME HTD-Vol 35, (ASME, New York) 33-42.
7. Dickakian, G. and Seay, S., 1988, *Oil and Gas J*, 86 (March 7): 47-50.
8. Engineering Science Data Unit, 1967, Item No 67016, (ESDU, London).
9. Engineering Science Data Unit, 1968, Item No 68006, (ESDU, London).
10. Downey, I. L., 1990, University of Bath, *unpublished work*.
11. Crittenden, B. D., Downey, I. L. and Kolaczkowski, S. T., 1988, *Proc Int Conf on Fouling in Process Plant, Oxford, 1988*: 32-51.
12. Bott, T. R. and Walker, R. A., 1971, *The Chemical Engineer*, No 255: 391-394.
13. Butler, R. C., McCurdy, W. N. and Linden, N. J., 1949, *Trans ASME*, 71: 843-847.
14. Weiland, J. H., McCay, R. C. and Barnes, J. E., 1949, *Trans ASME*, 71: 849-853.
15. Lambourne, G. A. and Durrieu, 1986, in *Heat Exchanger Source Book*, ed Palen, J. W., (Hemisphere, Washington).
16. Takemoto, T., Crittenden, B. D. and Kolaczkowski, S. T., 1991, *unpublished work*.
17. Watkinson, A. P. and Epstein, N., 1969, *Chem Eng Prog Symp Series*, 65(92): 84-90.
18. Crittenden, B. D., Hout, S. A. and Alderman, N. J., 1987, *Chem Eng Res Des*, 65: 165-170.
19. Taylor, W. F., 1969, *Ind Engng Chem Prod Res Dev*, 8: 375-380.
20. Vranos, A., Marteney, P. J. and Knight, B. A., 1981, in *Fouling of Heat Transfer Equipment*, eds Somerscales, E. F. C. and Knudsen, J. G., (Hemisphere, Washington) 489-499.
21. Crittenden, B. D., Kolaczkowski, S. T. and Hout, S. A., 1987, *Chem Eng Res Des*, 65: 171-179.

ACKNOWLEDGEMENTS

The authors are particularly grateful to the management and staff at the refinery operated by the Netherlands Refining Company (formerly BP Raffinaderij Nederland NV) for their time, enthusiasm and expertise in allowing the project to run smoothly over three years. The authors are also especially grateful to Dr M. F. Self and Mr D. King of BP International, and Mr D Cowie of BP Research for their continued enthusiasm and support. The project was funded jointly by the Science and Engineering Research Council and BP International.

ADDRESSES

Correspondence in connection with this paper should be addressed to Professor B. D. Crittenden, School of Chemical Engineering, University of Bath, Bath BA2 7AY. Miss I. L. Downey is currently at J. P. Kenny Technology Ltd, 59 Church Street, Staines, Middlesex TW18 4XS.

The manuscript was received 10 April 1992 and accepted for publication after revision 30 July 1992.

APPENDIX C

DETAILED RESULTS

C1 INTRODUCTION

This appendix contains all the data gathered at the refinery and any supplementary information used in the main part of the report. To Facilitate easy referal to the data it has been subdivided into the following sections;

- Temperatures measured on the refinery
- Crude types processed during the study
- Physical properties of the crude oils
- Physical properties of the process streams
- Tubeside velocities
- Average tubewall temperatures
- Clean heat transfer coefficients
- Dirty heat transfer coefficients
- Fouling resistances

Table C1 Temperature Data °C

Day No	29				107			
Exchanger	t_1	t_2	T_3	T_4	t_1	t_2	T_3	T_4
E2104a	123	148	200	169	129	146	178	168
E2104b	123	144	200	170	129	142	178	174
E2105	148	180	259	199	146	166	244	177
E2106	144	157	329	165	142	147	310	147
E2107a	180	191	225	203	166	184	225	194
E2107b	157	179	225	172	147	173	225	178
E2108ab	191	197	242	205	184	203	259	221
E2108cd	179	184	242	191	173	193	259	207
E2109a	197	224	268	235	203	221	255	228
E2109b	184	215	268	230	193	213	255	224
E2110ab	224	251	337	251	221	242	335	252
E2110cd	215	244	337	251	213	236	335	253

Day No	139				195			
Exchanger	t_1	t_2	T_3	T_4	t_1	t_2	T_3	T_4
E2104a	129	151	186	168	127	150	191	168
E2104b	129	146	186	170	127	146	191	174
E2105	151	172	243	196	150	183	269	212
E2106	146	158	324	172	146	153	324	189
E2107a	172	188	237	202	183	196	234	202
E2107b	158	182	237	206	153	176	234	208
E2108ab	188	202	268	228	196	210	269	222
E2108cd	182	196	268	219	176	192	269	207
E2109a	202	218	253	231	210	229	276	234
E2109b	196	210	253	230	192	215	276	231
E2110ab	218	224	335	259	229	252	345	254
E2110cd	210	231	335	263	215	241	345	255

Day No	261				303			
Exchanger	t_1	t_2	T_3	T_4	t_1	t_2	T_3	T_4
E2104a	132	153	186	173	134	153	186	168
E2104b	132	148	186	177	134	152	186	173
E2105	153	182	266	238	153	182	262	214
E2106	148	168	340	328	152	165	325	173
E2107a	182	201	232	216	182	198	237	211
E2107b	168	193	232	214	165	191	237	201
E2108ab	201	213	241	233	198	201	234	201
E2108cd	193	204	241	224	191	194	234	194
E2109a	213	230	272	245	210	221	271	238
E2109b	204	222	272	244	194	217	271	241
E2110ab	230	250	350	266	221	251	340	275
E2110cd	222	243	350	271	217	244	340	289

Day No	316				358			
Exchanger	t_1	t_2	T_3	T_4	t_1	t_2	T_3	T_4
E2104a	128	145	201	169	133	148	197	176
E2104b	129	148	201	169	132	145	197	175
E2105	148	171	251	208	148	175	264	192
E2106	145	152	328	315	145	157	332	215
E2107a	171	190	237	208	175	194	242	222
E2107b	152	183	237	210	157	187	242	220
E2108ab	190	198	217	210	194	207	267	246
E2108cd	183	190	217	202	187	198	267	242
E2109a	198	218	258	234	207	224	274	255
E2109b	190	210	258	235	198	214	279	251
E2110ab	218	226	244	277	224	241	349	296
E2110cd	210	238	350	292	214	232	349	291

Day No	400				414			
Exchanger	t_1	t_2	T_3	T_4	t_1	t_2	T_3	T_4
E2104a	126	145	202	171	131	146	195	181
E2104b	126	143	202	176	130	139	195	183
E2105	145	166	269	229	146	168	267	234
E2106	143	152	325	298	139	147	323	192
E2107a	166	181	252	228	168	182	251	231
E2107b	152	175	252	223	147	175	251	238
E2108ab	181	189	237	195	182	189	243	230
E2108cd	175	184	237	186	175	180	243	221
E2109a	189	196	274	246	189	211	277	252
E2109b	184	204	274	248	180	202	277	254
E2110ab	196	225	344	269	211	230	349	304
E2110cd	204	222	344	303	202	222	349	310

Day No	449				483			
Exchanger	t_1	t_2	T_3	T_4	t_1	t_2	T_3	T_4
E2104a	128	145	199	186	136	150	204	184
E2104b	128	140	199	190	136	144	204	187
E2105	145	162	264	226	150	168	267	239
E2106	140	166	329	198	144	150	314	267
E2107a	162	176	247	236	168	184	249	234
E2107b	166	184	247	233	150	174	249	228
E2108ab	176	197	248	236	184	193	254	238
E2108cd	184	192	248	234	174	183	254	231
E2109a	197	209	274	252	193	209	274	252
E2109b	192	213	274	259	183	194	274	255
E2110ab	209	217	343	304	209	221	342	309
E2110cd	213	218	343	310	194	211	342	311

Day No	499				552			
Exchanger	t_1	t_2	T_3	T_4	t_1	t_2	T_3	T_4
E2104a	135	151	204	185				
E2104b	135	142	205	189				
E2105	151	170	265	232				
E2106	142	153	305	178				
E2107a	170	187	256	238	116	198	236	199
E2107b	153	177	256	231	146	183	230	185
E2108ab	187	195	253	242	202	215	242	218
E2108cd	177	187	253	236	182	202	242	198
E2109a	195	211	276	255	215	228	257	230
E2109b	187	197	276	258	202	227	257	228
E2110ab	211	220	338	305	228	260	328	247
E2110cd	197	212	338	307	227	265	328	254

Day No	560				580			
Exchanger	t_1	t_2	T_3	T_4	t_1	t_2	T_3	T_4
E2104a	123	145	210	167	129	147	195	164
E2104b	123	146	201	171	129	150	195	169
E2105	145	171	249	178	147	166	242	199
E2106	146	160	317	163	150	157	293	159
E2107a	171	193	228	194	166	187	226	199
E2108b	160	187	228	187	157	180	226	201
E2108ab	193	207	256	208	187	185	231	200
E2108cd	187	205	256	205	180	191	231	198
E2109a	207	226	259	229	195	215	251	224
E2109b	205	229	259	229	191	216	251	229
E2110ab	226	256	337	257	215	246	325	276
E2110cd	229	258	337	258	216	247	325	268

Day No	608				664			
Exchanger	t_1	t_2	T_3	T_4	t_1	t_2	T_3	T_4
E2104a	129	148	203	170	127	147	198	170
E2104b	129	149	203	174	127	152	198	175
E2105	148	174	260	206	147	164	245	208
E2106	149	162	328	171	150	172	314	182
E2107a	174	193	242	211	164	186	243	217
E2107b	162	187	242	210	172	194	243	222
E2108ab	193	210	275	226	186	193	243	215
E2108cd	187	208	275	228	194	201	244	220
E2109a	210	239	270	244	193	210	259	241
E2109b	208	232	270	242	201	217	259	246
E2110ab	231	254	342	282	210	233	326	294
E2110cd	232	257	342	287	217	244	326	299

Day No	692				748			
Exchanger	t_1	t_2	T_3	T_4	t_1	t_2	T_3	T_4
E2104a	129	154	214	172	131	154	206	172
E2104b	129	155	214	177	131	155	206	176
E2105	154	170	256	217	154	175	253	212
E2106	155	172	325	183	155	157	282	155
E2107a	170	192	244	208	175	192	240	211
E2107b	172	197	244	217	157	182	240	205
E2108ab	192	203	244	224	192	199	241	211
E2108cd	197	217	244	226	182	191	241	217
E2109a	203	212	269	240	199	215	265	241
E2109b	217	224	269	245	191	209	265	242
E2110ab	212	232	336	283	215	241	332	284
E2110cd	224	238	336	291	209	237	332	289

Day No					752			
Exchanger	t_1	t_2	T_3	T_4	t_1	t_2	T_3	T_4
E2104a					120	148	199	163
E2104b	135	164	210	191	120	152	199	171
E2105					148	154	234	151
E2106	163	172	315	180	152	175	318	188
E2107a					154	180	222	182
E2107b	172	201	265	295	175	189	222	203
E2108ab					180	189	238	196
E2108cd	201	207	245	233	189	196	238	212
E2109a					189	209	248	232
E2109b	207	223	280	268	196	208	248	213
E2110ab					209	242	332	236
E2110cd	223	242	337	n/a	208	236	332	279

Day No	781			
Exchanger	t_1	t_2	T_3	T_4
E2104a	123	150	197	171
E2104b	122	148	197	174
E2105	150	166	243	168
E2106	148	152	302	154
E2107a	166	193	230	197
E2107b	152	178	230	199
E2108ab	193	198	232	204
E2108cd	178	188	232	201
E2109a	198	225	258	226
E2109b	188	200	258	236
E2110ab	225	233	335	252
E2110cd	200	225	335	274

Table C2 Crudes Processed

Date	Wt %	Crude type
13.11.86	42%	Brent Spa
	40%	Ekofisk
	13%	Helm Blend
	5 %	Statfjord
30.1.87	100%	Ninian
4.3.87	76%	Iran Heavy
	14%	Arab Light
	7 %	Slops
	3 %	Condensate
28.4.87	40%	Statfjord
	24%	Bonny Medium
	11%	Cabinda Export
	8 %	Algerian Condensate
	8 %	Hoorn
	5 %	Forcados
	1 %	Amna
3.7.87	28%	Fulmar
	20%	Cabinda Export
	15%	Bonny Medium
	11%	Algerian Condensate
	10%	Kotter
	5 %	Logger
	4 %	Hoorn
	4 %	Cabinda Takula
	3 %	Escravos
14.8.87	47%	Statfjord
	24%	Forties
	14%	Ninian
	5 %	Helm
	4 %	Saharan
	3 %	Cabinda Takula

Date	Wt %	Crude type
27.8.87	70%	Flotta
	8 %	Maya
	6 %	Iran Light
	5 %	Algerian Condensate
	3 %	Arab Light
	3 %	Leona
	3 %	Isthmus
	3 %	Urals
8.10.87	37%	Iran Light
	29%	Iran Heavy
	13%	Leona
	10%	Arab Light
	10%	Arab Heavy
	1 %	Algerian Condensate
19.11.87	79%	Flotta
	7 %	Arab Light
	11%	Algerian Condensate
	1.5%	Leona
	1.5%	Arab Medium
3.12.87	80%	Arab Light
	9 %	Algerian Condensate
	6 %	Iran Light
	4 %	Leona
	1 %	Brent Blend
7.1.88	88%	Es Sider
	6 %	Saharan
	2 %	Forcados
	2 %	Hoorn
	1 %	Statfjord
	1 %	Rijn
10.2.88	31%	Romashnko
	31%	Arab Heavy
	17%	Arab Light
	12%	Oman Export
	8 %	Algerian Condesate
	1 %	Leona

Date	Wt %	Crude type
25.2.88	41%	Forcados
	35%	Statfjord
	8 %	Hoorn
	3 %	Es Sider
	4 %	Ekofisk
	1 %	Algerian Condensate
	7 %	Cabinda Takula
19.4.88	44%	Ninian
	16%	Cabinda Takula
	10%	Helm
	9 %	Gullfaks
	5 %	Beryl
	5 %	Algerian Condensate
	4 %	Statfjord
	4 %	Amna
	2 %	Qua Iboe
	1 %	Rijn
27.4.88	74%	Urals
	17%	Arab Light
	8 %	Algerian Condensate
	1 %	Arab Med
17.5.88	75%	Statfjord
	13%	Forties
	3 %	Qua Iboe
	3 %	Helm
	2 %	Brent
	1 %	Rijn
	1 %	Argyll
	1 %	Cabinda Takula
	1 %	Ninian
14.6.88	37%	Romashkino
	31%	Arab Heavy
	12%	Flotta
	12%	Arab Light
	8 %	Algerian Condensate

Date	Wt %	Crude type
9.8.88	48%	Qua Iboe
	20%	Forties
	16%	Oguendjo
	10%	Helm
	3 %	Fulmar
	2 %	Nigerian Light
	1 %	Palaca
6.9.88	88%	Arab Light
	8 %	Romashkino
	2 %	Helm
	2 %	Algerian Condensate
12.10.88	39%	Ninian
	37%	Fulmar
	8 %	Ogendjo
	7 %	Cabinda Takula
	6 %	Bonny Light
	4 %	Helm
	4 %	Rijn
20.10.88	88%	Ninian
	5 %	Helm
	4 %	Fulmar
	1 %	Oguendjo
	1 %	Cabinda Takula
	1 %	Bonny Light
13.11.88	56%	Ninian
	30%	Beryl
	14%	Statfjord
14.12.88	58%	Bonny Light
	22%	Es Sider
	17%	Fulmar
	2%	Brent
	1%	Helm

Table C3 Crude oil Physical Properties

Physical properties Crude oil

Day No	Density	Specific Heat Capacity	Thermal Conductivity	Viscosity
	at 122oC kgm-3	at 122oC kJkg-1K-1	at 122oC Wm-1K-1	at 50oC cp
29	750.00	2.46	0.126	6.37
107	747.00	2.36	0.128	10.24
139	780.00	2.42	0.124	7.20
195	747.00	2.46	0.128	10.24
261	741.00	2.48	0.129	2.85
303	748.00	2.47	0.129	2.77
316	754.00	2.46	0.128	3.13
358	771.00	2.43	0.125	5.82
400	740.00	2.49	0.130	2.41
414	750.00	2.47	0.128	3.30
449	750.00	2.48	0.129	3.19
483	770.00	2.46	0.127	4.00
499	780.00	2.45	0.126	3.51
552	780.00	2.46	0.127	3.51
560	751.00	2.47	0.128	2.95
580	810.00	2.48	0.129	2.51
608	823.00	2.46	0.127	3.74
664	767.00	2.45	0.127	3.23
692	767.00	2.45	0.126	3.93
748	735.00	2.47	0.129	2.77
756	735.00	2.48	0.130	2.68
770	739.00	2.49	0.130	2.33
781	752.00	2.47	0.128	2.62

Table C4 Process Stream Physical Properties

TPA					LGO					HGO					RESIDUE				
Viscosity at 50oC cp	Density at 122oC kgm-3	Specific Heat Capacity at 122oC kJkg-1K-1	Thermal Conductivity at 122oC Wm-1K-1	Viscosity at 50oC cp	Density at 122oC kgm-3	Specific Heat Capacity at 122oC kJkg-1K-1	Thermal Conductivity at 122oC Wm-1K-1	Viscosity at 50oC cp	Density at 122oC kgm-3	Specific Heat Capacity at 122oC kJkg-1K-1	Thermal Conductivity at 122oC Wm-1K-1	Viscosity at 50oC cp	Density at 122oC kgm-3	Specific Heat Capacity at 122oC kJkg-1K-1	Thermal Conductivity at 122oC Wm-1K-1	Viscosity at 50oC cp
6.37	712.00	2.49	0.131	1.18	760.00	2.43	0.125	2.52	784.00	2.39	0.122	4.37	855.00	2.29	0.114	57.50
10.24	710.00	2.53	0.134	1.57	740.00	2.48	0.129	4.18	770.00	2.44	0.125	10.75	850.00	2.33	0.117	117.69
7.20	595.00	2.66	0.148	0.37	718.00	2.51	0.132	1.14	760.00	2.43	0.125	3.55	885.00	2.24	0.111	290.83
10.24	710.00	2.59	0.140	1.68	735.00	2.42	0.125	4.18	775.00	2.39	0.121	10.75	860.00	2.32	0.116	123.70
2.85	640.00	2.62	0.144	0.53	776.00	2.44	0.126	3.79	802.00	2.40	0.122	10.72	851.00	2.33	0.117	135.82
2.77	640.00	2.61	0.143	0.53	776.00	2.43	0.126	3.71	801.00	2.39	0.112	11.19	852.00	2.33	0.117	91.40
3.13	660.00	2.63	0.146	0.62	780.00	2.41	0.125	4.00	810.00	2.38	0.121	10.98	850.00	2.31	0.116	116.87
5.82	640.00	2.61	0.143	0.53	780.00	2.42	0.125	3.82	812.00	2.38	0.121	11.60	870.00	2.25	0.112	529.66
2.41	625.00	2.65	0.146	0.45	782.00	2.42	0.125	3.55	820.00	2.38	0.121	10.24	870.00	2.28	0.114	142.80
3.30	635.00	2.64	0.145	0.52	780.00	2.43	0.125	3.63	815.00	2.38	0.121	9.66	875.00	2.27	0.113	231.70
3.19	640.00	2.63	0.143	0.53	768.00	2.46	0.127	3.59	800.00	2.42	0.123	8.60	850.00	2.33	0.116	133.90
4.00	630.00	2.65	0.145	0.52	770.00	2.44	0.126	3.53	805.00	2.39	0.122	9.19	880.00	2.26	0.113	373.10
3.51	660.00	2.58	0.139	0.62	780.00	2.41	0.124	3.94	815.00	2.38	0.121	10.11	850.00	2.32	0.117	90.39
3.51	660.00	2.63	0.144	0.62	780.00	2.45	0.127	3.94	815.00	2.41	0.123	11.10	850.00	2.31	0.116	98.70
2.95	627.00	2.64	0.145	0.45	778.00	2.44	0.126	3.09	819.00	2.38	0.121	8.74	880.00	2.27	0.113	228.50
2.51	684.00	2.62	0.144	0.45	840.00	2.45	0.127	2.73	850.00	2.41	0.123	7.11	884.00	2.33	0.117	79.50
3.74	665.00	2.65	0.145	0.52	830.00	2.43	0.125	3.46	862.00	2.37	0.120	9.49	885.00	2.24	0.111	496.70
3.23	660.00	2.59	0.140	0.54	781.00	2.42	0.124	3.74	815.00	2.38	0.121	10.64	860.00	2.30	0.115	156.80
3.93	640.00	2.64	0.144	0.52	780.00	2.43	0.125	3.27	805.00	2.38	0.121	8.30	880.00	2.26	0.113	230.40
2.77	630.00	2.62	0.143	0.53	768.00	2.45	0.126	3.08	790.00	2.41	0.123	7.82	855.00	2.33	0.116	97.33
2.68	648.00	2.61	0.142	0.53	773.00	2.44	0.126	3.61	790.00	2.41	0.123	8.09	855.00	2.33	0.117	103.05
2.33	630.00	2.62	0.144	0.45	768.00	2.46	0.127	2.64	790.00	2.41	0.124	7.45	855.00	2.36	0.117	80.13
2.62	658.00	2.60	0.141	0.54	781.00	2.43	0.126	3.28	810.00	2.39	0.122	9.25	850.00	2.32	0.117	81.28

Table C5 Tubeside Velocities ms^{-1}

DAY NO	e2104a	e2104b	e2105	e2106	e2107a	e2107b	e2108ab	e2108cd	e2109a	e2109b	e2110ab	e2110cd
29	2.14	2.00	1.12	1.98	2.15	1.96	1.82	1.69	2.20	2.04	1.84	1.70
107	2.31	2.25	1.20	2.20	2.28	2.18	1.97	1.90	2.38	2.30	1.97	1.90
139	1.54	1.70	0.79	1.67	1.51	1.65	1.29	1.42	1.55	1.71	1.28	1.40
195	1.89	1.91	0.99	1.87	1.89	1.85	1.62	1.60	1.95	1.93	1.61	1.60
261	2.19	2.17	1.13	2.14	2.18	2.13	1.86	1.84	2.24	2.21	1.84	1.82
303	1.70	1.65	0.88	1.63	1.69	1.62	1.29	1.39	1.74	1.67	1.43	1.39
316	1.73	1.55	0.90	1.52	1.71	1.51	1.47	1.31	1.76	1.57	1.46	1.30
358	2.17	2.12	1.12	2.08	2.13	2.06	1.83	1.78	2.19	2.12	1.79	1.74
400	1.97	1.94	1.02	1.91	1.94	1.90	1.66	1.53	1.99	1.96	1.64	1.62
414	2.05	2.13	1.06	2.08	2.01	2.07	1.72	1.78	2.06	2.13	1.70	1.76
449	2.04	2.06	1.05	2.03	1.99	2.03	1.71	1.73	2.05	2.08	1.68	1.70
483	1.95	2.10	1.00	2.05	1.91	2.02	1.63	1.74	1.95	2.08	1.60	1.70
499	1.83	2.02	0.94	1.97	1.79	1.96	1.53	1.68	1.83	2.01	1.50	1.64
552					1.98	1.99	1.76	1.73	2.12	2.10	1.75	1.76
560	1.52	1.54	1.20	2.27	2.30	2.26	1.98	1.96	2.37	2.37	1.97	1.97
580	1.42	1.54	0.73	1.51	1.39	1.49	1.19	1.28	1.42	1.54	1.18	1.28
608	2.06	2.12	1.07	2.10	2.05	2.09	1.78	1.82	2.15	2.22	1.79	1.85
664	1.69	1.81	0.87	1.80	1.67	1.79	1.43	1.54	1.71	1.84	1.41	1.52
692	2.12	2.22	1.09	2.20	2.08	2.19	1.79	1.90	2.14	2.28	1.76	1.86
748	1.30	1.64	0.67		1.28	1.59	1.10	1.37	1.31	1.65	1.69	1.36
756		3.44		3.39		3.37		2.90		3.47		
770	2.24	1.56	1.16	1.56	2.19	1.55	1.89	1.33	2.27	1.59	1.89	1.31
781	1.58	1.61	0.82	1.58	1.57	1.57	1.33	1.36	1.62	0.00	1.34	1.34

Table C6 Average Tubewall Temperatures °C

DAY NO	e2104a	e2104b	e2105	e2106	e2107a	e2107b	e2108ab	e2108cd	e2109a	e2109b	e2110ab	e2110cd
29	175	174	202	172	202	176	198	184	227	217	254	251
107	153	157	170	147	182	168	204	201	218	211	239	234
139	166	165	196	174	196	197	212	205	225	220	248	247
195	164	166	220	171	202	191	222	199	234	223	254	249
261	171	172	226	291	213	204	223	212	237	227	258	257
303	164	167	210	176	202	198	201	193	227	229	266	269
316	164	167	202	248	196	199	206	198	227	224	258	263
358	168	166	196	192	210	208	227	218	241	233	268	262
400	164	160	211	222	203	199	190	184	214	227	247	262
414	170	164	217	171	207	216	206	199	232	230	268	269
449	173	174	206	193	210	212	219	209	228	239	249	257
483	173	169	222	204	213	207	204	202	232	224	264	267
499	174	168	216	171	215	207	218	209	233	226	256	259
552					201	186	216	199	229	228	256	257
560	162	165	183	168	193	187	207	204	224	228	258	259
580	161	165	192	161	193	192	197	194	219	223	263	259
608	166	168	203	174	202	199	216	216	236	237	268	273
664	164	169	197	187	202	210	201	208	227	233	269	279
692	173	169	205	186	201	208	212	219	223	232	258	262
748	168	171	205		202	194	204	201	228	226	266	267
756		182		179		159		216		163		
770	161	168	169	189	181	196	191	202	221	210	241	259
781	166	167	178	155	192	185	193	193	226		241	251

Table C7 Clean Heat Transfer Coefficients $W/m^2 K$

DAY NO	e2104a	e2104b	e2105	e2106	e2107a	e2107b	e2108ab	e2108cd	e2109a	e2109b	e2110ab	e2110cd
29	1351	1255	556	454	914	630	284	176	909	670	715	784
107	2402	2879	1102	454	1607	1448	1755	1772	1970	1857	1278	1312
139	982	1016	574	449	727	914	488	488	954	943	664	721
195	1079	1113	761	403	835	897	710	488	920	891	591	619
261	1005	1011	914	1669	1403	1261	1181	852	1107	784	744	772
303	1016	1062	653	449	653	534	244	182	596	920	823	846
316	926	636	630	863	664	903	596	386	999	920	664	698
358	971	903	613	556	1062	1119	835	698	1170	1033	835	789
400	1136	1147	721	840	920	977	460	403	733	1141	846	914
414	1192	1005	733	437	931	1283	687	619	1096	1136	891	971
449	1209	1221	670	767	1147	1181	1096	750	954	1329	659	795
483	971	903	698	653	1039	1073	500	591	999	948	801	954
499	1028	903	687	488	1011	1039	806	772	1022	954	693	897
552					1238	948	727	613	954	1147	857	914
560	852	982	681	539	1022	999	591	630	1033	1141	954	948
580	846	988	539	335	806	886	466	511	863	1045	829	829
608	1090	1175	738	517	977	1062	642	733	1164	1255	937	1033
664	909	1033	568	653	846	994	466	517	977	1130	931	1102
692	1073	1016	755	630	931	1124	721	750	784	812	857	835
748	733	914	500		647	789	409	505	733	903	693	863
756		1862		625		1772		1028		1868		
770	1153	1033	483	608	988	840	528	477	1374	664	840	801
781	965	994	273	182	608	1016	494	500	960		403	738

Table C8 Dirty Heat Tranfer Coefficients $W/m^2 K$

DAY NO	e2104a	e2104b	e2105	e2106	e2107a	e2107b	e2108ab	e2108cd	e2109a	e2109b	e2110ab	e2110cd
29	715	528	261	176	534	636	102	74	397	341	273	273
107	704	449	250	136	318	392	204	159	403	341	244	221
139	613	466	153	131	165	204	91	97	210	165	170	131
195	698	505	204	68	204	199	114	125	273	244	244	210
261	801	528	193	119	608	318	187	148	273	227	199	170
303	636	522	187	165	210	278	85	85	97	199	204	148
316	488	358	148	28	199	216	148	102	244	176	159	125
358	443	375	256	108	221	267	108	79	199	153	119	108
400	500	409	114	51	108	148	119	136	51	153	165	85
414	392	221	119	79	108	170	57	34	176	159	102	97
449	392	256	97	267	97	142	159	62	102	176	40	51
483	352	193	97	40	119	159	74	62	131	74	57	79
499	375	159	102	136	114	153	57	68	125	68	45	68
552					846	511	284	352	386	579	522	698
560	443	539	335	284	528	556	250	290	358	659	392	397
580	443	545	119	136	233	210	114	142	261	307	193	227
608	591	613	216	221	261	284	176	199	312	443	216	238
664	511	642	108	295	176	204	62	79	153	176	125	170
692	698	744	670	278	273	312	136	273	108	114	136	108
748	426	534	102		131	193	62	74	114	136	114	142
756		1261		267		352		125		233		
770	818	676	68	250	477	182	142	74	278	193	409	142
781	596	539	79	74	199	216	102	102	437		62	119

Table C9 Fouling Resistances K m^2/W

DAY NO	e2104a	e2104b	e2105	e2106	e2107a	e2107b	e2108a	e2108b	e2109a	e2109b	e2110a	e2110b
29	0.0007	0.0011	0.0021	0.0035	0.0007	0.0000	0.0063	0.0079	0.0014	0.0014	0.0023	0.0024
107	0.0010	0.0019	0.0031	0.0051	0.0025	0.0019	0.0043	0.0057	0.0020	0.0024	0.0033	0.0037
139	0.0007	0.0012	0.0048	0.0054	0.0047	0.0038	0.0090	0.0083	0.0037	0.0050	0.0044	0.0063
195	0.0005	0.0011	0.0036	0.0122	0.0037	0.0039	0.0074	0.0059	0.0026	0.0030	0.0024	0.0032
261	0.0002	0.0009	0.0041	0.0078	0.0009	0.0024	0.0045	0.0056	0.0028	0.0031	0.0037	0.0046
303	0.0005	0.0011	0.0039	0.0039	0.0032	0.0018	0.0076	0.0062	0.0086	0.0039	0.0037	0.0056
316	0.0010	0.0012	0.0052	0.0340	0.0035	0.0035	0.0051	0.0026	0.0031	0.0046	0.0048	0.0066
358	0.0012	0.0016	0.0023	0.0075	0.0036	0.0029	0.0081	0.0111	0.0042	0.0055	0.0072	0.0080
400	0.0011	0.0016	0.0074	0.0184	0.0081	0.0057	0.0062	0.0049	0.0182	0.0056	0.0049	0.0106
414	0.0017	0.0035	0.0070	0.0103	0.0082	0.0051	0.0161	0.0278	0.0048	0.0087	0.0093	0.0125
449	0.0017	0.0031	0.0089	0.0024	0.0095	0.0062	0.0091	0.0160	0.0087	0.0049	0.0236	0.0183
483	0.0023	0.0041	0.0092	0.0236	0.0074	0.0054	0.0115	0.0143	0.0067	0.0125	0.0164	0.0116
499	0.0017	0.0052	0.0083	0.0053	0.0078	0.0056	0.0164	0.0134	0.0070	0.0136	0.0206	0.0136
552	0.0011	0.0008	0.0015	0.0017	0.0007	0.0014	0.0032	0.0025	0.0023	0.0009	0.0014	0.0008
560	0.0011	0.0008	0.0065	0.0043	0.0009	0.0008	0.0023	0.0019	0.0018	0.0006	0.0015	0.0015
580	0.0008	0.0008	0.0033	0.0026	0.0030	0.0036	0.0067	0.0051	0.0027	0.0023	0.0040	0.0032
608	0.0009	0.0006	0.0075	0.0018	0.0028	0.0026	0.0041	0.0037	0.0023	0.0015	0.0036	0.0032
664	0.0005	0.0004	0.0002	0.0020	0.0045	0.0039	0.0139	0.0106	0.0055	0.0048	0.0069	0.0050
692	0.0010	0.0008	0.0078	0.0000	0.0026	0.0023	0.0059	0.0023	0.0080	0.0076	0.0062	0.0081
748	0.0004	0.0003	0.0126	0.0021	0.0061	0.0039	0.0136	0.0116	0.0074	0.0062	0.0074	0.0059
756	0.0006	0.0005	0.0089	0.0024	0.0011	0.0023	0.0051	0.0070	0.0029	0.0038	0.0012	0.0058
770		0.0008		0.0080	0.0034	0.0043	0.0078	0.0114	0.0012	0.0037	0.0135	0.0070
781						0.0036		0.0078		0.0000		

APPENDIX D

THERMOWELL EXPERIMENTS

D1 Thermowell experiments.

A series of experiments were carried out at the University of Bath to determine whether the temperature read by the thermocouple in the thermowell on the refinery was representative of the temperature of the fluid inside the pipe. The time required for the thermocouple reading to reach equilibrium with the temperature of the fluid inside the pipe, and the effect of debris in the thermowell, and the prevailing weather conditions on the refinery were also investigated.

D2 Experimental Procedure.

A thermowell of the same dimensions as those on the refinery was constructed and place in the wall of an oven (See Figure D1.1). A thin thermocouple (1mm diameter) was embedded in the wall of the thermowell at the base, enabling the wall temperature to be measured. The thermocouple used on the refinery was inserted into the thermowell and the oven switched on and the thermostat was set to 100°C. The system was then left for 30 minutes to reach equilibrium, the thermocouple readings were noted and equilibrium was defined as when the thermocouples in the oven and the wall of the thermowell had given a constant reading for fifteen minutes. Readings of each of the thermocouples were taken at minute intervals using the same indication box.

The thermostat setting was then changed and the experiment repeated at the new temperature. The series of experiments were then repeated with cool air from a gas cylinder blowing over the exposed part of the thermocouple,to simulate a cold windy day on the refinery.

Experiments were also carried out with a small amount of debris at the bottom of the thermowell, as although the thermowells are checked and cleaned before the thermocouple is inserted it is not always possible remove all the debris from the more remote fittings. The results are given in Tables D1 to D7.

D3 Conclusions.

The results show that the temperature measured by the thermocouple in the thermowell is the same as that of the fluid inside the tube provided sufficient time, fifteen to twenty minutes, is allowed for the thermocouple reading to reach equilibrium with the fluid temperature.

The results in Tables D6 and D7 show that the prevailing weather conditions, and a small amount of debris in the thermowell, should have no effect on the accuracy of the readings.

D4 Discussion.

All the temperature data taken on the refinery using the hand held thermocouples was taken in the following manner.

(i) The tubeside inlet and outlet thermowells were cleaned and the thermocouples were inserted. These were then left for twenty minutes.

(ii) The local tubeside temperature indicators were observed.
Provided local indicators had shown no or little ($\pm 1^{o}C$) change then the temperature readings were taken, otherwise the thermocouples were left in place until the local indicators were showing a steady reading.

(iii) The thermcouple readings were then compared to the local readings and if there was a large discrepancy ($> \pm 3^{o}C$) the thermocouples were swapped and left to come to equilibrium to check the readings.

(iv) The shellside thermocouples were cleaned and the thermocouples inserted. These were then left for twenty minutes.

(v) There are no local indictors for the shellside temperatures so the tubeside indicators were observed as these may give some forewarning of significant changes in the shellside temperatures.

Any vapour thermometers that had been removed to allow insertion of the thermocouples were replaced and the procedure was repeated on the next exchanger in the train.

Figure D1.1 Experimental Apparatus

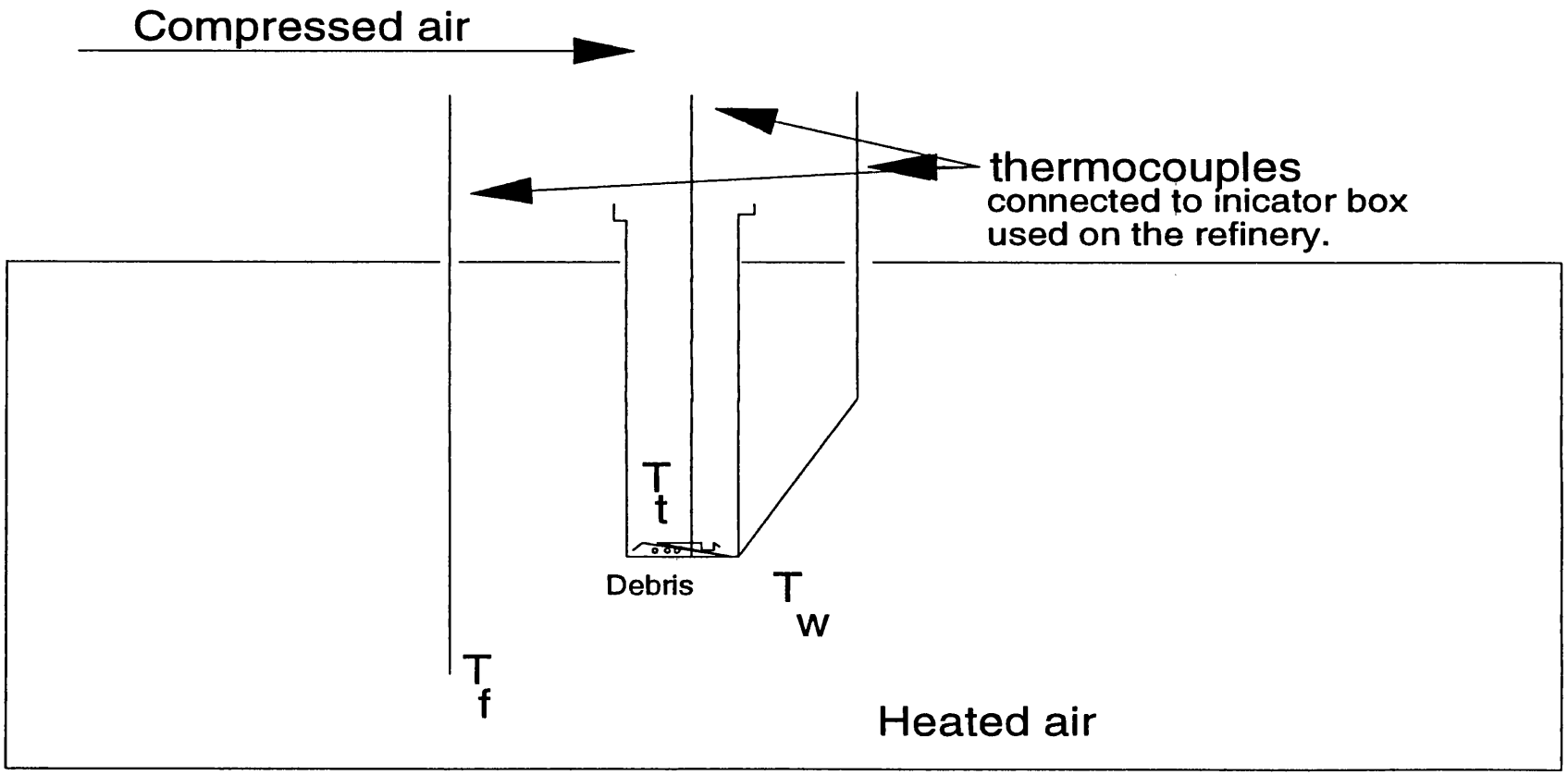

Table D1

Experiment 1 Oven setting 100°C

(readings taken 30 minutes after oven was switched on)

Time s	T_f °C	T_w °C	T_t °C
1	97	97	97
2	97	97	97
3	97	97	97
4	98	97	97
5	98	97	97
6	98	98	97
7	98	98	98
8	98	98	98
9	98	98	98
10	98	98	98
11	98	98	98
12	98	98	98
13	98	98	98
14	98	98	98
15	98	98	98
16	98	98	98
17	98	98	98
18	98	98	98
19	98	98	98
20	98	98	98

Table D2

Experiment 2 oven setting 150°C

(readings taken 30 minutes after oven was switched to the new setting.)

Time s	T_f °C	T_w °C	T_t °C
1	148	148	148
2	148	148	148
3	148	148	148
4	148	148	148
5	148	148	148
6	148	148	148
7	148	148	148
8	148	148	148
9	148	148	148
10	148	148	148
11	148	148	148
12	148	148	148
13	148	148	148
14	148	148	148
15	148	148	148
16	148	148	148
17	148	148	148
18	148	148	148
19	148	148	148
20	148	148	148

Table D3

Experiment 3 Oven setting 250 °C

(Readings taken 30 minutes after oven was switched to new setting.)

time s	T_f °C	T_w °C	T_t °C
1	247	247	247
2	247	247	247
3	247	247	247
4	247	247	247
5	247	247	247
6	247	247	247
7	247	247	247
8	247	247	247
9	247	247	247
10	247	247	247
11	247	247	247
12	247	247	247
13	247	247	247
14	247	247	247
15	247	247	247
16	247	247	247
17	247	247	247
18	247	247	247
19	247	247	247
20	247	247	247

Table D4

Experiment 4 Investigating the time taken for thermocouple to reach equilibrium with the surrounding temperature.(oven setting 200°C)

Time min	T^f °C	T^w °C	T^t °C
1	198	198	22
2	198	198	86
3	198	198	104
4	198	198	146
5	198	198	160
6	198	198	175
7	198	198	182
8	198	198	187
9	198	198	190
10	198	198	192
11	198	198	194
12	198	198	195
13	198	198	196
14	198	198	197
15	198	198	197
16	198	198	198
17	198	198	198
18	198	198	198
19	198	198	198
20	198	198	198

Table D5

Experiment 5 Investigating the time taken for the thermocouple to reach equilibrium with the surrounding temperature (Oven setting 250°C)

Time min	T_f °C	T_w °C	T_t °C
1	249	249	2
2	249	249	151
3	249	249	183
4	249	249	210
5	249	249	231
6	249	249	235
7	249	249	237
8	249	249	239
9	249	249	241
10	249	249	242
11	249	249	244
12	249	249	246
13	249	249	247
14	249	249	248
15	249	249	248
16	249	249	249
17	249	249	249
18	249	249	249
19	249	249	249
20	249	249	249

Table D6

Experiment 6 As for Experiment 1 with 6g of debris in the thermowell.

Time min	T_f °C	T_w °C	T_t °C
1	98	98	98
2	98	98	98
3	98	98	98
4	98	98	98
5	98	98	98
6	98	98	98
7	98	98	98
8	98	98	98
9	98	98	98
10	98	98	98
11	98	98	98
12	98	98	98
13	98	98	98
14	98	98	98
15	98	98	98
16	98	98	98
17	98	98	98
18	98	98	98
19	98	98	98
20	98	98	98

Table D7

Experiment 7 as Experiment 1 with compressed air blowing over the exposed section of the thermowell.

Time min	T_f °C	T_w °C	T_t °C
1	98	98	98
2	98	98	98
3	98	98	98
4	98	98	98
5	98	98	98
6	98	98	98
7	98	98	98
8	98	98	98
9	98	98	98
10	98	98	98
11	98	98	98
12	98	98	98
13	98	98	98
14	98	98	98
15	98	98	98
16	98	98	98
17	98	98	98
18	98	98	98
19	98	98	98
20	98	98	98